STUDIES ON DEEP EXCAVATION BEHAVIOUR IN ENGINEERED BACKFILLING ADJACENT TO NUCLEAR SAFETY RELATED STRUCTURES

By

PADMANABHAN.G

ENGG02201104028

INDIRA GANDHI CENTER FOR ATOMIC RESEARCH

A thesis submitted to the

Board of Studies in Engineering Sciences in partial fulfilment of requirements

for the Degree of

DOCTOR OF PHILOSOPHY

of

HOMI BHABHA NATIONAL INSTITUTE

December, 2018

Homi Bhabha National Institute

Recommendations of the Viva Voce Committee

As members of the Viva Voce Committee, we certify that we have read the dissertation prepared by Shri.G. Padmanabhan entitled "Studies on deep excavation behaviour in engineered backfilling adjacent to nuclear safety related structures" and recommend that it may be accepted as fulfilling the thesis requirement for the award of Degree of Doctor of Philosophy.

Dr.K.Veluṣamy, Chairman	Date: 6/3/2020
Dr.G.Sasikala, Guide	Date: 06/03/2020
Dr.A.Boominathan, IITM, Co-Guide	Date: 6/3/2020
Dr.J.S.Vinod, UOW, Australia, External Examiner	Date:06/03/2020
Dr.B.P.C.Rao, Member	Date: 6/3/2020
Dr.V.S. Srinivasan, Member	Date: 06/03/2020

Final approval and acceptance of this thesis is contingent upon the candidate's submission of the final copies of the thesis to HBNI.

We hereby certify that we have read this thesis prepared under our direction and recommend that it may be accepted as fulfilling the thesis requirement.

Date: 06/03/2020

Place:

Co-guide

Guide

STATEMENT BY AUTHOR

This dissertation has been submitted in partial fulfillment of requirements for an advanced degree at Homi Bhabha National Institute (HBNI) and is deposited in the Library to be made available to borrowers under rules of the HBNI.

Brief quotations from this dissertation are allowable without special permission, provided that accurate acknowledgement of source is made. Requests for permission for extended quotation from or reproduction of this manuscript in whole or in part may be granted by the Competent Authority of HBNI when in his or her judgment the proposed use of the material is in the interests of scholarship. In all other instances, however, permission must be obtained from the author.

G. Padmanabhan

DECLARATION

I, hereby declare that the investigation presented in the thesis has been carried out by me. The work is original and has not been submitted earlier as a whole or in part for a degree / diploma at this or any other Institution / University.

G. Padmanabhan

List of Publications arising from the thesis

Journals

1. ***Padmanabhan G,*** Sasikala G, Ravisankar A, (2018). "Site characterization for deep excavation and evaluation of stiffness properties of backfilled soil from field instrumentation", Innovative Infrastructure solutions, 2018, 3:59, https://doi.org/10.1007/s41062-018-0165-0
2. ***Padmanabhan G***, Sasikala G, Ravisankar A, (2018). Efficacy of engineered backfilling in limiting settlements during future deep excavations. International journal of geo synthetics and ground engineering. https://doi.org/10.1007/s40891-018-0149-3, ISSN 2199-9260
3. ***Padmanabhan G.***, Sasikala, G, Ravisankar A (2019). Geotechnical Characterization of Site for Deep Excavation Analysis. *i-manager's Journal on Civil Engineering*, 9(1), 26-33, https://doi.org/10.26634/jce.9.1.15371
4. ***Padmanabhan G***, Sasikala G, Ravisankar A, Boominathan A (2019) "Performance evaluation of an open deep excavation in a multi layered soil site for locating a critical facility in South Coast of India" International Journal of Geotechnical Engineering (Communicated).

Conferences:

1. ***Padmanabhan G***, Boominathan A, Jayakumar T, Evaluation of strength parameters for a deep excavation problem and prediction of behavior of deep excavation using soil constitutive laws, Indian Geotechnical Conference, IIT Madras, Chennai, December, 2016.
2. ***Padmanabhan G***, Sasikala G, Ravisankar A, Evaluation of stiffness parameters through numerical analysis. Research Scholars meet on Material Science and Engineering of Nuclear Materials, HBNI, Kalpakkam, May, 2018.

G. Padmanabhan

Dedicated to my Parents

Gurus

Wife, Sons & Family

ACKNOWLEDGEMENT

I am immensely grateful to my research guide Dr. G. Sasikala, Head, Materials Development & Technology Division, Metallurgy & Materials Group (MMG) for her valuable guidance in the right direction to complete this work. I am also thankful to Dr. A. Boominathan, Professor, IIT Madras for his guidance to complete the work and for allowing to use the infrastructure of IIT for carrying out this work. I am grateful to Dr. T. Jayakuamar, former Director, MMG for his guidance during the early part of work.

I am thankful to Dr. K. Velusamy, Chairman of the doctoral committee and members of my doctoral committee Dr. B.P.C. Rao and Dr. V.S. Srinivasan for their valuable suggestions and encouragement during the course of my work.

I owe my sincere thanks to Shri. P.V. Kumar, former Project Director, FRFCF for granting permission to carry out this work and for his constant follow ups and encouragement during the entire course of work. His encouragement and motivation is the key for completion of this work.

I would like to thank Dr. A.K.Bhaduri, Director, IGCAR, Dr. R. Natarajan, former Project Director, FRFCF, Dr. A. Ravisankar , Project Director, FRFCF and Dr.Anish Kumar, Dean, Engineering Sciences (Academic) for their constant support during the course of this work and also for allowing to use various resources at Indira Gandhi Center for Atomic Research.

I take this opportunity to thank Dr. M. Saibaba, former Director, Resources Management Group and Shri. R.V. Subbarao, former Head, IGCAR Training School for their constant support during my course work.

I am also grateful to Shri. B.M. Ananda Rao, Shri. L. Davy Herbert, Shri. C. Sundaramurthy, Shri.C. Sivathanu Pillai and Shri. Sudipta Chattopadhyay for their constant support during my research work. I am also thankful to Shri. R. Mano and Shri. P. Karthikeyan for their support in collection of instrumentation data.

I am thankful to my colleagues, relatives and friends without whose support the work could not have completed.

(G. Padmanabhan)

CONTENTS

SYNOPSIS

Traditionally, nuclear facilities are often located in virgin sites and various environmental aspects are considered in selection of sites for construction of these facilities. Currently, facilities are being set up similar to complexes, along with provisions for future expansions, which require future construction activities. This necessitates deep excavations adjacent to the existing operating nuclear facilities. Since open excavations are not viable in constrained areas, supported excavation needs to be carried out for reaching the competent strata and locating these facilities. Supported excavation systems, such as a diaphragm wall, strut wall, and anchored walls are commonly used in various infrastructure projects. The current practice followed in the Indian nuclear industry for deep excavation in constrained area is to design appropriate retaining walls and to construct them along with the main nuclear facility. Later, controlled engineered backfilling is carried out around the retaining wall and other main plant structures. During the expansion of the facility, excavation will be taken up in these engineered backfill soil with the help of existing retaining wall.

Most of the design methodologies to date, focus on the lateral displacement of the retaining wall system and predictions of ground movements. Nevertheless, large ground movements are usually observed near deep excavation sites. It is, therefore, important to assess the impact of these excavation-induced ground deformations on structures in close proximity, so as to ensure the integrity, availability and serviceability of these structures. The effect of excavation-induced ground movements on structures has recently received considerable attention since excavations are often carried out close to the existing nuclear safety related structures.

Even though, retaining walls are conventionally designed for strength and stability, the performance of this system and engineered backfilling around retaining walls are not

studied in Indian context. Such studies help in identifying the critical areas of settlement as well as the precautions to be taken up to restrict the settlements within the permissible limits in order to ensure safety of critical structures in the zone of influence. Presently, empirical methods are adopted to predict ground surface settlement and displacement of the retaining structures from various case histories. Even though these empirical methods are useful for a preliminary analysis and design of a deep excavation, a site-specific analysis accounting for the stiffness properties of the soil, retaining system, construction sequence and dewatering effect is essential to identify the area of maximum settlement of soil mass for critical structures like nuclear power plants. This can be achieved by a numerical analysis of the deep excavation accounting for these parameters and with appropriate constitutive models that describe site-specific properties of subsurface.

Prediction of deep excavation behaviour mainly depends on accurate evaluation of stiffness properties of subsurface material. Overestimation of stiffness values and its usage in analysis may lead to under-prediction of settlement, which may be exceeded during actual excavation imposing damage to existing structures. On the other hand, use of lower stiffness leads to uneconomical design.

Various researchers and practitioners are recently using field monitoring of deep excavation and calibration of numerical models with observed and computed parameters through back analysis. These back analyses are mostly carried out for excavation involving in-situ soil; in the present study, this approach is extended to calibrate the stiffness properties of engineered backfill soil. These calibrated models are further applied to evaluate the efficacy of engineered backfilling in limiting the settlements and displacements during future excavation near critical structures. This calibrated model can be used in predicting deep excavation behaviour in sites of similar geology. The study carried out in the present work was motivated by the need to (a) identify a suitable constitutive model to predict the

behaviour of deep excavation involving engineered backfill and multilayered soil site (b) evaluate the stiffness of engineered backfill soil through field calibration using field instrumentation data (c) study the efficacy of already placed engineered backfilling soil in limiting the settlements during future excavation and (d) finalize an excavation scheme and to specify engineered backfilling requirements for future excavation sites of similar geology.

A systematic literature review was carried out on the methods of deep excavation as well as the empirical and numerical methods for design and analysis of deep excavation. Various soil constitutive laws required to define stress-strain relation of soil mass were identified and the current practice of geotechnical site characterization to obtain these parameters were critically reviewed. The stiffness properties determined using empirical relations showed wide variation and indicated the necessity of accurate stiffness determination of soil mass to define accurate behaviour of excavation. Also, the current practice of design of deep excavation employing empirical methods does not take in to account the effects of continuous dewatering. To address these issues, stiffness properties of soil is determined through a comprehensive field instrumentation scheme, which was evolved and implemented to monitor the behaviour of deep excavation carried out in virgin sites and in constrained areas involving engineered backfill.

As identified from the literature review, to account for the gap area in accurate estimation of soil stiffness and site specific continuous dewatering, the following two cases were analyzed in PLAXIS 2D idealizing the problem as a plane strain case (i) open deep excavation in a multi

layered soil site for locating a nuclear facility and (ii) deep excavation in engineered backfill soil adjacent to an infrastructure building. Stiffness properties of engineered backfill soil were calibrated from field instrumentation and then used in predicting the behaviour of supported deep excavation.

The work carried out in this study is mainly divided into three parts, namely, (a) characterization of site for an open deep excavation analysis and validation of the results using field instrumentation (b) caliberation of stiffness properties of engineered backfill soil from field instrumentation and (c) numerical analysis of deep excavation adjacent to safety related structures using various soil constitutive laws and performance evaluation of engineered backfill and retaining systems.

As the first part of the study, geotechnical characterization of a deep excavation (500 m x 300 m x 18.0 m) carried out in a multi-layered soil site was undertaken. Strength and stiffness properties of the various soil layers were determined using conventional correlations between SPT N values available in literature. The geotechnical investigation carried out at the site indicates that the site consists of loose to medium sand followed by dense sand. This sand layer is followed by silty sand/clayed soil and residual soil. Hard rock is available at a depth of 15 to 20 m below the ground level in most of the area.

Currently open excavations are designed with stable slopes and are never monitored for their performance. In the present study, considering the importance of critical structures, a comprehensive field instrumentation was developed to monitor the performance of excavation. Four inclinometers (Model SME 2190) were installed along the boundary of excavation at a distance of 2.0 m from the top edge.

The problem was idealized as a plane strain case and stage analysis was carried out in PLAXIS 2D considering initial ground conditions. The stress-strain relation of soil mass is defined using Mohr-Coulomb (MC) model and Hardening Soil (HS) model accounting the nonlinear behaviour of the soil mass. In addition to the conventionally required parameters, dilatency and incremental increase of stiffness were considered for top sandy layer, and behaviour of adjacent soil mass were determined. Dewatering effect is also considered in the analysis by lowering the water table after each stage.

As a part of the performance evaluation of this open excavation, four inclinometers and bench marks were provided to monitor the displacements and settlements of adjacent soil mass. The numerical models were validated by comparing the displacements obtained numerically with those measured using field instrumentation. It was shown that the behaviour of excavation can be computed by combining MC model (modified taking into account the dilatency of sand and incremental increase in stiffness) for the sandy layer with HS model for silty sand and residual soil. The maximum surface displacement computed numerically, 9.6 mm is in good agreement with the displacements10.86 mm and 8.18 mm observed from the two inclinometersplaced at190 m from the corner of the excavation.

The displacements observed from inclinometers kept closer to the corner of excavation (at 100 m) provided a smaller displacement of 1.75 mm and 0.9 mm indicating the corner effects of the excavation. The numerically computed displacement fairly matches with the inclinometer readings obtained from the middle of the excavation, validating the plane strain assumption adopted in this analysis. The calibrated model predicted a settlement of 38 mm at a distance of 11.0 m behind the excavation which was also verified by the bench mark observations during last phase

of excavation. The displacements were computed by varying the thickness of each layer and the values were compared with the field observed values.

The work was further extended to evaluate the actual in-situ site-specific stiffness of sandy layer by carrying out a parametric study by varying SPT N values and stiffness of sandy layer. A series of back calculations were performed and it was concluded that the empirical relations between stiffness of soil and SPT N values, overestimate the stiffness of top loose to medium sand layer and underestimate the stiffness of dense layer. The present study provided the in-situ stiffness of sandy layer, which can be used for predicting behaviour of deep excavations in similar sites. This was validated by comparing the numerical results obtained from the site-specific in-situ stiffness with those from the instrumentation readings.

In the second part of study, current practice of deep excavation in engineered backfill soil carried out adjacent to critical structures was examined. Stiffness properties of engineered backfilling soil determined from various field investigations were used for numerical analysis. Since the displacement profiles computed using MC model did not match with the field observations, higher order constitutive model, viz., HS model was employed for evaluating the displacements.The results highlighted the requirement of such models in predicting the behaviour of excavation in engineered backfilled soil. The present study showed that the stiffness parameter of engineered backfilled soil obtained from conventional pressuremeter tests (8000 kPa) is conservative and that from full scale plate load tests (32000 kPa) overestimate the actual stiffness. The actual in-situ stiffness of backfilled soil is almost 50% higher than that estimated from conventional pressuremeter test. This calibrated stiffness is further used for predicting deep excavation to be carried out employing retaining walls.

In the third part of this study, future excavation adjacent to critical facility employing retaining wall was studied. The settlement of adjacent soil mass and displacements of retaining wall were computed and compared with those from available empirical methods. In this study, the field-calibrated stiffness was used in predicting the settlements of adjacent soil mass. The study highlighted the non-conservatism involved in assuming linear behaviour of soil mass; the computed settlements using nonlinear HS model is higher than that obtained from conventional MC model. This study indicated that while the available empirical formulations for predicting deep excavation behaviour are adequate to define the maximum settlements in primary zone, a site specific analysis accounting in-situ stiffness and dewatering effects is warranted for evaluating secondary zone of settlements. Both the primary and secondary zone of settlements computed from numerical analysis are higher than the permissible value of 25 mm, and hence appropriate measures need to be adopted to ensure the stability of structures supported on this backfilled soil.

Application of strut load and improvement of stiffness of engineered backfilled soil proved to be useful in limiting the settlement to the permissible value of 25 mm, which is essential to ensure the stability of foundations of adjacent critical structures during future excavation. Further, this study recommends that implementation of an instrumentation scheme is essential during future excavation to observe the settlement of adjacent soil mass and to take remedial measures at each stage of excavation.

The results obtained from the studies carried out as part of the thesis clearly establish the inadequacy of present system of retaining wall assisted deep excavation in engineering backfilling to limit the settlements during future excavation. The conclusions drawn from the study are valuable inputs to design of future excavation

systems in engineered backfill soil. Further research needs to be taken up to identify appropriate methods for improving the stiffness of engineered backfilling in the primary settlement zones. Cement stabilization, lime stabilization etc in combination with geo grids need to be studied to find out optimum percentage of stabilization. Various laboratory and field investigations need to be carried out to evaluate the parameters of stabilized soil for numerical analysis. Implementation of a comprehensive instrumentation scheme and monitoring of excavation at each stage would be beneficial to take any corrective action to restrict the settlement of adjacent soil mass to within the permissible limits.

LIST OF FIGURES

LIST OF TABLES

Chapter 1

Introduction

The per capita energy consumption per year is one of the main indicators of developed countries and developing countries such as India; the average energy consumption in India is approximately 1075 kWh per year, which is approximately one-third of the world average demand and is much lower than the International per capita consumption per year. The main sources of energy in developing countries are hydel, coal and oil, which are not environmental friendly. Therefore, alternative energy sources are required for sustainable development in such countries. To this end, India has planned a three-stage nuclear programme to generate sustainable energy by utilizing indigenously available resources (Srikumar Banerjee, 2017). Accordingly, various nuclear power plants and the associated facilities are being constructed. The sites for locating these facilities are selected with consideration of various environmental aspects and are often located in virgin sites. Currently, these facilities are being set up similar to complexes, along with provisions for future expansions, which require future construction activities and necessitate deep excavations adjacent to the existing operating plants.

1.1 Necessity and current practice of Deep excavations

Deep Excavations are required for construction of infrastructure projects, power plant structures and underground transport systems. However, deep excavation often creates displacement and settlement of adjacent soil mass, and this can damage nearby infrastructures especially in case of adjacent deep excavations. Open excavation and supported excavation are two basic types of excavation systems and open excavation is feasible only in virgin sites. Open excavation designed as per conventional slope stability analysis is generally adopted in virgin sites where space is not a constraint. However, the choice of open excavation often

depends on ground water level, method of dewatering, and area availability for storage of excavated material which can be used for backfilling at a later date. Since open excavations are not viable in constrained areas, supported excavation needs to be carried out for reaching the competent strata and locating facilities. Supported excavation systems, such as diaphragm wall, strut wall, and anchored walls, are commonly used in various infrastructure projects.

The current practice of deep excavation followed in the Indian nuclear power plant construction is to design open excavation in virgin site with stable slopes which are obtained from classical slope stability analysis. The material excavated is used for later backfilling. In constrained areas and where future excavation is planned later along with the main plant structures, retaining walls are designed during the planning stage and constructed along with the main plant. Later, engineered backfilling is carried out around the retaining walls. During expansion of the facility, excavation is taken up in this engineered backfilling with the help of the already constructed retaining wall. In the current practice, these retaining walls are generally designed for stability; however, the settlements of the adjacent soil mass and the displacement of the excavation support are not studied. These parameters need to be evaluated in order to adopt appropriate measures to ensure that these are within the permissible limits.

In Indian Nuclear construction programme, conventionally designed systems are seldom monitored for their performance. The conventionally designed slopes are stable and need not to be monitored for its performance; however, implementation of a comprehensive filed instrumentation in a regular excavation programme often provides insight into the behaviour of adjacent soil. The data so generated can be effectively used for analysis, design and monitoring the performance of supported excavation systems which is essential for carrying out deep excavations adjacent to nuclear safety related structures for future expansion.

One of the main design constraints in deep excavation problems is that the damage to adjacent infrastructure should be prevented/ minimized. To date, much of the design methodologies are aimed at minimizing lateral displacement of the retaining system, settlements and ground movement. Nevertheless, large ground movements are usually observed in various deep excavation projects. It is, therefore, important to assess the impact of these excavation-induced ground deformations on structures in close proximity to ensure the integrity and serviceability of the nearby structures. Displacements and settlements are to be minimized and monitored to ensure the safety of structures. This aspect is vital in the case of Nuclear Power Plants, where excessive displacement and settlement of soil mass can jeopardize the safety of adjacent nuclear safety related structures and services.

Presently, empirical methods, e.g., Peck (1969), Goldberg et al. (1976), Clough and Rourke (1990), Ou and Hsieh (2000) and Ou et al. (2005) are used to predict the ground surface settlement and displacement of the retaining structures. These empirical methods were developed from various case histories of deep excavation.

1.2 Infamous excavation failures

The effect of excavation induced ground movements on nearby structures has recently received considerable attention since excavations especially for infrastructure development, are often to be carried out close to existing important structures. Even though several methods for design of deep excavation are available, various deep excavation failures are reported; notable among the recent ones are Nicoll Highway collapse in Singapore in 2004, failure of open excavation in Washington DC in 1990 and Subway collapse in Hangzhou, China. Photographs of these failures are given in Fig 1.1 to 1.3. Recent metro rail construction in Chennai also raised concern on the stability of structures near to the tunnelling works and underground construction. Heritage structures like CSI Wesley Church

and Rippon building are among those which developed cracks during this tunnelling works. Photograph of cracks developed in Rippon building is given in Fig 1.4.

Fig 1.1: Nicoll Highway collapse in Singapore

Fig 1.2: Failure of an open excavation Washington DC

Fig 1.3: Subway collapse in Hangzhou, China

Fig 1. 4: Cracks in Rippon building due to excavation for Chennai Metro Rail construction

1.3 Need of site specific studies

Even though excavation systems are designed using empirical methods, such failures are widely reported. Considering the importance of the safety of nuclear power plant structure in view of the long-term consequences of any failures, the stability of these structures needs to be maintained during adjacent deep excavation. Hence, a site-specific analysis of excavation accounting for the stiffness properties of the soil and dewatering effects is warranted to identify the area of maximum settlement and to adopt appropriate measures to limit these so that the safety of the adjacent structures which are supported on this soil mass are ensured.

Constitutive laws describing strength and stiffness properties of soil are essential for a site specific analysis and to predict the behaviour of deep excavation. Strength properties are generally obtained from conventional site investigation and empirical correlations between Standard Penetration Test (SPT) values. However, stiffness properties obtained from conventional investigations and empirical relations show a wide range of scatter which needs to be properly accounted in a site specific analysis. Therefore, to define the constitutive laws,

advanced methods of field investigations need to be often adopted for evaluating stiffness parameter. Finite element analysis describing soil constitutive law accounting for the non linear behaviour of soil is commonly used in today's world of infrastructure development for solving various deep excavation problems. Advances in computing facilities and availability of finite element methods are effectively used in identifying critical areas near excavation where proper precautions and control measures need to be taken to protect the adjacent critical facilities.

1.4 Motivation for current study

As a part of location of a nuclear facility, a site along the East Coast of India (Fig 1.5) is selected which comprises beach deposits. The sediments are made up of sand, and yellowish brown silty sands more oxidized owing to relative age. There exists a minor topographical break between this unit and the younger geomorphic unit indicating receding of the sea in geological time. The older beach is made up of fine to medium grained sand. Geologically the area is comprised of two distinct formations, namely crystalline rocks of Archaean to late Proterozoic age mainly composed of Charnockite rocks and recent sediments (Sivakumar et al. (2008) and Boominathan (2004)).

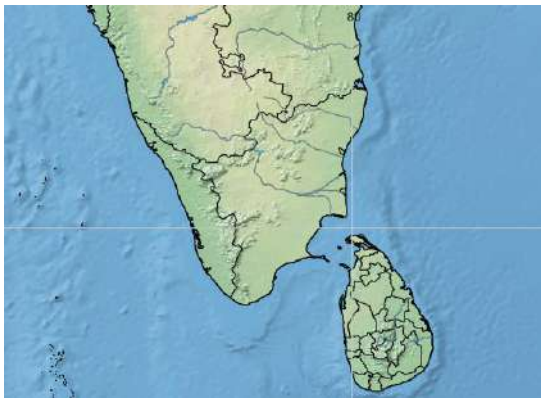

Fig 1.5: Location Map of the Study area

The study carried out in the present work was motivated by the need to (a) identify a suitable constitutive model to predict the behaviour of deep excavation involving engineered backfill and multilayered soil site (b)evaluate the stiffness of engineered backfill soil (c) study the efficacy of already placed engineered backfilling soil in limiting the settlements during the future excavation and (d) finalize an excavation scheme and to specify engineered backfilling requirements for future excavation sites of similar geology.

Prediction of deep excavation behaviour from such numerical analysis mainly depends on accurate evaluation of stiffness properties of subsurface material. Use of higher stiffness values in analysis will lead to lower values of computed settlement which will be exceeded during actual excavation causing damage to the existing structures. On the other hand, use of lower stiffness may lead to uneconomical design. Field instrumentation is widely used nowadays for monitoring the performance of deep excavation and to calibrate the soil stiffness used in constitutive models. Field monitoring of deep excavation and calibration of numerical models with observed and computed parameters through back analysis is recently used by various researchers in deep excavation research and practice. This approach of back analysis is generally used for estimating the stiffness properties of the soil at deep excavation sites. In the present study, this is extended to calibrate the in-situ stiffness properties of the engineered backfill soil using field monitoring of displacements. These calibrated models are further applied to evaluate the efficacy of engineered backfilling in limiting the settlements and displacements during future excavation near critical structures.

The objective of the proposed research is to study the influence of deep excavations on the nearby critical structures at Kalpakkam. Three cases of deep excavation are studied: (a) in virgin site involving a mass excavation (b) excavation in constrained area, which require steeper slopes and (c) supported excavation system for deep excavation in engineered

backfilled soil. Factors affecting deep excavation behaviour like soil stiffness, depth of excavation, size of excavation and dewatering are examined.

1.5 Method of study

A systematic literature review was carried out on deep excavation methods as well as design and analysis of deep excavation including empirical and numerical methods. Various soil constitutive laws required to define stress-strain relation of soil mass were identified and the current practice of geotechnical site characterization to obtain these parameters were critically reviewed. The stiffness properties determined using empirical relations showed wide variation and indicated the necessity of accurate stiffness determination of soil mass while predicting deep excavation behaviour. Also, the current practice of deep excavation design employing empirical methods does not predict effect of continuous dewatering. A comprehensive field instrumentation scheme addressing these issues was evolved to monitor the behaviour of deep excavation and was implemented for excavation carried out both in virgin site and in constrained area involving engineered backfill.

As identified from the literature review, to account for the gap area in accurate estimation of soil stiffness and site specific continuous dewatering, the problem of open deep excavation in a multi layered soil site for locating a nuclear facility and deep excavation in engineered backfill soil adjacent to an infrastructure building was analyzed in PLAXIS 2D idealizing the problem as a plain strain case. Inclinometers and settlement monitors were deployed near an open excavation carried out in a multi layered virgin soil site for locating a nuclear facility. Displacement of soil mass and settlement were observed and compared with the model results and the model was calibrated. Also, stiffness properties of engineered backfill soil were calibrated from field instrumentation and then used in predicting the behaviour of deep excavation to be carried in engineered backfilled soil using retaining

structure. Even though the retaining structure is designed for conventional stability the displacement of retaining system and settlement of soil mass is beyond the permissible limit and required additional safety measures to be implemented during excavation.

The work carried out during the study is mainly divided into three parts namely (a) Characterization of site for an open deep excavation analysis and validation of the results using field instrumentation (b) evaluation of stiffness properties of engineered backfill soil through model calibration and back analysis (c) numerical analysis of deep excavation adjacent to safety related structures using various soil constitutive laws and performance evaluation of engineered backfill and retaining systems. The study provided a frame work for selection of appropriate soil model for describing excavation behaviour in open excavation, evaluation of stiffness property of backfilled soil which in turn is used for describing soil constitutive law in finite element software and to predict the behaviour of supported deep excavation adjacent to existing structures.

1.6 Organization of thesis

In the ***Chapter 1,*** a brief introduction to the research work, an overview about current practice of deep excavation followed in Indian nuclear industry identifying the gap area is covered.

Chapter 2 reviews various deep excavation methods, design and analysis methods of deep excavation including empirical and numerical methods. Application of field instrumentations in predicting behaviour of deep excavation is also addressed in this chapter.

Chapter 3 provides a comprehensive review on soil constitutive laws for prediction of deep excavation behaviour, parameters required for characterization of soil constitutive models and geotechnical characterization required for defining the soil constitutive model.

Current practice of geotechnical investigation carried out for analyzing deep excavation behaviour is also addressed in this chapter.

Chapter 4 analyzes the performance of a conventionally designed open deep excavation carried out in a virgin multilayered soil site for locating a nuclear facility using comprehensive filed instrumentation.

In ***Chapter 5*** stiffness of engineered backfilled soil to be used for predicting deep excavation, behaviour was determined from the field instrumentation through a parametric study. The displacement obtained from field instrumentation was compared with that obtained through numerical analysis and series of back calculations were performed to evaluate the accurate stiffness of backfill soil.

In ***Chapter 6,*** the efficacy of retaining wall and engineered backfilling was studied in limiting the settlement during future excavation.

Chapter 7 summarizes the works carried out during this study, conclusions drawn from the study and possible area of future work.

Chapter 2

Deep Excavation methods, analysis and soil constitutive laws: A review

Excavations with depths smaller than their widths are classified as shallow excavations while those with depth larger than their width as deep excavations (Terzaghi, 1943). Peck (1969) categorized excavation of depth lesser than 6 m as shallow excavation and greater than 6 m as deep excavation. Some of the commonly used excavation methods are open excavation, retaining system assisted excavation, braced excavation, island excavation, anchored excavation, top-down construction and zoned excavation. Choice of method of deep excavation depends on various factors (i) cost, (ii) time period of construction, (iii) water table, (iv) presence of adjacent structures, (v) their condition and type of foundation (vi) availability of area, (vii) equipment for excavation.

2.1 Types and choice of deep excavation

Open excavation is generally adopted in virgin sites where space is not a constraint since it requires side slopes. As the depth of excavation increases, the volume of excavated material increases and more space is required to keep the excavated material, which is required at a later stage for backfilling works. Further, the scheme of open excavation depends on type of soil, water table and depth of excavation. As the depth increases, intermediate berms need to be provided for a stable slope and continuous dewatering needs to be employed to lower the ground water level.

Structural systems like cantilever retaining walls, counter-fort retaining walls, soldier pile, sheet pile, diaphragm walls are commonly used for the retaining system for deep excavation in constrained areas and for deep excavation adjacent to existing structures. Choice of the retaining system depends on various factors like economy, soil conditions,

requirements for protection of adjacent structures, ease of construction and environmental factors. Cantilever walls are generally used for excavations upto 6.0 m and to retain earth by the passive resistance provided by the soil below the excavation. For retaining earth more than 6.0 m height counter fort retaining walls are generally adopted.

The continuous diaphragm wall, also referred to as slurry is a structure formed and cast in a slurry trench (Xanthakos, 1994). The trench excavation is initially supported by either bentonite or polymer based slurries that prevent soil incursions into the excavated trench. The term "diaphragm walls" refers to the final condition when the slurry is replaced by tremied concrete that acts as a structural system either for temporary excavation support or as part of the permanent structure.

Sheet pile walls are constructed by driving prefabricated sections into the ground. Soil conditions may allow the sections to be vibrated into ground instead of it being hammer driven. The full sheet pile wall is formed by connecting the joints of adjacent sheet pile sections in sequential installation. Sheet pile walls provide structural resistance by utilizing the full section. Steel sheet piles are most commonly used in deep excavations, although reinforced concrete sheet piles are being used successfully.

Secant pile walls are formed by constructing intersecting reinforced concrete piles. The piles are reinforced with either steel rebar or with steel beams and are constructed by drilling under mud. Primary piles are installed first with secondary piles constructed in between primary piles once the primary piles gain sufficient strength. Pile overlap is typically of the order of 3 inches (8 cm). In a tangent pile wall, there is no pile overlap as the piles are constructed flushed to each other.

When retaining walls are supported with horizontal struts to resist earth pressure, such excavation is known as braced excavation. In case of anchored excavation methods, the struts

are replaced with anchors to resist the lateral earth pressure. These methods of excavation are commonly used for staged excavation.

Presently, in Indian nuclear industry, since nuclear power plants are constructed in virgin sites, spaces is not a constraint and hence open excavation with slope of 2H: 1V and intermediate berms are generally adopted in combination with multistage well point system of dewatering. In constrained areas where space available is limited, steeper slopes are adopted. However, for future excavation near adjacent structures, supported excavation needs to be adopted due to limited space considering the safety of the existing structures. Currently, retaining walls are designed and constructed along with the main nuclear power plant buildings. Later, excavation is planned to be taken up with the help of these retaining wall, which are designed for strength and stability.

2.2 Design of deep excavation system using empirical methods

One of the main objectives of the design of deep excavation is to evaluate the stability, stress and deformation induced by excavation. While the objective of stability analysis is to avoid collapse of the excavation, stress analysis is necessary for the design of structural components. Deformation analyses are usually carried out to estimate the soil movements and wall deflection caused by excavation in order to take adequate measures to protect adjacent structures. The stress and deformation caused by excavation arises from unbalanced forces, construction defects and dewatering. When the unbalanced forces are beyond the acceptable limits, the movement of soils within the range of excavation can damage adjacent structures. The stress and deformation analysis of deep excavation includes simplified methods and numerical methods. Simplified methods generally classify the monitored results from excavation case histories and relate with the stress and deformation characteristics of retaining system and soil mass. These empirical methods are applicable for construction in

similar geological sites using the same construction methods as in the case histories considered. However, these simplified methods do not address the site specific issues like continuous dewatering and soil stiffness.

Peck (1969), Lambe (1969), Goldberg et.al (1976), O'Rourke (1981), Clough and O'Rourke (1990) made significant contributions in evaluating the characteristics of deep excavations. The major findings of these studies are (i) Soil type is an important factor in the performance of deep excavation (ii) Deep excavation dewatering is a major source of settlement. (iii) Construction sequencing is another important factor in the performance of deep excavation.

2.2.1. Ground Settlement induced by construction of diaphragm walls

Clough & O' Rourke (1990) established from the monitored results of various excavations that the maximum settlement induced by the construction of diaphragm walls is 0.15% of the depth of the trench. The envelope is shown in Fig 2.1. This indicates that the settlement near diaphragm wall panels is significant and necessitates utmost care in protecting adjacent structures.

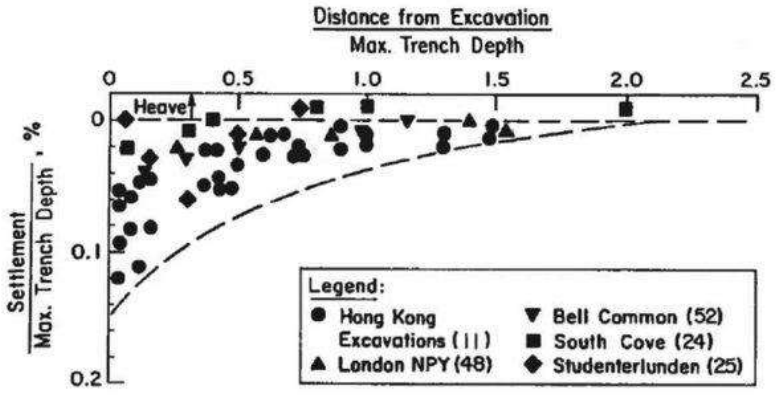

Fig 2.1 Envelope of ground surface settlement induced by trench excavations
(Clough and O'Rourke, 1990)

The legend in the Fig 2.1 indicates the data points obtained from various sites and the number inside the parenthesis indicates the number of data points.

Ou and Yang (2000) studied the settlement induced by the construction of diaphragm walls for the excavation in the Taipei Rapid Transit System and found that maximum settlement (δ_v) induced by a single panel is about 0.05% of the depth of trench (H_t) and this occurs within a distance of 0.3 times the depth of trench as per Fig 2.2 . They also noticed that the effect of excavation is not felt beyond a distance equal to depth of excavation. The study conducted by Poh and Wong (1998) also indicated that the in sand-clay alternated layers, the maximum settlement induced by a single trench panel is 10-15 mm while that in Singapore marine clay the maximum settlement is is around 24 mm. Ou and Wang (2000) also found that the maximum accumulated settlement after the completion of several test panels was about 0.07 times depth of trench and its location and influence range were similar to those of single panel induced settlement. Multiple panels of diaphragm walls induced more settlements and the total settlement was about 0.13% of the depth of trench and occurs at a distance of 0.3 times the depth of trench. These results were less than those observed by Clough and O'Rourke (1990).

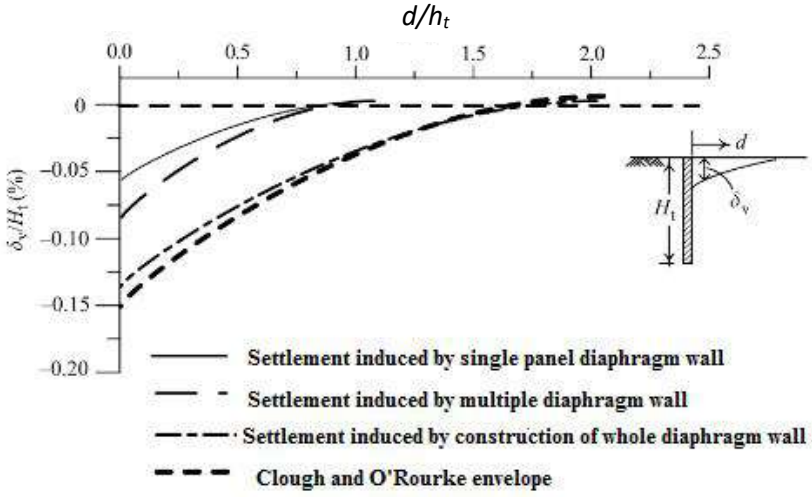

Fig 2.2 Envelope of ground surface settlement induced by diaphragm wall construction (Ou and Yang, 2000)

2.2.2 Retaining Wall movements induced by excavation

Magnitude of wall movement depends on the stiffness of the retaining system and excavation induced unbalanced forces. A thick retaining wall, narrow and shallow excavation, and high strut stiffness will reduce the wall deflection. Clough and O'Rourke (1990) found that as the width of the excavation increased deformation of the retaining wall increases. They also found that as stability of the excavation increases the wall deformation decreases. Relation between maximum lateral deflections of walls (δ_{Hmax}), stiffness of retaining system (EI) and factor of safety against basal heave (F_b) of the excavation pit is shown in Fig 2.3. In the Fig 2.3, H_e is the depth of excavation, h is the distance between struts, h_{avg} denotes average distance between struts and γ_w is unit weight of water.

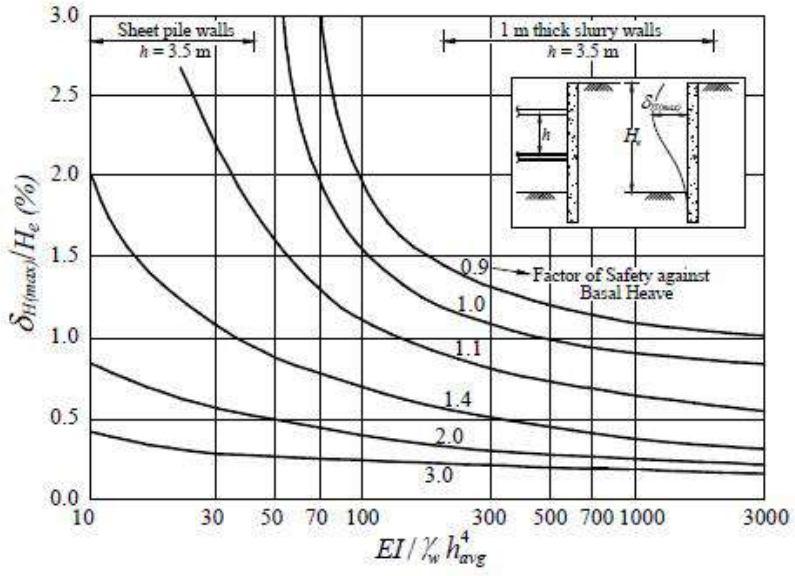

Fig 2.3: Maximum lateral wall movements and ground surface settlements for support systems in clay (Clough et al., 1989).

Ou et al. (1993) studied the relation between the deformations of excavation and their depths in Taipei area. They observed that the deformation of retaining wall system increases with the depth of excavation. They also found that the deformation of wall in soft clay is generally greater than that in sand. They proposed a maximum wall deformation of

respectively 0.2% and 0.5% of excavation depth for sand and soft clay. There also exists a relation between wall penetration depth and deflection. As the depth of penetration of retaining wall decreases, a phenomenon called “kicking” occurs at the bottom of retaining wall and excavation fails. However, as long as the retaining wall is stable, penetration depth does not affect the retaining wall deflections.

The studies by Hsieh (1999) observed that the increase in retaining wall thickness decrease the wall deformation. However, this decrease does not have a linear relationship with the increase in stiffness. They also found that the increase in retaining wall thickness is effective upto certain extent. Apart from the wall thickness the strut stiffness, strut spacing and strut pre load also affect the deformation of the retaining wall.

Deflection of wall is a function of stiffness of struts; if the stiffness of strut is high, retaining wall rotates about the contact point between the strut and the wall and the maximum wall deformation occurs near the excavation surface. If the soil below the excavation surface is weak the location of maximum deformation will be below the excavation surface. For stiff soils, the location of maximum deformation will be above excavation surface. If the stiffness of strut is low, the displacements of wall will be larger at the contact points and the profile of the deformation will be cantilever and the maximum deformation will be at the top of the retaining wall (Ou et al 1998). Decreasing the horizontal spacing increases stiffness of the strut per unit width and while decreasing the vertical spacing increases stiffness of the strut system and deformation of the retaining wall system reduces.

2.2.3 Characteristics of ground surface movement

Hsieh and Ou (1998) observed that the settlement produced by excavation can be classified into spandrel and concave types. Under normal conditions, excavations in soft clay

will produce concave type of settlement while excavation in sandy or stiff soil produces spandrel type of settlement as shown in Fig 2.4 (Clough and O'Rourke 1990).

According to Peck (1969), the influence zone of settlement is around two to three times the depth of excavation. Clough and O'Rourke (1990) observed that the influence zone for excavation in sandy soil is around twice the depth of excavation, while that in stiff soil is around three times the depth. In all these cases, the location of maximum settlement is only a function of depth; however, as per Ou (2006) the zone of influence of ground settlement also depends on excavation width and location of hard soil. Hsieh and Ou (1998) also proposed two zones of influence, namely, Primary influence Zone (PIZ) and secondary influence zone (SIZ). Fig 2.4 indicates the various types of settlement profiles.

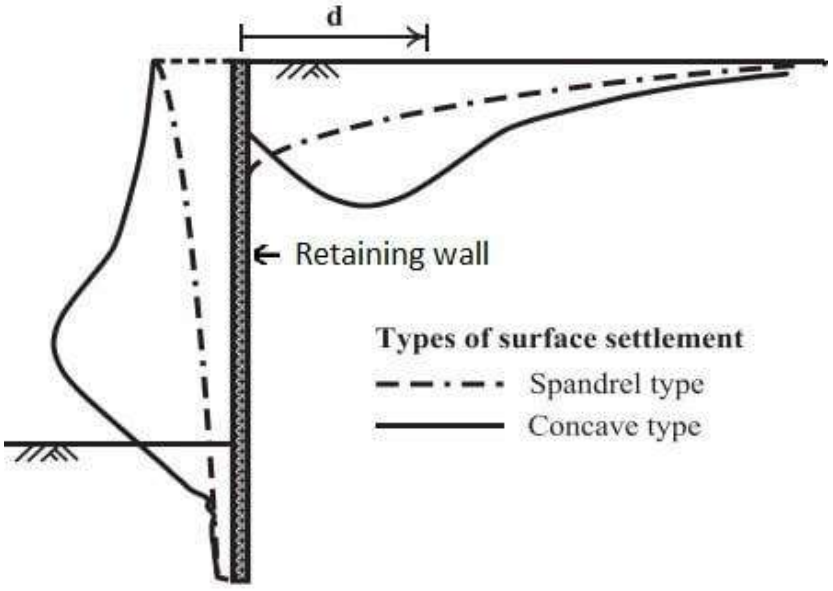

Fig 2.4 : Schematic diagram of Settlement Profile

Nichloson (1987), and Ou.et al (1993) from various case studies indicated that the location of maximum ground settlement of the concave type would occur at a distance of 0.5 H_e from the wall, where H_e is the depth of excavation. However, the monitoring of excavation by Ou (2005) indicated that the location of the maximum settlement does not change with the increase in depth of excavation. According to Ou et al. (2005) the maximum

settlement occurs at one third a distance of PIZ. Clough and O'Rourke (1990) established a relationship between the maximum settlement and the excavation depth in stiff clay, sandy soil, and soft to medium soft clays, based on various case histories. The established relation is shown in the Figure 2.5. The legend in the Fig 2.5 indicates the location of case histories.

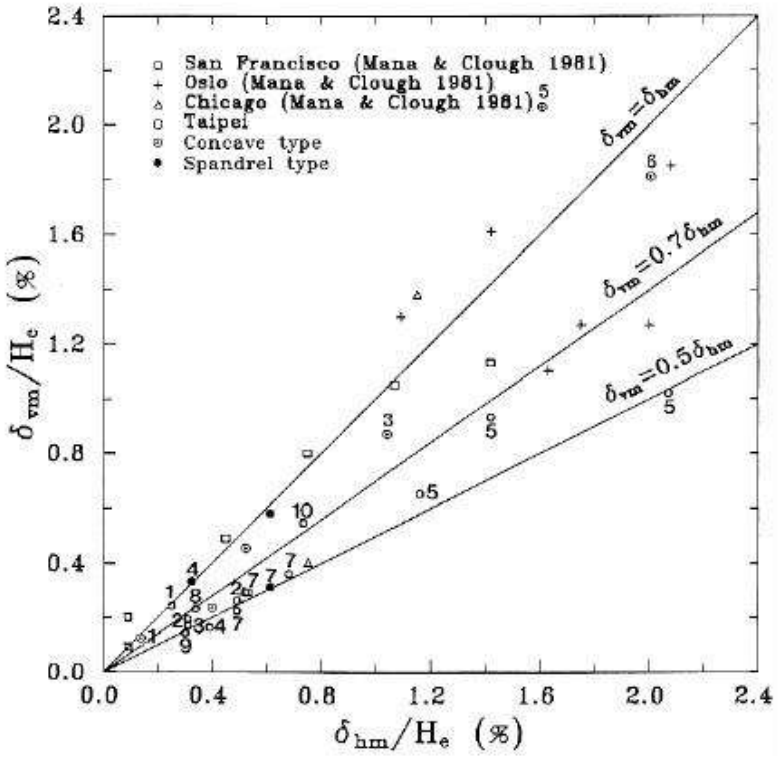

Fig 2.5: Maximum ground surface settlement and lateral wall deflection (Ou et al., 1993)

These relations are obtained from various case histories observed in Taipei, Chicago, San Francisco and Oslo (Ou et al., 1993). From the figure, it can be noted that the maximum vertical settlement is around 0.5 times to 0.75 times the horizontal movement of wall. δ_{hm} corresponds to horizontal displacement, δ_{vm} corresponds to vertical displacement and H_e is the depth of excavation. While the lower value is for sandy soils, upper limit is for clays. For very soft soil, the maximum vertical and horizontal displacements are same.

2.2.4 Analysis of ground movement induced by Excavation

Peck (1969) summarized information from previous case histories to correlate settlement around excavations. He proposed three zone of settlement profile based on soil type and workmanship. These are Type I : Sand and soft to stiff clay with average workmanship, Type II : Very soft to soft clay and Type III – Very soft to soft clay to a significant depth below the excavation bottom. The figure summarizing the results of case histories by Peck (1969) is reproduced in Fig 2.6.

Peck (1969) mainly employed the results of field monitoring of case from histories in Chicago and Oslo and established the relation curves between the ground surface settlement and distance from the wall. These results are from case histories before 1969, which employed sheet piles, and different from the present day advanced design and construction methods like diaphragm walls and hence need not to be applicable for all excavations. Peck (1969) proposed that the influence zone of settlement should be two or three times of the excavation depth.

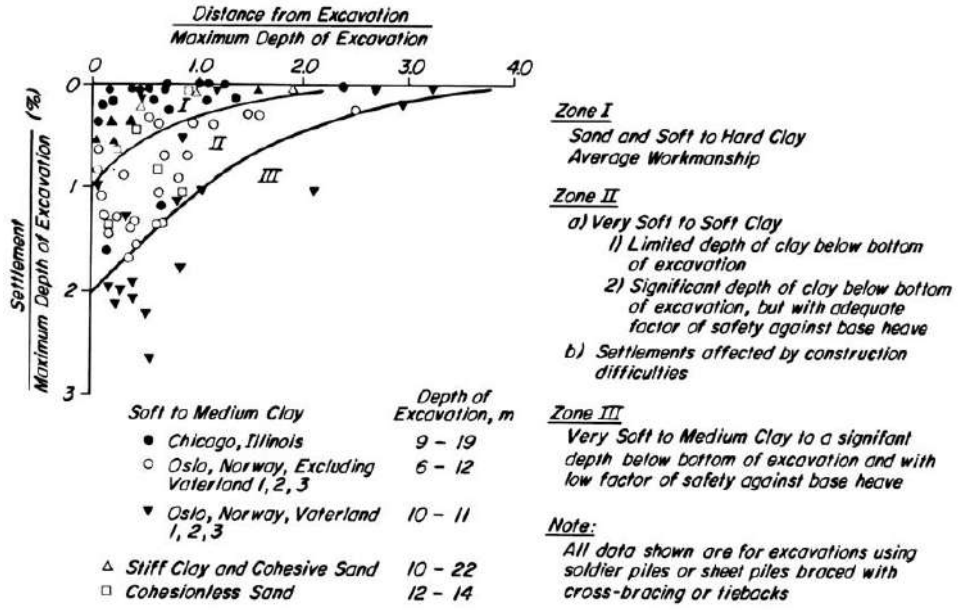

Fig 2.6: Summary of settlement profile adjacent to Open cuts (Peck 1969)

Goldberg et al (1976) and Colugh and Rourke (1990) showed that the pattern of the settlement adjacent to excavation depends on soil type. Fig 2.7 below shows the normalized settlement profiles proposed by Colugh and Rourke (1990) for estimating settlement pattern adjacent to excavation.

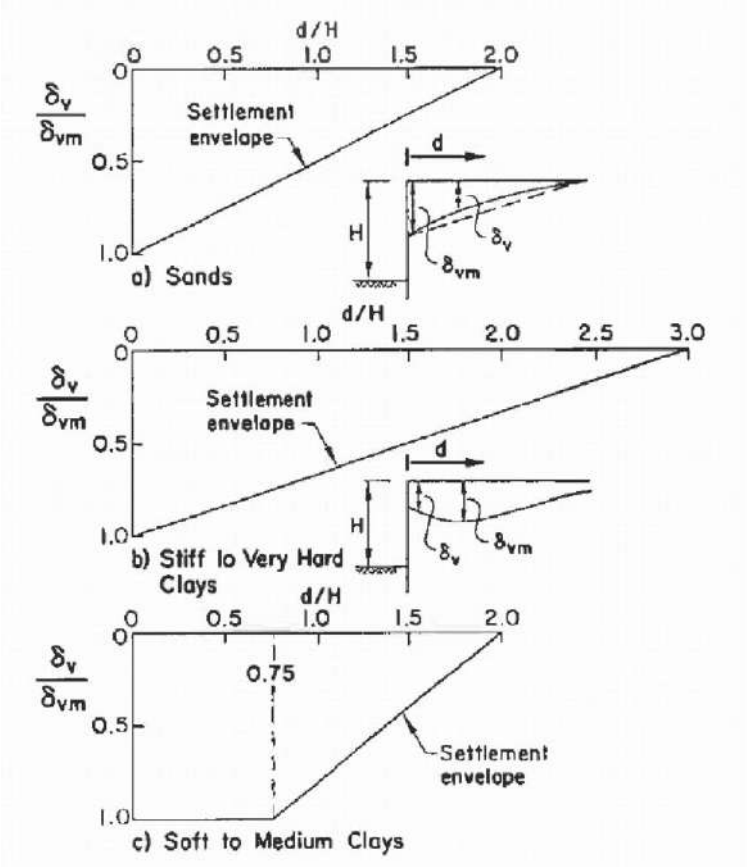

Fig 2.7 : Normalized settlement profile for estimating settlement adjacent to excavation of various soil types (Clough and Rourke 1990)

They found that the ratio of the maximum settlement induced by the construction of diaphragm walls to the depth of the trench is 0.15%. According to their studies, excavation in sand or stiff clay tend to produce triangular ground surface settlement. The maximum settlement is found to be near the retaining wall. These curves are envelopes predicting ground surface settlement induced by excavation and is simple to apply.

As earlier mentioned Clough and O'Rouke (1990) proposed, excavation in sandy soil may induce an influence zone of settlement about twice of the excavation depth. The influence zone for stiff to very stiff clay is three times the excavation depth and that of soft or medium soft clay is twice the excavation depth. Ou and Hsieh (2000) and Ou et.al (2005)developed a method to predict the ground surface settlement. The proposed settlement curves for the spandrel and concave types are shown in the Fig 2.8 and 2.9. They computed ground settlement based on influence zone, maximum settlement, and its location. They showed that the primary settlement zone generates larger angular distortion for adjacent structures.

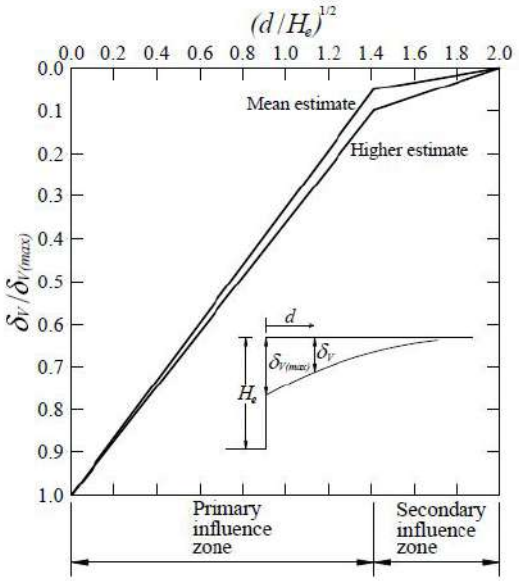

Fig 2.8: Shape of Spandrel type of settlement Profile (Ou and Hsieh, 2000; Ou et al.,2005)

Generally, soil back of the retaining wall moves forward and down with the retaining wall deforming under normal conditions producing ground settlement. It is also observed that factors causing wall deformation also produce ground settlement.

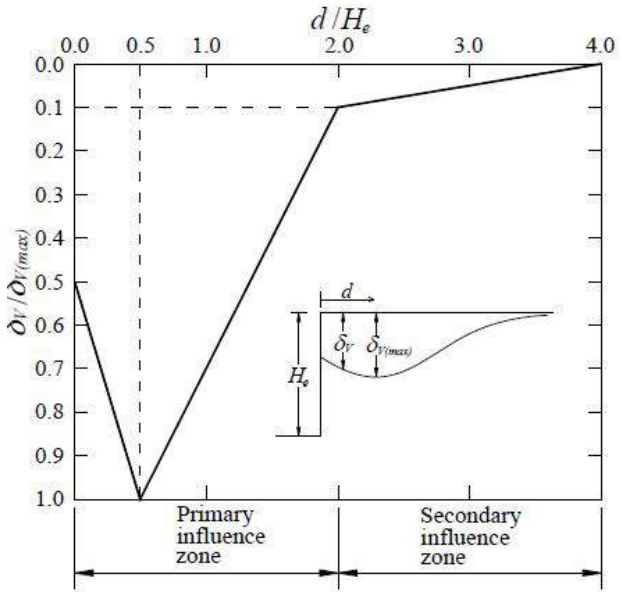

Fig 2. 9: Shape of concave type of settlement Profile (Ou and Hsieh, 2000; Ou et al.,2005)

2.3 Comparison of the various empirical methods

Chang-Yu Ou (2005) showed that settlement profile derived from Clough and O'Rourke method lead to a satisfactory settlement envelope for the primary influence zone, though the secondary influence zone is ignored. Settlement profile computed from Ou and Hsieh's method is in reasonable agreement with the field measurements. On the other hand, the results computed using Clough and O'Rourke's method are not comparable with the field measurements. Various case studies showed that angular distortion can be computed by Ou and Hsieh's method.

This literature review indicates that the simplified methods are reasonable for predicting the excavation behaviour. However, large deformations and failures were noticed in deep excavations indicating the necessity of advanced techniques for numerical and observational methods of analysis.

2.4 Numerical methods of deep excavation analysis

The results of empirical analysis depends on many factors like soil type, its thickness, water table and its variations, excavation depth and width. These parameters are often simplified in empirical methods of design of deep excavation and can lead to unsafe design. In order to simulate the effect of various factors advanced numerical analysis is often employed in today's growing world of infrastructure development. '*Beam on elastic foundation'* is a classical numerical analysis often used to solve soil-structure interaction problems and to study the behaviour of axially loaded pile, raft foundations, and retaining walls. However, this simplified numerical analysis does not provide information on overall stability of excavation, movement of retaining system and the effect of construction on excavation. In such cases, a full numerical analysis can provide information on all the design requirements.

Various researchers have carried out analytical studies and conducted parametric studies to identify the effects of various parameters, which affect the deep excavation behaviour. Numerical methods are expected to be a flexible tool to study the impact of deep excavation in each stage and to evaluate the effect of ground water dewatering, stiffness of retaining wall. The important numerical methods in continuum mechanics include Finite Element Method (FEM), Boundary Element Method (BEM) and Finite Difference Method (FDM). A numerical excavation model is able to deal with the construction processes that take place during the sequential removal of soil during deep excavation process. Based on the review carried out, FEM appears to be particularly suited for solving geotechnical problems and for the stress and deformation analysis of deep excavation and underground constructions like tunnels. Excavation problems are typical Boundary value problems and can be solved using Finite Element methods. FEM studies are often performed using software like ABAQUS, ANSYS, PLAXIS and Zsoil. PLAXIS is user-friendly to predict the

behaviour of deep excavation and is most commonly used for static problems. Finite element methods can simulate factors that affect magnitude of unbalanced force created due to excavation and hence provide more accurate results than those derived from semi empirical methods.

Finite element analysis can be classified into plane strain analysis, axisymmetric analysis and three-dimensional analyses. The wall deformation, ground settlement, excavation bottom movement and the related empirical formulas discussed refer to two dimensional plane strain behaviour and are not necessarily valid in the vicinity of the corners of the excavation. Three-dimensional analyses are required to correctly predict the displacement of diaphragm walls at corners. The most important aspects of Finite element analysis are the selection of the constitutive model for describing soil behaviour and characterization of site for defining various model parameters. Appropriate modelling of construction sequence and drainage conditions also are important for accurately predicting the behaviour of deep excavations.

2.5 Observational method of analysis

Excavation design using empirical methods were developed from the limited observations and mostly led to conservative design. Still, a few failures were reported in the fast developing world of infrastructure. This is attributable to various site-specific factors which are not accounted for in the design of excavation system. In the present practice of geotechnical engineering, field instrumentations are commonly deployed to monitor the slopes by measuring displacements and settlements and to take remedial measures during construction. These field monitored instrumentation data can be effectively used to calibrate the soil model used in finite element analysis. These calibrated model parameters can be used

for analysis of future excavations and also for similar geotechnical problems in similar geology area.

The objective of geotechnical instrumentation is to ensure the safety of excavation and surrounding area, to confirm the design conditions and calibrate the soil models and to predict the long-term behaviour of excavation. Commonly used field instrumentation in geotechnical deep excavation problems are settlement monitors and inclinometers. Settlement monitors measure the settlement in the adjacent areas while inclinometer monitors the inclination of the retaining system and adjacent soil mass. In addition, ground water pressure is also monitored in various projects. Presently, for all the critical projects of deep excavation inclinometers are widely used. For diaphragm walls, strain gages and embedment gages were used in a few cases to monitor the moments and axial forces in the slurry walls. Inclinometers can be fixed either inside the retaining wall or within the retained soil.

Slope inclinometers are the commonly used geotechnical instrument to measure horizontal displacements of deep excavation. According to Erikson et al.,1992, slope inclinometers are the most important source of geotechnical data during construction. These are widely used to measure lateral displacement of soil and wall movements in slurry wall and deep excavations (Fig. 2.10). Inclinometers are broadly classified into probe inclinometers and fixed- in-place inclinometers (Laplante, 1998). Most of the geotechnical engineering practice uses probe inclinometers.

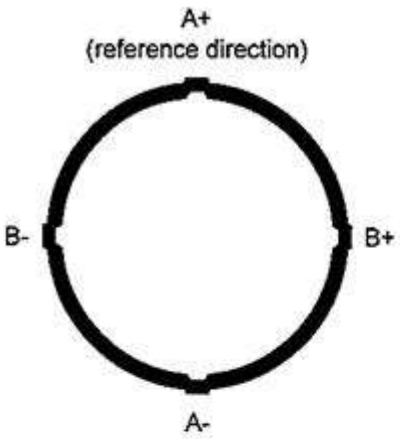

Inclinometer grooves, A +, A - is the primary direction, B + , B - is the secondary direction

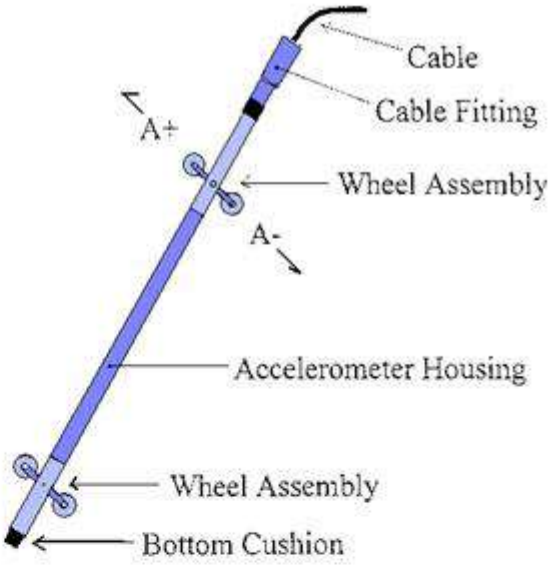

Inclinometer probe

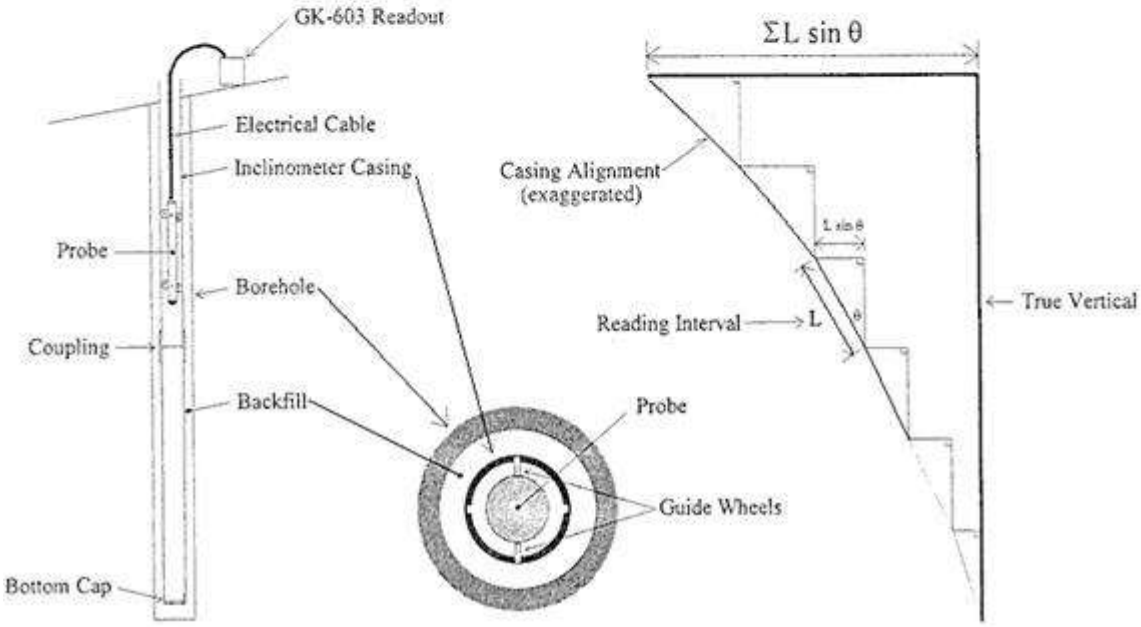

Fig 2.10 Assembly of slope inclinometers

Field instrumentations were effectively used by various researchers to monitor the performance of supported deep excavations, stability of structures adjacent to ongoing

infrastructure activities like tunnelling etc. Nikolinakou (2011), Gorska (2012), Becker (2013), Hsiung (2014), Whittle (2015) and Hsiung et al. (2016) employed field instrumentation to monitor the performance of deep excavation and calibrated the numerical model parameters using back calculations. Use of such advanced field instrumentation and back calculation provides a platform to evaluate the deep excavation performance which can be further utilized for calibrating the soil constitutive models used in finite element analysis. This coupled numerical analysis with field instrumentation is the requirement of today's developing infrastructure world and can be effectively used to identify the site specific requirements in deep excavation analysis and design.

This method of finite element analysis and back calculations matching the field instrumentation data was used for determining the stiffness properties of engineered backfill soil and performance of existing soil retaining system adopted in Indian Nuclear Industry for future expansion works was studied in this work. The results were compared with the commonly used empirical methods; the study highlighted the requirement of site specific analysis accounting for the soil variability, dewatering effects, stiffness of soil properties and effect of soil constitutive laws for predicting the behaviour of deep excavation.

2.6 Soil Constitutive Modelling

Numerical analysis requires defining stress-strain properties of soil that is usually described through soil constitutive laws. The stress –strain relation of soil has non-linear, plastic characteristics and often depends on confining pressures. In addition, soil behaves differently during loading and unloading stresses. Soil is a complicated material that shows anisotropic and time dependent behaviour when subjected to stresses. Generally, it exhibits non-linear behaviour well below failure condition with stress dependent stiffness. Soil also exhibits low stiffness at very low strains and upon stress reversal. Various soil constitutive

models have been proposed for the analysis and prediction of the soil behaviour, which can be used in the characterization of the site.

Brinkgreve (2004) indicated that the mechanical behaviour of soils may be modelled at various degrees of accuracy. Hooke's law of linear, isotropic elasticity is the simplest available stress-strain relationship however is too crude to capture essential features of the non linear soil behaviour. On the other hand, a large number of constitutive models have been proposed by several researchers to describe various aspects of soil behaviour in detail. Brinkgreve highlighted the importance of selection of parameters, which need to be accurately obtained from detailed field tests. However, in practice, soil parameters often need to be estimated from limited or insufficient data. Various features of different soil models are explained in the following sections.

2.6.1 Liner Elastic-Perfectly Plastic Model (Mohr-Coulomb Model)

Mohr-Coulomb model is a first order elastic-perfectly plastic soil model. It assumes that under general stress state, soil behaves linearly in the elastic range. Basic parameters required to define this model are Young's Modulus (E) and Poisson's ratio (υ). Other parameters required to define this model are friction angle, cohesion and dilatency. The idealization in Mohr- Coulomb Model is shown in the Fig 2.11.

Plasticity is the development of irreversible strains. In order to evaluate the plasticity, a yield function 'f' is introduced as a function of stress and strain in Mohr- Coulomb model. When the yield function $f = 0$, plastic yielding occurs. A perfectly plastic model is a constitutive model with a fixed yield surface.

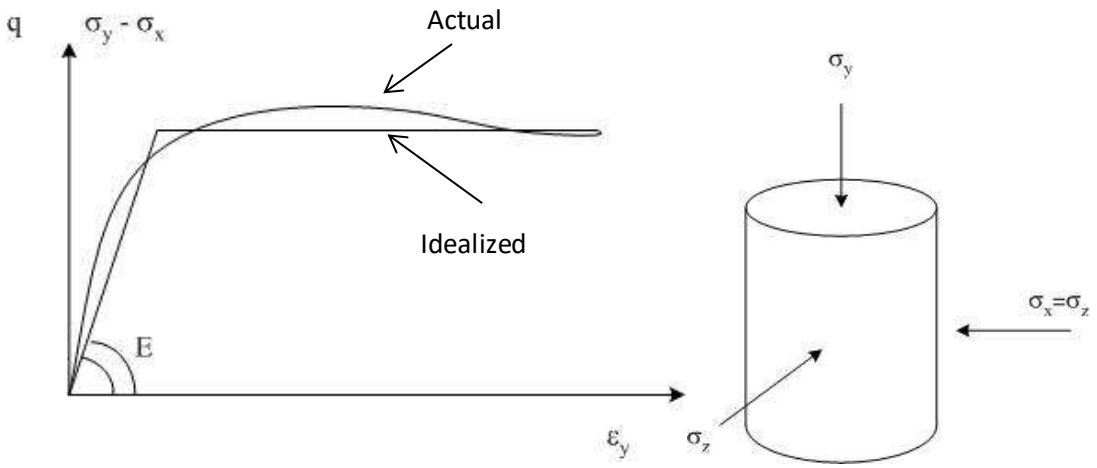

Fig 2.11: Stress –Strain relation in Mohr-Coulomb model

The basic principle of elasto-plasticity is that strains and strain rates can be decomposed in to an elastic part and a plastic part, which is given in the following equation (2.1).

$$\varepsilon = \varepsilon^{e} + \varepsilon^{p} \text{ -------- } (2.1)$$

where ε = Total strain

ε^{e} = Reversible elastic strain and

ε^{p} = Irreversible plastic strain.

$\varepsilon^{p} = 0$ for $f<0$

Mohr-Coulomb yield condition is an extension of Coulomb's friction law to general states of stress. Smith and Griffith (1982) defined six yield functions in terms of principal stresses to define Mohr-Coulomb yield conditions. The six yield functions are given in the following equations 2. 2 to 2.7.

$$f_{1a} = \tfrac{1}{2}(\sigma_2' - \sigma_3') + \tfrac{1}{2}(\sigma_3' + \sigma_2')\sin\phi - C \times \cos\phi \le 0 \text{ --------- } (2.2)$$

$$f_{1b} = \frac{1}{2}(\sigma_3' - \sigma_2') + \frac{1}{2}(\sigma_3' + \sigma_2')\sin\phi - C \times \cos\phi \leq 0 \text{ ---------- (2.3)}$$

$$f_{2a} = \frac{1}{2}(\sigma_3' - \sigma_1') + \frac{1}{2}(\sigma_3' + \sigma_1')\sin\phi - C \times \cos\phi \leq 0 \text{ ----------(2.4)}$$

$$f_{2b} = \frac{1}{2}(\sigma_1' - \sigma_3') + \frac{1}{2}(\sigma_1' + \sigma_3')\sin\phi - C \times \cos\phi \leq 0 \text{ ----------(2.5)}$$

$$f_{3a} = \frac{1}{2}(\sigma_1' - \sigma_2') + \frac{1}{2}(\sigma_1' + \sigma_2')\sin\phi - C \times \cos\phi \leq 0 \text{ ---------- (2.6)}$$

$$f_{3b} = \frac{1}{2}(\sigma_2' - \sigma_1') + \frac{1}{2}(\sigma_2' + \sigma_1')\sin\phi - C \times \cos\phi \leq 0 \text{ ---------- (2.7)}$$

Two plastic model parameters appearing in the above equations are friction angle (ϕ) and cohesion (C). The condition, $f = 0$ for all yield functions together represent a fixed hexagonal cone in principal stress space as shown in Figure 2.12.

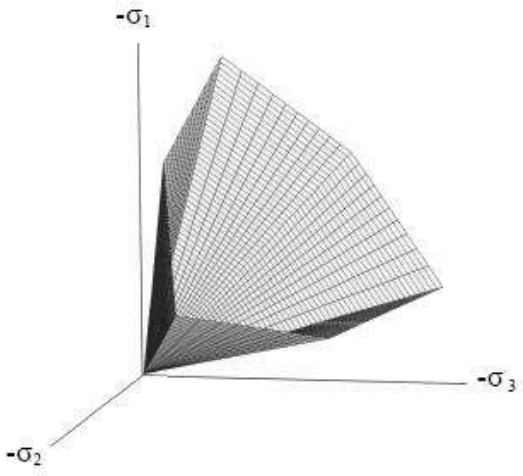

Fig 2.12: The Mohr-Coulomb yield surface in principal stress space

In addition to the yield function, six plastic potential functions are also defined for the Mohr-Coulomb model. These equations are given in the following equations 2.8 to 2.13.

$$g_{1a} = \frac{1}{2}(\sigma_2' - \sigma_3') + \frac{1}{2}(\sigma_2' + \sigma_3')\sin\psi \text{ ---- (2.8)}$$

$$g_{1b} = \tfrac{1}{2}(\sigma_3' - \sigma_2') + \tfrac{1}{2}(\sigma_3' + \sigma_2')\sin\psi \text{ ----- (2.9)}$$

$$g_{2a} = \tfrac{1}{2}(\sigma_3' - \sigma_1') + \tfrac{1}{2}(\sigma_3' + \sigma_1')\sin\psi \text{ ------ (2.10)}$$

$$g_{2b} = \tfrac{1}{2}(\sigma_1' - \sigma_3') + \tfrac{1}{2}(\sigma_1' + \sigma_3')\sin\psi \text{ ------ (2.11)}$$

$$g_{3a} = \tfrac{1}{2}(\sigma_1' - \sigma_2') + \tfrac{1}{2}(\sigma_1' + \sigma_2')\sin\psi \text{ ------(2.12)}$$

$$g_{3b} = \tfrac{1}{2}(\sigma_2' - \sigma_1') + \tfrac{1}{2}(\sigma_2' + \sigma_1')\sin\psi \text{ ----- (2.13)}$$

These plastic potential functions contain a third parameter, namely, dilatency angle 'ψ'. This parameter is required for modelling of dense sand to simulate positive plastic volumetric strain increment. Thus, the Mohr-Coulomb model requires five basic parameters for modelling the soil behaviour. These are Young's Modulus (E), Poisson Ratio (v), Cohesion (C), Angle of internal friction (ϕ) and dilatency angle (Ψ).

2.6.2 Hardening Soil Model (Isotropic Hardening)

Soil behaviour for loading and unloading problems are different and soil behaves nonlinearly well below the failure conditions. Also, stiffness of soil depends on stress level. These characteristics of soil necessitate the use of advanced constitutive models to predict the behaviour of soil. The hardening soil (HS) model proposed by Brinkgreve & Vermeer (1992) is derived from the hyperbolic model of Duncan and Chang (1970). The model proposed by Schanz (1998) is a true second order model, which is applicable for both soft and hard types of soil. In the special case of drained triaxial test, relation between axial strain and deviator stress can be represented by a hyperbola. Thus, the basic characteristics of the model are (i) stress dependent stiffness, (ii) plastic strain hardening due to primary deviator loading (shear

hardening), (iii) plastic strain hardening due to compression, (iv) elastic unloading/reloading and (v) failure according to Mohr-Coulomb Law.

Shear hardening is used to model irreversible strains due to primary deviatoric loading while compression hardening is used to model irreversible plastic strains due to primary compression in oedometer and isotropic loading. Yield contour of the model in three-dimensional space is shown in Fig 2.13 below. Failure is defined by means of Mohr-Coulomb failure criterion. Because of the two types of hardening, the model is accurate for problems involving a reduction of mean effective stress and at the same time mobilization of shear strength. Such situations occur in excavation (retaining wall problems) and tunnel construction projects.

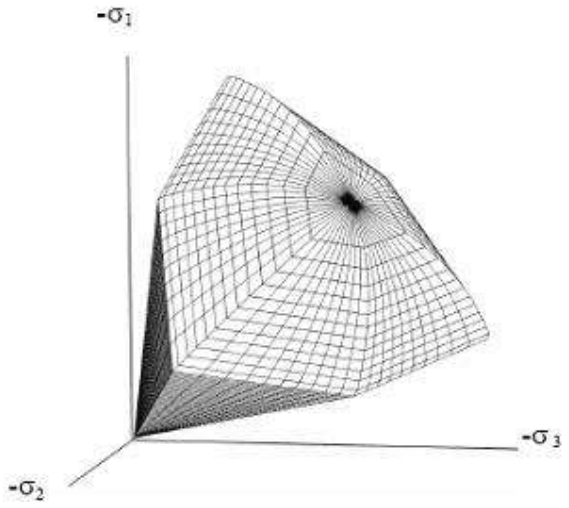

Fig 2.13: Total yield contour of hardening soil model in principal stress space

The basic feature of the Hardening soil model is the stress dependency of soil stiffness. For oedometer conditions of stress and strain, the HS model uses the relation given in equation (2.14) given below.

$$E_{oed} = E_{oed}^{ref} \left(\frac{\sigma}{\rho^{ref}}\right)^{m} \text{ ------- (2.14)}$$

The formulation of HS model is based on the hyperbolic relationship between the vertical strain and deviator stress in primary triaxial loading. The relationship is plotted in the Fig 2.14.

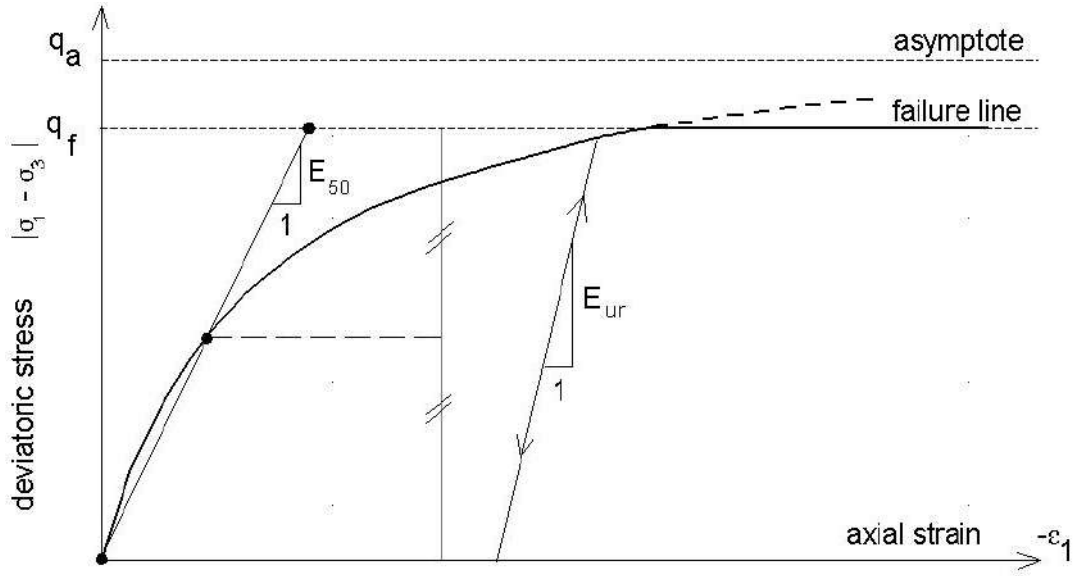

Fig 2.14: Hyperbolic stress-strain relation in primary loading for a standard drained triaxial test.

Some basic characteristics of the model are: stress dependent stiffness according to a power law (m), plastic straining due to primary deviatoric loading (E_{50}^{ref}), plastic straining due to primary compression (E_{oed}^{ref}), elastic unloading/reloading input parameters (E_{ur}^{ref}, υ_{ur}) and failure criterion according to the Mohr-Coulomb model(C, ϕ and ψ). The definition of E_{50}^{ref} and E_{oed}^{ref} are shown in the Figures 2.15 and 2.16 respectively. For most of the engineering applications E_{50}^{ref} is same as E_{oed}^{ref}.

The parameter E_{50} is the confining stress dependent stiffness modulus for primary loading and is given by the following equation 2.15.

$$E_{50} = E_{50}^{ref}\left(\frac{\sigma_3^{'} + c\cot\varphi}{p^{ref} + c\cot\varphi}\right)^m = E_{50}^{ref}\left(\frac{\sigma_3^{'}\sin\varphi + c\cos\varphi}{p^{ref}\sin\varphi + c\cos\varphi}\right)^m \quad \text{---- (2.15)}$$

where E_{50}^{ref} is a reference stiffness modulus corresponding to the reference confining pressure of 100 kPa. The extent of stress-dependency is given by the exponent m. For unloading and reloading stress paths, another stress-dependent stiffness modulus is used which is known as Young's Modulus during unload. For all practical purpose this is equal to three times the value of E_{50}^{ref} (Obrzud, 2010) . The advantage of the hardening soil model over the Mohr-Coulomb model is not only the use of a hyperbolic stress strain relation but also the control of stress level dependency. In Mohr-Coulomb model, Young's Modulus is a fixed value but in actual case, the Young's Modulus is dependent on stress level.

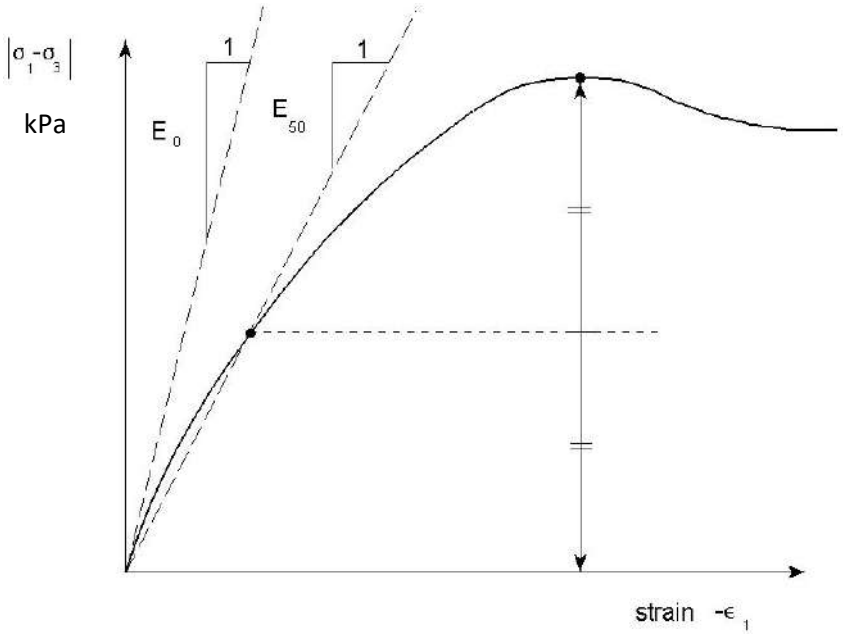

Fig 2.15: Definition of E_{50}^{ref} in standard triaxial test

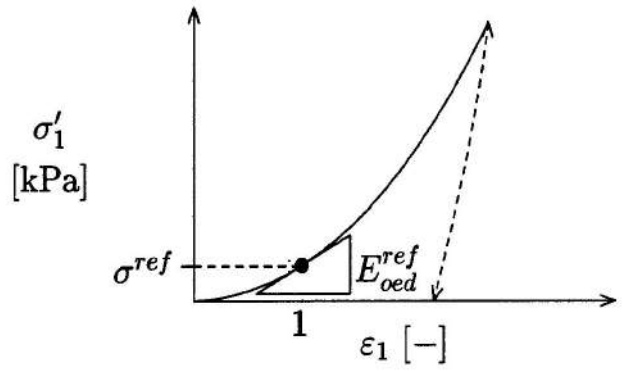

Fig 2.16 : Definition of E_{oed}^{ref}

2.7 Applicability of the material models

Mohr-Coulomb model is generally used as a first order approximation for all types of soils and various types of geotechnical problems like slope stability, excavation, foundation and tunnelling. Mohr-Coulomb model also provides a reasonable estimate for unloading problems like excavation. Hardening soil model is used for predicting the behaviour of sand, silt and clayey soil with reasonable accuracy. It is also used to predict the behaviour of foundations, excavations, embankments and other geotechnical problems.

Several researchers (Ou& Lai, 1994; Hsieh , 1999; Ou et al. 2000; Yoo& Lee, 2008; Hsiung, 2009; Usmani et al., 2010; Pan & Fu, 2012; Parkbaz et al., 2013; Khoiri and Ou, 2013; Zheng et al., 2014; Law et al., 2014, Hsiung et al., 2016; Bhatkar et al., 2017; Goh et al., 2017) have studied the excavation behaviour and computed ground surface settlements, wall displacements, earth pressure and bending moment distributions of walls using different soil models. In all these studies, a single constitutive model, either MC model or HS model, is used to define the stress-strain behaviour of the soil, and deep excavation behaviour in the virgin sites was computed. However, in multilayered sites, a combination of soil constitutive laws defining the stress-strain relation of various soil layers is essential to evaluate the

excavation behaviour. In addition, to evaluate the characteristics of deep excavation involved in engineered backfill soil, a proper soil constitutive model is to be identified. Various geotechnical investigations ranging from conventional borehole drilling to field and laboratory investigations are required to define the various parameters of constitutive laws describing stress-strain parameters. The current practice of geotechnical investigation carried out in Indian Nuclear industry sites is elaborated in the next section. Various parameters required to define stress-strain relation is evaluated from the investigations and addressed in Chapter 3.

Chapter 3

Site characterization for deep excavation analysis

General geotechnical investigation includes drilling of boreholes to identify the various soil layers and laboratory investigations like grain size analysis, shear tests and consolidation tests. In addition, results from field investigations like plate load tests, plate-bearing tests and advanced geotechnical investigations like pressuremeter tests are also required to define the parameters of various soil constitutive laws. In the present study, geotechnical characterization of a multi-layered soil site and engineered backfilling soil was carried out to identify the various parameters defining soil constitutive laws. Stiffness properties were established from the empirical correlations available between Standard Penetration Test (SPT N) values and Young's Modulus (E) of soil. Additionally, the stiffness properties of engineered backfill soil were experimentally established using plate load test, plate bearing test and pressuremeter tests.

3.1 The soil profile

As the part of siting of the facility, geotechnical investigation comprising drilling of 146 boreholes and laboratory investigation and field investigation was carried out at the site. The geotechnical investigation indicated that the site consists of loose to medium sand followed by dense sand. This sand layer is followed by silty /clayey sand and residual soil. Extensive seismic refraction survey was also conducted to determine the depth of bed rock. Hard rock is available at a depth of 15 to 20 m below the ground level at most of the area. Idealized soil profile is shown in Fig 3.1. The ranges of SPT N values for the different layers are also indicated in the same figure.

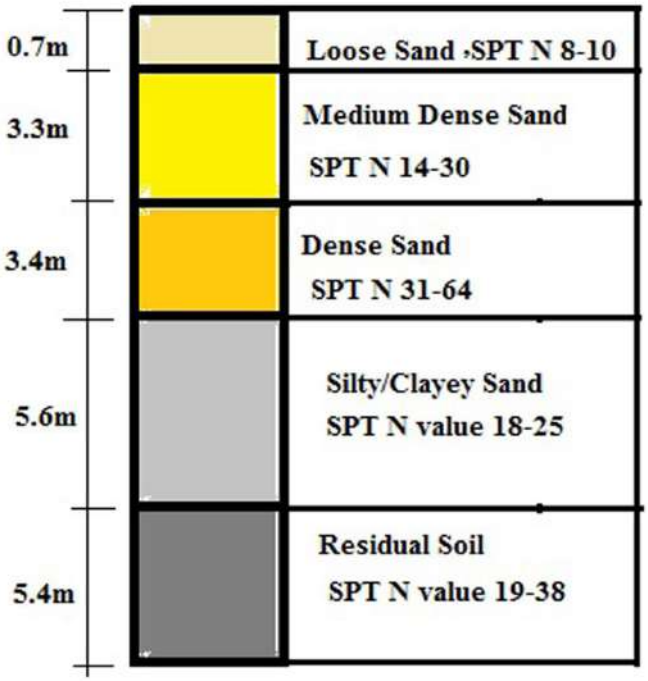

Fig 3.1 – Idealized soil profile

This idealized soil profile is arrived at by averaging the thickness of each layer encountered in each borehole and is used for the analysis of deep excavation carried out in the virgin site.

3.2 Strength properties of soil layers

The finite element analysis requires strength properties of various soil layers. In order to determine the strength properties of soil layers, various laboratory investigations namely Consolidated Undrained (CU) shear test for sandy layer and Consolidated Drained (CD) tests with Plasticity Index for Silty/ clayey sand and Residual soil were carried out . SPT N values are generally correlated with strength properties of soil material and hence site specific correlations were established for strength properties of soil, namely, Drained cohesion (C') and Drained angle of internal friction (ϕ') between SPT N values. In this analysis sand is considered as drained during the entire excavation process and accordingly drained

parameters are required for modelling. CU tests were carried out for sandy soil being simple and quick and it was intended to use the data from simple CU test to obtain the drained parameters of sandy soil from empirical correlations. As these empirical relations are developed using wide set of data these relations are generally found acceptable for obtaining drained parameters.

3.2.1 Consolidated Undrained (CU) Shear Test

Consolidated Undrained Shear Test (CU) is carried out on remoulded soil samples using 60 mm shear box in accordance with the methods specified in Indian Standard Method of Test for Soils IS:2720 -Part 13- Direct Shear test (2002). The shear box with the specimen, plain grid plate over the base plate at the bottom of the specimen, and plain grid plate at the top of the specimen is fitted into position in the load frame. The loading pad is then placed on the top grid plate. A normal stress is then applied and the rate of longitudinal displacement/shear stress application is adjusted so that no drainage occurs in the sample during the test. The test is conducted by applying horizontal shear load to failure or to 20 percent longitudinal displacement, whichever occurs first. The shear load readings indicated by the proving ring assembly and the corresponding longitudinal displacements are noted at regular intervals of displacement. The test is repeated for different normal stresses and plotted against corresponding shear stress. The slope of the relation between normal stress and shear stress provided undrained friction angle (ϕ). Further, SPT N values were corrected for standard 60% efficiency and then normalized to 1 atmosphere overburden stress.

Variation of undrained friction angle (ϕ) vs corrected SPT N value obtained from CU direct shear test carried out on loose to dense sand as the part of site characterization is given in Fig 3.2. The data used for generation of the predictive relation is given in Table 3.1. The linear relation between ϕ and SPT N also is indicated in same figure, which is given in Eq 3.1.

The predictive relation shows a correlation coefficient of 0.784 and can be used for obtaining undrained friction angle of various sandy soil found in similar geology.

$$\phi = 0.177 \times (N_{60})_1 + 28.02^{\circ} \quad \text{------- (3.1)}$$

Using these predictive relation undrained friction angle was estimated for sandy layer as 29.6, 32.46 and 34.9 respectively for loose, medium and dense sand which corresponds to average SPT N value of 9, 25 and 39 respectively.

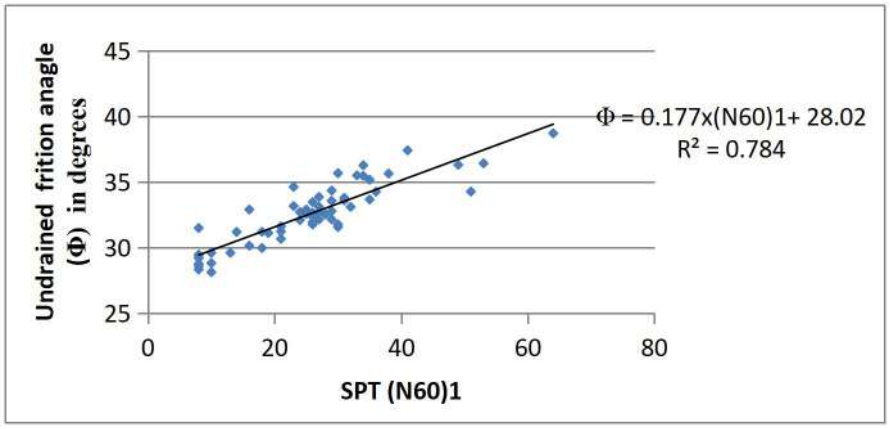

Fig 3.2: Variation of undrained friction angle vs corrected SPT N value from undrained direct shear test

The cohesion of sand layer is to be considered as zero for consolidated drained cases. The drained friction angle (ϕ') of loose, medium and dense sand is estimated using the equation proposed by Hatanaka & Uchida (1996) which is given in Eq: 3.2.

$$\phi' = [15.4 \times (N_{60})_1]^{0.5} + 20^{\circ} \quad \text{-------} \quad (3.2)$$

For SPT N value of 9, 25 and 39 corresponding drained friction angles are estimated as 32°, 39°and 44° respectively using Eq. 3.2.

Table 3.1: Undrained friction angle obtained from direct shear test for various sand layers and corresponding corrected SPT N values from bore holes

BH No	***Depth (m)***	***SPT N***	***N60***	***Effective Overburden Stress (kN/m^2)***	***Overburden correction***	***$(N60)_1$***	***Sand type***	***Φ°***
1T	0.5	6	4	8	1.6	10	Loose	28.83
1T	5	16	11	80	1.12	18	Medium	31.21
2T	1.5	19	13	24	1.6	30	Medium	31.57
2T	8.5	44	31	136	0.86	38	Dense	35.64
3T	9.5	29	21	152	0.81	23	Medium	33.17
4T	2	10	7	32	1.6	16	Medium	30.15
7T	6	48	34	96	1.02	49	Dense	36.31
8T	2	22	16	32	1.6	35	Medium	33.67
10T	0.5	13	9	8	1.6	21	Medium	31.24
11T	9.5	42	30	152	0.81	34	Dense	36.27
11T	14	46	33	224	0.67	31	Dense	33.8
20	2	12	9	32	1.6	19	Medium	31.12
22	6.5	37	26	104	0.98	36	Dense	34.26
23	3.5	20	14	56	1.34	27	Medium	33.87
28	5	57	40	80	1.12	64	Dense	38.71
32	0.5	6	4	8	1.6	10	Loose	28.14
34	0.5	5	4	8	1.6	8	Loose	29.47
42	3.5	18	13	56	1.34	24	Medium	32.71
44	2	16	11	32	1.6	26	Medium	31.77
44	5	23	16	80	1.12	26	Medium	32.65
46	8	34	24	128	0.88	30	Dense	31.78
47	12.5	22	16	200	0.71	16	Medium	32.9
48	0.5	6	4	8	1.6	10	Loose	29.61
50	0.5	5	4	8	1.6	8	Loose	29.41
51	3.5	19	13	56	1.34	25	Medium	32.91
53	12.5	41	29	200	0.71	29	Dense	34.35
55	3.5	23	16	56	1.34	31	Medium	33.6
59	2	16	11	32	1.6	26	Medium	31.95
60	2	18	13	32	1.6	29	Medium	32.78
61	0.5	9	6	8	1.6	14	Loose	31.2
63	5	47	33	80	1.12	53	Dense	36.42
68	0.5	5	4	8	1.6	8	Loose	29.21
69	0.5	8	6	8	1.6	13	Loose	29.61
69	6.5	42	30	104	0.98	41	Dense	37.41
70	2	13	9	32	1.6	21	Medium	31.62
72	3.5	20	14	56	1.34	27	Medium	32.68
74	2	17	12	32	1.6	27	Medium	32.15
77	6.5	34	24	104	0.98	33	Dense	35.51

BH No	*Depth (m)*	*SPT N*	*N60*	*Effective Overburden Stress (kN/m^2)*	*Overburden correction*	*$(N60)_1$*	*Sand type*	*Φ°*
79	3.5	18	13	56	1.34	24	Medium	32.11
77	9.5	29	21	152	0.81	23	Medium	34.63
84	6.5	31	22	104	0.98	30	Dense	35.67
88	0.5	5	4	8	1.6	8	Loose	28.34
88	6.5	27	19	104	0.98	26	Medium	32.37
90	5	24	17	80	1.12	27	Medium	33.11
100	3.5	21	15	56	1.34	28	Medium	32.54
101	3.5	19	13	56	1.34	25	Medium	32.58
108	2	11	8	32	1.6	18	Medium	29.98
109	3.5	24	17	56	1.34	32	Medium	33.11
112	5	23	16	80	1.12	26	Medium	33.47
113	0.5	5	4	8	1.6	8	Loose	31.5
115	5	30	21	80	1.12	34	Dense	35.47
116	0.5	5	4	8	1.6	8	Loose	28.61
118	2	13	9	32	1.6	21	Medium	30.67
120	3.5	22	16	56	1.34	29	Medium	33.57
127	2	18	13	32	1.6	29	Medium	32.16
131	0.5	5	4	8	1.6	8	Loose	28.78
133	6.5	36	26	104	0.98	35	Dense	35.17
145	2	32	23	32	1.6	51	Dense	34.27

3.2.2 Plasticity Index Test

Plasticity Index test is conducted as per Indian standard Method of test on soils IS 2720 part 5. A sample weighing about 20 g from the thoroughly mixed portion of the material passing 425-micron IS Sieve, is mixed thoroughly with distilled water in an evaporating dish or on the flat glass plate till the soil mass becomes plastic enough to be easily moulded with fingers. A ball is formed with about 8 g of this plastic soil mass and rolled between the fingers and the glass plate with just sufficient pressure to roll the mass into a thread of uniform diameter of 3 mm throughout its length. The soil is then kneaded together to a uniform mass and rolled again. This process of alternate rolling and kneading is continued until the thread crumbles under the pressure required for rolling and the soil can no longer be

rolled into a thread. The pieces of crumbled soil thread was collected in an air-tight container and the moisture content is determined as described in Indian Standard Method of Test on soil IS : 2720 Part 2. The corresponding moisture content in '%' is the Plasticity Index (PI) of the soil .

3.2.3 Consolidated Drained (CD) shear test

Characterization of silty/clayey sandlayer and residual soil layer was carried out using Consolidated Drained (CD) shear test results and described in the section. The Consolidated Drained (CD) shear test is carried out as per Indian Standard Method of test on soils IS: 2720 part 15. The shear box with sample and perforated grid plates and porous stones is used for simulating drainage condition. After application of incremental normal stress the sample is allowed to consolidate. After the successful completion of consolidation, the shear test is carried out at such a slow rate that at least 95 percent pore pressure dissipation occurs during the test. The test is repeated for different normal stresses and plotted against corresponding shear stress. Since continuous dewatering is in place during the entire period of excavation, consolidated drained test (CD) is performed for silty/clayey sand layers to obtain the drained parameters. The details of data points used for generating the relation for silty/clayey sand layer is shown in table 3.2.

Table 3.2 Drained Friction angle obtained from consolidated drained direct shear test for silty/clayey sand samples and corresponding Corrected SPT N values from bore holes

BH No	***Depth***	***SPT N***	***N60***	***Effective Overburden Stress***	***Overburden Correction***	***(N60)1***	***Dilatency Correction***	***PI***	***C (kPa)***	***Φ'***
50	8.45	23	16	57.52	1.32	21	18	20	17	30.2
50	12.95	43	30	89.875	1.05	32	24	22	56	35.6
51	9.95	28	20	68.305	1.21	24	20	20	27	30.5
68	8.45	23	16	57.52	1.32	21	18	18	18	30.35
74	8.45	23	16	57.52	1.32	21	18	25	55	31.8
84	9.95	30	21	68.305	1.21	25	20	22	38	31.9
118	8.45	36	26	57.52	1.32	34	25	20	26	32.6

BH No	*Depth*	*SPT N*	*N60*	*Effective Overburden Stress*	*Overburden Correction*	*(N60)1*	*Dilatency Correction*	*PI*	*C (kPa)*	*Φ'*
120	8.45	22	16	57.52	1.32	21	18	16	18	30.8
120	9.95	31	22	68.305	1.21	27	21	21	32	33.2
131	9.95	29	21	68.305	1.21	25	20	19	18	30.9

The slope of the relation between normal stress and shear stress provided drained friction angle (ϕ') and intercept of the 'y' axis provides drained cohesion (C'). Plasticity index determined according to section 3.2.2 is correlated with drained cohesion (C') in Fig 3.3. A linear correlation with a correlation coefficient of 0.716 is obtained for silty/clayeysandis given in Eq 3.3

$$C' = 5.095 * PI - 72.31 \text{ -----(3.3)}$$

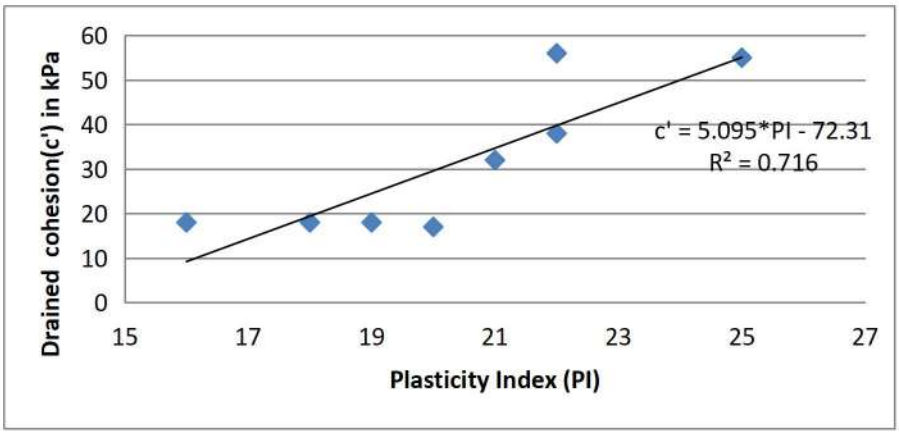

Fig 3.3 : Variation of drained cohesion vs Plasticity Index for silty/clayey sand layer

The predictive relation between drained friction angle and Plasticity Index shows a linear relation with a correlation coefficient of 0.716 and can be used for estimation of drained cohesion from PI for silty/clayeysand obtained from similar geology. The data points used for developing the predictive relations of residual soil between SPT N , PI and drained friction angle and drained cohesion is shown in Table 3.3.

Table 3.3: Drained Friction angle obtained from consolidated drained direct shear test of residual soil samples and corresponding corrected SPT N values from bore holes

SPT N	*N60*	*Effective Overburden Stress (kN/m^2)*	*Correction for overburden*	*(N60)1*	*Correction for dilatency*	*PI*	*C' (kPa)*	*ϕ'*
38	27	79.09	1.12	30	23	20	23	31.1
39	28	100.66	1	28	22	25	43	29.5
43	30	100.66	1	30	23	32	52	30.25
42	30	89.875	1.05	32	24	29	48	30.6
31	22	79.09	1.12	25	20	23	22	30.3
30	21	46.735	1.46	31	23	17	12	29.9
58	41	89.875	1.05	43	29	21	39	31.1
70	50	68.305	1.21	61	38	19	34	32.1
35	25	46.735	1.46	37	26	18	29	30.6
32	23	89.875	1.05	24	20	25	44	30.7
18	13	35.95	1.67	22	19	13	16	30.4
45	32	35.95	1.67	53	34	15	29	32.1

PI and Drained cohesion of residual soil were correlated and indicated in the Fig 3.4. A liner correlation is obtained with a correlation coefficient of 0.686 for residual soil too is given in Eq 3.4

$$C' = 1.668 * PI - 2.267 \text{ ----- (3.4)}$$

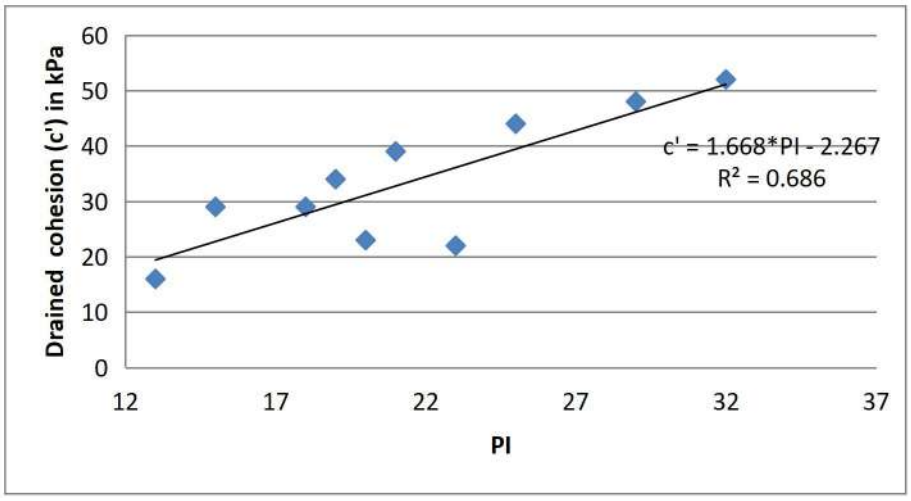

Fig 3.4 : Variation of drained cohesion vs Plasticity Index values for residual soil

Further, SPT N values were corrected for standard 60% hammer efficiency and then normalized to 1 atmosphere overburden stress. Consolidated drained cohesion (C') and drained friction angle (ϕ') were obtained from the relations established between Plasticity index and corrected SPT N values. These relations between SPT N value and drained friction angle for silty/clayey sand layer and residual soil obtained respectively from Fig 3.5 and 3.6 are given in Eq 3.5 and 3.6.

$$\phi = 0.779 \times (N_{60})_1 + 16.55 \text{ ------ (3.5) for Silty/Clayey sand soil}$$

$$\phi = 0.097 \times (N_{60})_1 + 28.42 \text{ -------- (3.6) for residual soil}$$

These empirical relations show a good correlation coefficient of 0.81 to 0.845 and hence can be used for estimation of strength properties of various soil layers.

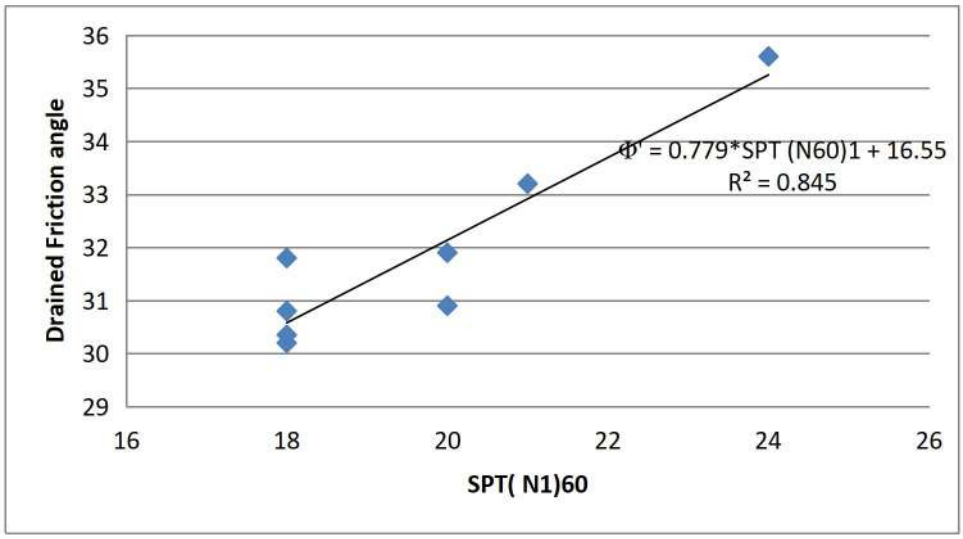

Fig 3.5 : Variation of drained friction angle vs Corrected SPT N values for silty/clayey sand layer

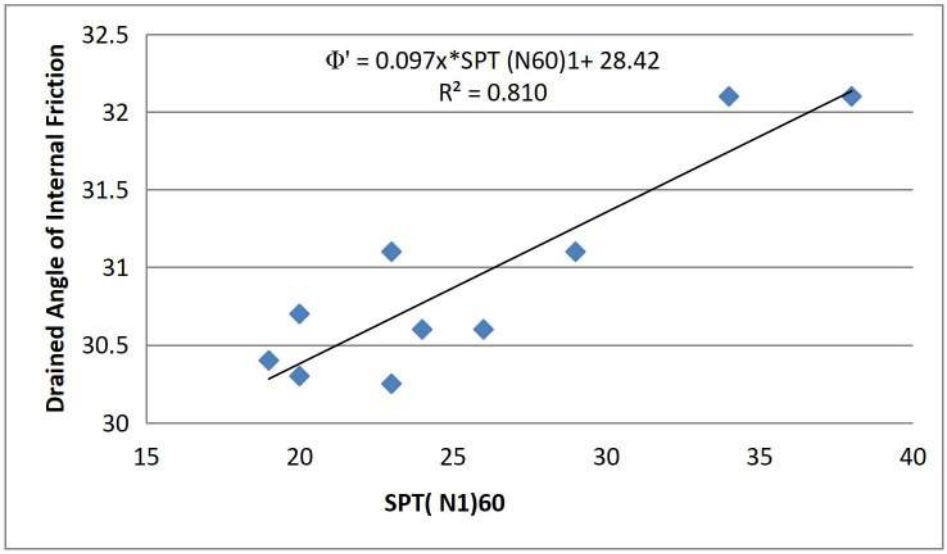

Fig 3.6: Variation of drained friction angle vs Corrected SPT N values for residual soil

3.3 Stiffness Properties of Soil layers

Young's Modulus (E) is the essential stiffness parameter required for defining the stress-strain property of soil mass. Various empirical relations are available in literature for describing the relation between E and SPT N values (Bowles, 1988; Kulhawy and Mayne, 1998). The E values obtained from these empirical relations show wide variations.

$$E = 500\ (N + 15) \text{ -------- (3.7)}$$

$$E = 300\ (N + 6) \quad \text{-------} \ (3.8)$$

$$E = 18000 + 750^{*}\ N \text{ -----} \quad (3.9)$$

Bowles, (1988); proposed three equations for various types of soil of these, Eq 3.7 is applicable for sandy soil in normally consolidated state and Eq 3.8 is proposed for silty sand while Eq 3.9 is applicable for over consolidated soil state which is used for residual soil encountered at the site, considering the overburden pressure over the residual soil encountered at the site.

Alternatively, stiffness of sand, silty/clayey sand layer and residual soil can be computed using the equations 3.10 to 3.12 proposed by Kulhawy&Mayne, 1998.

$$\frac{E}{P_a} = 10 * N \text{ --- } (3.10)$$

$$\frac{E}{P_a} = 5 * N \text{------} (3.11)$$

$$\frac{E}{P_a} = 15 * N \text{---- } (3.12)$$

where P_a is the atmospheric pressure and E is the stiffness.

Apart from the stiffness parameters required for Mohr-Coulomb Model, additional stiffness parameters like unloading stiffness (E_{ur}^{ref}) and tangent stiffness (E_{oed}^{ref}) required for HS model can be evaluated using the following relations proposed by Obrzud (2010).

$$E_{ur}^{ref} = 3 * E_{50}^{ref} \text{ ------ } (3.13)$$

$$E_{oed}^{ref} = E_{50}^{ref} / 1.25 \text{ ---- } (3.14)$$

Range of Young's Modulus *(E)* values for the design SPT N value is given in Table 3.4.

Table 3.4: Range of Young's Modulus for various soil layers

Layer	***Range of E (kPa)***
Loose sand	9000-12000
Medium Sand	21000-27000
Dense sand	31500-48000
Silty/Clayey Sand	8400-11040
Residual soil	39750-43500

3.4 Stiffness evaluation of engineered backfilled soil

As a part of future expansion, deep excavation needs to be carried out in engineered backfilled soil. Oedometer tests, field tests like plate load or plate bearing tests and in-situ tests such as pressuremeter tests are required to be conducted to evaluate the stiffness of engineered backfill soil. In the present study, oedometer tests were conducted on remoulded soil samples and the stiffness properties were obtained. In addition, plate load tests and plate bearing tests were carried out to determine stiffness of backfilled soil. However, considering the limitations of oedometer tests conducted on remoulded samples due to sample disturbance, and plate size effect in plate load test, pressuremeter tests were conducted on engineered backfill soil to determine the stiffness. Site specific relations were established between limit pressure (P_L) and pressuremeter modulus (E_P). The pressuremeter modulus is related to stiffness properties of soil and this was used for defining the stiffness of engineered backfilled soil. The stiffness of engineered backfilling obtained from various investigations are elaborated in the following sections.

3.4.1 Stiffness from oedometer test

Oedometer tests are the commonly used tests to evaluate the stiffness properties of soil. In the present study, already excavated material was used for backfilling and these excavated materials were remoulded and Oedometer tests were performed as per IS 2720 Part 15, Method of test for soil for consolidation properties. The properties of materials used for backfilling obtained from the excavation are also given in Table 3.5.

Table 3.5 – Properties of soil used for engineered backfilling

Property	***Value***
Dry unit weight (γ_{dry}) kN/m^3	18
Saturated unit weight (γ_{sat}) kN/m^3	20
Cohesion (C) kN/m^2	5
Angle of internal friction (ϕ) in Degree	30

Drainage is allowed through both top and bottom surfaces. Volume change after every stress application is recorded at intervals of 0, ½, 1, 4, 9, 16, 25, 36,49, 64 min; 1½, 2, 4, 8 and 24 hours. Initial specimen height is 18 mm in all the cases. Three samples were tested and applied pressure and strain noted for all the three samples are shown in Tables 3.6 to 3.8 .

Log scale plotting is generally adopted for sedimentary soils for obtaining pre consolidation pressure. Wesley (1983), Pender et al, (2000) employed linear scales for presenting oedometer data of residual soil. Since the present site consists of silty/clayey sand layer which is residual in nature , linear scale is adopted for presenting oedometer data.

Table 3.6 – Stress –strain values obtained from Oedometer test for sample 1

Applied pressure (kN/sq:m)	***Settlement "mm"***	***Strain***
0	0	0
10	0.02	0.001111
20	0.144	0.008
50	0.61	0.033889
100	1.004	0.055778
200	1.54	0.085556
400	2.278	0.126556
800	3.354	0.186333
50	3.068	0.170444
20	2.736	0.152

Table 3.7– Stress –strain values obtained from oedometer test for sample 2

Applied pressure (kN/sq:m)	***Settlement "mm"***	***Strain***
0	0	0
10	0.044	0.002444
20	0.15	0.008333
50	0.318	0.017667
100	0.942	0.052333
200	1.396	0.077556
400	1.72	0.095556
800	2.214	0.123
50	2.044	0.113556
20	2.004	0.111333

Table 3.8 – Stress –strain values obtained from oedometer test for sample 3

Applied pressure (kN/sq:m)	***Settlement "mm"***	***Strain***
0	0	0
10	0.01	0.000549
20	0.102	0.005604
50	0.44	0.024176
100	0.896	0.049231
200	1.708	0.093846
400	2.028	0.111429
800	3.254	0.178791
50	3.078	0.169121
20	2.99	0.164286

In the present case, since pre consolidation pressure is not essential to get Young's Modulus from oedometer, linear scale is used. Stress -strain curve obtained from oedometer test for all the samples is show in Fig 3. 7 (a-c) .

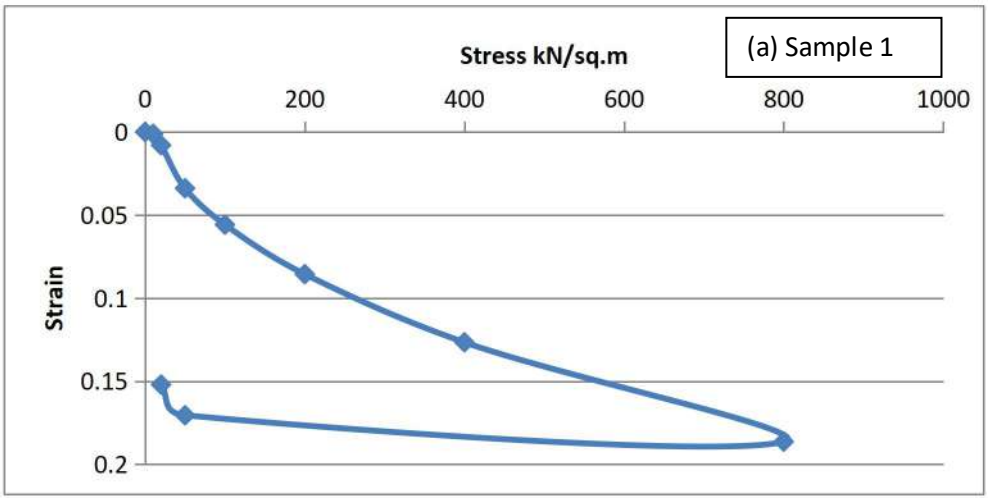

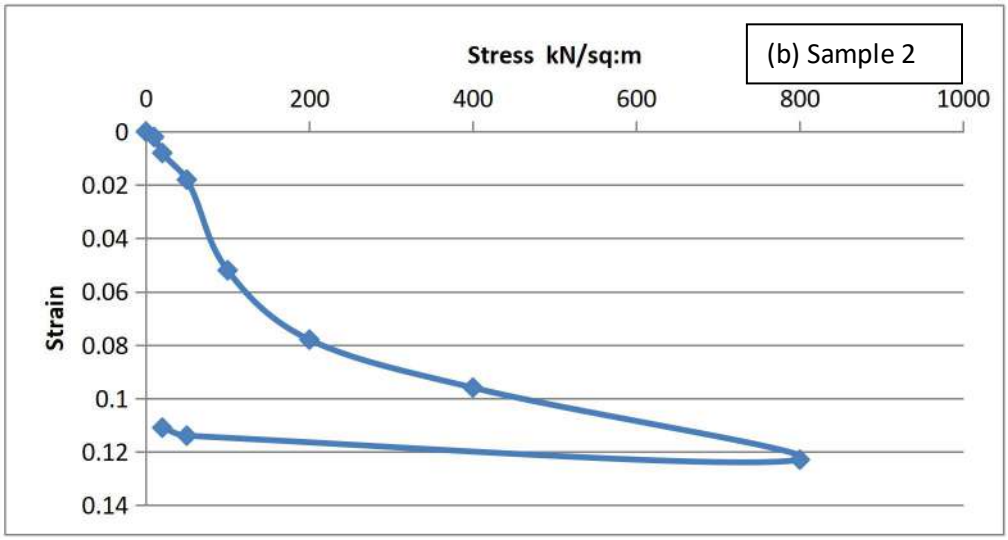

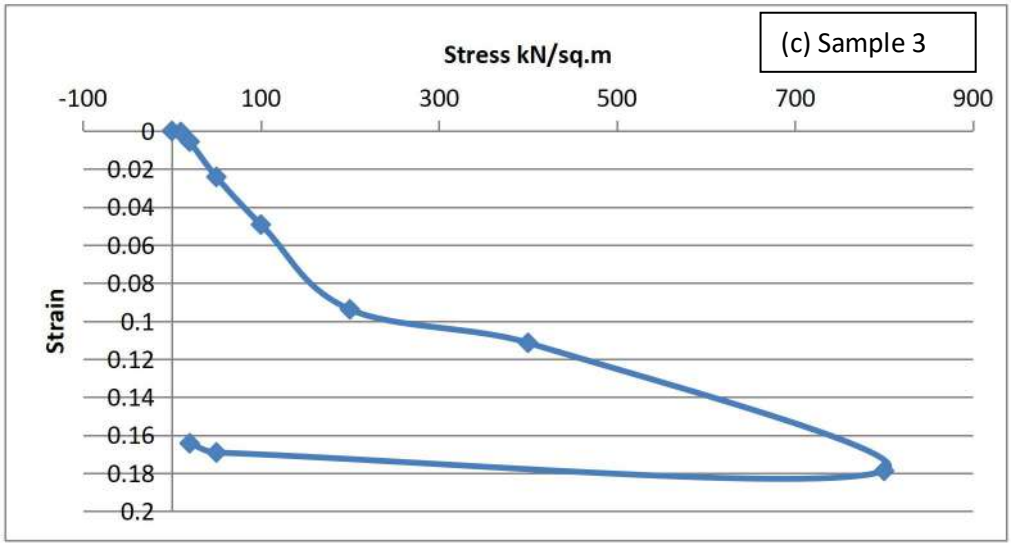

Fig 3.7 Stress – Strain relation from Oedometer test (a) Sample 1 (b) Sample 2 (c) Sample 3

The oedometer based stiffness obtained for samples 1,2 and 3 are 2500 kN/m^2, 3000 kN/m^2 and 1560 kN/m^2 respectively. The stiffness values were obtained from the slope of the linear portion of the Stress-Strain graph from Oedometer stiffness. These stiffness values are applicable for the stress range of 0 to 400 kN/m^2. Since Undisturbed soil samples were not available, soil samples were remoulded to the field density and Oedometer tests were conducted on this remoulded soil samples. This may be one reason for greater settlement at small stress and lower settlement at higher stress.

3.4.2 Stiffness from plate load and plate bearing tests

Field plate load test was carried out in engineered backfilled soil as per Indian Standard IS 1888, Method of Load Test on Soils. 600 mm x 600 mm plate is used for carrying out the test. Pressure is applied through ram, and settlement was observed for applied pressure. Load settlement graph obtained from Plate load test is shown in Fig 3.8.

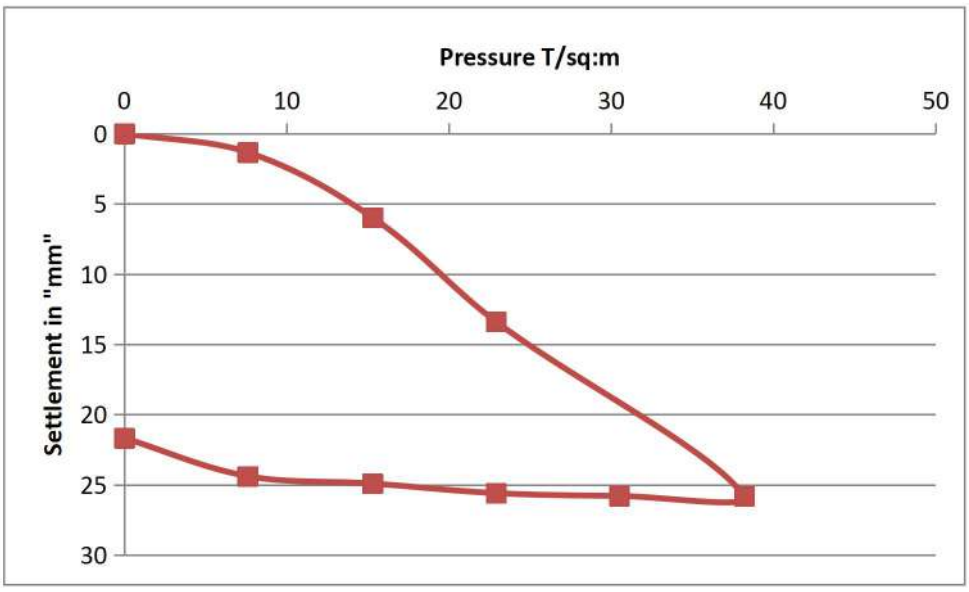

Fig 3.8 – Load settlement graph from Plate load test

An initial settlement (δ) of 1.33 mm corresponding to a pressure of 7.6 t/m^2 under the plate of 0.6m x 0.6m was obtained .Stiffness parameters were determined from theory of elasticity using Eq 3.15.

$$\delta = c_d * q * B * \frac{1-\upsilon^2}{E} \text{ --------- (3.15)}$$

where δ = Settlement in m.

c_d = Correction factor 0.95

q = Load intensity 7.6 t/m^2

υ = Poisson Ratio (0.2)

B= Width of the plate

The Young's modulus obtained from the relation is 33000kN/m^2.

3.4.3 Stiffness from plate bearing test

Alternatively, Young's modulus (E) can also be determined from plate bearing tests. In the present site, plate bearing was also conducted as per IS:1888, Method of Load tests on soils to evaluate the stiffness parameters of engineering backfill soil. The deflection of plate and plate pressure are plotted and shown in Fig 3.9.

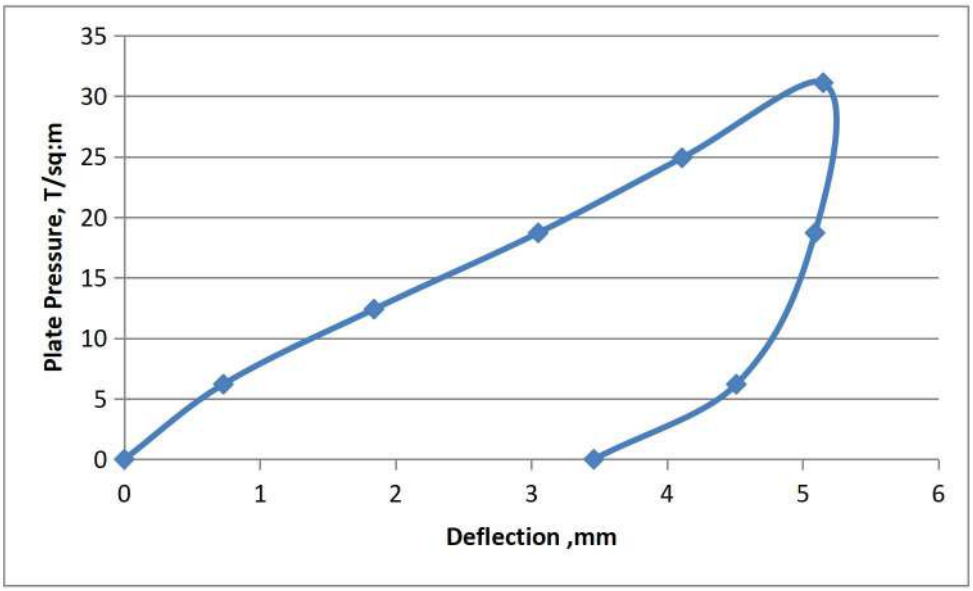

Fig 3.9 : Plate bearing test : Variation of plate pressure against deflection

From Fig 3.9, the Plate pressure corresponding to 1.25 mm settlement is calculated and modulus of sub grade reaction (k_s) is then estimated as 6 kg/cm^2/cm from the plate bearing test. From theory of elasticity, solution for a rigid plate on a semi-infinite elastic soil medium subjected to a concentrated load (Timoshenko and Goodier, 1951) indicated that the modulus of sub-grade reaction, ks, can be expressed using the following expression Eq. 3.16

$$k_s = 1.13 * \frac{E}{1-v^2} * \frac{1}{\sqrt{A}} \qquad \text{---------- (3.16)}$$

where k_s is Modulus of Subgrade Reaction

v = Poission's ratio (0.2)

A = Area of plate 0.442 m^2

The E value obtained from eq 3.16 is 33800kN/m^2. Thus, the E values obtained from different tests as discussed above varies widely from a value 8000 kN/m^2 to 33800 kN/m^2 with an average value of 25000 kN/m^2.

3.4.4 Stiffness from Pressuremeter Test

Pressuremeter tests were carried out to determine the field stiffness of backfilled soil as per ASTM D 4719 Standard Test Methods for Pre bored pressuremeter test in soils. The aim of the test was to determine the insitu deformation modulus of soil using an expanding probe that exerts pressure on the wall of a drill hole. The resulting diametric hole expansion is determined from measurements of the volumetric expansion of the probe. Deformability characterstics of the soil are then calculated from the relation between pressure and dilation. NX size bore hole is first drilled to the desired depth and casing is provided to protect the side of the bore holes. Calibrated probe is then placed at test location and then pressure is applied in equal increments of 0.5 MPa. At each load increment the pressure is held constant for a

period of 60 s. Application of pressure increment is continued upto failure point or maximum specified pressure of 180 MPa and then unloaded. The limit pressure is defined as the maximum pressure where no further increase in the pressure is observed with increase in the deformation reading. The plots of test pocket radius against the pressure obtained form pressuremeter test data for all the four locations are presented in Fig 3.10.

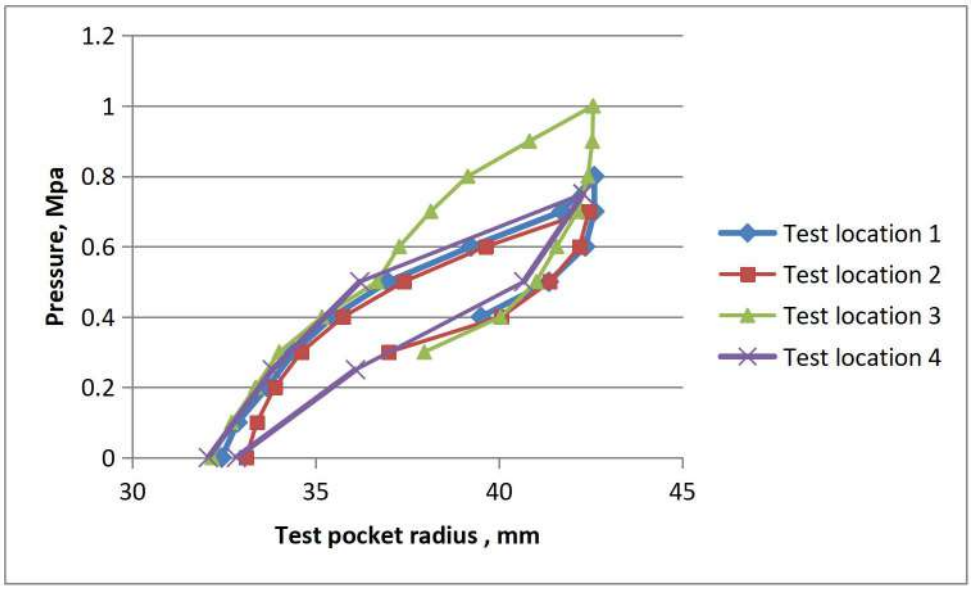

Fig 3.10 – Relation between Test pocket radius and Pressure from Pressuremeter Test

The pressuremeter modulus (E_p) provides a direct correlation for the horizontal modulus of the soil and is related empirically to the Young's modulus (E) of the soil as $E_p/E = \alpha$, (Menard, 1975), where α is the rheological coefficient and has a value between 0 and 1 (Baguelin et al., 1978). For the present case, α is considered to be 0.3. A series of pressure meter tests were carried out on the engineering backfilled soil at an adjacent site where backfill was carried out using the same material and with the same compaction specification with an objective to determine the deformation modulus of soil. Hole expansion is then determined from measurement of volumetric expansion of the probe. Application of pressure increment was carried up to failure point which corresponds to limit pressure (P_L). Pressure

meter modulus is then determined using relation 3.17 between Pressure interval *(ΔP)*, Radius interval (*ΔR*) , Poisson's Ratio (υ) and intermediate Radius (R_{av}).

$$E_p = (1 + v) * R_{av} * (\frac{\Delta P}{\Delta R}) \text{ -- -----(3.17)}$$

The Limit pressure and Pressuremeter Modulus (E_p) is tabulated in Table 3.9.

Table 3.9 – Limit pressure and Pressuremeter Modulus at various locations

Area	***Limit Pressure (kPa)***	***Pressuremeter Modulus***
Location 1	7	18.2
Location 2	7.5	27.0
Location 3	8	28.2
Location 4	10	37.4

From the field obtained data a site-specific relation between the limit pressure (P_L) and the Pressure meter modulus (E_p) was established (Fig 3.11) as eq 3.18 with a correlation coefficient of 0.926 which can be used for determination of stiffness properties of backfilled soil.

$$Ep = 6.397 * P_L - 23.75 \text{ ------- } (3.18)$$

The limit pressure obtained shows a variation ranging from 0.7 MPa to 1 MPa and this order of limit pressure obtained matches well with that of silty soils and old fills (Gambin M.P. & Rousseau, J 1988). Considering this, the correlation is used for determining the Pressuremeter Modulus of engineered backfilled soil.

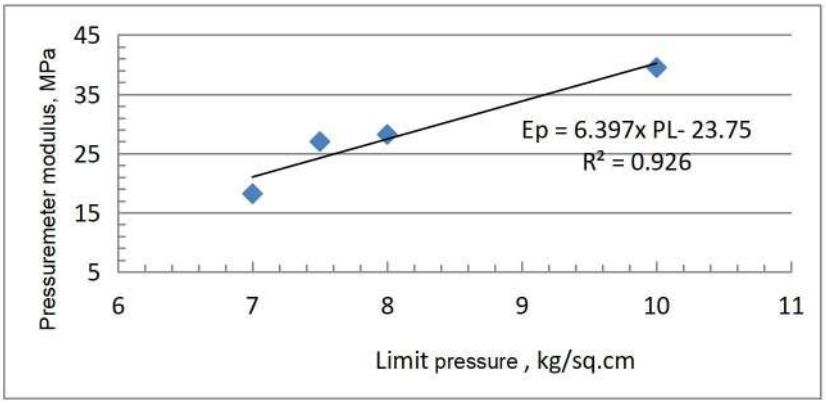

Fig 3.11: Correlation between Limit Pressure and Pressuremeter Modulus

A correlation was developed to obtain and average value of limit pressure and to obtain the pressuremeter modulus. Considering an average P_L value of 8 kg/cm^2, the site specific pressuremeter modulus is 27 kg/cm^2 using eq 3.18 and the corresponding modulus of elasticity is 8000kN/m^2 from the equation proposed by (Menard, 1975).

The stiffness of engineered backfilled soil evaluated from various methods shows wide variation. Stiffness estimated from oedometer is the lowest, which is attributable to sample disturbance while that obtained from plate load and plate bearing tests are higher owing to plate size effect. Since the Oedometer test is conducted on samples collected from engineered backfilled soil and then remoulded to the same density and water content. Sample disturbance can besignificant .Pressuremeter test provides intermediate reasonable values and hence used for predicting the behaviour of deep excavation carried out in engineered backfilled soil.

Chapter 4

Performance of open excavation in a multi layered virgin site

4.1 Definition of the problem

An open excavation of 15-20 m deep was carried out as a part of construction of a nuclear facility. The area of open excavation is around 500 m x 300 m at bottom and 600m x 400 m at top. This type of excavation is massive and involves removal of around 3 x 10^6 m^3 of soil. Based on the safety guidelines provided in AERB SG CSE 2 (2008) and IAEA NS-G-3.6 (2004), stable slopes of 1 V: 2 H for sandy soil and 1 V: 1 H for residual soil were provided. Intermediate berms of 2.0 m width are also provided after every 3.5 m of excavation to facilitate manual movement and erection of dewatering pipes. The width of the excavation is 49.0 m and the depth of excavation is 18.4 m.

The entire excavation of the site was carried out in eight stages; (i) top loose sand layer up to a depth of 0.7 m (ii) to 3.5 m (iii) to 4.0 m and creation of first berm (iv) to 7.0 m (v) to 7.3 m and creation of second berm (vi) to 10.5 m and creation of third berm (vii) to 12.9 m and creation of third berm (viii) to 18.4 m. Initial ground water at 2.0 m below the ground level was lowered to 10.0 m, 15.0 m and 18.3 m after 3rd, 5th and 7th stages of excavation respectively. Multistage well point dewatering system was employed to lower the ground water during each stage of the excavation.

Conventional slope stability analysis indicated a factor of safety of 1.51 to 1.56, which is higher than required factor of safety 1.3 as per guidelines of AERB. Idealized excavation plan and typical section is shown in Fig 4.1.

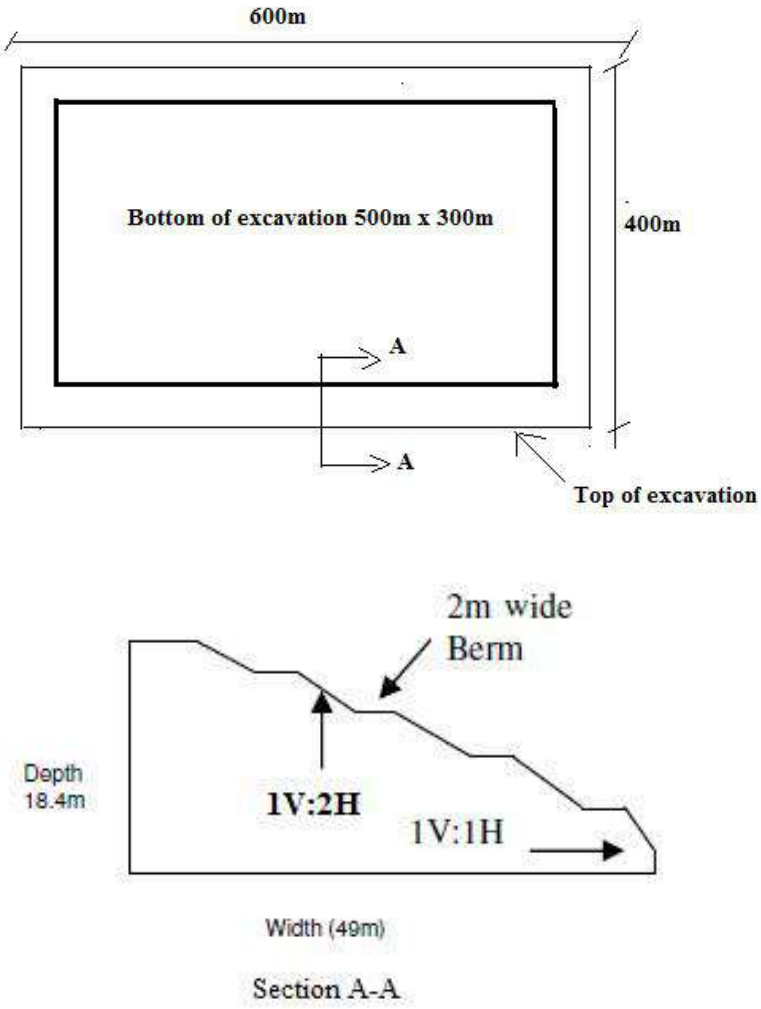

Fig 4.1 Idealized excavation plan and section

(Fig not to scale & Stage of excavation not shows for clarity)

Photographs of excavated profile are presented in Fig 4 .2 and 4.3

Fig 4.2 Excavation profile

Fig 4.3 Formed Excavation profile

4.2 Field instrumentation programme

Field instruments have been effectively used by various researchers to monitor the performance of supported deep excavations, stability of structures adjacent to ongoing infrastructure activities like tunnelling etc. These include inclinometers, settlement monitors, tilt meters, vibration wire gauge, piezometers etc. Various reserchers Nikolinakou (2011), Gorska (2012), Becker (2013), Hsiung (2014), Whittle (2015), Hsiung et al. (2016) used the data from field instrumentation not only to monitor the performance of deep excavation but also to calibrate the numerical model parameters using back calculations. In the present study, inclinometers and settlement monitors were deployed to monitor the performance of conventionally designed slope.

Even though field monitoring of supported excavation system is widely in place, conventionally designed slopes are seldom monitored for its performance. Also, current practice in Indian nuclear industry is to provide a conservative stable slope arrived at from classical slope stability analysis. However, considering the safety critical nature of important structures near the excavation, field instrumentation has been proposed for monitoring the performance of deep excavation so as to ensure the stability of slopes during the period of excavation and construction at this nuclear facility site. This would also enable adopting appropriate corrective actions if required.

As a part of slope stability monitoring, four inclinometers (Model SME 2190 make) were provided at 5.0 m away from battery limit locations of open excavation. Inclinometers were designated as I1, I2, I3 and I4 and the relative locations of the inclinometers with reference to the overall excavation size are indicated in Fig 4.4. The termination depth of these inclinometers is 20 m, which is hard rock. This inclinometer system is used for

monitoring lateral movement of slopes during excavation in order to assess the requirement of any corrective measures and their timings, and to assess the stability of the slopes. The probe consists of two precision accelerometers, which sense the inclination of the access tube in two planes at right angle to each other.

4.2.1 Installation of inclinometers

Standard practices described by Dunnicliff (1993), Mikkelsen (1996, 2003) and Cornforth (2005) were used for installation of inclinometers. 125 mm diameter holes were drilled using rotary wash boring technique up to 30 m depth below the existing ground levels. PVC casings were provided and bentonite slurry was used to prevent the collapse of side wall and to protect the side walls of bore holes. The casing is also provided with a bottom cap and safety clamps. One pair of grooves was provided perpendicular to the direction in which the lateral movement of soil needs to be measured. The casing is grouted using cement, bentonite and water and the compressive strength of the grout is around 700 kPa to ensure that the assembly itself does not move. The casing is flushed with water after grouting to prevent any leaked grout sticking to the case which will obstruct the movement of sensor. Top of the casing is kept at a level of 150 mm below the ground and protected by a top cap and lockable cover. Grooves were marked in casing as A+, A- , B+ and B - where A+ is pointed in direction of the major principal plane of movement and B+, A- and B- are marked clockwise from A+. The locations of the inclinometer assembly, its distance fromthe excavation edgeand read out unit are shown in Fig 4. 4 and 4.5 . Final assembly of inclinometer at location I2 is given in Fig 4. 6.

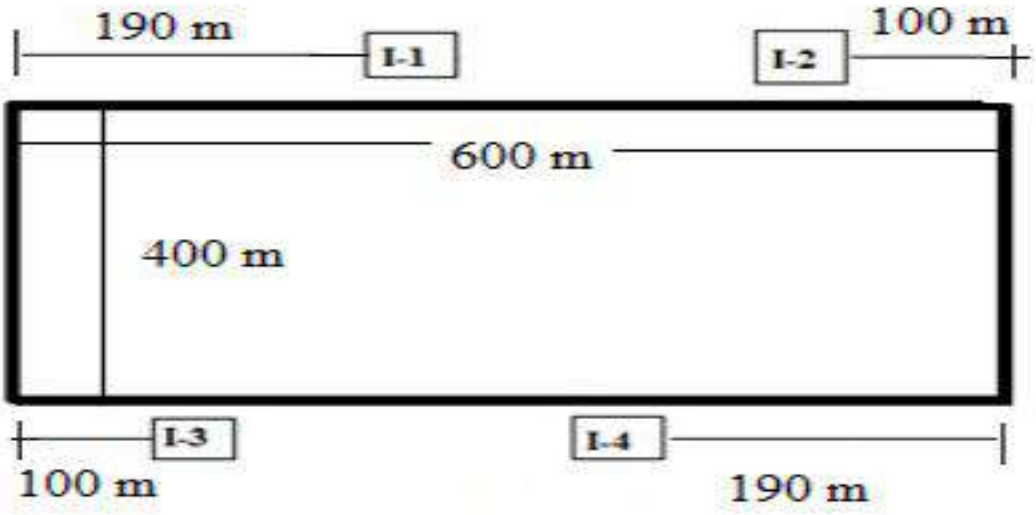

Fig 4.4 –Schematic diagram indicating inclinometer locations

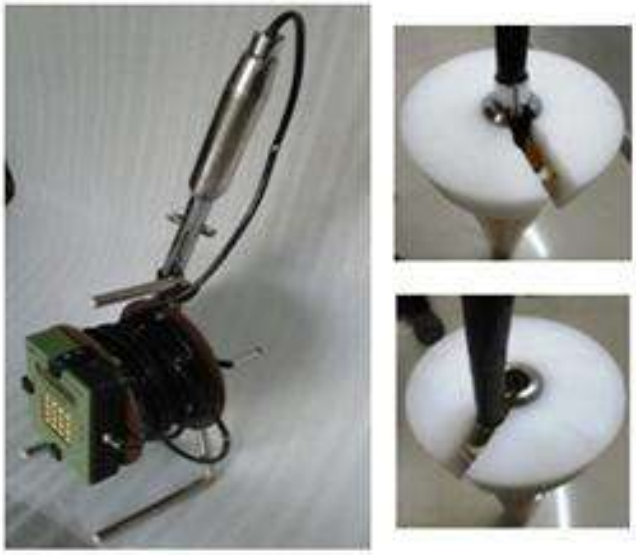

Fig 4. 5: Inclinometer sensor and readout unit with hole and guide assembly

Fig 4.6: Assembly of inclinometer and read out unit at location I2.

4. 2.2 Data measurement and Interpretation

The sensor located in the probe senses the inclination of the probe. A set of initial base readings taken within the gage well form the reference datum. All subsequent readings are taken at identical depth intervals, thereby indicating rate, magnitude, and direction of lateral deformation. The inclinometer probe is then lowered to the bottom of the gage well with uppermost torpedo wheel pointing to direction marked A+ and then is raised along entire length of bore holes from bottom to top taking readings at intervals of 0.5 m. This sequence is repeated with the torpedo wheel pointing in direction A-. Results of these two sets of measurements are then averaged to reduce the error and to account for the sensitivity of the probes. The inclinometer measures the tilt, which is then converted in to displacement according to the theoretical aspects of tilt measurement described in Wilson and Mikkelsen (1977) and Dunnicliff (1988). The basic principle involves measuring tilt, an angle, and the hypotenuse of a right angle, which is the measuring interval. If θ_i is the tilt angle for i^{th} measurement and L_i is the measuring interval, then displacement is given by the following equation

$d_i = L_i \text{ Sin } \theta_i$ ---------- (4.1)

The summation of all d_i gives the total displacement. The principle of displacement measurement and cumulative displacement is indicated in Fig 4.7 & Fig 4.8 respectively.

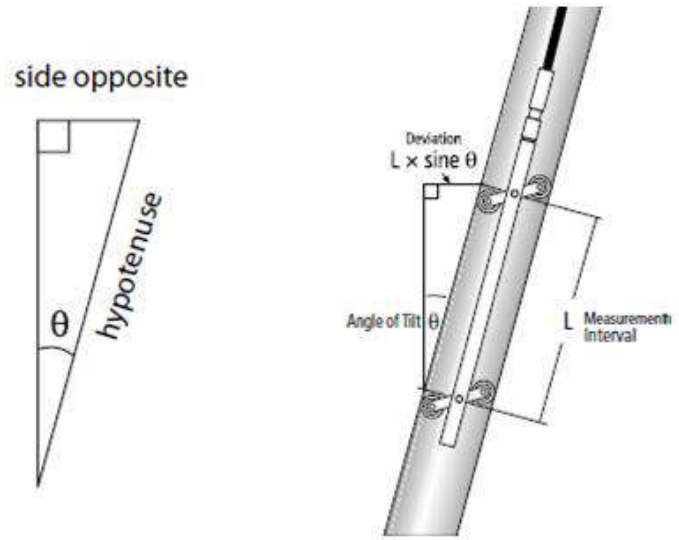

Fig 4.7 – Principle of displacement measurement

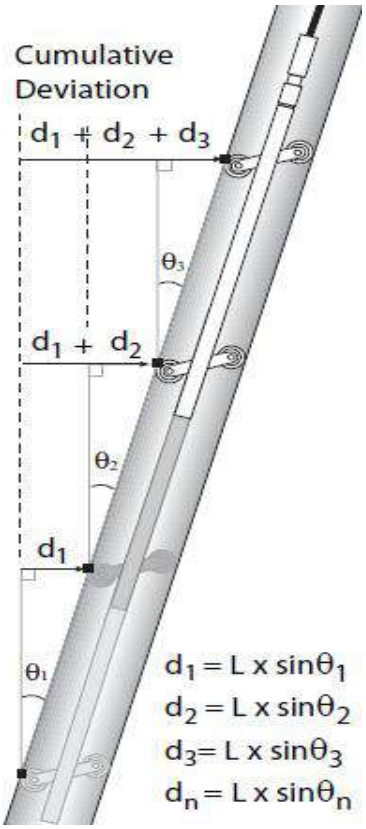

Fig 4.8 – Cumulative deviation from inclinometer

By summing and plotting the deviation values obtained at each measurement interval the displaced profile of the casing is obtained.

4.3 Numerical analysis of the problem

This staged excavation problem defined in section 4.2 was idealized as a plane strain case considering the length of the excavation and analyzed using finite element method in PLAXIS software. 15 node triangular elements provided in the software were used for discretization of the soil volume. Since the thickness of different soil layers are different, mesh size is not uniform and typical mesh distribution at the end of excavation is given in Fig 4.9. The excavation slope and the location of inclinometer is also indicated in the fig. Total number of elements in the numerical model is 253.

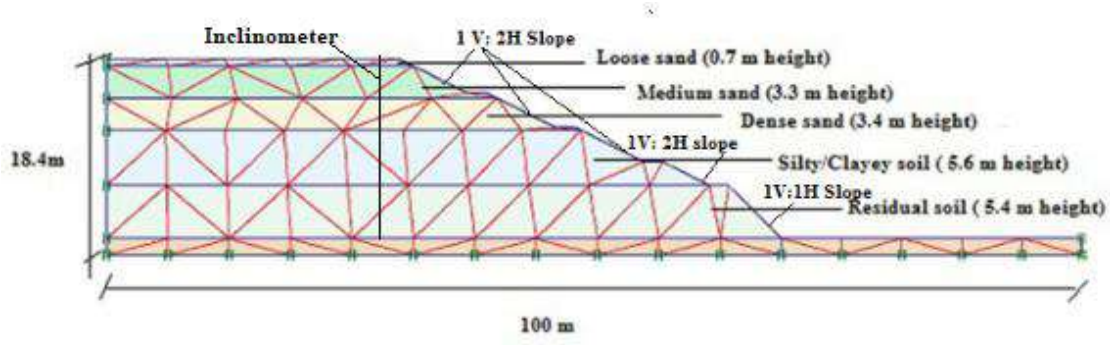

Fig 4.9 : Finite Element Mesh along with soil layers

Standard fixities were adopted for the model boundary where vertical geometry line in the model is assumed with a horizontal fixity and horizontal geometry line in the model is assumed with a total fixity. Finite element analysis was carried out using 12 Point Gauss Integration method and the interaction between different soil layers were ignored in the analysis. Generallythe boundary of the model from the excavation zone is considered as 4 times the depth of excavation for retaining wall cases. However, considering the open

excavation scenario, the boundary was assumed at 1.5 times the excavation depth in the present analysis.

4.3.1 Properties of the soil defining the soil constitutive laws

Strength and stiffness properties of various soil layers estimated as described in Chapter 3 were used for the numerical analysis of the excavation. Design SPT N values were considered and existing empirical relations between SPT N values and Young's Modulus proposed by Bowles (1988), Kulhawy& Mayne (1998) were considered for estimating Young's Modulus of various layers encountered at the site. Young's Modulus (Secant Modulus) obtained from these empirical relations shows a wide range of values as given in Table 4.1. Conservatively, the lower bound value computed was used in numerical analysis. Apart from the stiffness parameters required for MC Model, unloading stiffness (E_{ur}^{ref}) and tangent stiffness (E_{oed}^{ref}) parameters required for HS model were evaluated using the relations defined in Chapter 3.

Table 4.1: Young's Modulus of different soil layers obtained from SPT N values using empirical relations (Bowles 1988, Kulhave & Mayne 1998)

Layer	***Design SPT N value***	***Range of Young's Modulus (kPa)***	***Design Young's Modulus (kPa)***
Loose sand	9	12000-48300	12000
Medium sand	27	21000-72500	21000
Dense sand	48	31500-85100	31500
Silty/ clayey sand	22	8400-11800	8400
Residual soil	29	39750-70450	39750

The fact that Young's Modulus increases with increase in confining pressure is accounted for in MC Model using the method proposed by Janbu (2011). In general, soil

shows an increase in stiffness properties with depth. In order to account for this, an increment value (E_{inc}) needs to be defined in PLAXIS which is obtained from the formulation of Janbu (2011). In addition, the effect of dilatency (ψ) of sandy soil is seldom studied in deep excavation behaviour. Since the site in the present study consists of loose to dense sand layer at top, dilatency (ψ) is also considered in MC Model. The dilatency of sandy layer is estimated using the formulation proposed by Bolton (1986) for quartz sands.

$$\Psi = \Phi - 30° \text{ for } \Phi > 30° \quad \text{------ Eq: 4.2}$$

$$= 0 \text{ for } \Phi < 30°$$

The parameters for numerical analysis of MC and HS Model are given in Table 4.2.

Table 4.2: Parameters of MC and HS Model for Numerical analysis

Parameter	***Loose Sand***	***Medium Sand***	***Dense Sand***	***Silty/Clayey Sand***	***Residual soil***
Dry density (γ_{dry}) kN/m^3	16	16	18	18	18
Saturated density (γ_{sat}) kN/m^3	19.68	19.68	20.88	20.88	20.88
Secant stiffness (E_{50}^{ref}) kN/m^2	12000	21000	31500	8400	39750
Tangent stiffness (E_{oed}^{ref}) kN/m^2	9600	16800	25200	6720	31800
Unloading - reloading stiffness (E_{ur}^{ref}) kN/m^2	36000	63000	94500	25200	119250
Poisson's Ratio (υ)	0.37	0.32	0.32	-	-
Unloading - reloading Poisson's Ratio (υ_{ur})	-	-	-	0.32	0.2
Power for stress level dependency (m)	-	-	-	0.5	0.5
Dilatency (Ψ°)	1°	3°	5°	-	-
Increase in Stiffness , E_{inc}(kN/m^2/m)	1900	2800	2800	-	-

Other engineering parameters of the soil, such as angle of internal friction (ϕ) and cohesion (C) were estimated using the site specific relations established between SPT N

values described in Chapter 3. This SPT N value was used for estimating the undrained (ϕ_u) friction angle of sandy layer using correlations of Peck (1977) and the drained friction angle is then evaluated using the correlation proposed by Hatanaka & Uchida (1996). Laboratory investigations were carried out for estimating drained cohesion (C_d) and friction angle (ϕ_d) of silty/clayey sand and residual soil layer as described in Chapter 3. The results are presented in Table 4.3 . Drained strength parameters shown in Table 4.3were used in analysis. However, since drained tests were not conducted in sand, these parameters were obtained using empirical formulations eloborated in Section3.2.1 using data obtained from Undrained tests . Drained cohesion was assumed as zero for sandy layer and the values obtained from drained shear tests were used for silty/clayey sand and residual soil.

Table 4.3 : Engineering properties of various soil layer

Layer	***Design SPT N value***	***Drained Cohesion (kPa)*** C_d	***Drained angle of internal friction*** ϕ_d ***(°)***	***Undrained angle of internal friction*** ϕ_u***(°)***
Loose Sand	9	0	32	30
Medium Sand	27	0	40	35
Dense Sand	48	0	45	41
Silty/clayey Sand	22	29	32	-
Residual Soil	29	31	31	-

4.3.2 Cases of analysis

Sequential drained analysis was carried out for predicting the behaviour of open excavation using the strength and stiffness properties defined. Since continuous multi stage well point dewatering system was established for dewatering, and water table was lowered before each stage of excavation, the drained parameters were considered for all the soil layers. Initial stress values were generated using K_0 procedure where K_0 is the coefficient of

earth pressure at rest. The following analyses were carried out to predict the behaviour of open excavation.

(i) Case (a) assuming MC model for the entire soil layer

(ii) Case (b) assuming MC Model for sand layer and HS Model for silty/clayey sand layer and residual soil

(iii) Case (c) accounting for incremental increase of stiffness with depth and dilatency of sand layer in MC Model along with HS Model for silty/clayey sand layer and residual soil.

4.3.2.1 Case (a) MC model for soil layers

Surface heaves were observed at the bottom of excavation and settlements were observed behind the excavation during the initial phase. Typical plots of computed vertical displacement at the end of 1st, 3rd , 5th,7th and final stages of excavation are shown in the Fig 4.10 (a-e). Surface heave of 10.8 mm was observed upon completion of first stage which increased to 53.26 mm upon completion of third stage of excavation. However, the settlement of 7mm behind the excavation at the end of first stage reduced to 1.2 mm at the end of third stage.

Settlement behind excavation increases considerably with further increase in the depth of excavation and at the end of 5th stage, the settlement computed is 26 mm at a distance of 13.7 m. At the end of 7th stage of excavation, the settlement computed is 34.6 mm at a distance of 14.1 m. At the end of excavation, the settlement computed is 36.7 mm which occurs at a distance of 15.8 m. Maximum surface heave was observed at the end of 5th stage is 70 mm. Surface heave at the bottom of excavation subsequently reduces to 20 mm at the end of 7th stage. However, the location of the maximum vertical displacement shifts towards third bench during 7th stage of excavation. The maximum vertical displacement is 62.51 mm

at the face of excavation and this vertical displacement reduced to 60.3 mm at the end. The vertical displacement computed behind the excavation at various phases is given in Table 4.4.

Table 4.4 : Computed vertical settlement at the end of each stage of excavation (Case a)

Stage	*Maximum Vertical settlement (mm)*
Stage1	10.8
Stage 3	53.26
Stage 5	69.99
Stage 7	62.52
Last stage	60.35

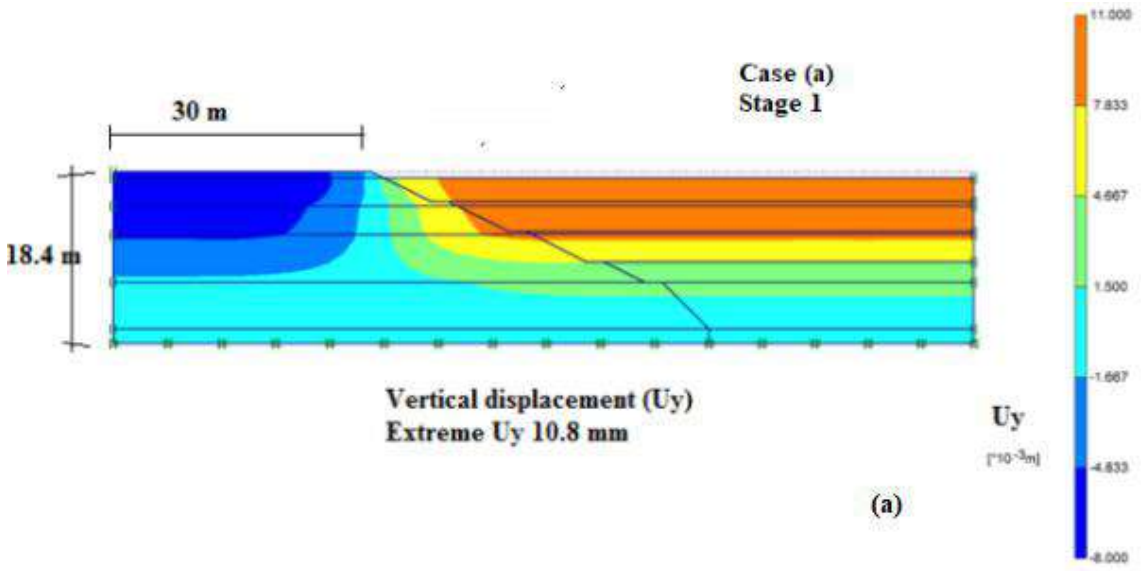

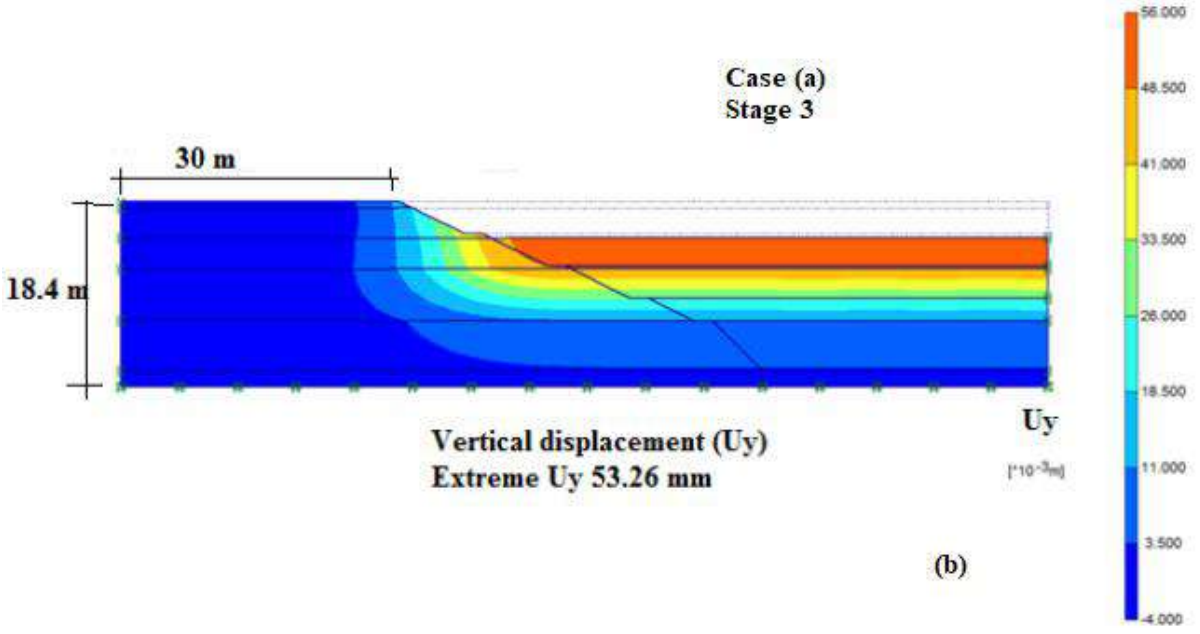
Case (a)
Stage 3
30 m
18.4 m
Vertical displacement (Uy)
Extreme Uy 53.26 mm
Uy
[*10^-3m]
56.000
48.500
41.000
33.500
26.000
18.500
11.000
3.500
-4.000

(b)

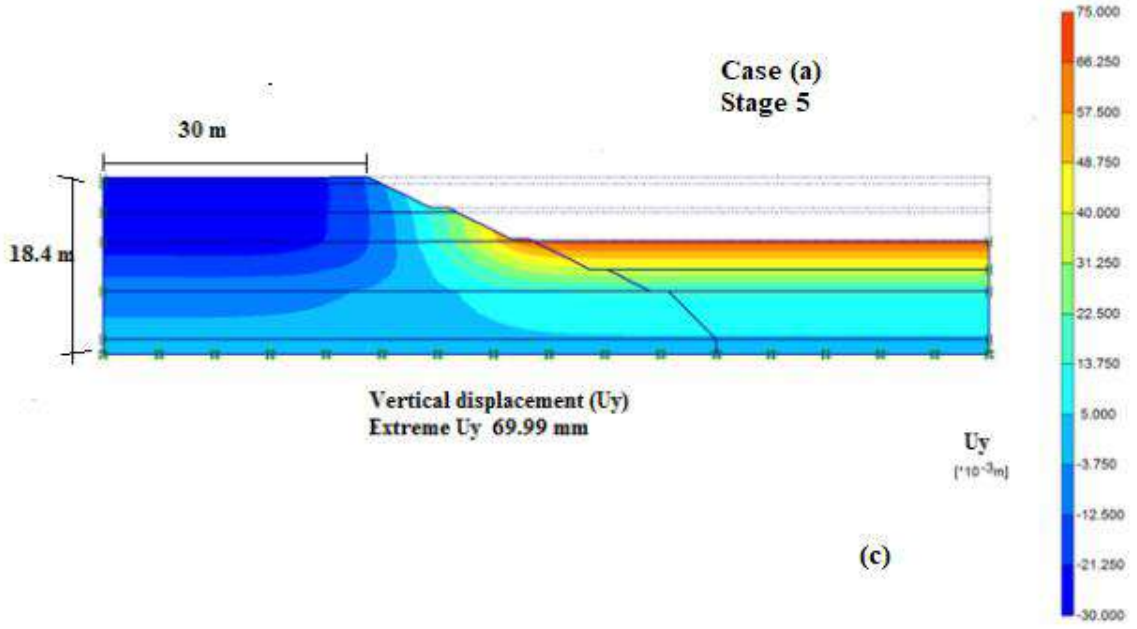
Case (a)
Stage 5
30 m
18.4 m
Vertical displacement (Uy)
Extreme Uy 69.99 mm
Uy
[*10^-3m]
75.000
66.250
57.500
48.750
40.000
31.250
22.500
13.750
5.000
-3.750
-12.500
-21.250
-30.000

(c)

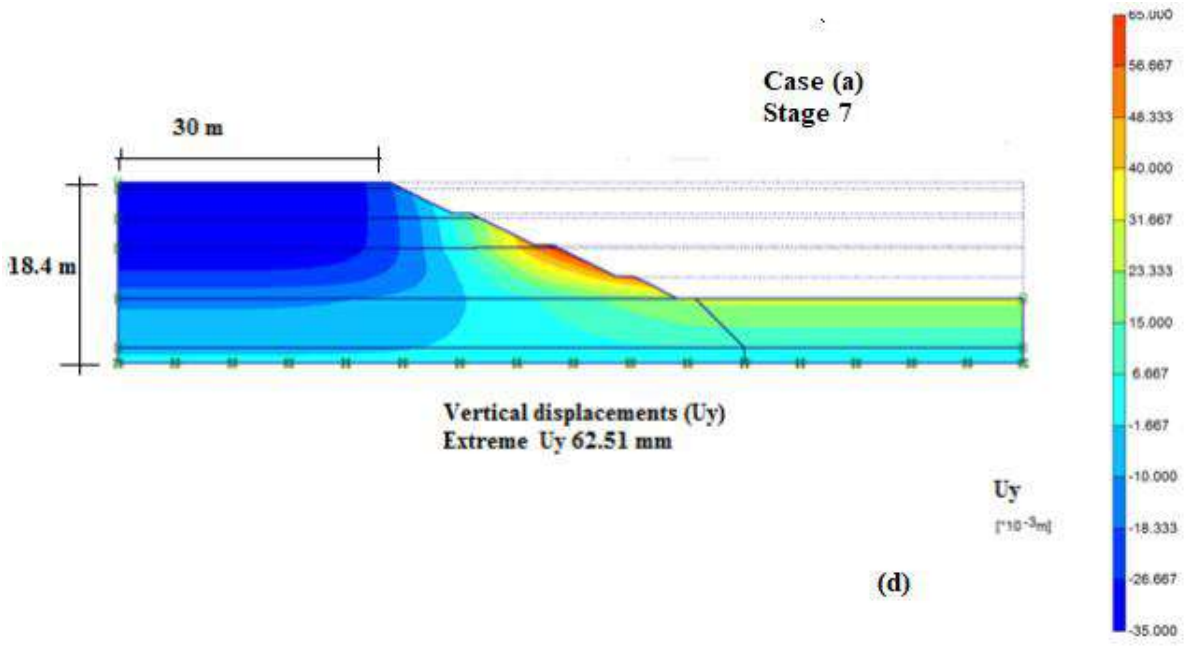

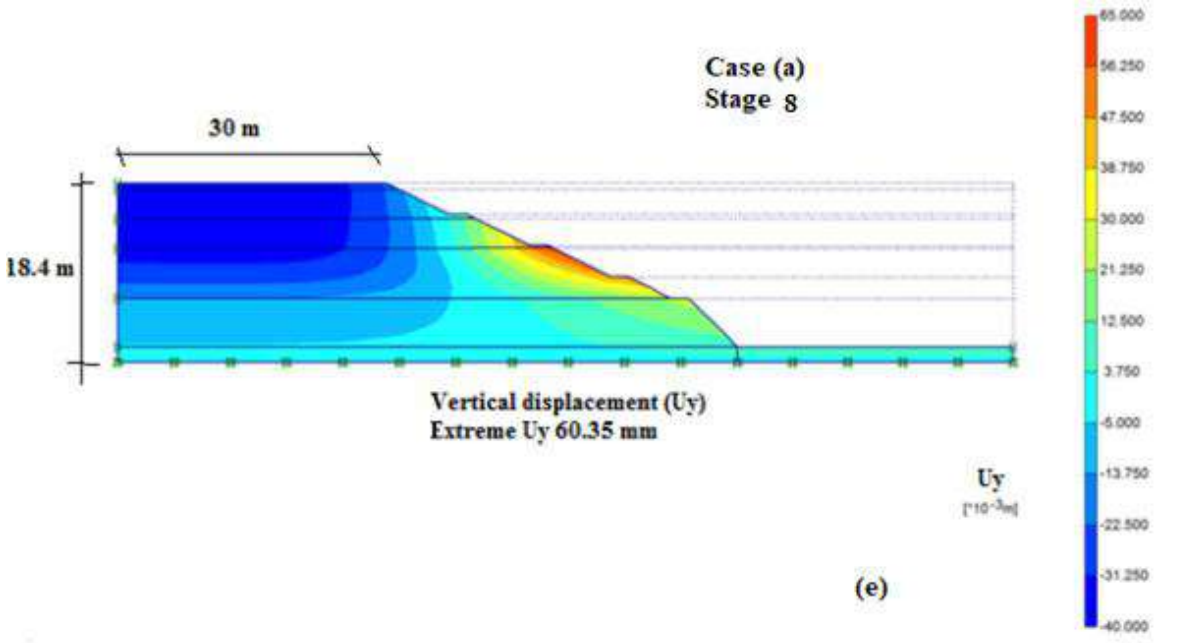

Fig 4.10 : Vertical displacements computed in Case (a), MC Model at the end of various stages (a) 1st (b) 3rd (c) 5th (d) 7th (e) 8th

The vertical displacement data from Fig 4.10 (a) to (e) are summarized in Fig 4.11 and shown below.

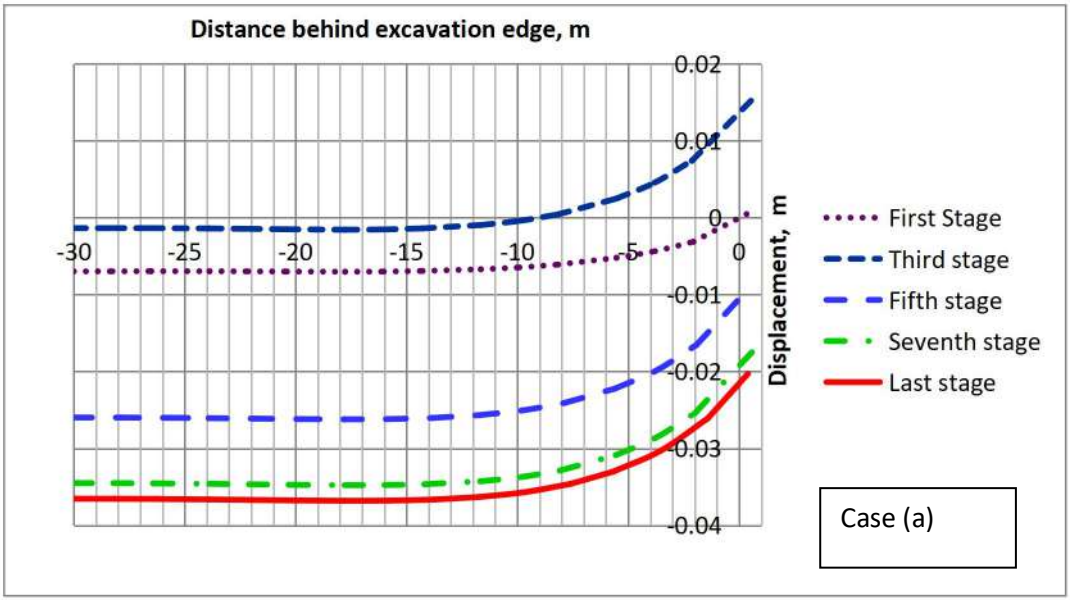

Fig 4.11 : Vertical displacements computed using MC model (Case a).

Typical plots of horizontal displacements at the end of 1st, 3rd, 5th, 7th and last stages of excavation at a distance of 1.0 m away from the edge is shown in the Fig 4.12 (a-e). The horizontal displacement at the surface at the end of first stage is 3.02 mm. This increases to 9.47 mm at the end of third stage and a maximum of 11.55 mm is observedat the end of 5th stage .

Surface displacement at the end of 7th and last stages are lower than that computed at the end of 5th stage; 10.7 mm and 10.56 mm respectively. Displacement towards the excavation increases as the depth of excavation increases and the maximum displacement occurs at the end stage; 6.9 mm at a depth of 9.7 m below. The computed maximum horizontal displacement at a distance of 1.0 m away from the excavation edge is given in Table 4.5

Table 4.5 : Computed horizontal displacement at the end of each stage of excavation (Case a)

Stage	*Maximum Horizontal displacement (mm)*
Stage1	-3.02
Stage 3	-9.47
Stage 5	-11.55
Stage 7	11.64
Last stage	12.91

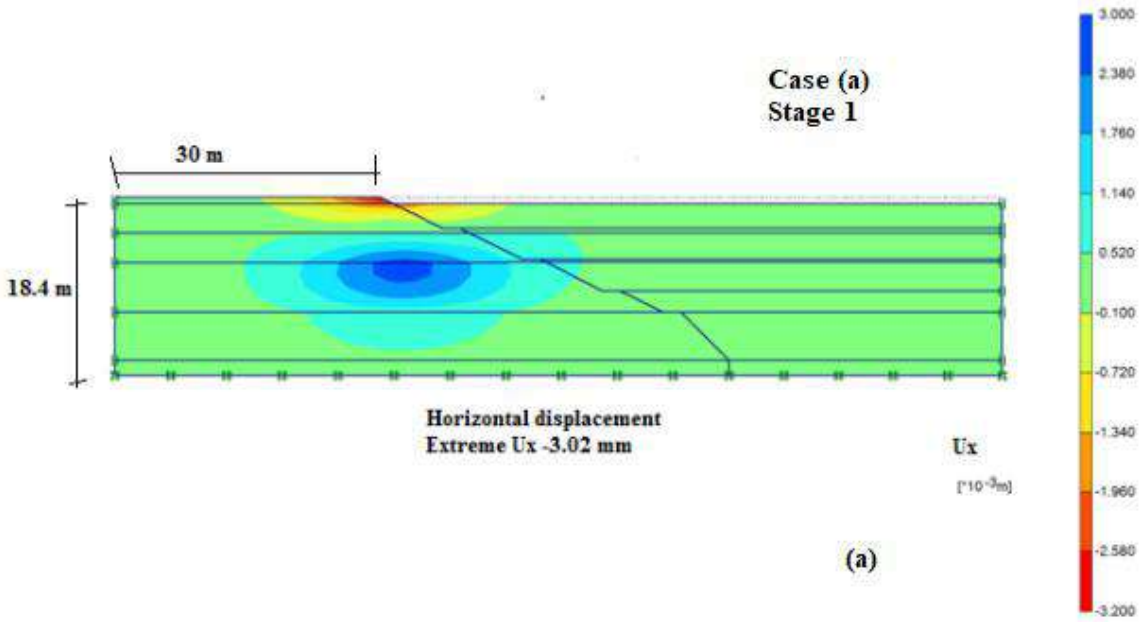

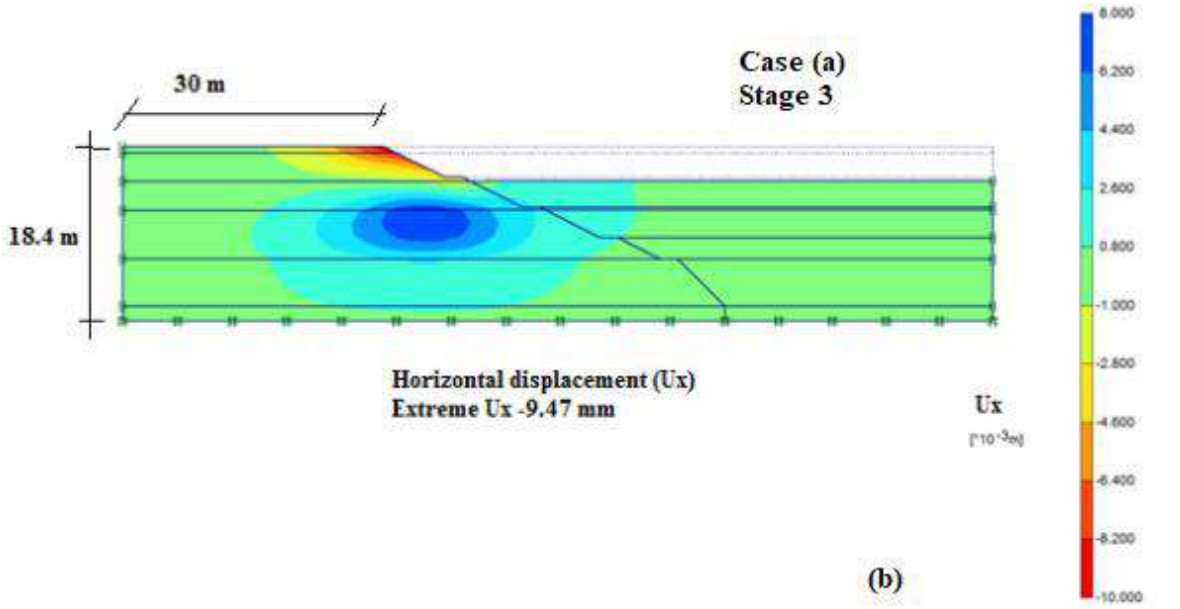
Case (a)
Stage 3
30 m
18.4 m
Horizontal displacement (Ux)
Extreme Ux -9.47 mm
Ux
[*10^-3 m]
8.000
6.200
4.400
2.600
0.800
-1.000
-2.800
-4.600
-6.400
-8.200
-10.000

(b)

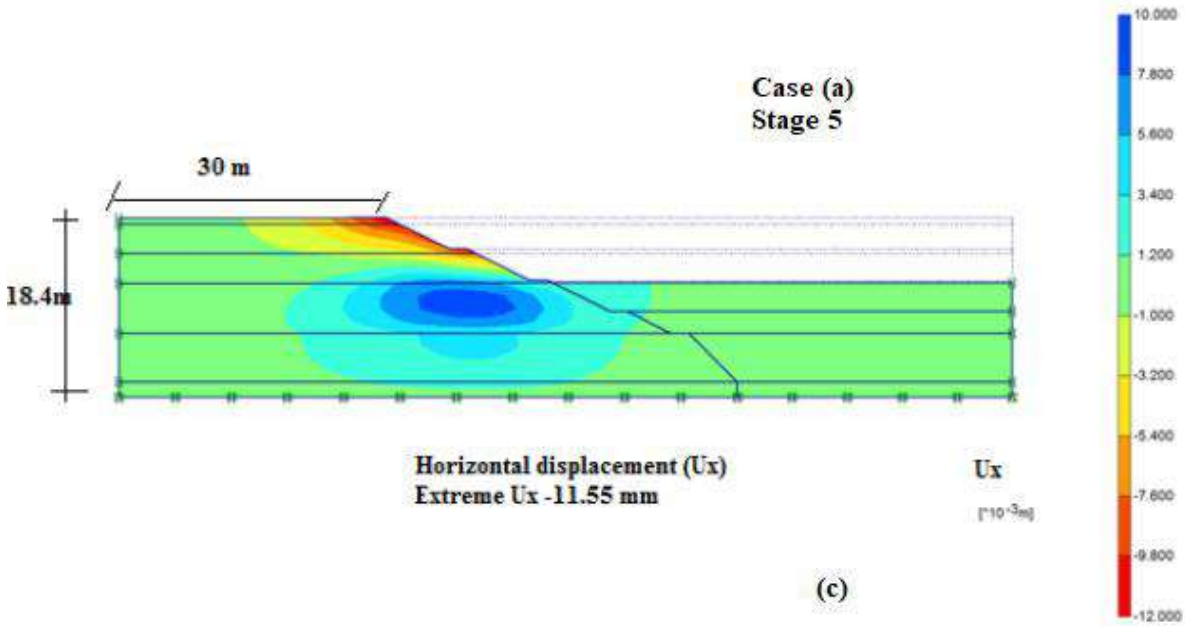
Case (a)
Stage 5
30 m
18.4m
Horizontal displacement (Ux)
Extreme Ux -11.55 mm
Ux
[*10^-3 m]
10.000
7.800
5.600
3.400
1.200
-1.000
-3.200
-5.400
-7.600
-9.800
-12.000

(c)

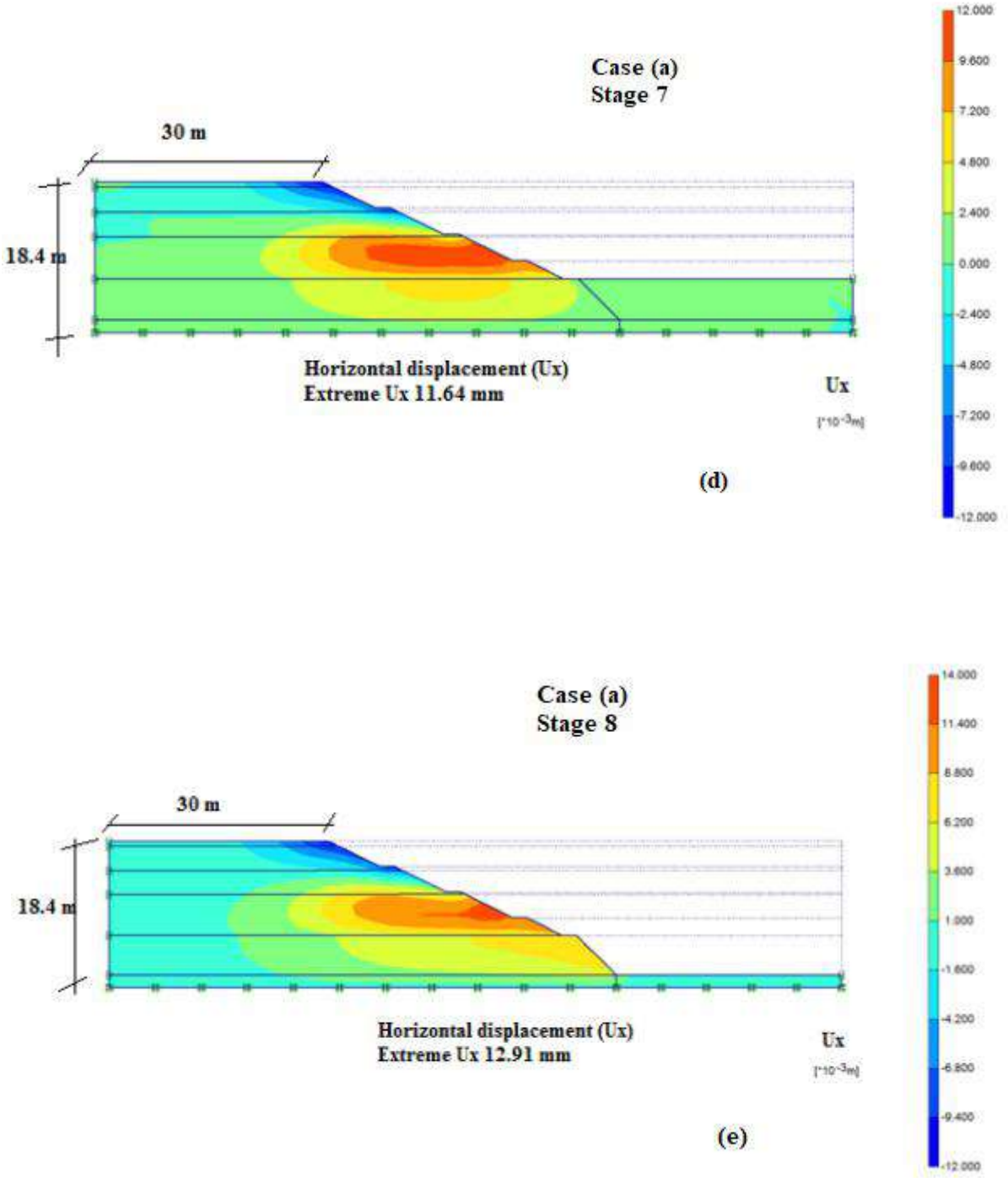

Fig 4.12 : Horizontal displacement at the end of various stages of excavation computed by MC Model for all layers (Case a) (a) 1st (b) 3rd (c) 5th (d) 7th (e) 8th

The horizontal displacement profiles behind the edge at the end of 1st , 3rd, 5th, 7th and last stages of the excavation are given in Fig 4.13.

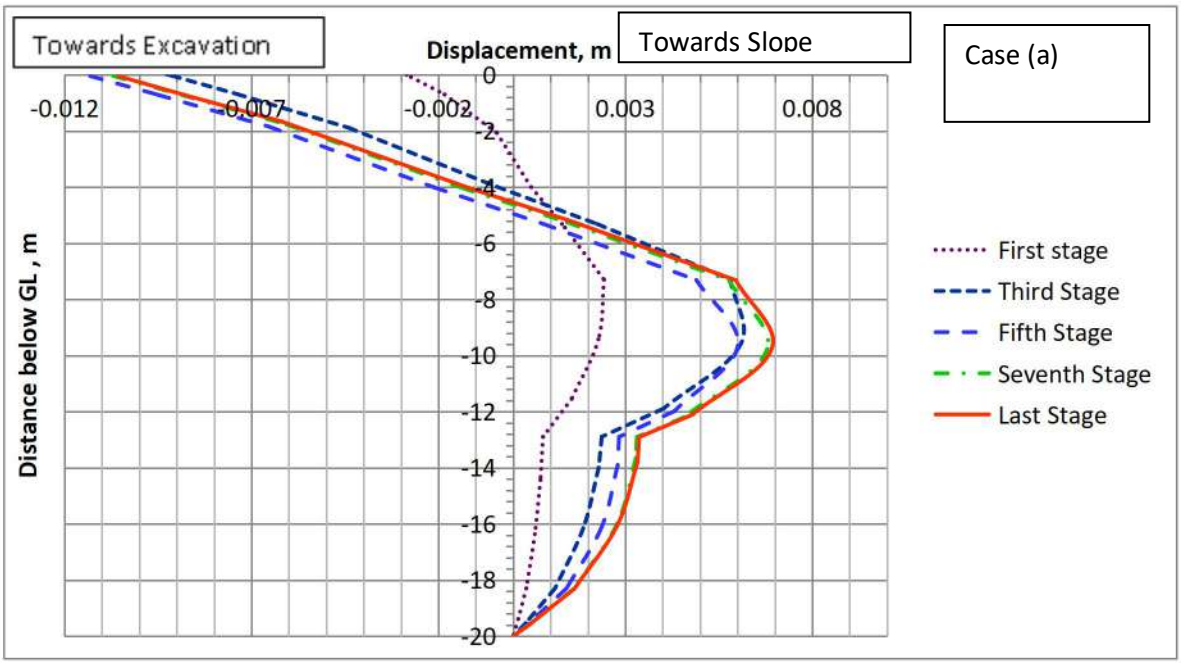

Fig 4.13: Computed Horizontal displacement profiles at various stages of excavation for Case (a) MC model

A sensitivity analysis was carried out to evaluate the adequacy of the medium coarser finite element mesh sizes considered for the analysis. The mesh sizes were further refined in PLAXIS for the case explained above. The maximum vertical settlement and horizontal displacement observed for fine mesh are 60.14 mm and 12.98 mm respectively. This when compared to the results of numerical analysis carried out using medium coarser mesh size is found to be 60.35 and 12.91 mm for vertical settlement and horizontal displacements . The difference in vertical settlement is (+) 0.3 % and that in horizontal displacement is (-) 0.5%. This difference is less than 1% and considering the computation time required for fine mesh, the entire analysis was carried out with medium coarser mesh. Moreover, as the structural responses were not evaluated in this study, and hence the use of fine mesh is not envisaged.

4.3.2.2 Case (b) MC model for top sandy layers and HS Model for silty/clayey sand and residual soil

As in case (a), in case (b) also surface heaves were computed during the initial stage of excavation at the bottom and settlements were observed behind the edge of excavation.

Typical plots of vertical displacement at the end of 1st, 3rd, 5th, 7th and last stage of excavation is shown in the Fig 14 (a-e). Surface heaves of 6 mm was observed upon completion of first stage of excavation, which increases to 25.28 mm upon completion of third stage of excavation. However, the settlement behind at the end of first stage of excavation is 7.26 mm which reduces to 6 mm at the end of third stage.

Settlement increases considerably as the depth of excavation increases and at the end of 5th stage of excavation the settlement computed is 27.5 mm at a distance of 14.9 m. At the end of 7th stage of excavation the settlement computed is 36.1 mm at a distance of 15.26 m and at the end of excavation, the settlement is 38.1 mm which occurs at a distance of 16.1 m behind the edge. Maximum surface heave was observed at the end of 5th stage is 30.61 mm which is considerably less than that computed using MC model Case (a). Surface heave at the bottom subsequently reduces to 16 mm at the end of 7th stage. However, the vertical displacements of the order of 28 mm were computed at the third bench during 7th and last stage of excavation. The vertical displacement computed behind the excavation at various phases is given in Table 4.6.

Table 4.6 : Computed vertical settlement at the end of each stage of excavation (Case b)

Stage	***Maximum Vertical displacement (mm)***
Stage 1	-7.26
Stage 3	25.28
Stage 5	30.61
Stage 7	-36.3
Last stage	-38.21

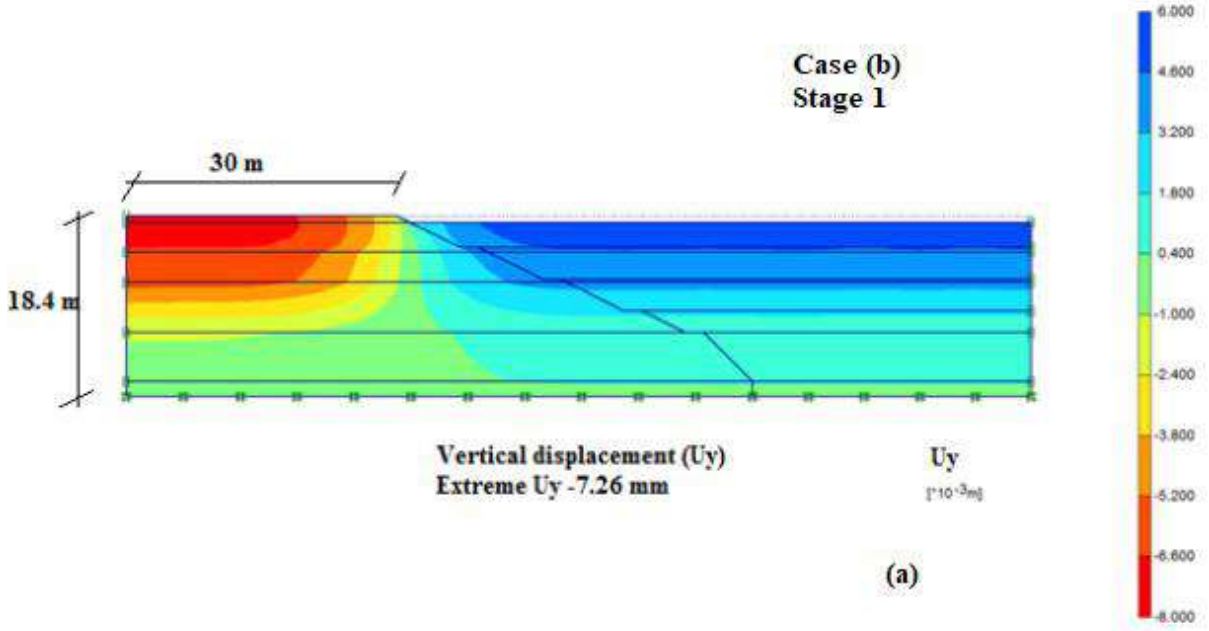
Case (b)
Stage 1
30 m
18.4 m
Vertical displacement (Uy)
Extreme Uy -7.26 mm
Uy
[*10^-3m]
6.000
4.600
3.200
1.800
0.400
-1.000
-2.400
-3.800
-5.200
-6.600
-8.000

(a)

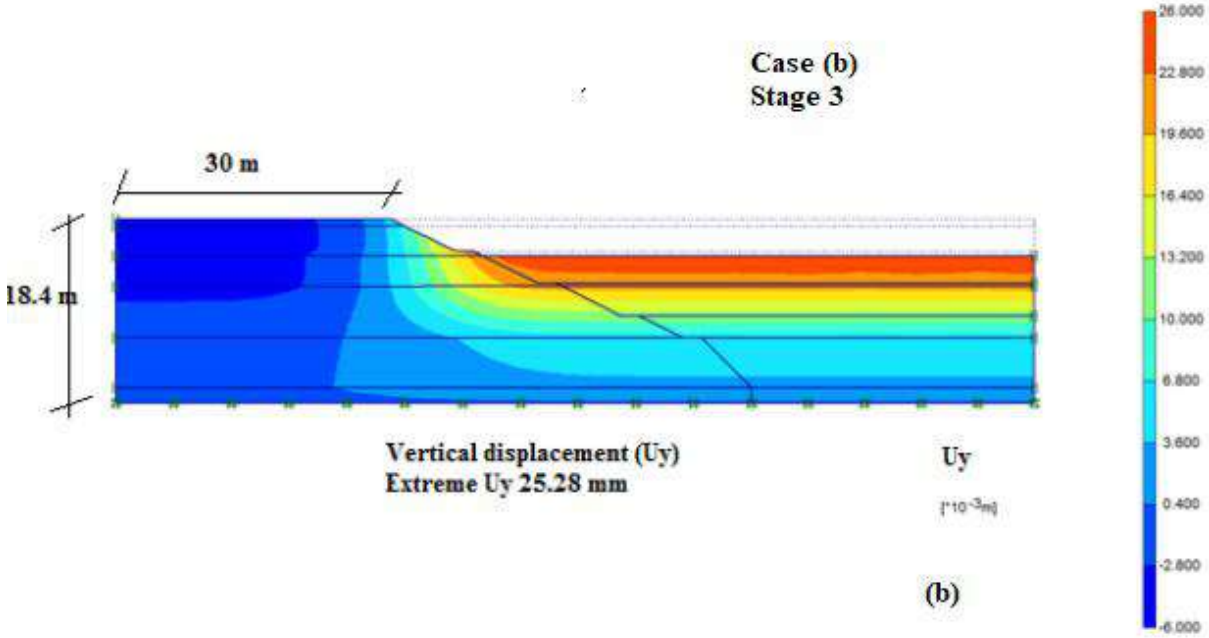
Case (b)
Stage 3
30 m
18.4 m
Vertical displacement (Uy)
Extreme Uy 25.28 mm
Uy
[*10^-3m]
26.000
22.800
19.600
16.400
13.200
10.000
6.800
3.600
0.400
-2.800
-6.000

(b)

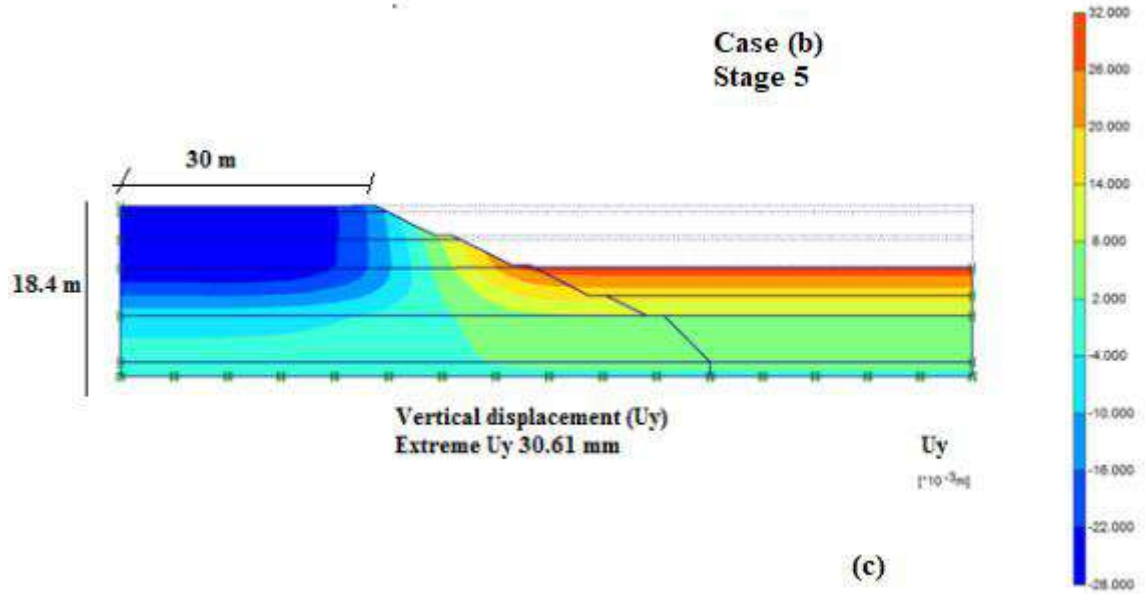
Case (b)
Stage 5
30 m
18.4 m
Vertical displacement (Uy)
Extreme Uy 30.61 mm
Uy
[*10^-3m]
32.000
26.000
20.000
14.000
8.000
2.000
-4.000
-10.000
-16.000
-22.000
-28.000

(c)

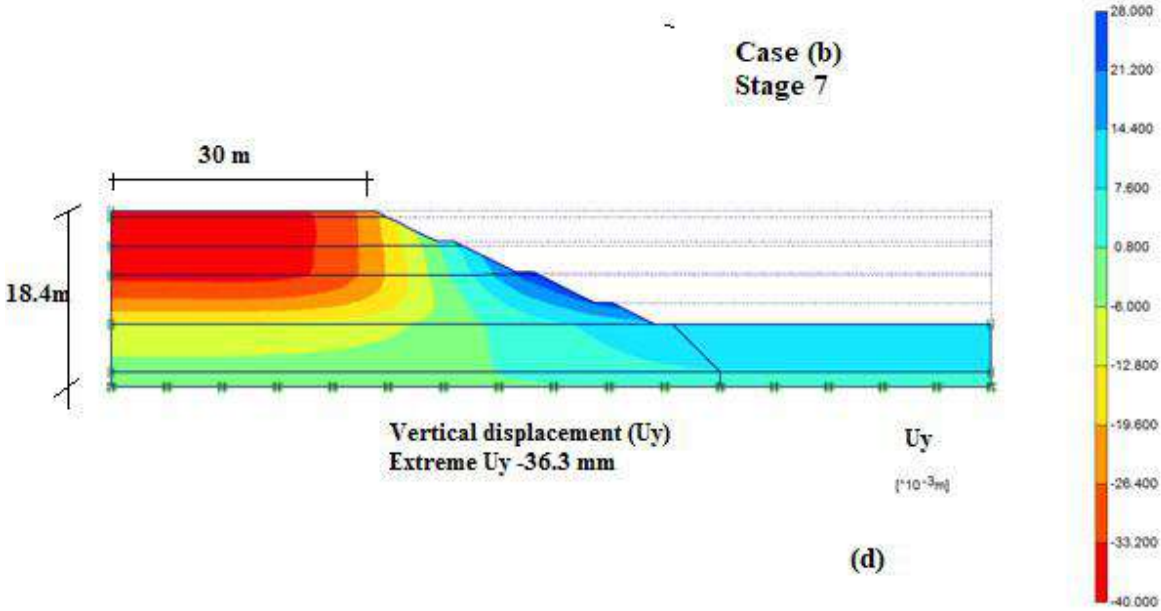
Case (b)
Stage 7
30 m
18.4m
Vertical displacement (Uy)
Extreme Uy -36.3 mm
Uy
[*10^-3m]
28.000
21.200
14.400
7.600
0.800
-6.000
-12.800
-19.600
-26.400
-33.200
-40.000

(d)

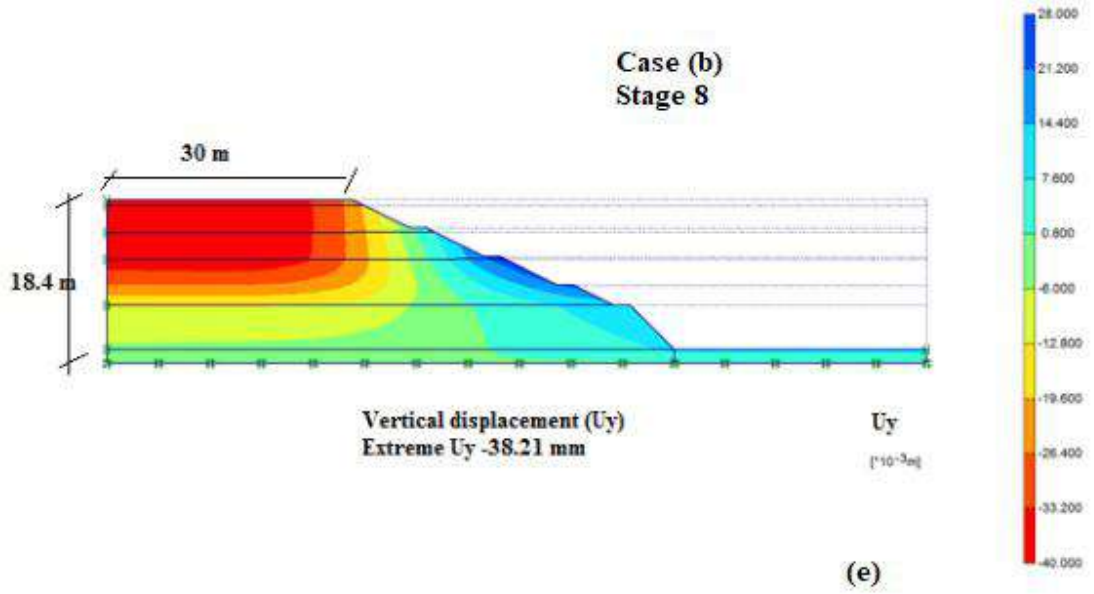

Fig 4.14 : Vertical displacement profile at the end of various stages of excavation computed by MC + HS Model, Case (b) for all layers (a) 1st (b) 3rd (c) 5th (d) 7th (e) 8th

The horizontal displacement profiles for the case (b) behind the excavation edge after the 1st, 3rd , 5th, 7th and last stage of the excavation is given in Fig 4.15.

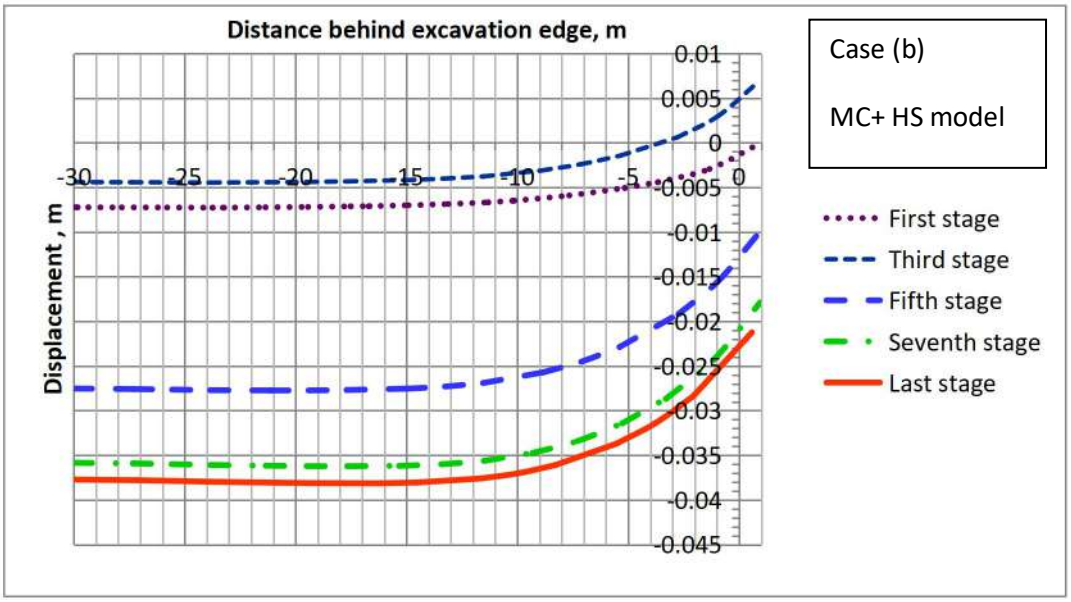

Fig 4.15 : Computed Vertical displacement profiles behind excavation edge using combined MC & HS model, Case (b)

Typical plots of horizontal displacement at the end of 1st, 3rd, 5th, 7th and last stage of excavation at a distance of 1.0 m away from the excavation edge are shown in the Fig 4.16 (a-e) for Case (b), MC + HS model. The horizontal displacement at the surface is 2.66 mm at the end of first stage of excavation and increases to 5.72 mm at the end of third stage. At the end of 5th stage, the surface displacement was observed is 10.85 mm. This surface displacement increases to 11.07 mm at the end of 7th stage of excavation and further reduces to 11.02 mm.

Displacement towards the excavation increases as the depth of excavation increases and the maximum displacement is 5.6 mm which occurs at the end at a depth of 9.7 m below the edge. This displacement is lower than that computed using MC model. The computed maximum horizontal displacement at a distance of 1.0 m away from the excavation edge is given in Table 4.7

Table 4.7 : Computed horizontal settlement at the end of each stage of excavation (Case b)

Stage	***Maximum Horizontal displacement***
Stage1	-2.66
Stage 3	-5.72
Stage 5	-10.85
Stage 7	-11.27
Last stage	-11.02

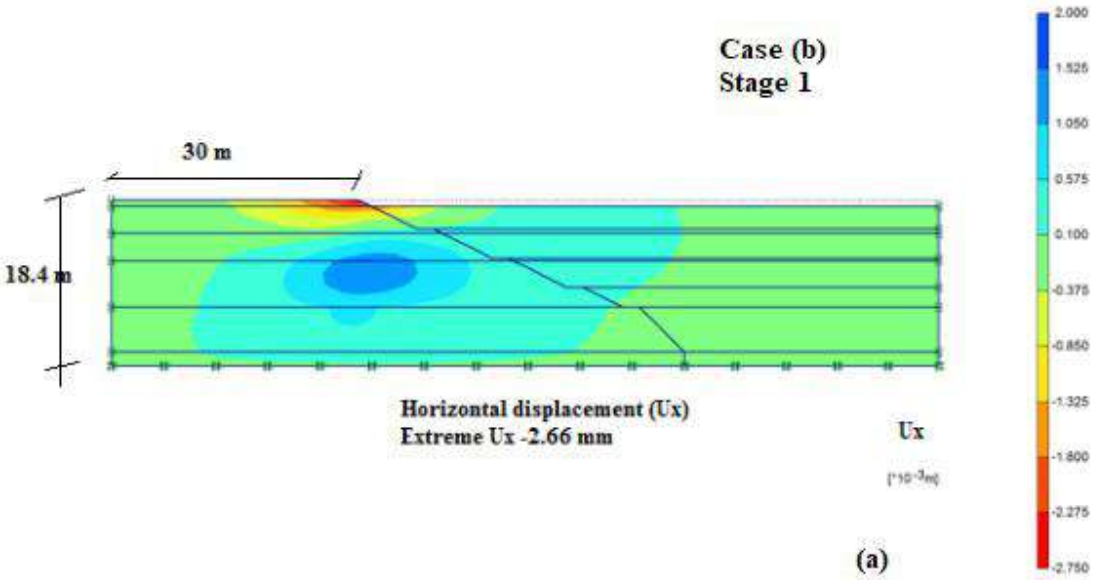
Case (b)
Stage 1
30 m
18.4 m
Horizontal displacement (Ux)
Extreme Ux -2.66 mm
Ux
[*10^-3m]
2.000
1.525
1.050
0.575
0.100
-0.375
-0.850
-1.325
-1.800
-2.275
-2.750

(a)

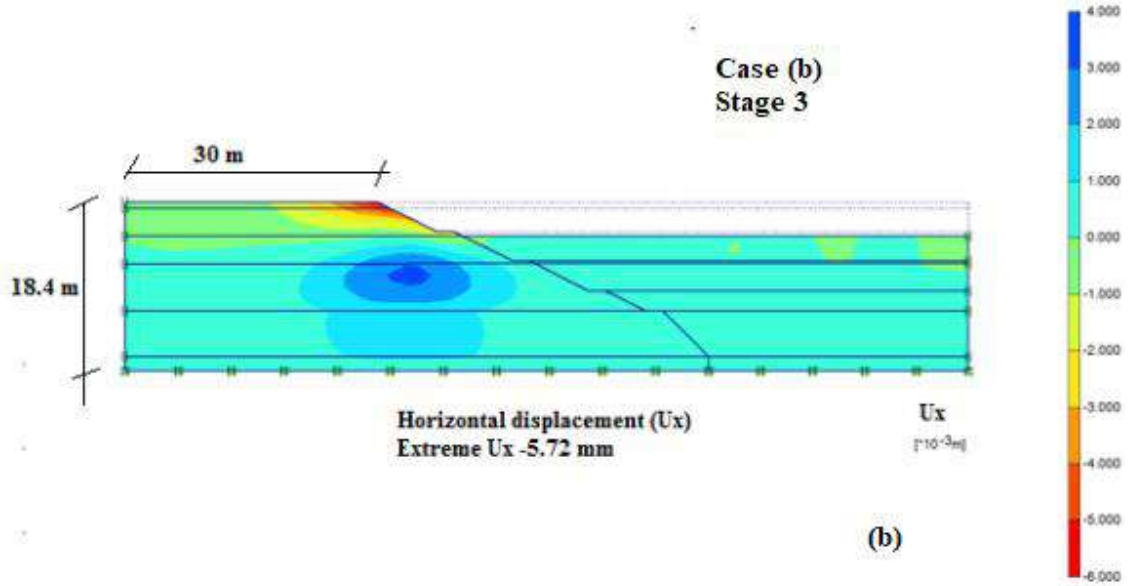
Case (b)
Stage 3
30 m
18.4 m
Horizontal displacement (Ux)
Extreme Ux -5.72 mm
Ux
[*10^-3m]
4.000
3.000
2.000
1.000
0.000
-1.000
-2.000
-3.000
-4.000
-5.000
-6.000

(b)

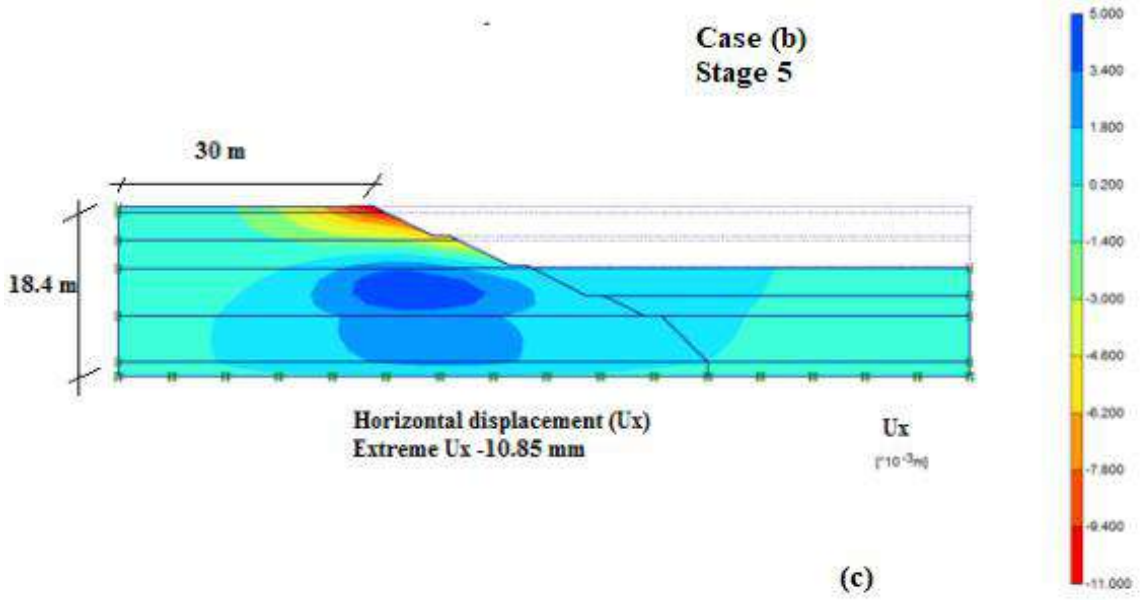
Case (b)
Stage 5
30 m
18.4 m
Horizontal displacement (Ux)
Extreme Ux -10.85 mm
Ux
[*10^-3m]
5.000
3.400
1.800
0.200
-1.400
-3.000
-4.600
-6.200
-7.800
-9.400
-11.000

(c)

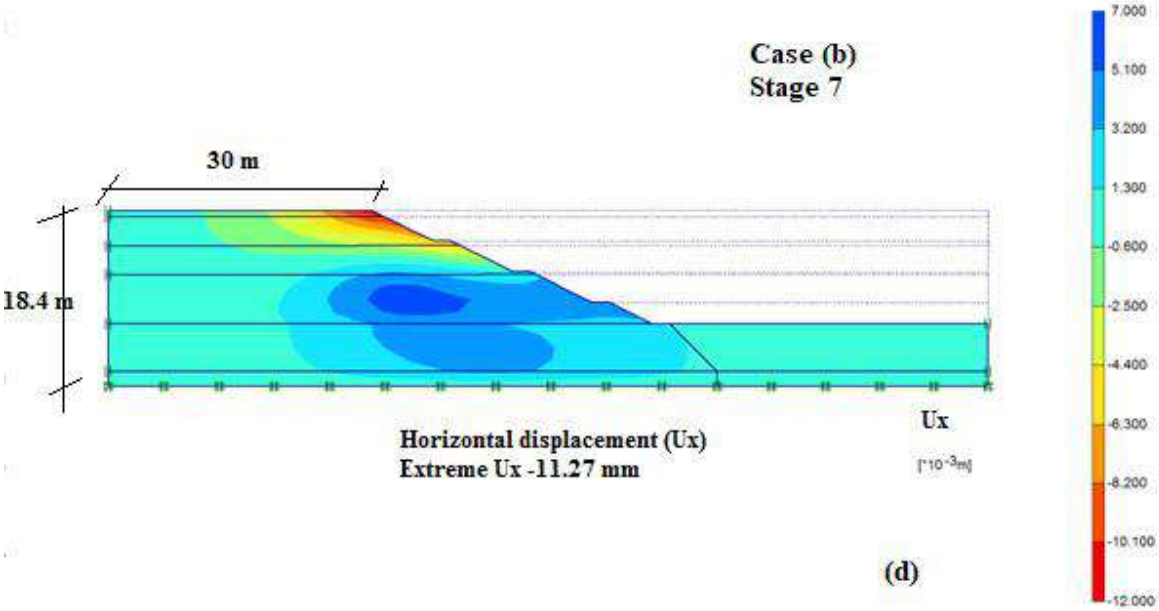
Case (b)
Stage 7
30 m
18.4 m
Horizontal displacement (Ux)
Extreme Ux -11.27 mm
Ux
[*10^-3m]
7.000
5.100
3.200
1.300
-0.600
-2.500
-4.400
-6.300
-8.200
-10.100
-12.000

(d)

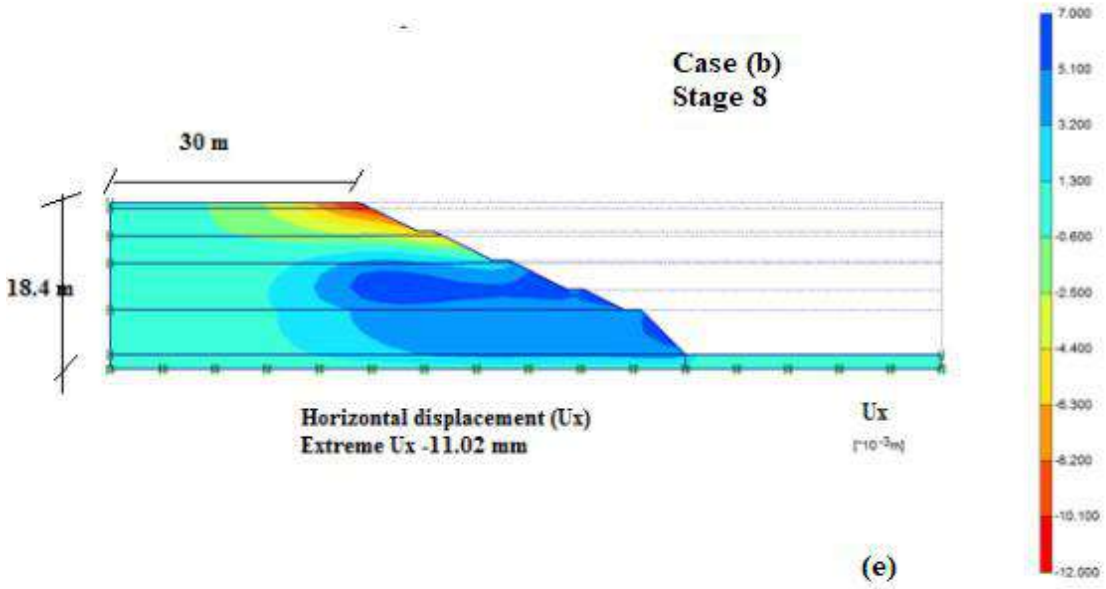

Fig 4.16: Computed Horizontal displacement profile from MC + HS model, Case (b) at the end of different stages of excavation (a) 1st (b) 3rd (c) 5th (d) 7th and (e) 8th

The horizontal displacement profiles behind the excavation edge after the 1st, 3rd, 5th, 7th and last stage are given in Fig 4.17.

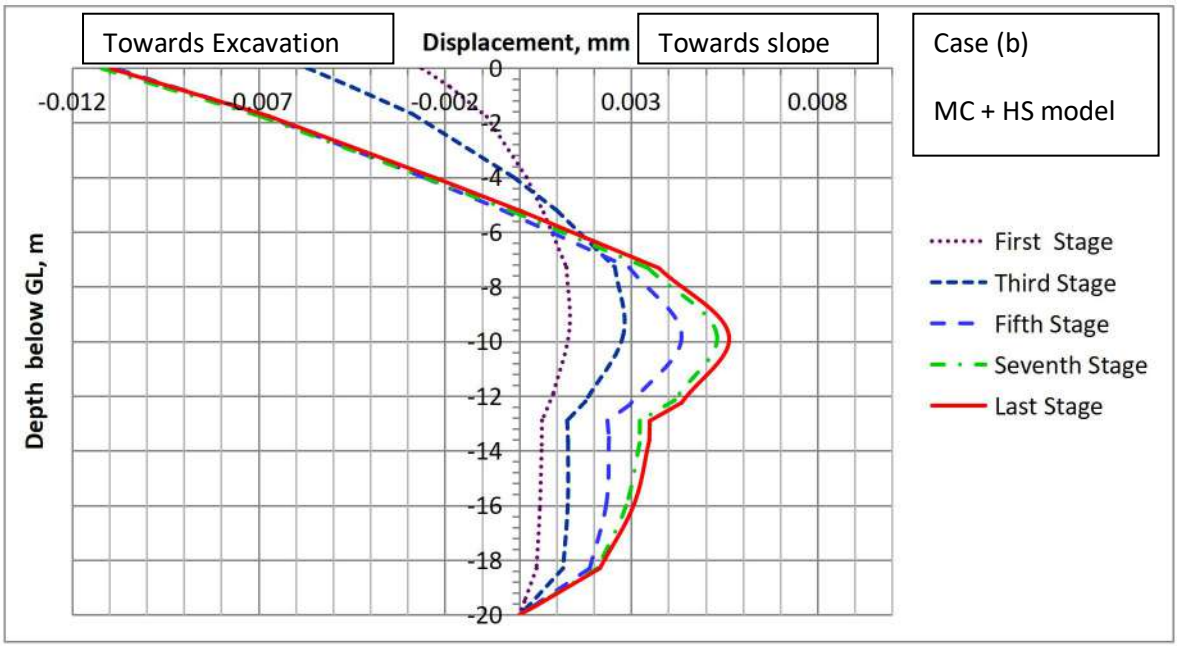

Fig 4.17: Computed Horizontal displacement profiles at the end of each stage of excavation for Case (b)

4.3.2.3 Case (c): MC model for top sandy layers with incremental stiffness and dilatency and HS model for silty/clayey sand and residual soil

Like in previous cases, surface heaves were observed during the initial phase of excavation at the bottom of excavation and settlements were observed behind the excavation edge in this case too. Typical contour plots of vertical displacement at the end of 1st, 3rd, 5th, 7th and last stage of excavation are shown in the Fig 4.18 (a-e). Surface heaves of 6 mm were observed upon completion of first stage of excavation, which increases to 23.42 mm upon completion of third stage. However, the settlement behind the excavation at the end of first stage is 7.01 mm which reduces to 6 mm at the end of third stage.

Settlement behind excavation increases considerably as the depth of excavation increases, at the end of 5th stage, the settlement computed is 27.6 mm at a distance of 15.4 m behind the excavation edge. At the end of 7th stage, the settlement computed is 36.3 mm at a distance of 16.3 m behind the excavation edge. At the end of excavation, the settlement computed is 38.24 mm which occurs at a distance of 17.5 m behind the excavation. Maximum surface heave was observed at the end of 5th stage which is 30.61 mm and considerably less than that computed using MC model Case (a). Surface heave at the bottom of excavation subsequently reduces to 12 mm at the end of 7th stage. However, vertical displacements of the order of 24 mm were computed at the third berm during 7th stage and last phase of excavation. The vertical displacement computed behind the excavation at various phases is given in Table 4.8.

Table 4.8 : Computed vertical settlement at the end of each stage of excavation (Case c)

Stage	*Maximum Vertical displacement*
Stage1	-7.01
Stage 3	23.42
Stage 5	30.61
Stage 7	-36.4
Last stage	-38.3

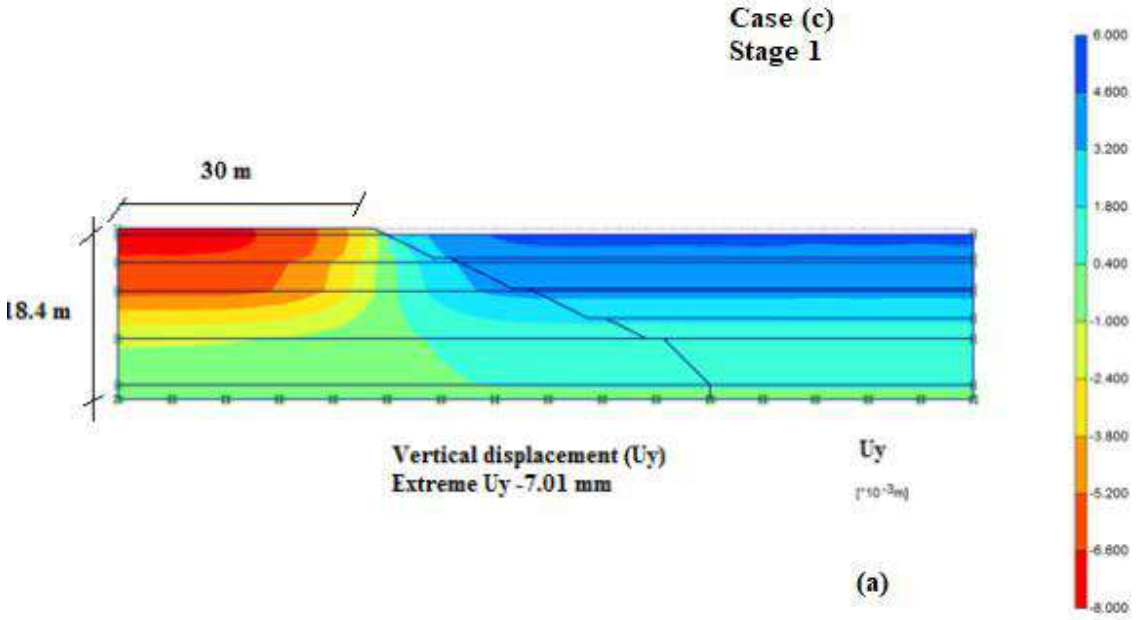

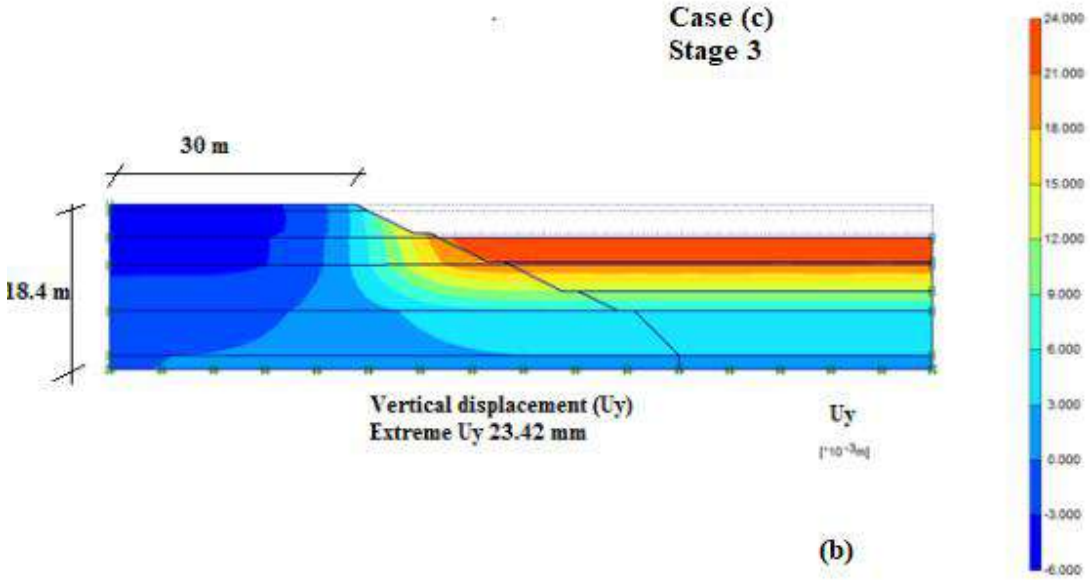
Case (c)
Stage 3
30 m
18.4 m
Vertical displacement (Uy)
Extreme Uy 23.42 mm
Uy
[*10^-3m]
24.000
21.000
18.000
15.000
12.000
9.000
6.000
3.000
0.000
-3.000
-6.000

(b)

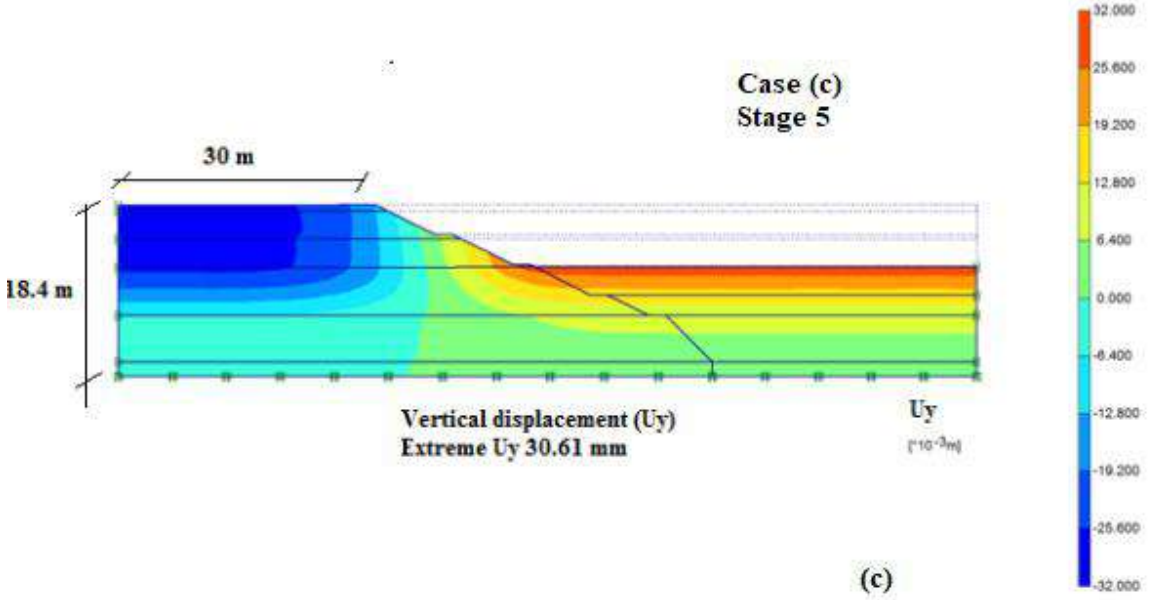
Case (c)
Stage 5
30 m
18.4 m
Vertical displacement (Uy)
Extreme Uy 30.61 mm
Uy
[*10^-3m]
32.000
25.600
19.200
12.800
6.400
0.000
-6.400
-12.800
-19.200
-25.600
-32.000

(c)

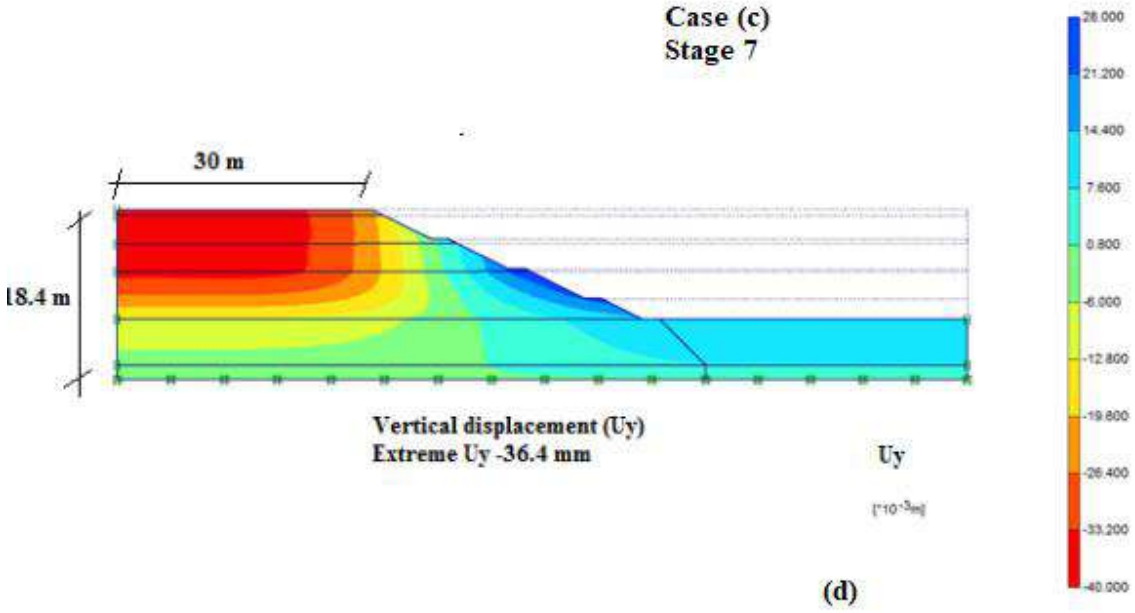

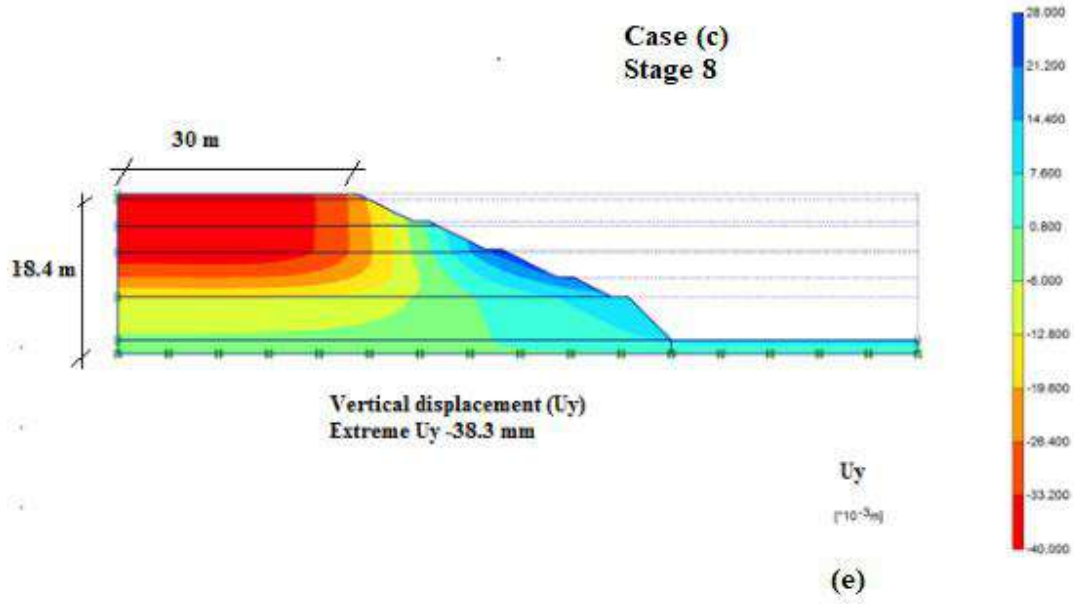

Fig 4.18 Vertical displacements computed from Case (c) at the end of different stage of excavation (a) 1st (b) 3rd (c) 5th (d) 7th (e)8th

The vertical displacement profile for the case (c) behind the excavation edge after the 1st, 3rd , 5th, 7th and last stage of the excavation are given in Fig 4.19.

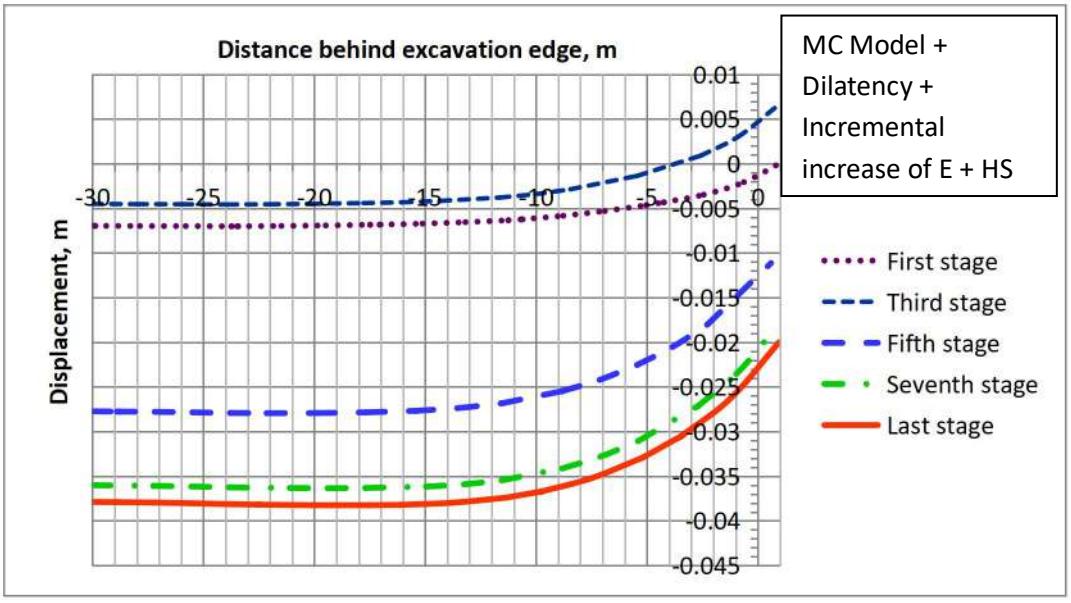

Fig 4.19 Computed vertical displacement profile behind excavation (Case c)

Typical plots of horizontal displacement at a distance of 1.0 m away from the edge computed by Case (c) analysis at the end of different stages and last phase of excavation is shown in Fig 4.20 (a-e). The horizontal displacement at the surface of excavation at the end of 1st stage is 2.62 mm which increases to 5.75 mm at the end of 3rd stage. At the end of 5th stage surface displacement observed is 10.86 mm which increases to 11.31 mm at the end of 7th stage and further reduces to 11.07 mm at the end of excavation.

Displacement towards the excavation increases as the depth increases and the maximum displacement occurs at the end stage which is 5.6 mm at a depth of 10.4 m below the excavation. The maximum computed horizontal displacement at a distance of 1.0 m away from the excavation edge is given in Table 4.9.

Table 4.9 : Computed horizontal settlement at the end of each stage of excavation

Stage	***Maximum Horizontal displacement***
Stage1	-2.62
Stage 3	-5.75
Stage 5	-10.86
Stage 7	-11.31
Last stage	-11.07

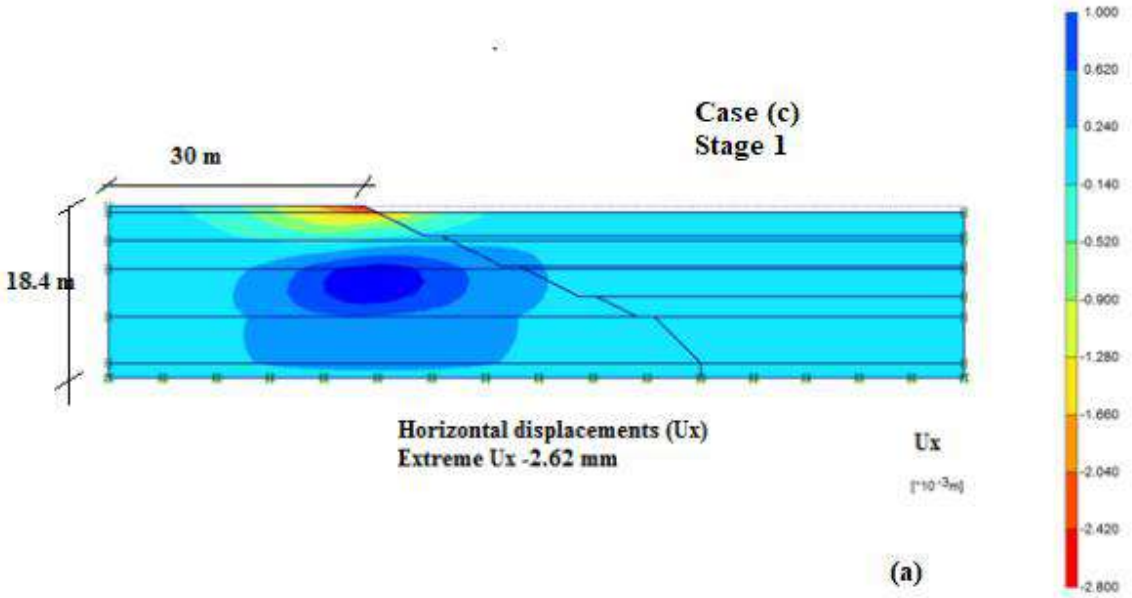

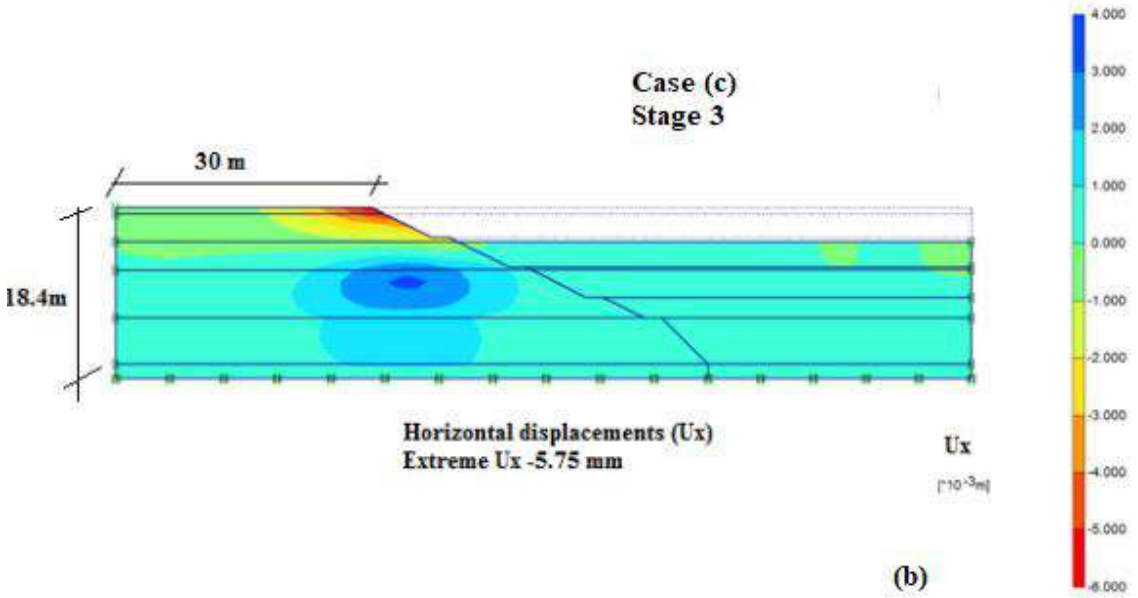
Case (c)
Stage 3
30 m
18.4m
Horizontal displacements (Ux)
Extreme Ux -5.75 mm
Ux
[*10^-3m]
4.000
3.000
2.000
1.000
0.000
-1.000
-2.000
-3.000
-4.000
-5.000
-6.000

(b)

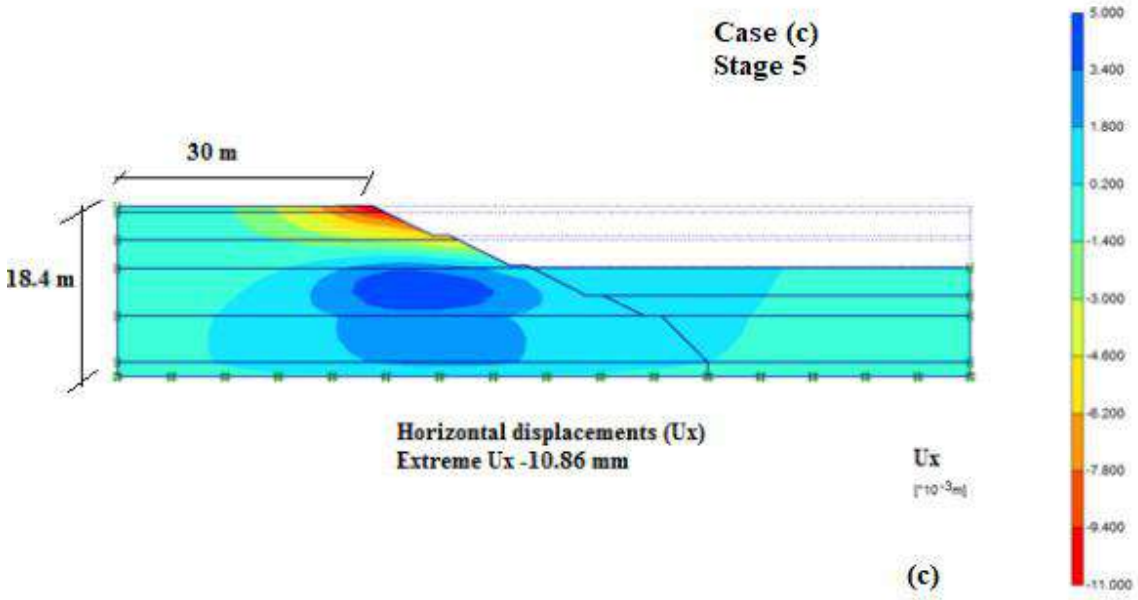
Case (c)
Stage 5
30 m
18.4 m
Horizontal displacements (Ux)
Extreme Ux -10.86 mm
Ux
[*10^-3m]
5.000
3.400
1.800
0.200
-1.400
-3.000
-4.600
-6.200
-7.800
-9.400
-11.000

(c)

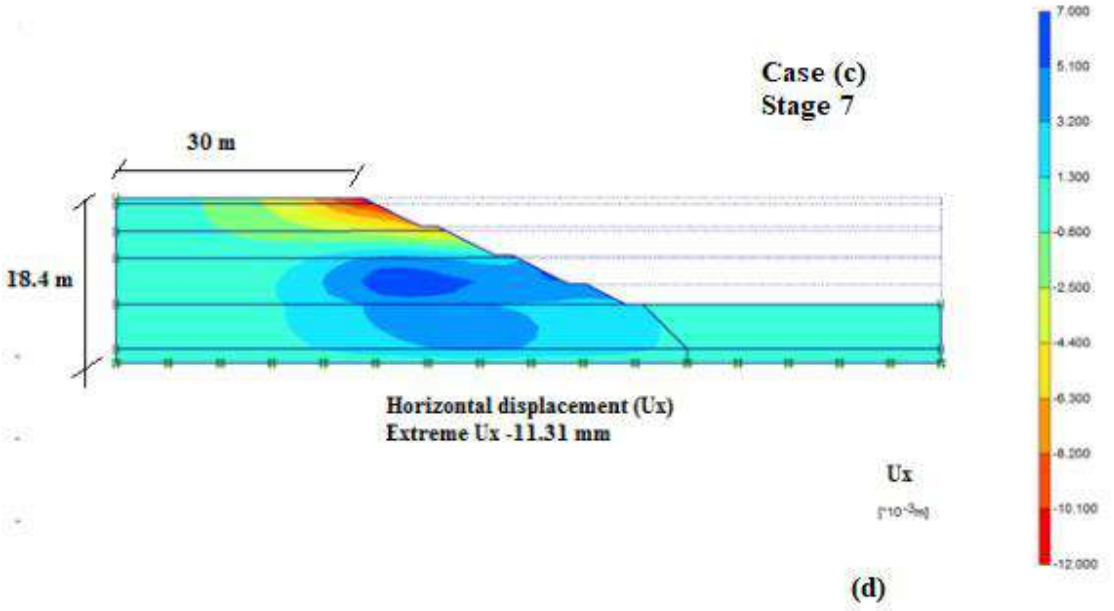

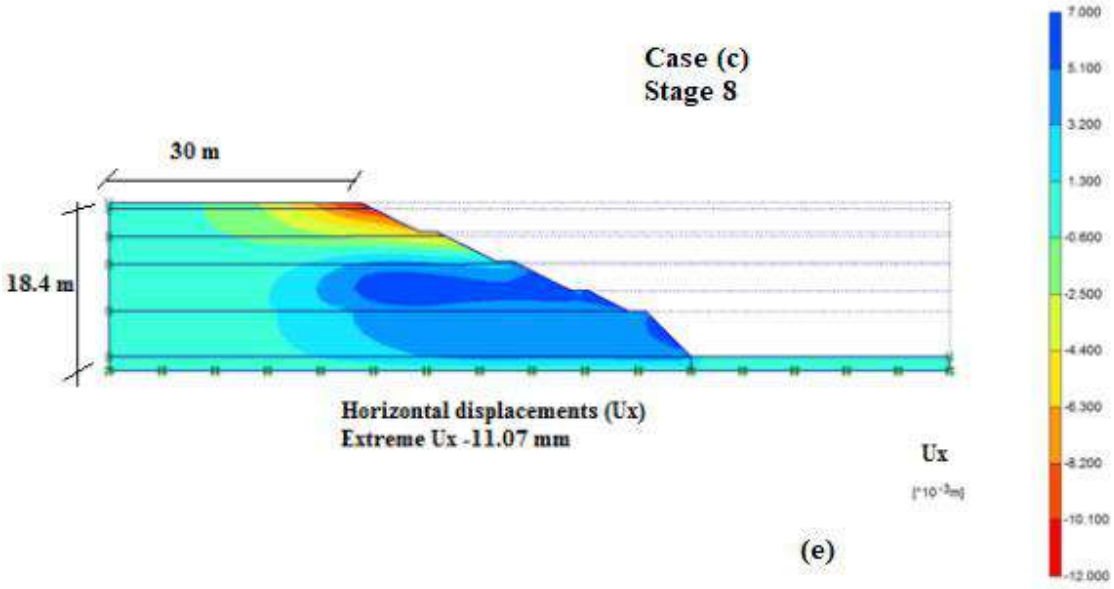

Fig 4.20: Horizontal displacement computed by analysis using Case (c) at the end of different stages (a) 1st (b) 3rd (c) 5th (d) 7th (e) 8th

The horizontal displacement behind the excavation edge after the 1st, 3rd, 5th, 7th stage and end of the excavation is given in Fig 4.21.

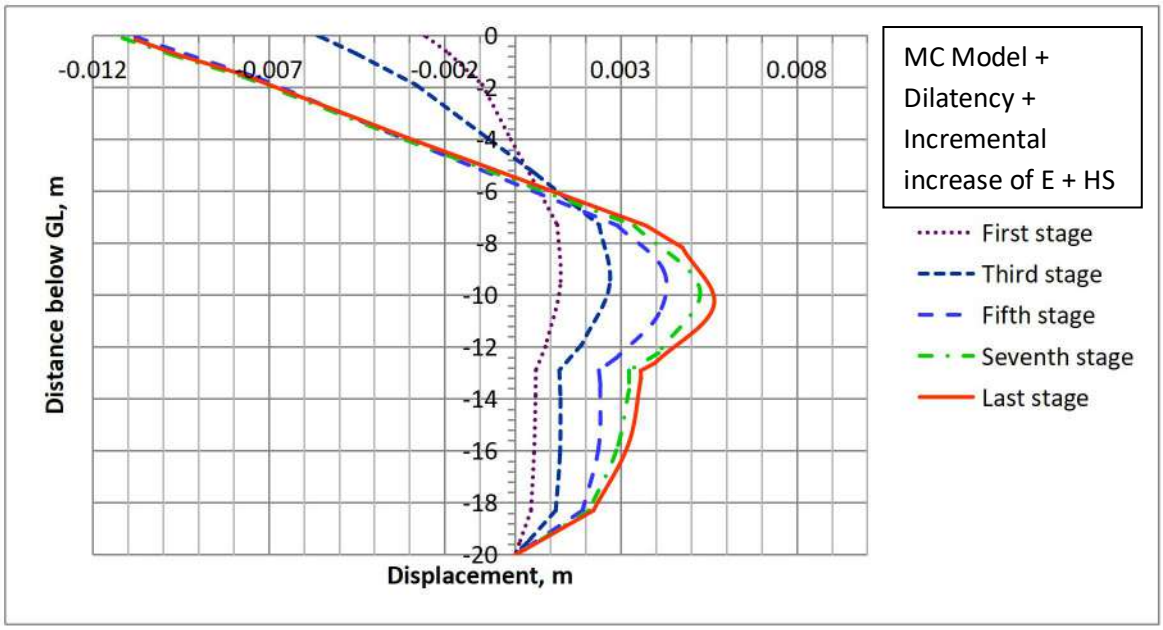

Fig 4.21 Computed Horizontal displacement profile behind excavation edge (Case c)

4.3.3 Comparison of the Results of analyses

The vertical displacement computed by the three analyses carried out for the excavation problem are compared for 1st, 3rd, 5th, 7th and last stage of excavation in Fig 4.22 (a-e). The results shows that the settlement computed by MC Model (Case a) is lower than that computed from the other two analysis (Case b & Case c) except for the first stage. However, towards the later stages this difference reduces. At the end of excavation, the settlement computed from Case (a) is 36.7 mm which occurs at a distance of 15.8 m behind the excavation fig 4.22 (e). At the end of excavation stage 8, the settlement computed from Case (b) is 38.2 mm which occurs at a distance of 16.1 m behind the excavation. For case (c) the settlement is 38.24 and occurs at a distance of 17.5 m. This indicates that the settlement is marginally higher for the model accounting for dilatency and incremental increase of stiffness for sandy layer along with HS model for silty/clayey soil and residual layer. The distance of maximum settlement for all the cases is around 0.85 times to 0.95 times the depth of

excavation. The results from Case (b) and Case (c) are similar at all the stages, except for the first stage.

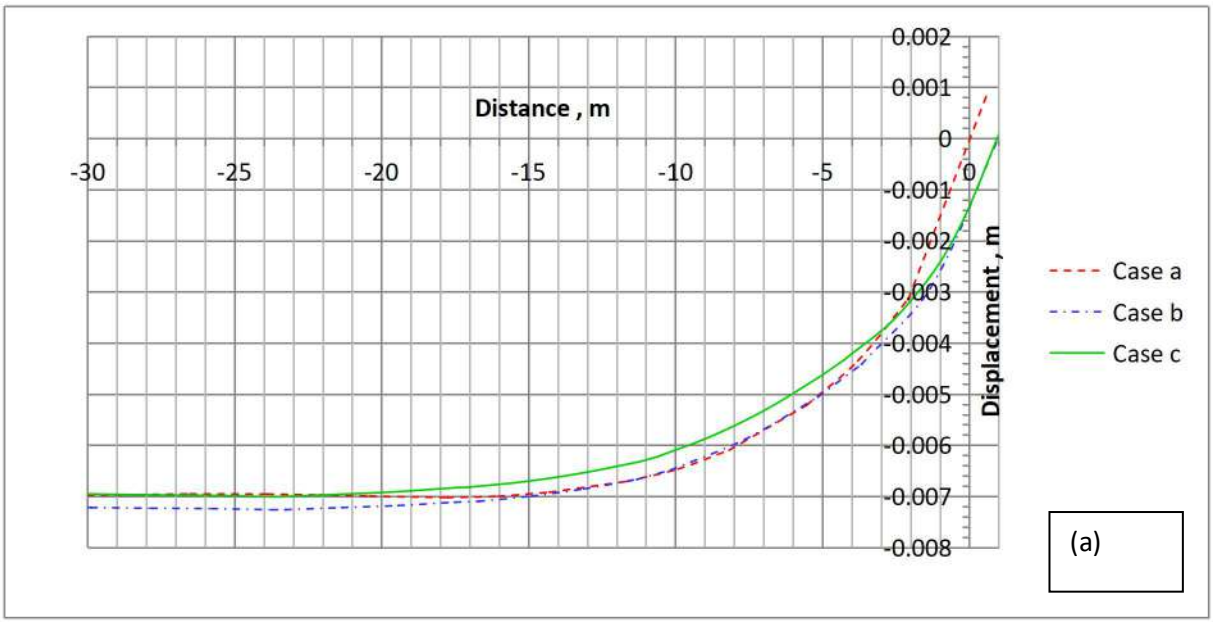

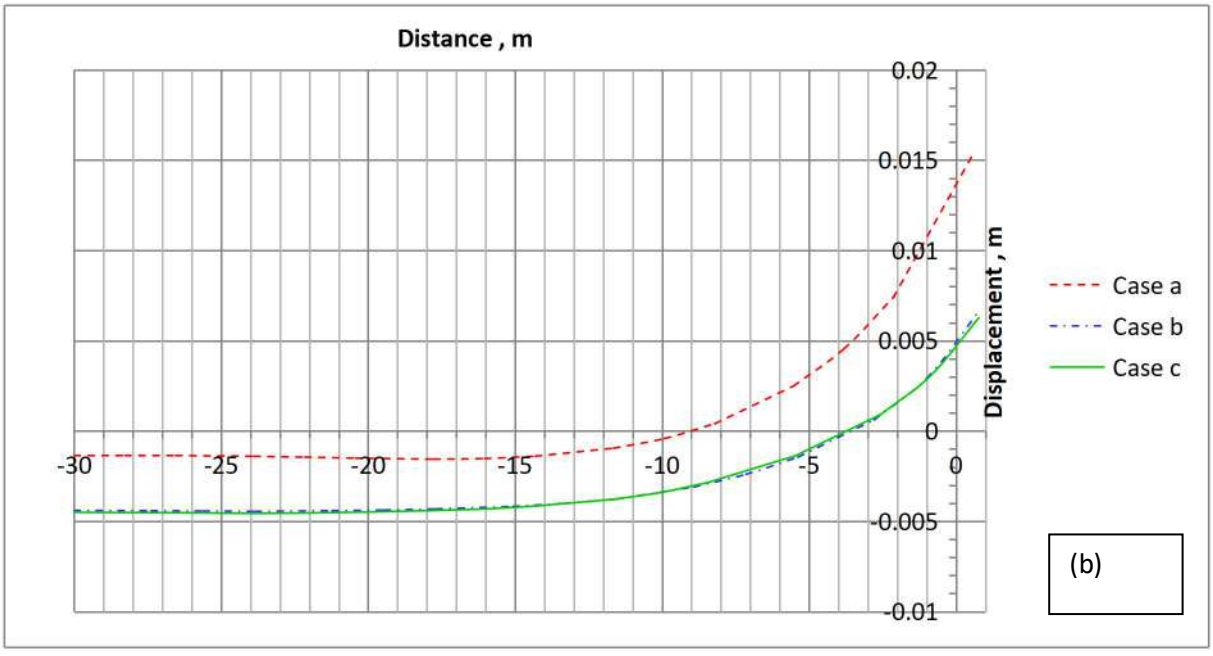

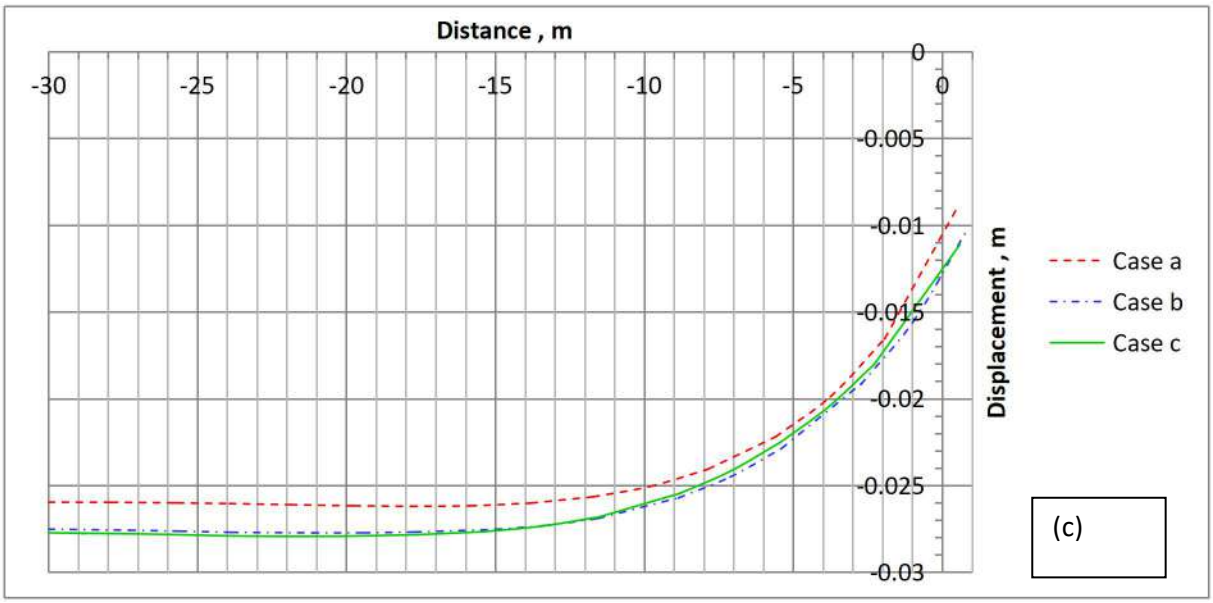
Distance , m
-30
-25
-20
-15
-10
-5
0
0
-0.005
-0.01
-0.015
-0.02
-0.025
-0.03
Displacement , m
Case a
Case b
Case c
(c)

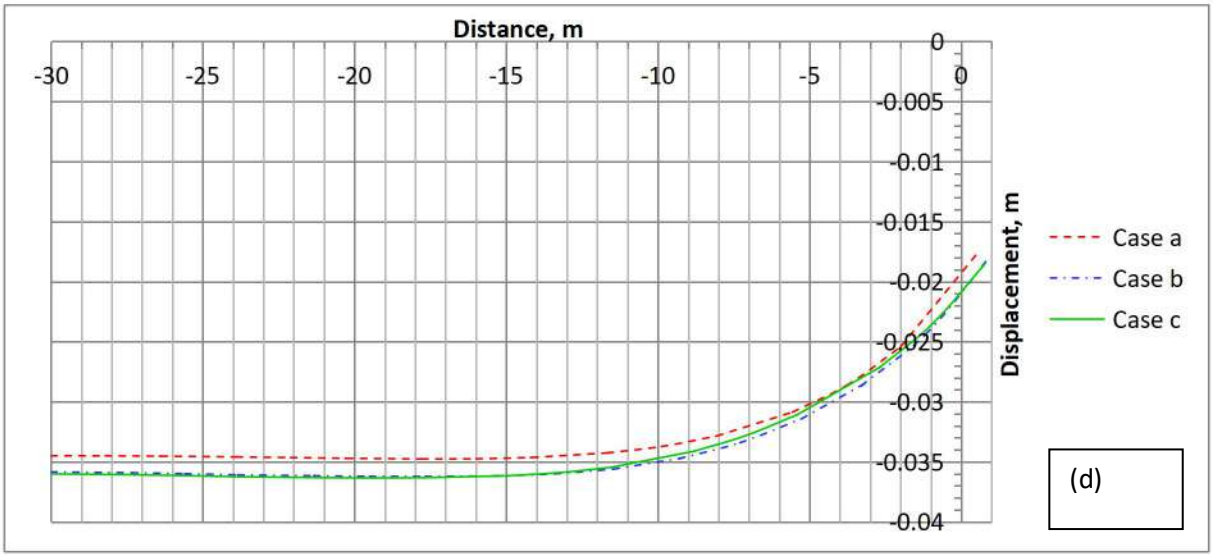
Distance, m
-30
-25
-20
-15
-10
-5
0
0
-0.005
-0.01
-0.015
-0.02
-0.025
-0.03
-0.035
-0.04
Displacement, m
Case a
Case b
Case c
(d)

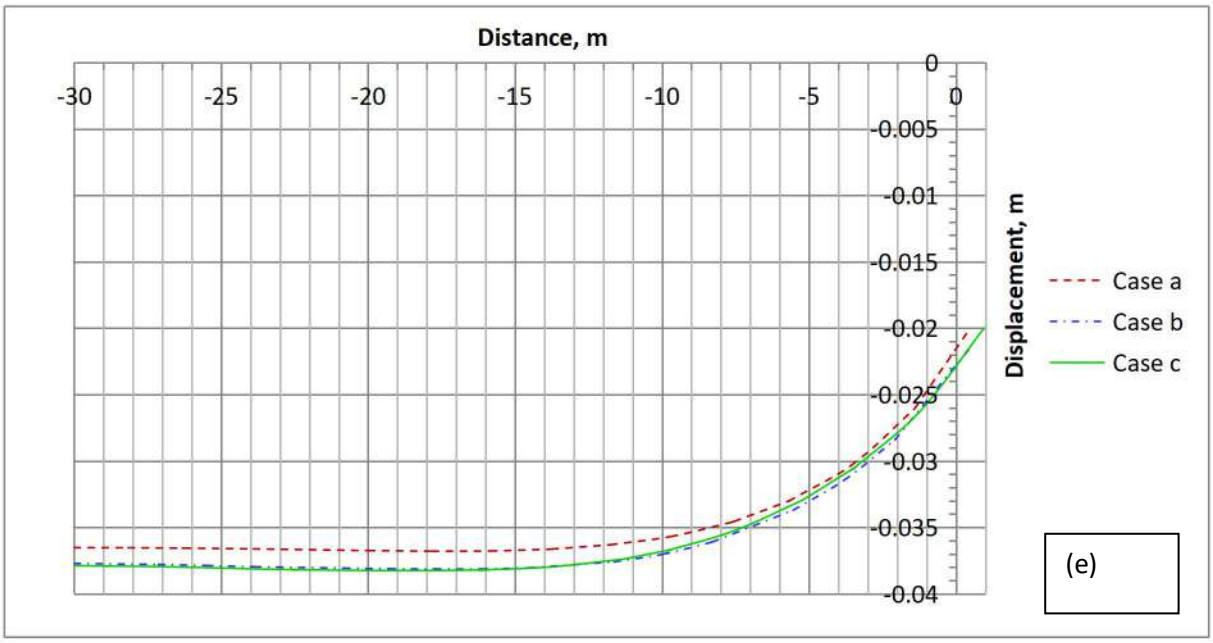

Fig 4.22– Comparison of computed vertical displacement from different models at the end of various stages (a) 1st (b) 3rd (c) 5th (d) 7th (e)8th

Horizontal displacement obtained for all the three models for first, third , fifth , seventh and last stage of excavation is shown Fig 4.23 (a-e).

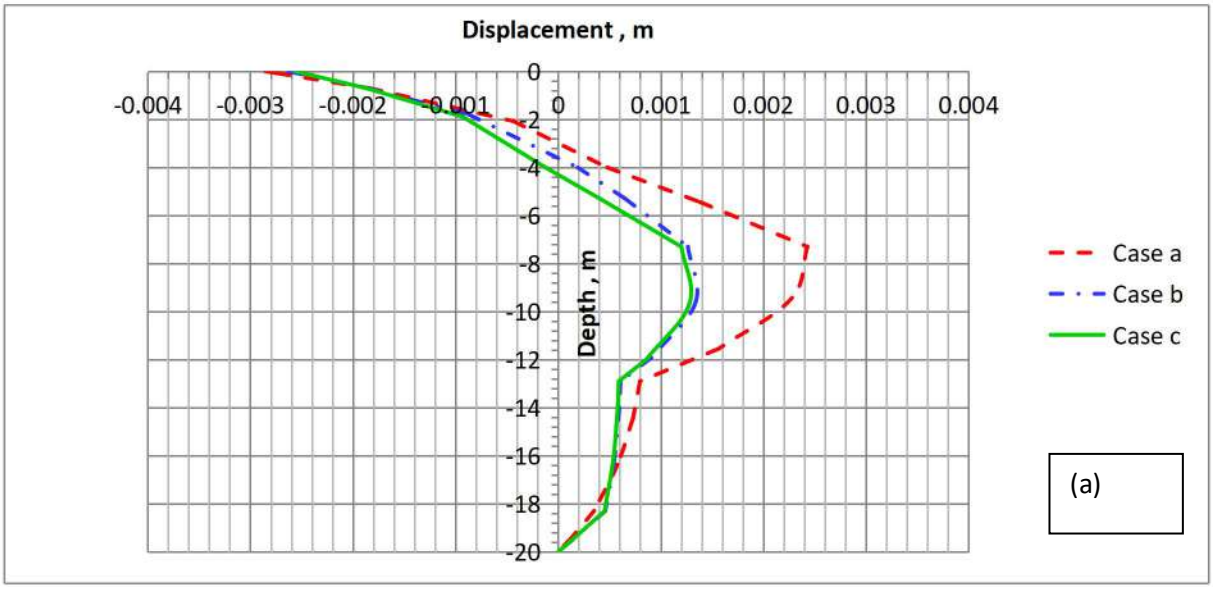

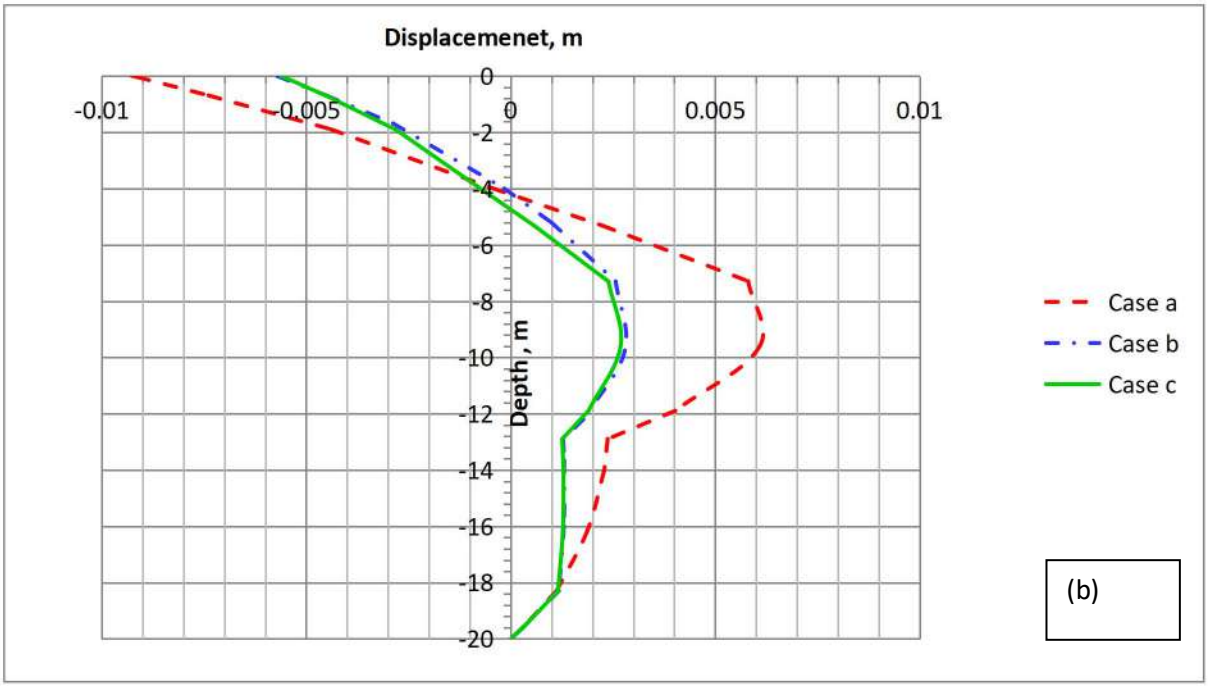
Displacemenet, m
-0.01
-0.005
0
0.005
0.01
0
-2
-4
-6
-8
-10
-12
-14
-16
-18
-20
Depth, m
Case a
Case b
Case c
(b)

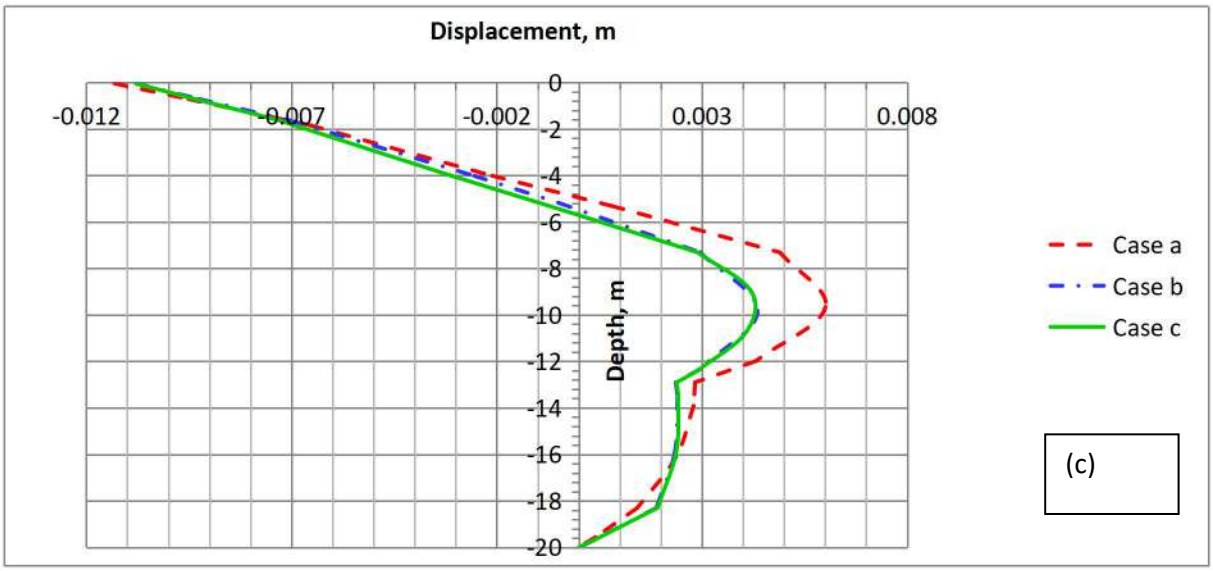
Displacement, m
-0.012
-0.007
-0.002
0.003
0.008
0
-2
-4
-6
-8
-10
-12
-14
-16
-18
-20
Depth, m
Case a
Case b
Case c
(c)

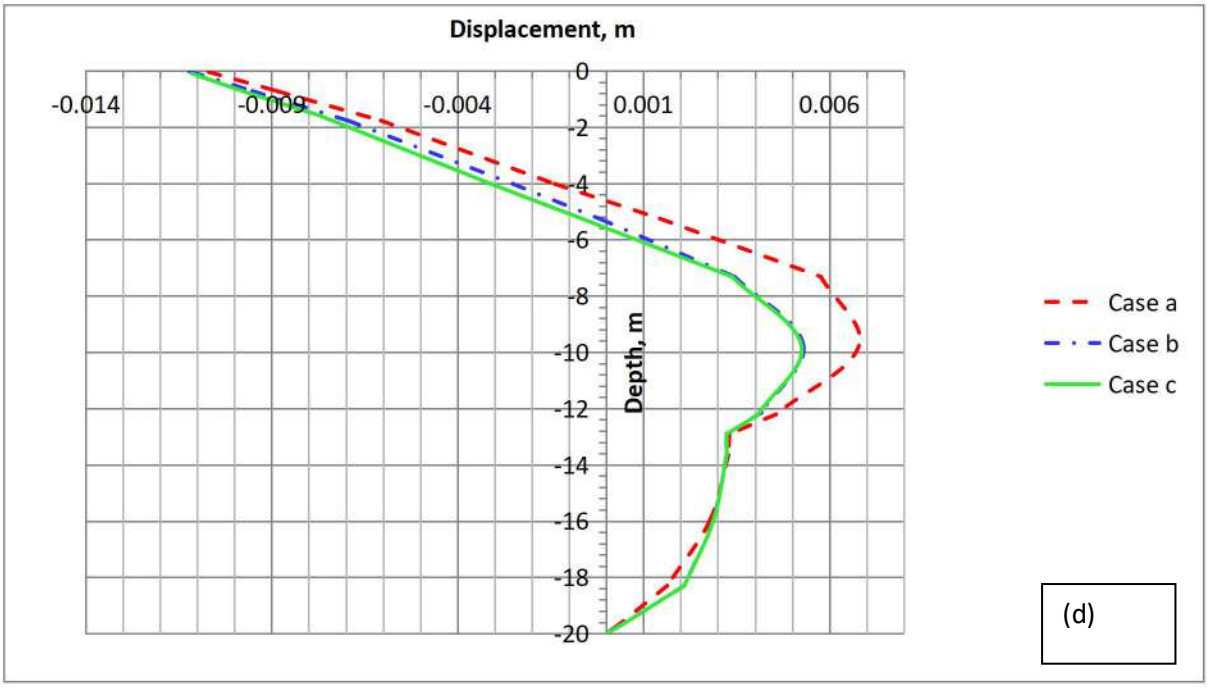

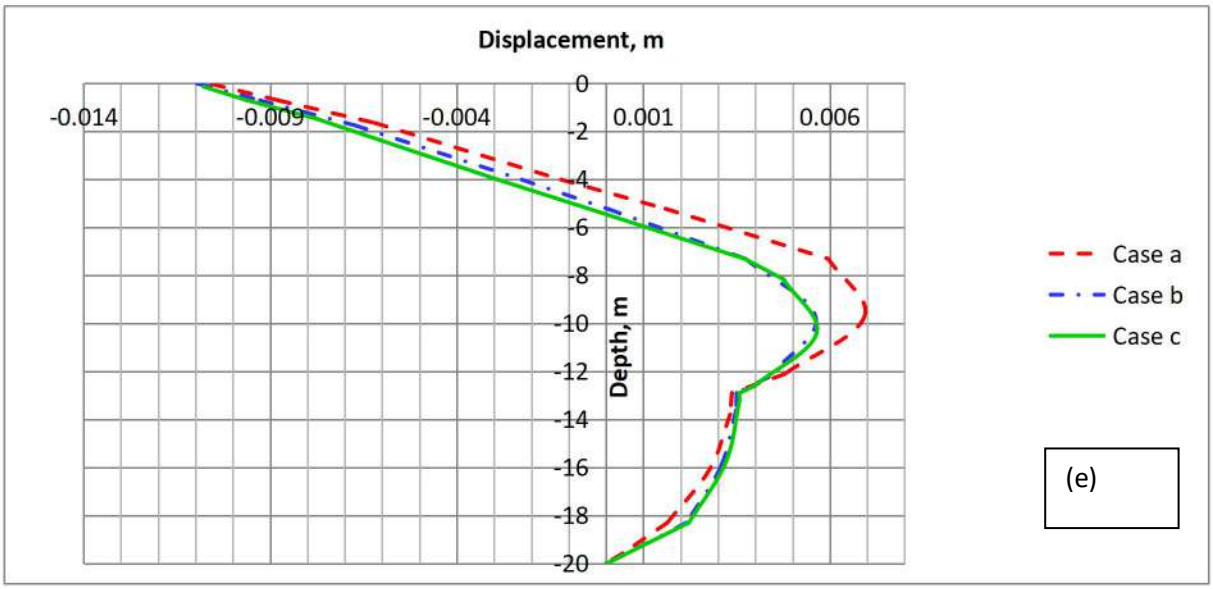

Fig 4.23– Comparison of computed horizontal displacement from different models at the end of various stages (a) 1st (b) 3rd (c)5th (d) 7th (e)8th

The comparison of results indicates that the horizontal displacement towards excavation increases as the depth of excavation increases and MC model predicts more displacement towards excavation. At the end of last stage, the displacement towards excavation computed by MC Model (Case a) is 6.9 mm at a depth of 9.7 m below the ground

level whereas the displacement computed by other two models are around 5.6 mm at depths of 9.7 m and 10.4 m respectively for Case b and Case c as shown in Fig 4.23 (e). The surface displacement computed by MC model is higher than that computed by the other two models during the initial phase of excavation as indicated in Fig 4.23 (a). However, towards the end of excavation, the other two models (Case b & Case c) predicts more surface displacement than MC model (Case a). The maximum surface displacement is computed at the end of 7^{th} phase which is 11.4 mm for the case c and reduces to 11 mm at the end of excavation.

4.4 Comparison of the results with field monitored data

The field instrumentation installed as described in Section 4.2 of this chapter was monitored during fifth stage of excavation at instrumentation I1 & I4 located at the center of the excavation. The horizontal displacement observed and that computed from case (c) are plotted in Fig 4. 24. The model computed value for the fifth stage of excavation indicates a surface displacement of 10.78 mm. The displacements that were observed at instrumentation location I1 and I4 are 8.8 mm and 8.17 mm respectively. The maximum displacement towards the excavation computed by Case (c) analysis is 4.2 mm at a depth of 9.0 m below ground level. However, the maximum displacement towards excavation observed at location I1 and I4 are respectively 1.7 mm at a depth of 8.0 m and 2.2 mm at a depth of 9.5 m below ground level.

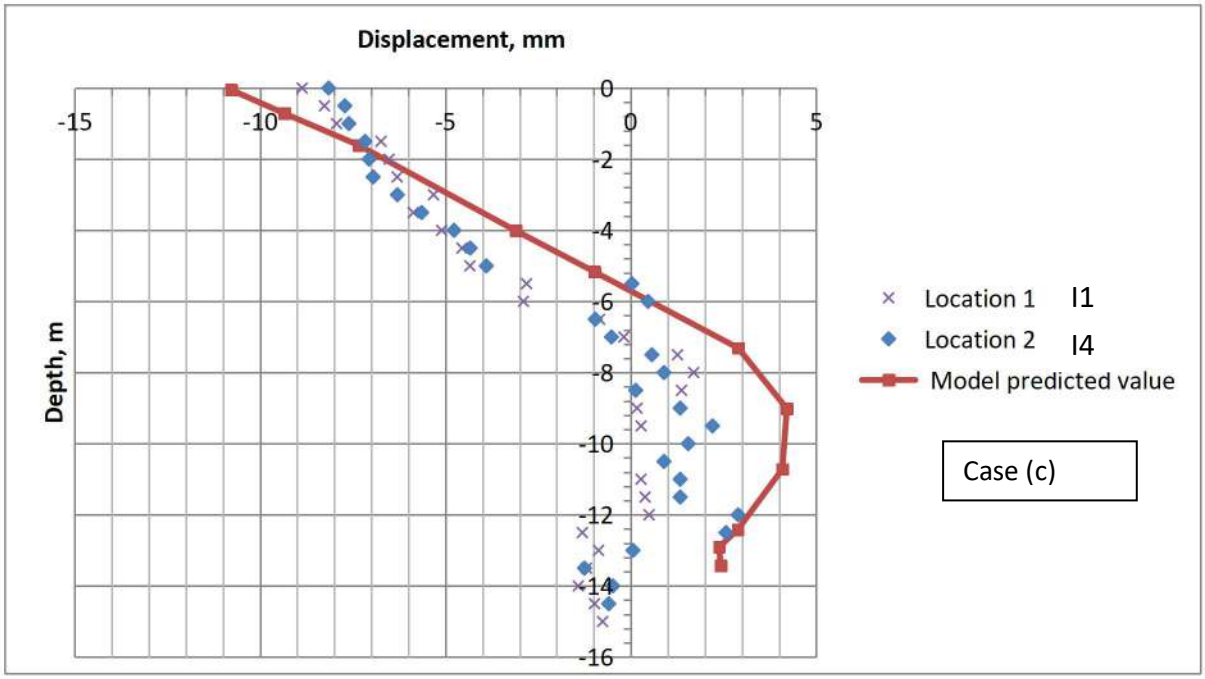

Fig 4.24 Comparison of computed and measured displacements at the end of 5th stage of excavation at the center for Case (c)

All the inclinometers were monitored during the last phase of excavation . The plot of observed variation of horizontal displacement as a function of depth at the end of last phase for centreand corner inclinometer is presented in Fig 4.25 (a&b). Results of the numerical analysis using various constitutive relations for the different cases (a) to (c) are also compared with the field results and shown in Fig 4.25 . Maximum surface displacement is observed at the inclinometer location I1 which is -10.86 mm. Surface displacement observed at I4 location is 8.18 mm. Surface displacements from other inclinometers at the locations I2 and I3 are 1.75 mm and 1 mm respectively. The maximum horizontal displacement towards excavation obtained from inclinometer locations I1, I2, I3 and I4 are 1.57, 5.67, 4.98 and 3.92 mm respectively. The corresponding depths are at a depth of 9.0, 9.5, 10 and 10.5 m respectively.

The surface displacement computed from the cases (a), (b) and (c) are nearly same and in agreement with that observed from the inclinometers at locations I1 and I4. However,

the surface displacement observed at location I2 and I3 are not close with the values computed by any of these methods. The maximum displacements observed towards excavation for instrumentation locations I1, I2, I3 and I4 are 1.85 mm, 5.67 mm, 4.98 mm and 3.92 mm respectively. The maximum displacement computed from the numerical analyses by cases (b) and (c) fairly matches with the observed results for inclinometer locations I2 and I3. It is also evident that the MC model (Case a) predicts a larger maximum displacement towards excavation.

Negative displacements observed in the top sandy layer is due to dilatency effect and negative dispalcements at corner of the excavation is small as shown in Fig 4.25 (a)while higher negative displacements were observed in center of the excavation as indicated in Fig 4.25 (b) .Upon comparison of these results, the corner effect of deep excavation is evident. The surface displacement is higher at the centre locations (I1 and I4) when compared to the instrumentation readings obtained from the locations I2 and I3 which are located close to the corner of the excavation. The displacements towards the excavation monitored from the instrument location I2 and I3 are comparable with that obtained from numerical analysis.

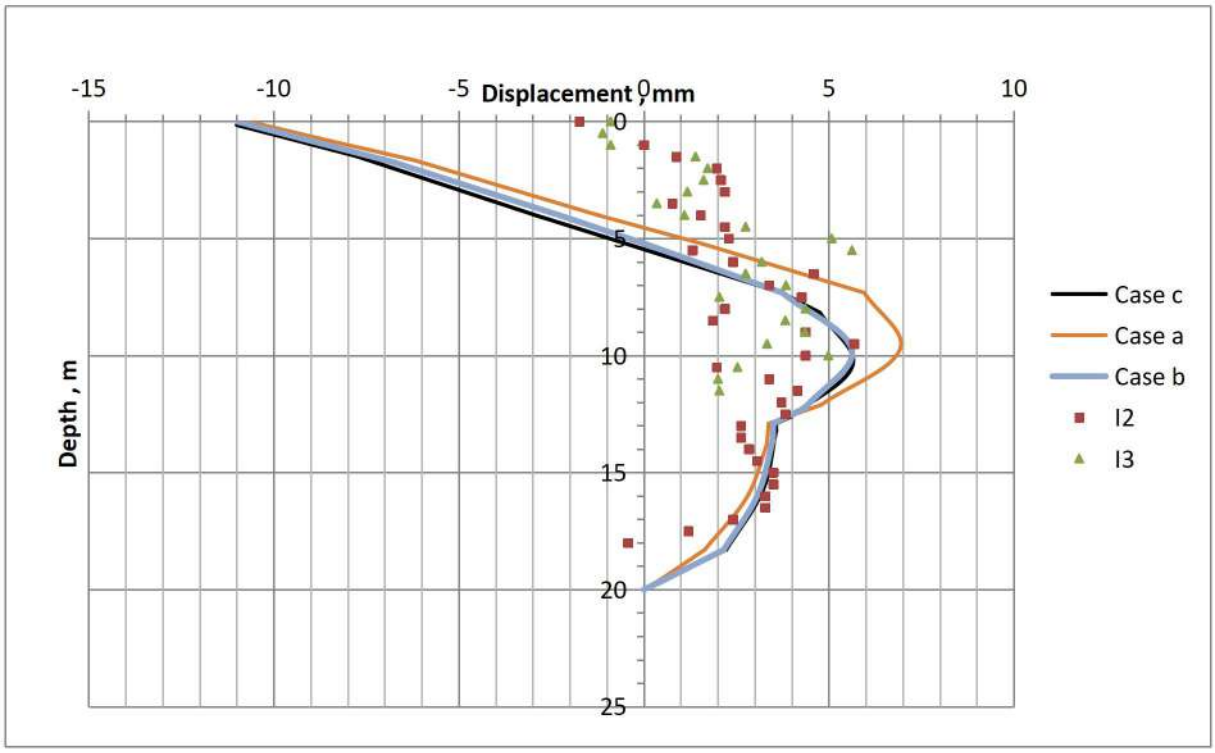

Fig 4.25 (a) : Comparison of computed and measured displacement for corner inclinometer (I-2& I-3) at the end of excavation

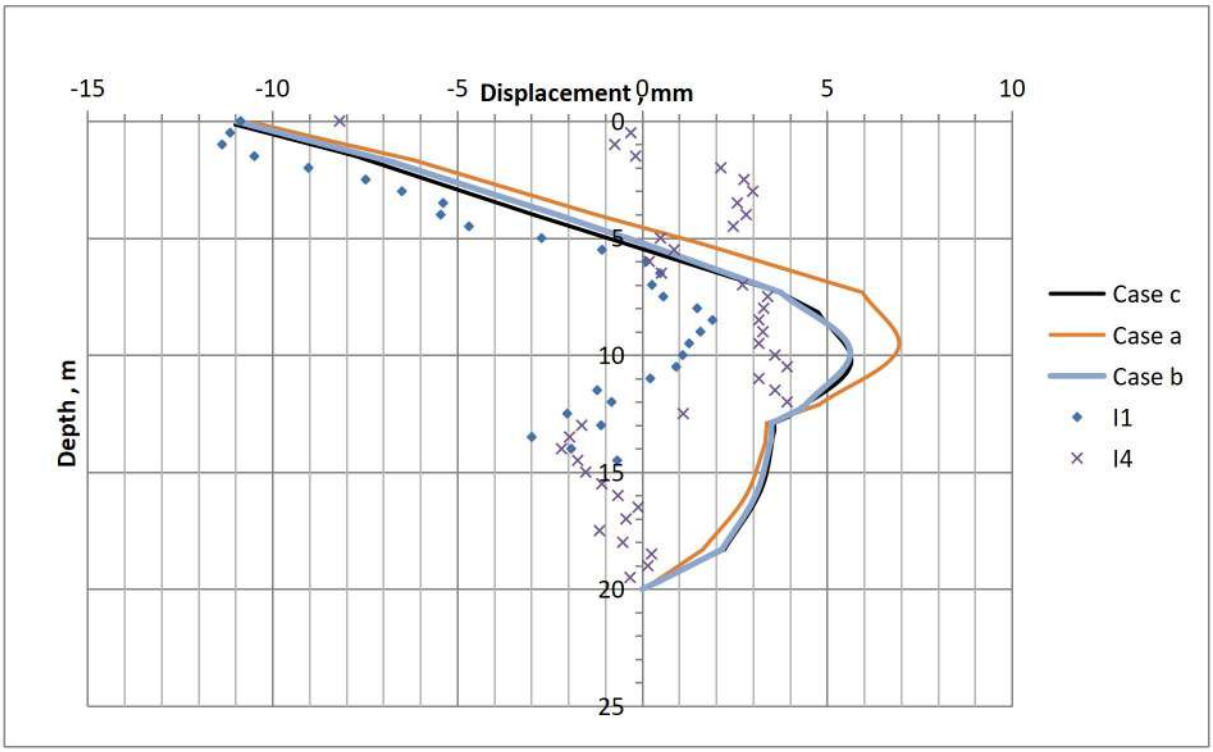

4.25 (b) : Comparison of computed and measured displacements for centre inclinometer (I-1 & I-4) at the end of excavation

However, the displacement observed towards the excavation from the instrument location I1 and I4 are less than that obtained from numerical analysis. In addition, negative displacements were observed below the maximum displacement point, which clearly indicates plane strain condition and corner effects of excavation. Corner effects of excavation in retaining wall are widely studied; however, the present study and calibration of the results with instrumentation readings established the corner effects in massive open excavation. Considering the close prediction of MC model with field monitored displacement values, accounting for dilatency and incremental increase of stiffness of sandy layer and HS Model for silty/clayey layer and residual soil was considered as the ideal model for predicting the performance of open deep excavation carried out in multi layered soil site.

As a part of settlement monitoring, benchmarks were kept at different distances from the excavation edge. The final stage settlement observed from field is compared with the model computed settlement case (c) and plotted in the Fig 4.26.

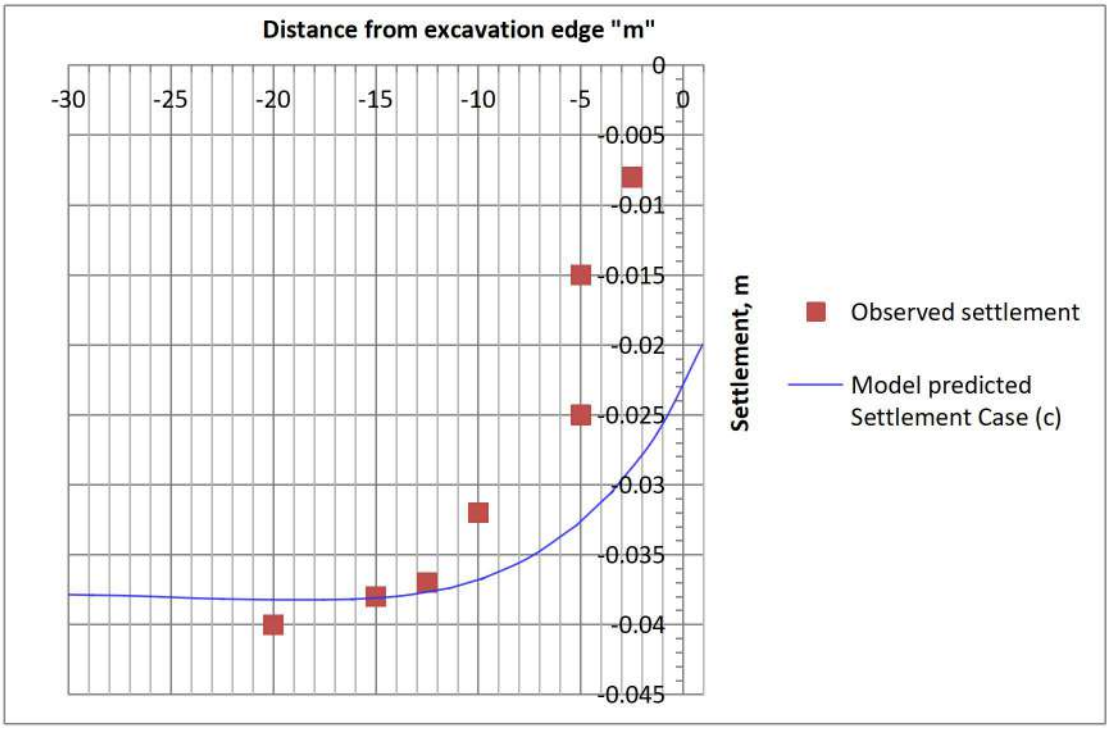

Fig 4.26 – Comparison of field monitored and model Case (c) computed settlement

The field monitored settlement in the primary settlement zone is less than the model computed value. However, beyond 10 m distance, the model computed values and field observed values are in reasonable agreement and the maximum settlement zone observed from the field is 40 mm at a distance of 20 m behind the excavation edge while the computed settlement is 38.24 mm at a distance of 17.5 m behind the excavation.

4.5 Parametric study on the effect of soil layer thickness

Since the study carried out used an idealized soil profile, a parametric study was carried out considering the variability of soil thickness and compared with the field observations. From the bore holes, it was observed that the thickness of sandy layer is more than the earlier assumed soil profile in the East side and thickness of silty/clayeysand and residual layers are more than the earlier assumed soil profile in the West side of the site. Accordingly, for the parameteric study two different soil profiles as in Fig 4.27 (a) and Fig 4.27 (b) were considered for the East and West sides in line with the actual profiles.

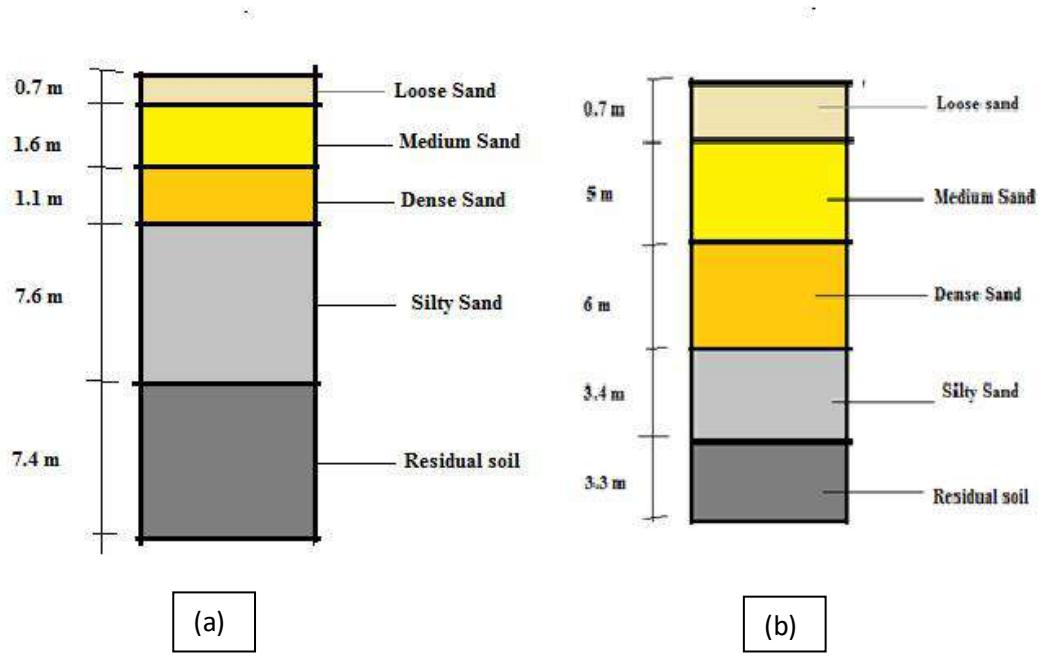

Fig : 4.27 Soil profiles considered for (a) East (b) West

The displacements were computed for both the soil profiles using the model Case (c) in PLAXIS and the results are presented in Fig 4.28. The properties of soil assumed were same as defined in the previous sections. The analysis indicates that as the depth of sandy layer increases, surface displacement decreases and displacement towards excavation increases. The surface displacement observed during the last stage of excavation, in the case of soil profile considered for East side is 5.5 mm and displacement towards excavation is 6.62 mm at a depth of 11.0 m below the ground level. In case of the soil profile considered for West the surface displacement is 9.9 mm and the displacement towards excavation is 3.95 mm at a depth of 9.9 m below the ground level. Whereas, the surface displacement and displacement towards excavation for idealized soil profile is 11.07 mm and 5.6 mm at a depth of 10.4 m below edge respectively.

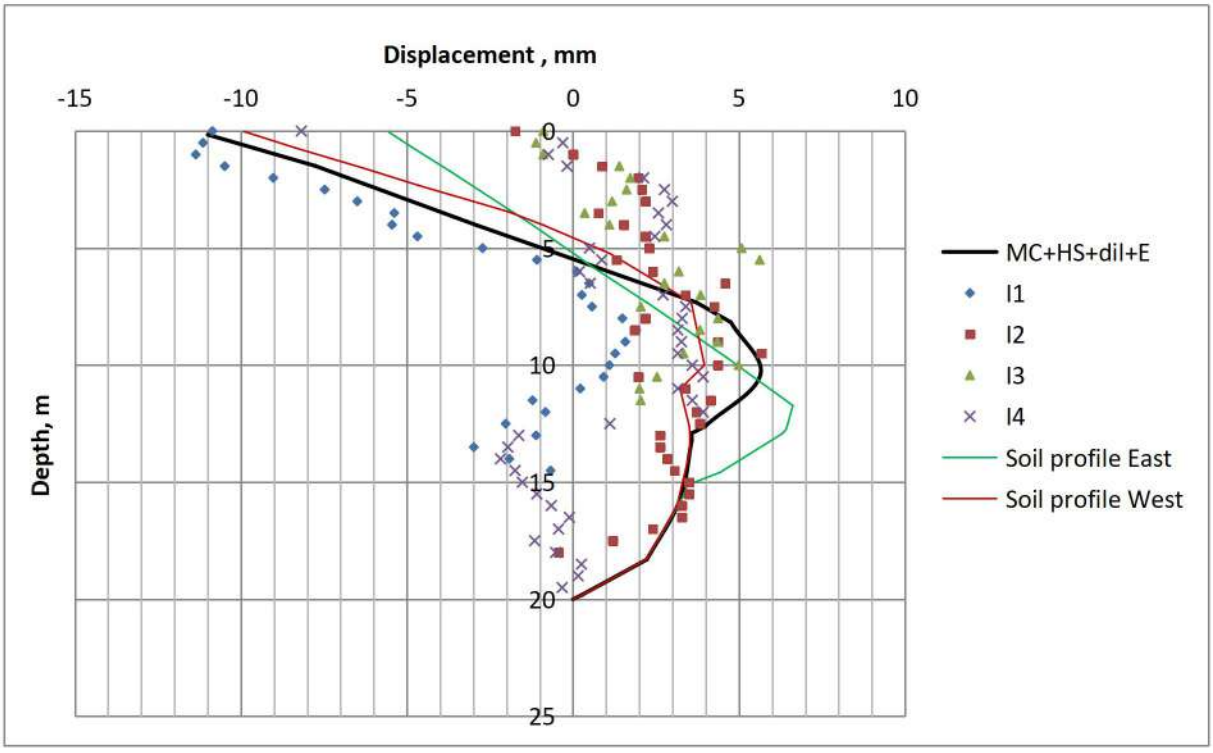

Fig 4.28 : Displacement of soil mass computed using Case (c) for various soil thickness

The settlement observed behind the excavation for various soil thicknesses is presented in Fig 4.29 shows that the maximum settlement is higher for the West profile where

the thickness of sandy layer is higher and is lower for the East profile where the thickness of silty/clayey sand and residual soils are higher. The maximum settlement observed is 33.8 mm at a distance of 19.5 m behind the excavation for the West profile, while for the East profile it is 31.89 at a distance of 16.17 m behind the excavation edge. However, these are less than that computed for the idealized soil profile that is 38.24 mm at a distance of 17.5 m behind the excavation edge. This analysis indicates the idealized soil profile predicts conservatively the surface settlement and displacement in comparison with analysis accounting for the soil thickness variation.

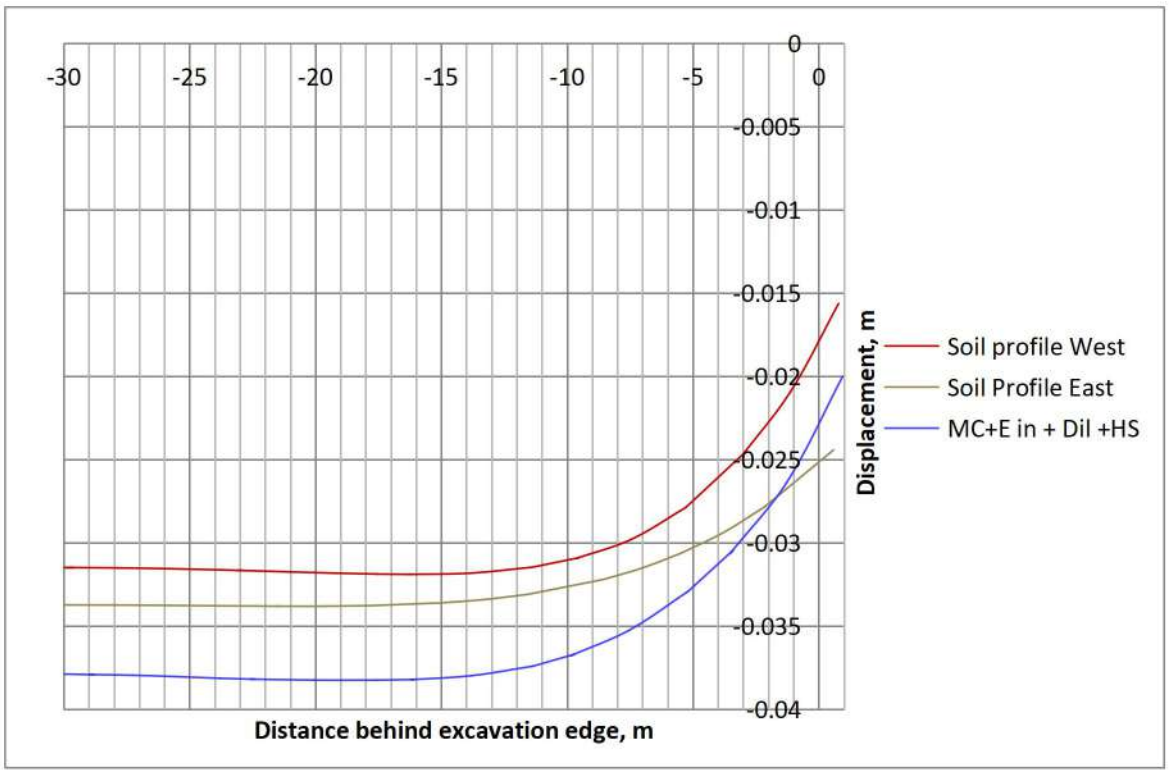

Fig 4.29: Vertical displacement of soil mass for various soil thicknesses at the end of excavation

4.6 Evaluation of sand stiffness through back calculations

Stiffness evaluation of sandy soil is usually carried out using empirical correlations with SPT N values as it is difficult to obtain the undisturbed soil samples. Commonly used empirical relations are the ones proposed by Bowles (1988) and Kulhawy and Mayne (1998)

as already described in Chapter 3. The relation proposed by Kulhawy and Mayne predicts lower *E* value compared to that obtained from Bowles. In the analysis presented in the previous section, stiffness values proposed by Kulhawy were used. The comparison of field monitored and model computed displacement in Fig 4.30 indicates that the displacement profile observed in sand is in reasonable agreement with that computed using the stiffness estimated by the lower bound equation, i.e, Kulhawy et al., (1998). However, for silty/clayey sand and residual soil, the observed displacement matches with that computed by upper bound values of Bowles (1988). However, the numerical value of displacement computed by lower bound *E* values is not in agreement with that of observed displacements in sandy soil.

Considering this, a series of back calculations were performed in the PLAXIS model by varying the stiffness of sandy layer till a depth of 7.5 m and the model computed displacement were matched with that observed from the field. While carrying out the back calculations, other parameters such as cohesion and angle of internal friction were kept unchanged. In this study, first two analyses were performed; one with lower bound and another with upper bound *E* values obtained from the range for both the equations. As a third case, *E* value of sandy layer was varied and displacement was computed. The computed displacements are shown in Fig 4.30. In this case, stiffness of loose sandy layer, medium sand and dense sand are considered as 4000 kPa , 10000 kPa, 54000 kPa respectively and displacement were evaluated and compared with field observed values. These *E* values were corresponding to N values of 9, 27 and 48 of loose sand, medium sand and dense sand as observed from the boreholes.

The surface displacement computed is − 11.97 mm and is in reasonable agreement with the field monitored values. Hence, the actual insitu stiffness of loose, medium and

dense sandy layer are estimated as function of SPT N value and is given below in equations 4.2, 4.3 and 4.4 respectively .

$$E = 166\,(N + 15)$$ -------- 4.2

$$E = 233\,(N + 15)$$ ---------4.3

$$E = 860\,(N + 15)$$ ---------4.4

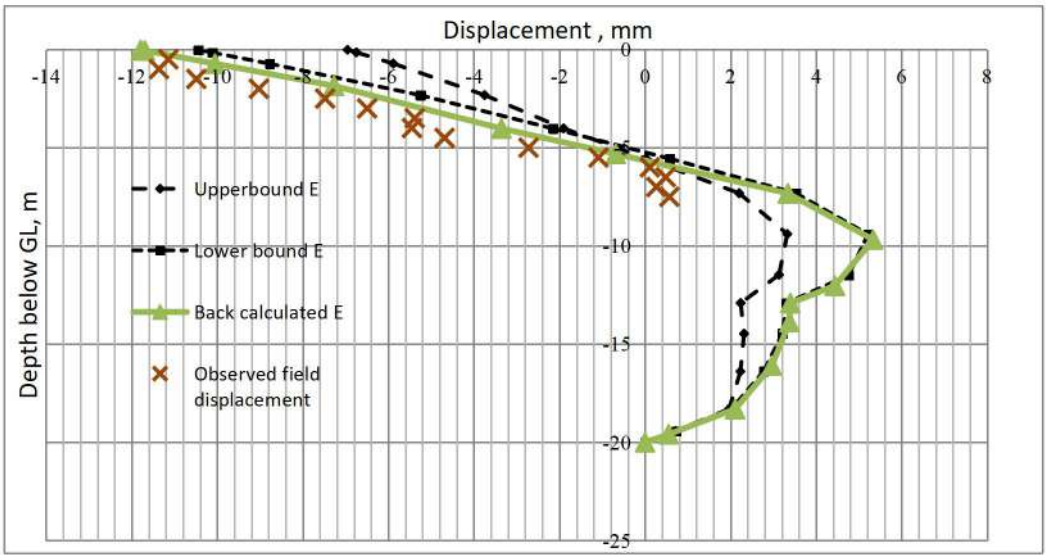

Fig 4.30 – Displacement profile with back calculated *E* value

This study indicated that that the stiffness of loose and medium sandy soil is overestimated by the conventional correlations available and the stiffness of dense sand layer is underestimated by relations. Site specific empirical relations were proposed which can be used for site of similar geology and characteristics.

4.7 Summary

The analysis carried out for the open excavation indicated that for a multi layered soil site, single conventional constitutive model is not adequate to describe the deep excavation behavior. A combination of constitutive models namely MC model accounting for the dilatency and incremental increase in stiffness of the soil layer and HS model for silty/clayey sand layer is required to predict excavation behavior. Conventional MC model is not always

conservative in predicting the settlements and higher order models are essential. The study indicated that the influence of excavation is felt upto a distance of 20 m behind the excavation which is nearly same as the depth of excavation. Also, the back calculation indicated that the stiffness of loose and medium sandy soil is overestimated by the available empirical correlations and the stiffness of dense sand layer is underestimated by relations.

Chapter 5

Evaluation of stiffness of backfilled soil through numerical analysis

Studies reported in the previous Chapter indicated the importance of accurate determination of stiffness properties in predicting the behaviour of excavation. Even though empirical correlations are available for determining the stiffness properties of natural soil deposits, field investigations explained in Chapter 3 are commonly used to evaluate the stiffness of engineered backfill soil. However, as seen it Chapter 3, these values show wide range of variation and need to be verified before using for prediction of deep excavation behaviour. In an attempt to validate the stiffness properties of backfilled soil, numerical analysis was carried out for a deep excavation near an existing facility and results were compared with that obtained from field instrumentation. A series of back calculations were performed in PLAXIS by varying stiffness of backfilled soil matching the instrumentation displacements and field displacements. The results of this study are presented in this present chapter.

5.1 Definition of the problem

As a part of infrastructure development, an 18.4 m deep excavation was carried out adjacent to an ongoing construction supported on engineered backfill soil. Proximity of the excavation to the ongoing construction facility necessitates a steep slope of 1 V: 1 H for excavating the top layer of backfilled soil. This slope is steeper than the normal slopes used for open excavations discussed in Chapter 4. In this study, strength and stiffness properties of engineered back filled soil was obtained from chapter 3. Since the proposed excavation is close to the ongoing construction, inclinometers were provided for monitoring the displacement of slope so that necessary timely measures can be adopted to ensure the safety of slopes and adjacent structures. The effect of stiffness of engineered backfilled soil on the

displacement was assessed by carrying out a parametric study by varying the stiffness properties of backfilled soil. A series of back calculations were performed by varying the stiffness properties, and comparing the displacement obtained from finite element analysis with that obtained from field, till a reasonable agreement was obtained.

The site is located adjacent to the infrastructure facility and comprises beach deposits. The geotechnical investigation carried out at the site indicated that it consists of loose to medium sand followed by dense sand. This sand layer is followed by silty sand/clayed soil and residual soil. Hard rock is available at a depth of 15 to 20 m below the ground level in most of the area. Idealized bore log is shown in Fig 5.1. This idealized profile is different from that of open excavation described in Chapter 3 and arrived based on the specific bore hole details adjacent to the on going construction.

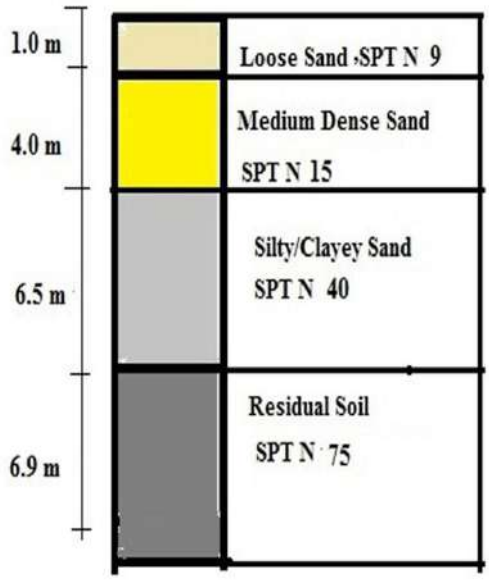

Fig 5.1 – Typical soil profile at the site

The design SPT N values are also given in the Fig 5.1. The SPT N values of the top layers are low and not suitable for supporting heavy load transfer form superstructure. Therefore, the top 9.5 m of the profile, comprising the loose and medium sandy layer and part of the slity sand layer,

was removed and replaced with engineered backfill upon which the foundation for the new infrastructure was constructed. Subsequently, a deep excavation of 18.4 m was carried out near to this ongoing construction to construct a nuclear safety related structure. The available horizontal distance between the ongoing construction and excavation site was only 5.0 m and hence conventional normal slopes of 1 V: 2 H could not be provided. Therefore, a nearly 1 V: 1 H slope was adopted for excavation in the top layer of backfill soil and 1 V: 2 H slope was provided for excavation in silty/ clayey sandlayers. Excavation of the bottom residual soil layer was carried out with a slope of 1 V: 1.35 H to reach the required depth of foundation. Intermediate berms of 2.0 m were also provided in two stages to increase the stability of slope. Water table was observed at a depth of 15.0 m below the existing ground level. To facilitate the excavation below water table, after reaching the level, it was lowered by continuous dewatering.

The idealized problem indicating soil layers and location of inclinometer is provided in Fig 5.2. The sequence of construction, deep excavation and dewatering was analysed in PLAXIS using constitutive laws namely Mohr-Coulomb (MC) Model and Hardening Soil (HS) Model as defined in Chapter 2 using the soil properties elaborated in Chapter 3. Since the backfilled soil is silty in nature dilatency effect was not accounted.

5.2 Numerical analysis of the problem

The excavation problem defined in the previous section and idealized in Fig 5.2 was modelled in PLAXIS 2D and stage analysis was carried out to evaluate the effect of excavation. In the first stage, before commencement of excavation for infrastructure building, a uniformly distributed construction load of 10 kN/m^2 arising from general construction activity was assigned. Subsequently in the second stage, the top loose sandy layer, medium sandy layer and silty/clayey sandy layer was removed upto top 9.5 m and engineering backfill

was carried out. This was carried out to simulate the actual site condition of engineered backfilled soil.

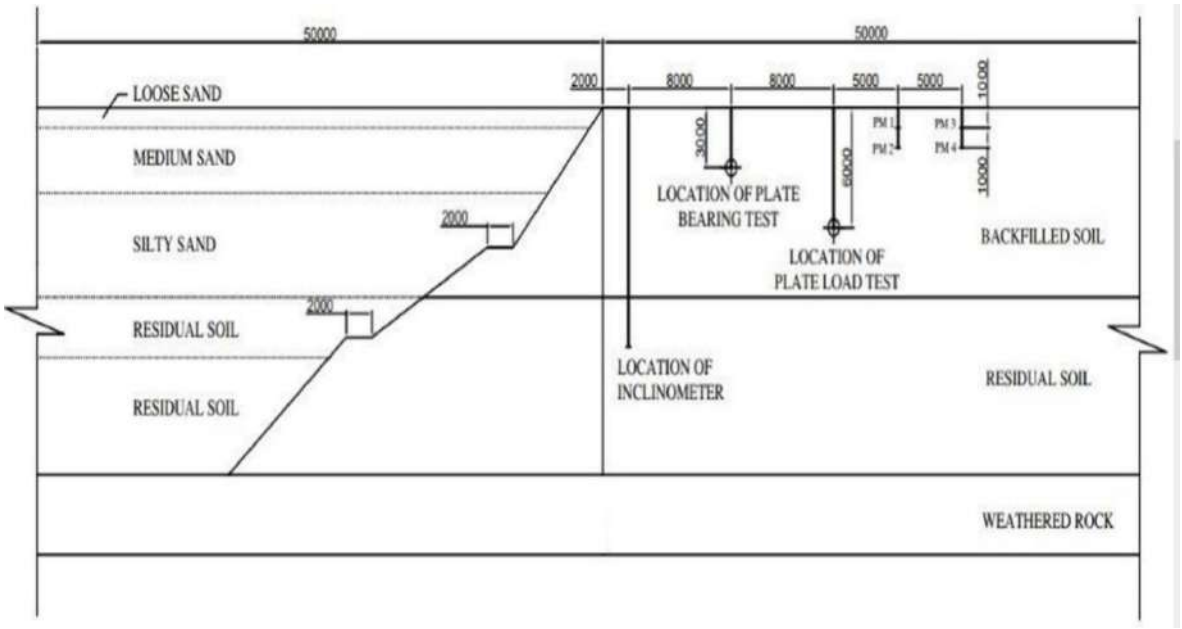

Fig 5.2 – Excavation profile with location of field tests

At this stage, the construction of foundation of the facility was simulated by providing a uniform load of 50 kN/m^2 accounting the load coming from the foundation. Subsequently a deep excavation of 18.4 m was carried out near to this existing ongoing construction. As a part of this excavation, in the third stage, top loose sandy layer of 1.0 m thick was excavated and effect of construction was simulated by increasing the construction load to 55 kN/m^2. In the fourth stage of excavation, medium sandy layer was excavated up to 5.0 m and construction load was increased by an increment of 10 kN/m^2 to 65 kN/m^2. In fifth stage, silty/clayey sandy layer was excavated up to 9.5 m below the ground level. During sixth phase of excavation, residual layer was removed upto 12.5 m and during the last phase, excavation was carried out upto a depth of 18.4 m below ground level. Construction load was increased to 85 kN/m^2 during the last stage of excavation to account for construction of super structures. This staged excavation problem was idealized as a plane strain problem and analyzed using finite element method in PLAXIS software using soil parameters described in

the previous chapter. 15 node triangular elements were used for descretization of the soil volume. Typical mesh of the excavation at the end of excavation is given in Fig 5.3. Total number of elements in the numerical model is 214. Standard fixities were adopted for the model boundary where vertical geometry line in the model is assumed with a horizontal fixity and horizontal geometry line with a total fixity. Finite element analysis was carried out using 12 Point Gauss Integration method. Sequential drained, plastic analysis was carried out for predicting the behaviour of open deep excavation. Initial stresses were generated using K0 (Earth pressure at rest) procedure. Parameters required for MC model and HS model are indicated in Tables 5.1 and 5. 2 respectively.

Table 5.1: Strength and stiffness properties of various soil layers for MC Model

Layer	***Design SPT N value***	***Drained Cohesion (kPa)***	***Drained angle of internal friction***	***Young's Modulus in kPa***	***Dry density kN/m^3***	***Saturated Density kN/m^3***
Loose Sand	9	0	28	4500	16	19.68
Medium Sand	15	0	32	15200	16	19.68
Silty/clayey Sand	40	29	30	17600	18	20.88
Residual Soil	75	25	31	75000	18	20.88
Weathered rock	>50	30	31	500000	20	22
Backfill soil		5	30	8000	18	20.88

The finite element model is shown in Fig 5.3 indicating the thickness of various layers and depth of excavation.

Table 2: Parameters of backfilled soil for HS Model

Parameter	***Backfilled soil***
Secant stiffness (E_{50}^{ref}) kN/m^2	8000
Tangent stiffness (E_{oed}^{ref}) kN/m^2	6400
Unloading stiffness (E_{ur}^{ref}) kN/m^2	24000
Poisson Ratio (v)	0.20
Poisson Ratio (v_{ur})	0.20
Power for stress level dependency (m)	0.50

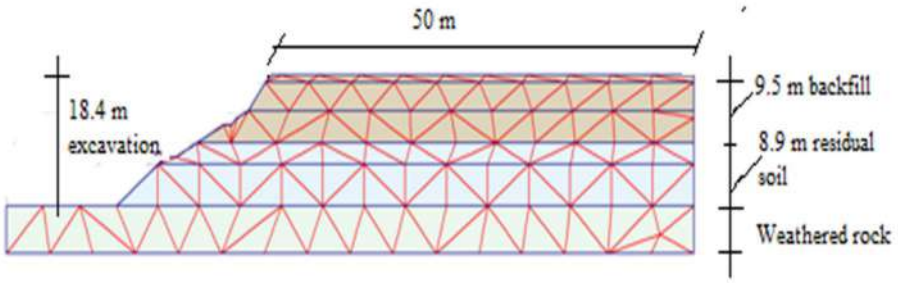

Fig 5.3 Finite element model of the excavation

5.3 Results of Numerical analysis

The excavation problem was analyzed by MC model using soil properties defined in Table 5.1 to predict the horizontal displacements before commencement of excavation and at the final stage of excavation. The displacement profiles are shown in Fig 5.4. Maximum horizontal displacement computed during initial phase before the commencement of excavation is - 1.82 mm (negative sign indicates the displacement is towards slope side) at a depth of 5.0 m below ground level. At the final stage of excavation, the displacement is + 14 mm (towards excavation side) at a depth of 9.5 m below ground level. The displacement

contours at the initial and final stages of excavation are shown in Fig 5.5 (a) & (b) respectively.

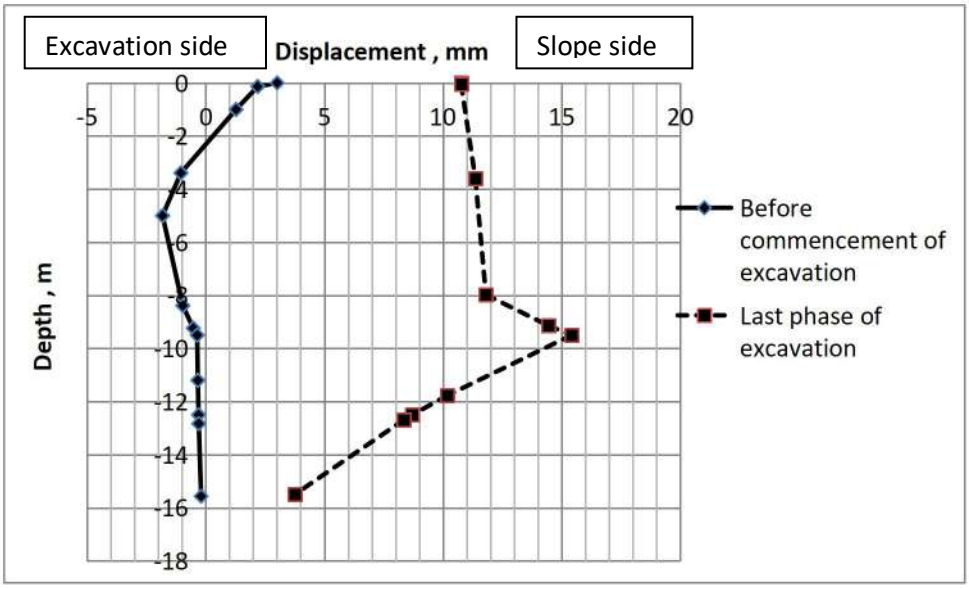

Fig 5.4 - Horizontal displacement profile obtained from MC Model for stiffness value of 8000 kPa

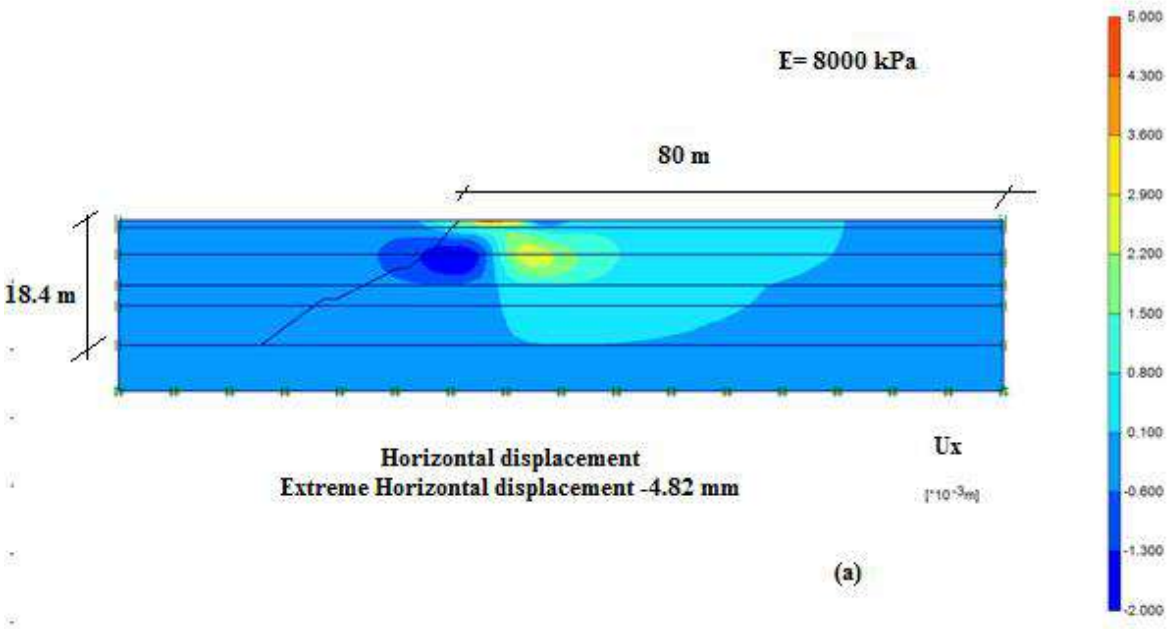

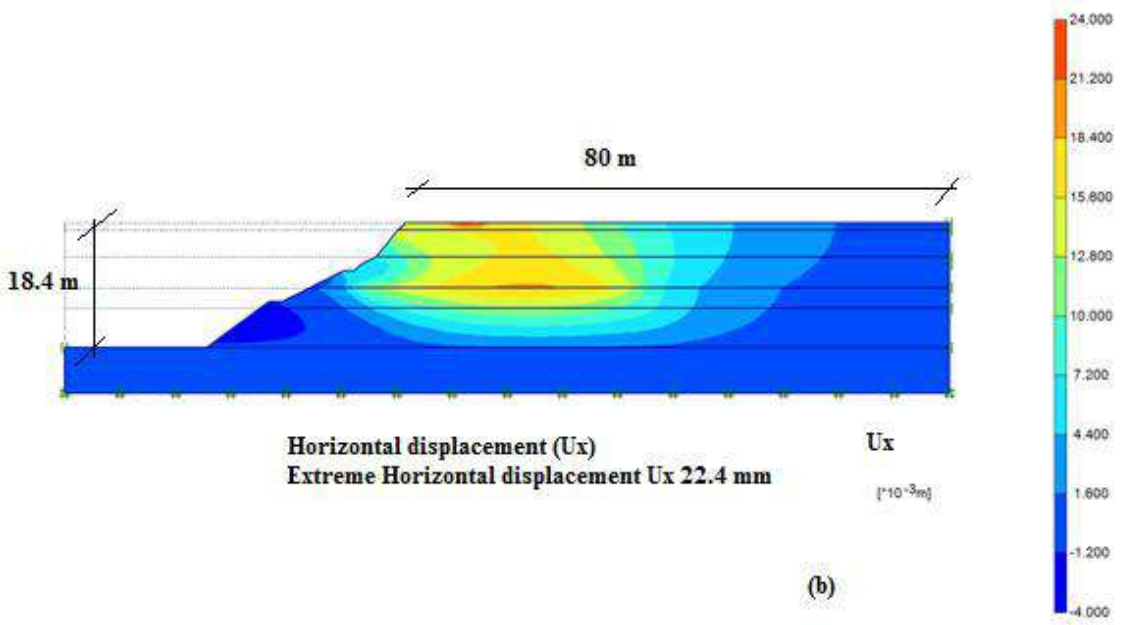

Fig 5.5: Displacement contours obtained with E = 8000 kPa at (a) Before commencement of excavation and (b) after last phase of excavation

As the stiffness *(E)* of the backfill soil obtained from various investigations shows a wide variation, in order to account for the effect of stiffness in predicting displacement, a parametric study was performed by varying the stiffness from 8000 kPa to 30000 kPa using MC model. However, other model parameters like cohesion and angle of internal friction were not varied. The displacement obtained for each case using MC model indicates that as *E* value increases, the computed displacement is away from the excavation face. The displacement contour obtained at the last phase of excavation for *E* values of 10000 kPa to 30000 kPa are shown in Fig 5.6 (a-c).

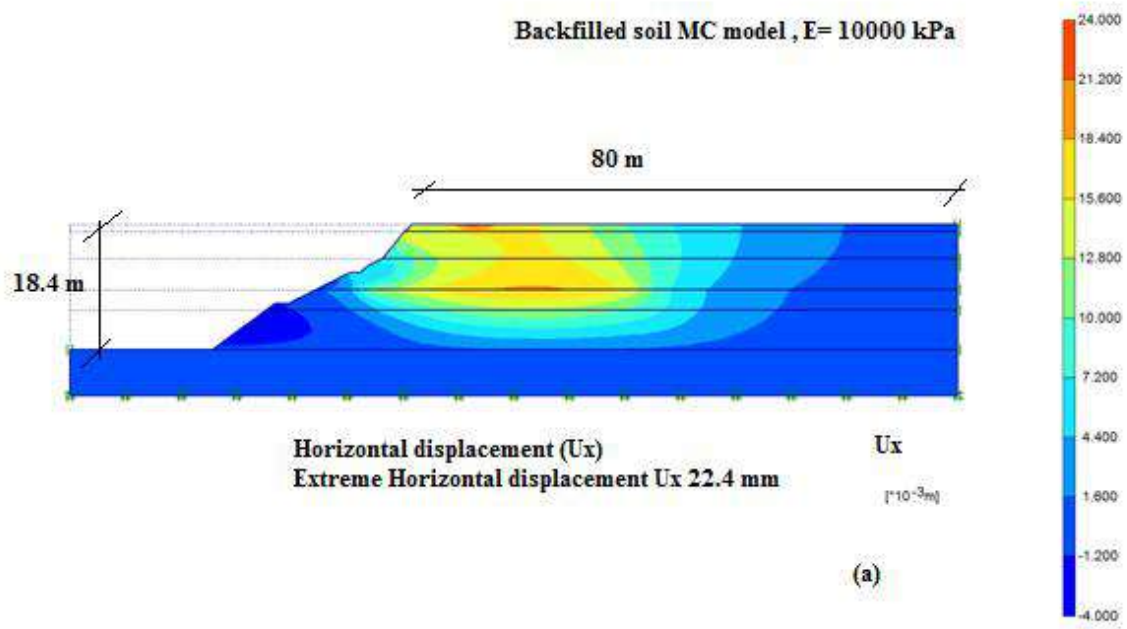
Backfilled soil MC model , E= 10000 kPa
80 m
18.4 m
Horizontal displacement (Ux)
Extreme Horizontal displacement Ux 22.4 mm
Ux
[*10^-3m]
24.000
21.200
18.400
15.600
12.800
10.000
7.200
4.400
1.600
-1.200
-4.000

(a)

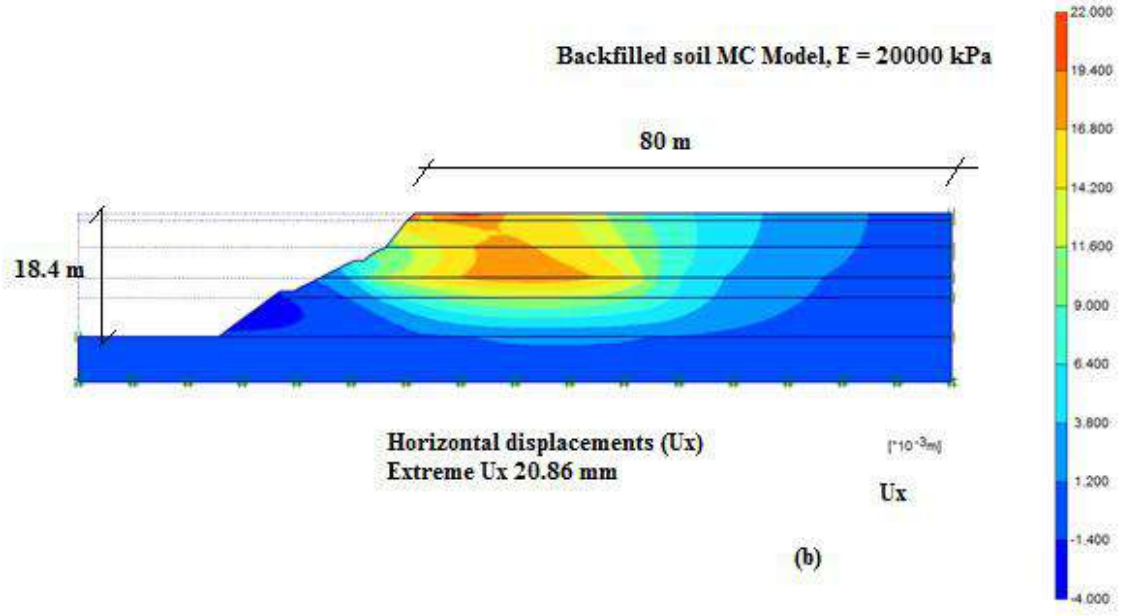
Backfilled soil MC Model, E = 20000 kPa
80 m
18.4 m
Horizontal displacements (Ux)
Extreme Ux 20.86 mm
[*10^-3m]
Ux
22.000
19.400
16.800
14.200
11.600
9.000
6.400
3.800
1.200
-1.400
-4.000

(b)

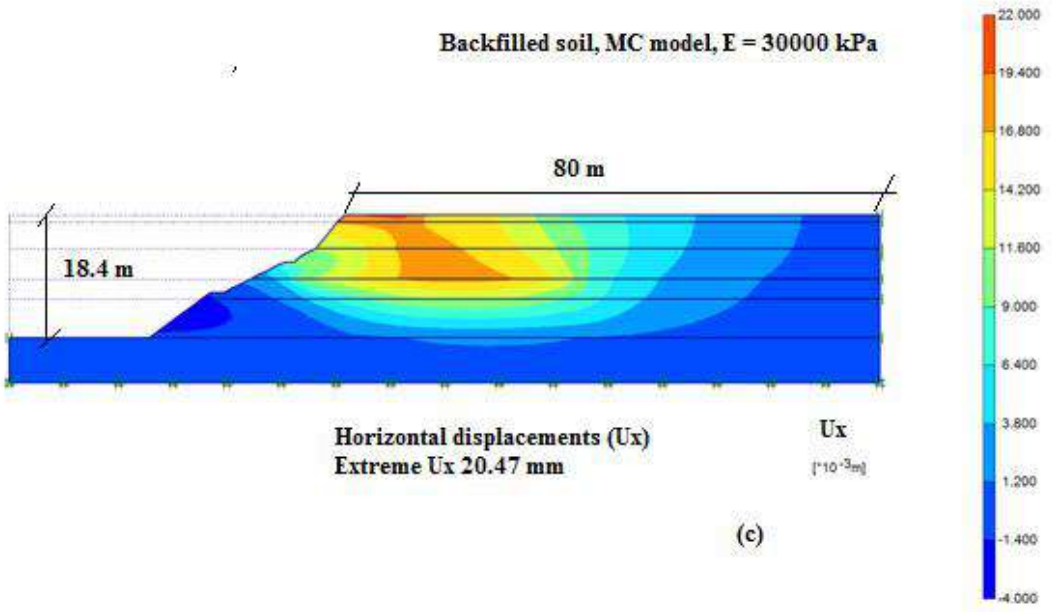

Fig 5.6 - Displacement contours during last phase of excavation for backfilled soil using MC model with (a) E= 10000 kPa (b) E = 20000 kPa and (c) E = 30000 kPa

The computed horizontal displacement profiles are shown in Fig 5.7. Surface displacement varies from 10.7 mm to 18 mm showing wide variation indicating significance of soil stiffness in predicting the behaviour of excavation and surface displacement. The extreme displacement is found to decrease and stiffness of soil increases however, the surface displacement increases as stiffness value increase. Displacement profile indicates that for low value of *E*, displacement is relatively towards the slope and as *E* value increases the displacement increases. Surface displacements for higher *E* values are almost same.

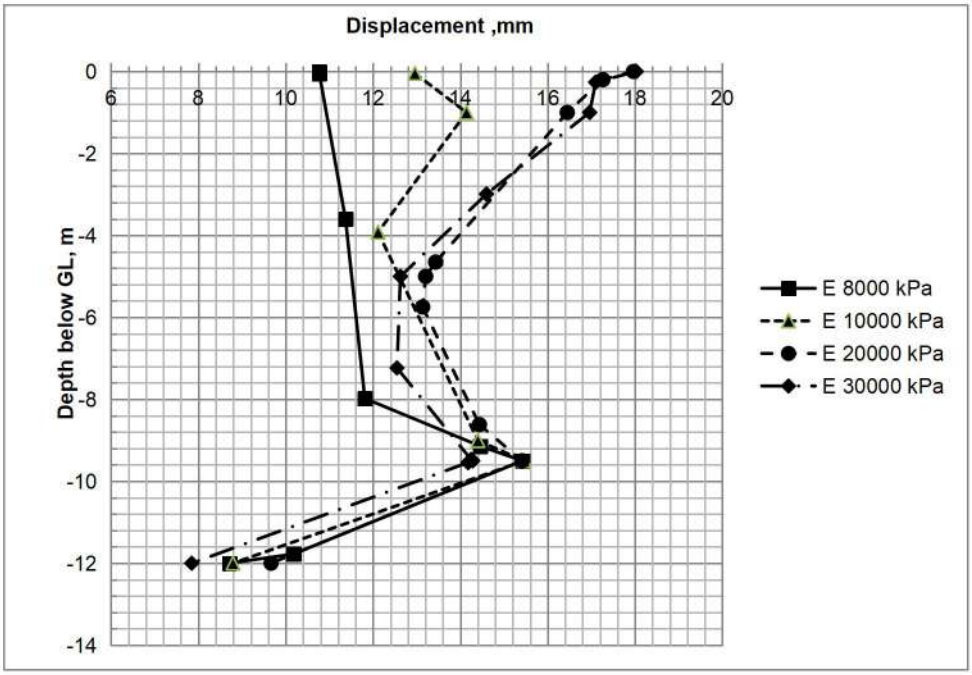

Fig 5.7 - Horizontal displacement profile for backfilled oil obtained from MC model for various stiffness values

Surface settlements for each case of *E* are also computed from numerical analysis and indicated in Fig 5.8. The surface settlement behind the excavation decreases as the stiffness *E* increases as expected. Low *E* value (8000 kPa) indicates surface heaves of 9 mm at a distance of 4.6 m away from the excavation. For E = 8000 kPa, the maximum surface settlement observed is around 14.5 mm at a distance of 18.0 m behind the excavation edge. For *E* = 30000 kPa, it is − 13 mm at a distance of 7.0 m behind the excavation. Even though the order of settlement is more or less matching for different E values, the location at which maximum settlement occurs widely differs. For higher *E* values, the location of maximum settlement is close to excavation edge. This wide variation obtained in displacement and surface settlements locations indicates the importance of accurate estimation of soil stiffness and importance of site characterization in excavation design.

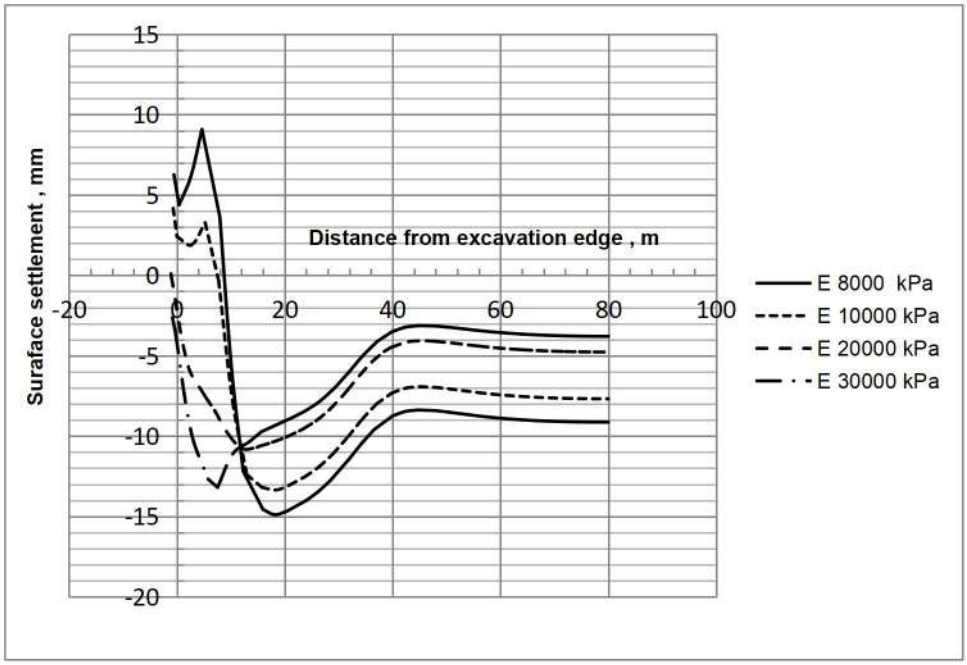

Fig 5. 8: Surface settlements for various stiffness values using MC Model for backfilled soil

Plots of surface settlement computed for various E values are given in Fig 5.9 (a-d)

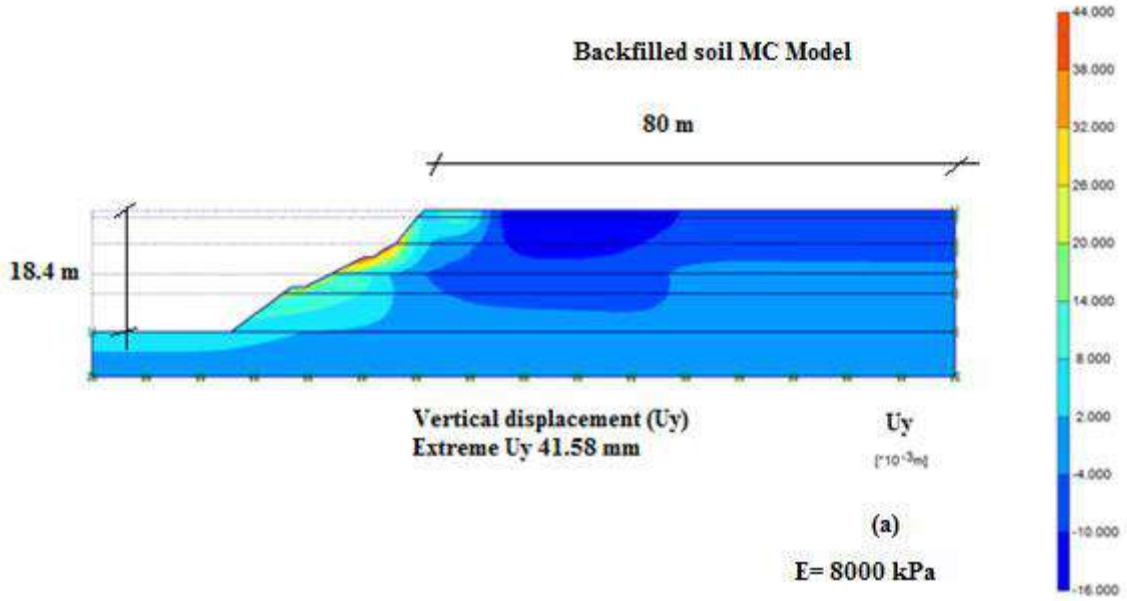

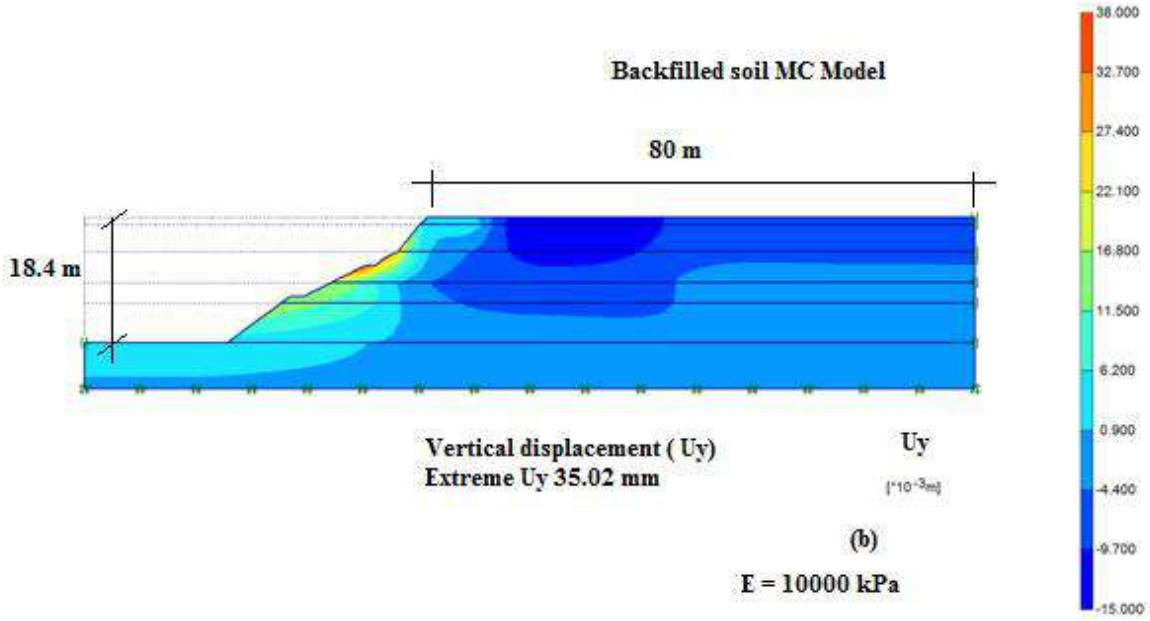

(b)

E = 10000 kPa

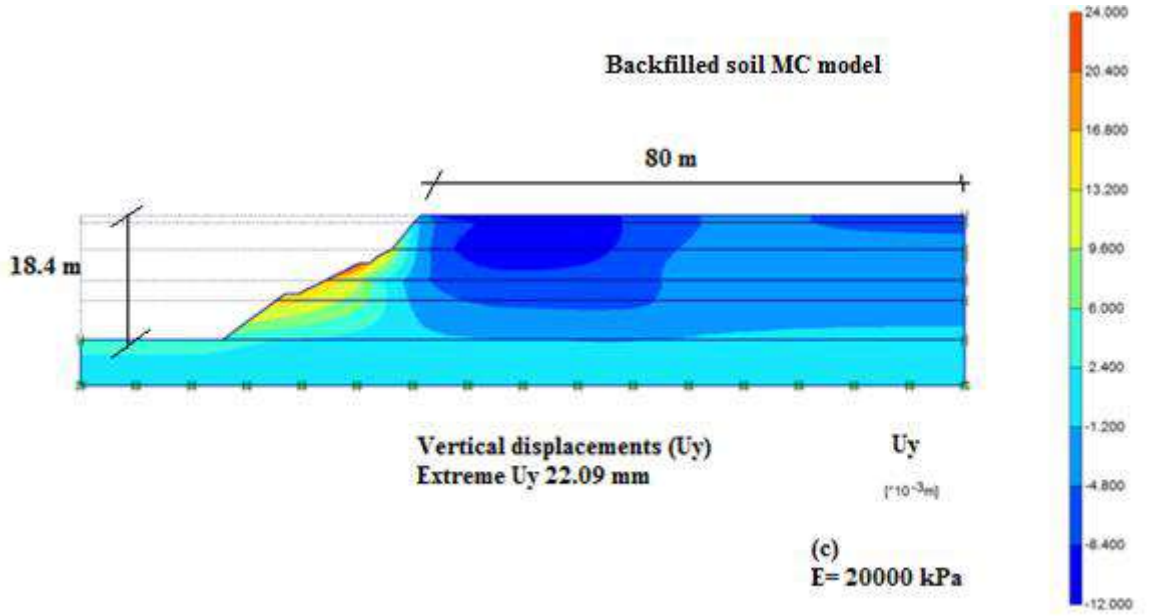

(c)

E= 20000 kPa

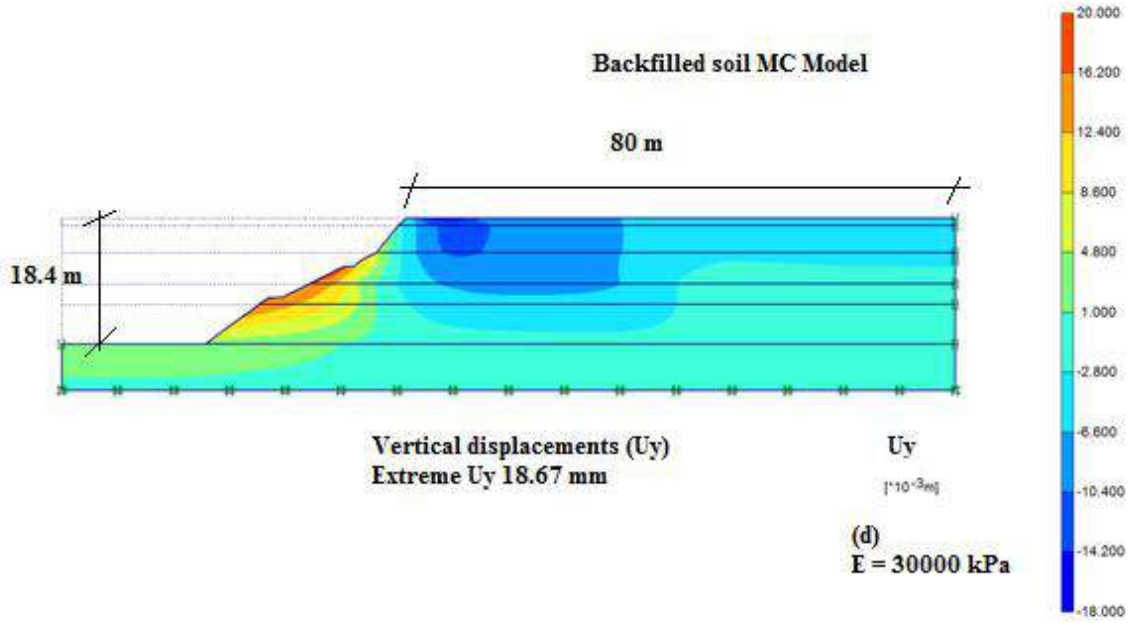

Fig 5.9- Surface settlement contours for backfiiled soil from MC Model for E value of (a) 8000 kPa (b) 10000 kPa (c) 20000 kPa and (d) 30000 kPa

Conventional investigations provided a wide range of *E* values and it is evident that use of higher stiffness need not always produce conservative results in terms of surface settlements and displacements. Hence, an accurate determination of stiffness properties is essential in predicting the behaviour of excavation. As an alternate approach, data obtained from field instrumentation can be effectively used for back calculating and matching the field data with the model computed surface displacement obtained from FE analysis for different *E* values and actual in-situ stiffness can be evaluated. This method of calibrating the model, evaluating the displacement and further matching with field observed displacement used for evaluating field stiffness of backfilled soil is addressed further in the following sections.

5.4 Field instrumentation programme

As a part of field instrumentation programme, inclinometers were deployed to monitor the stability of excavation slopes. The field displacements obtained from these

measurements were used for calibration of the numerical model generated using soil properties (Table 5.1) obtained from conventional investigations. Field instrumentations can be effectively used to monitor the performance of supported deep excavations, stability of structures adjacent to ongoing construction activities for locating infrastructures like tunnelling, basement constructions etc. Various field instrumentation including inclinometers, settlement monitors, telemeters, vibration wire gauge and piezometers were used to predict the behaviour of excavation. Also, field instrumentation data have been used for calibration of the numerical model parameters using back calculations.

Conventionally, designed slopes are seldom monitored for its performance. In addition, current practice in Indian Nuclear Industry is to provide a conservative stable slope estimated based on classical slope stability analysis and carry out an open excavation to reach the desired depth. However, considering the long-term safety requirements based on the possible consequences of failure if any, it is important to monitor the performance of slopes. This will indicate safety of conventionally designed slopes in order to ensure the safety of nearby existing structures. As a part of slope stability monitoring, one inclinometer of make (Model SME 2190) was installed near the battery limit location of open excavation at a distance of 2.0 m from the excavation edge to a depth of 12.0 m to monitor the horizontal movement of soil. This inclinometer system was used for monitoring lateral movement of slopes and to evaluate the requirement for any corrective measures to be implemented.

The horizontal displacement data obtained from inclinometer before commencement of excavation for foundation of infrastructure, and after reaching final phase of excavation (18.4 m) are plotted against depth in Fig 5.10. The Maximum displacement obtained from instrumentation is 2.0 mm towards excavation at a depth of 8.5 m before the commencement of excavation and is nearly constant, 15 mm at depths of 3.5 to 8 m below the ground level during the last phase of excavation. In general, excavation leads to displacement towards

excavation. However, in the present case as construction work was in progress adjacent to the ongoing excavation, the net displacement was away from the excavation as observed from the inclinometer readings.

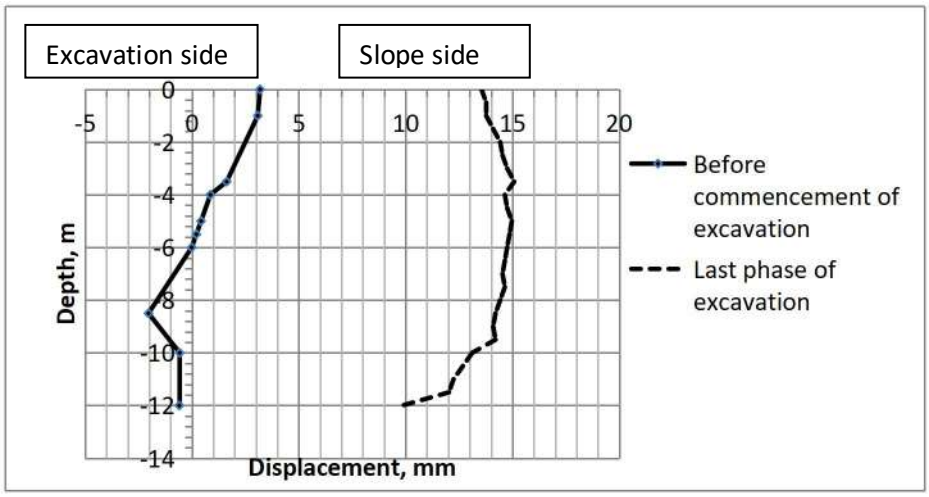

Fig 5.10 Displacement monitored from inclinometer in backfilled soil excavation

Field observed instrumentation data before the commencement of excavation was compared with that obtained from numerical analysis in Fig 5.11. While the displacement profiles for both the cases are very similar and the maximum displacements are in close agreement, − 1.8 mm at a depth of 5.0 m below ground level and – 2 mm field measurement, the location of maximum displacement differs and it is at a depth of 5 m below ground level from the MC model and at 8.5 m below ground level from field instrumentation.

The comparison of instrumentation readings obtained during the last phase excavation with that obtained using MC Model for a stiffness value of E 8000 kPa in the FE analysis is presented in Fig 5.12.

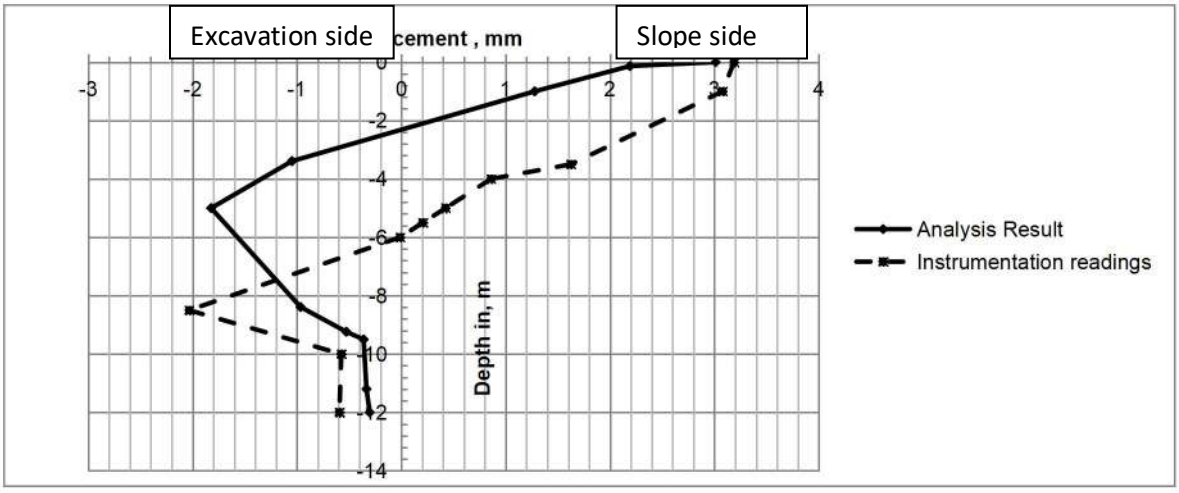

Fig 5.11 Comparison of field observed and computed (MC model) displacements before commencement of excavation

It is seen that the displacement of backfill soil obtained from the analysis is not matching with the instrumentation data above a level of – 9.0 m even though the displacement profile is similar.

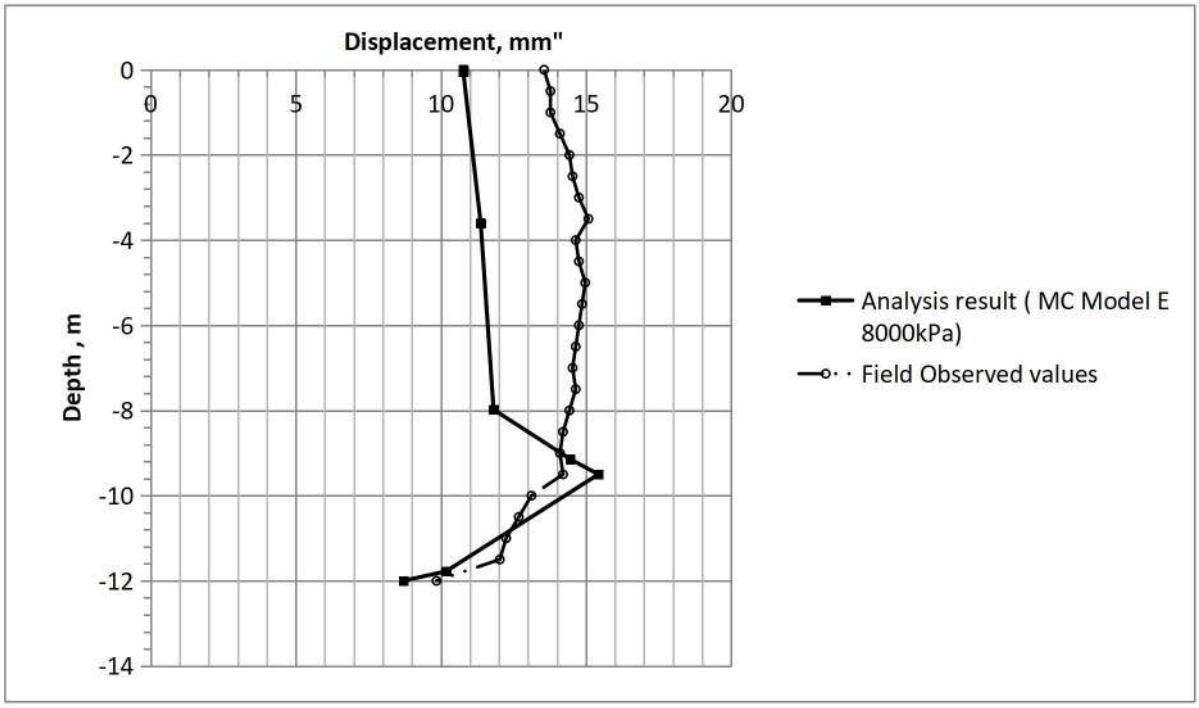

Fig 5.12 Comparison of field observed and computed displacement after last phase of excavation

In the range of 0 to −9 m depth, the difference if about 3 mm. Maximum surface displacement obtained from field instrumentation is 13.5 mm while that obtained from analysis is 10.7 mm. This shows that the stiffness value of 8000 kPa used in analysis does not match with the actual in situ stiffness of the soil. This difference is attributable to non linear behaviour of soil and variation in stiffness property with depth which is not addressed in conventional MC model. This also suggests the requirement of higher order soil models and accurate determination of stiffness properties in predicting the behaviour of soil during excavation as discussed earlier.

Considering this, analysis was carried out using higher order HS model for *E* value of 8000 kPa and the horizontal and vertical displacement contour obtained from HS model at the end of the excavation are presented in Fig 5.13 (a-b). This analysis indicated that the maximum horizontal displacement computed using HS model is 20.95 mm and is lower than that computed from MC Model which is 22.4 mm. However, the maximum vertical settlement computed by HS model is 24.58 mm and is higher than 18.67 mm computed by MC model

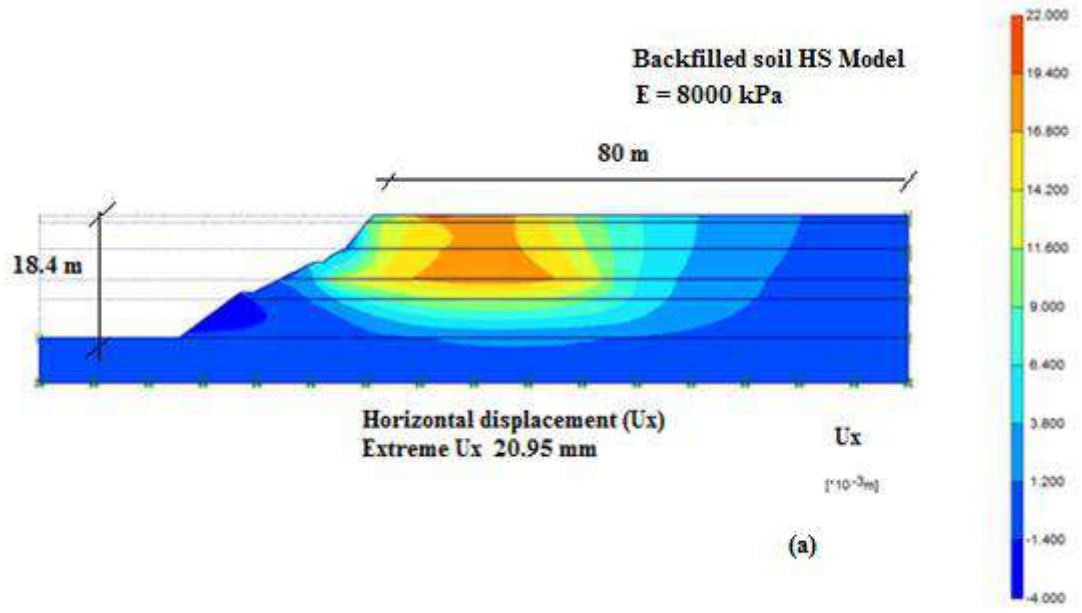

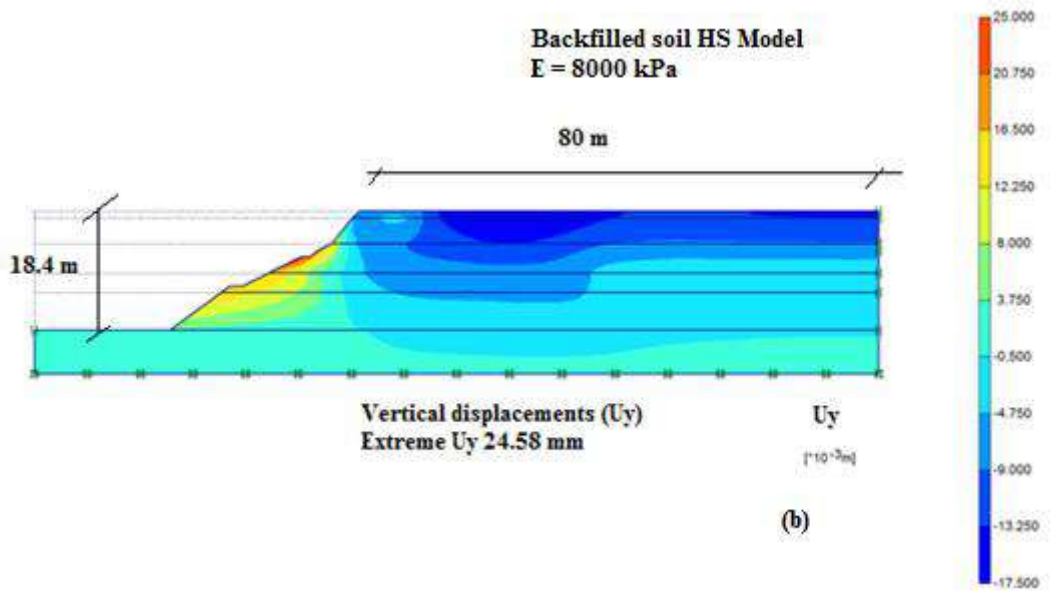

Fig 5.13: Final displacement contour after the end phase of excavation using HS Model with E value of 8000 kPa (a) Horizontal displacement (b) Vertical displacement

5.5 Stiffness evaluation through back calculation approach

In this section, the measured model horizontal displacement is compared with that obtained from back calculation by varying stiffness property of backfilled soil to match the computed and measured displacements by carrying out a parametric study for various *E* values using HS Model.

Surface displacement and settlements computed for backfilled soil using MC model by varying *E* values from 8000 kPa to 30000 kPa computed in previous sections indicate a wide variation in results signifying the importance in accurate stiffness properties in predicting the behaviour of excavation and adjacent soil mass. Higher order soil models like HS models is required to be included in the parametric study apart from varying the stiffness properties for predicting deep excavation behaviour. In this parametric study, HS model was used for defining backfilled soil properties and surface displacement was evaluated by

varying E values. Since low-level deformations at shallow depth is not sensitive to other prameter like cohesion and angle of internal friction (Pakbaz et al., 2013) these parameters were not varied in this parametric study. Properties of other layers were also not varied.

A series of calculations were performed in PLAXIS using Secant modulus (E_{50}^{ref}) values varying from 8000 kPa to 15000 kPa. Poisson ratio of backfilled soil was considered as 0.2 and the exponent for stress level dependency of soil was considered as 0.5. Additional stiffness parameters like unloading stiffness (E_{ur}^{ref}) and tangent stiffness (E_{oed}^{ref}) required for HS model were evaluated using the relations described in chapter 4.

This parametric study conducted by varying the stiffness property and employing higher order HS Model computed a displacement of 9.5 mm away from excavation for an E value of 8000 kPa at the end phase of excavation which is less than the value of 10.7 mm computed using MC Model for the same E value . From the parametric study, it was also evident that the displacement away from excavation increases as E value increases. Displacement obtained using HS Model for various secant moduli is shown in Fig 5.14. For an E_{50} 15000 kPa, computed surface displacement of 14.9 mm is almost 55% higher than the 9.5 mm computed for E_{50} = 8000 kPa. Field observed surface settlement of 13.5 mm at the last phase of excavation is in reasonable agreement with the value of 13.15 mm obtained from numerical analysis for E_{50}= 12500 kPa. The displacements computed for various depths are not as sensitive to change in E_{50} values as the surface displacement.

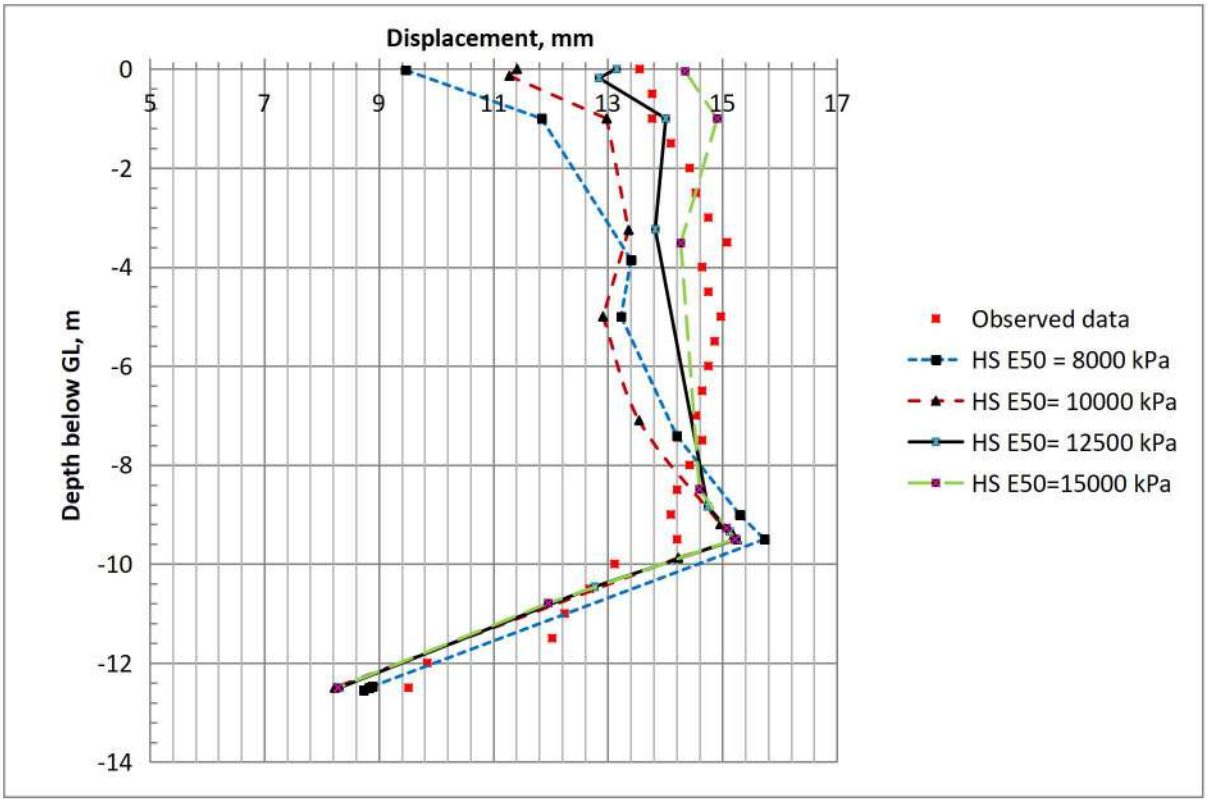

Fig 5.14 Horizontal displacement obtained using HS Model for various stiffness values

This shows that the insitu stiffness of soil is higher than that evaluated from Pressuremeter test (8000 kPa) however it is less than that obtained from full scale plate load test (30000 kPa to 33000 kPa) as indicated in Chapter 3. This analysis indicates that the prediction of stiffness parameters through conventional site investigation programme using Pressure meter test provides a conservative Young's Modulus that is almost 50% lower than that obtained from back analysis. Also, it is evident from the above discussion, higher order soil models like HS model is required for predicting the accurate behaviour of backfilled soil during excavation. The horizontal displacement contours for various values of E_{50} are shown in Fig 5.15 (a-c).

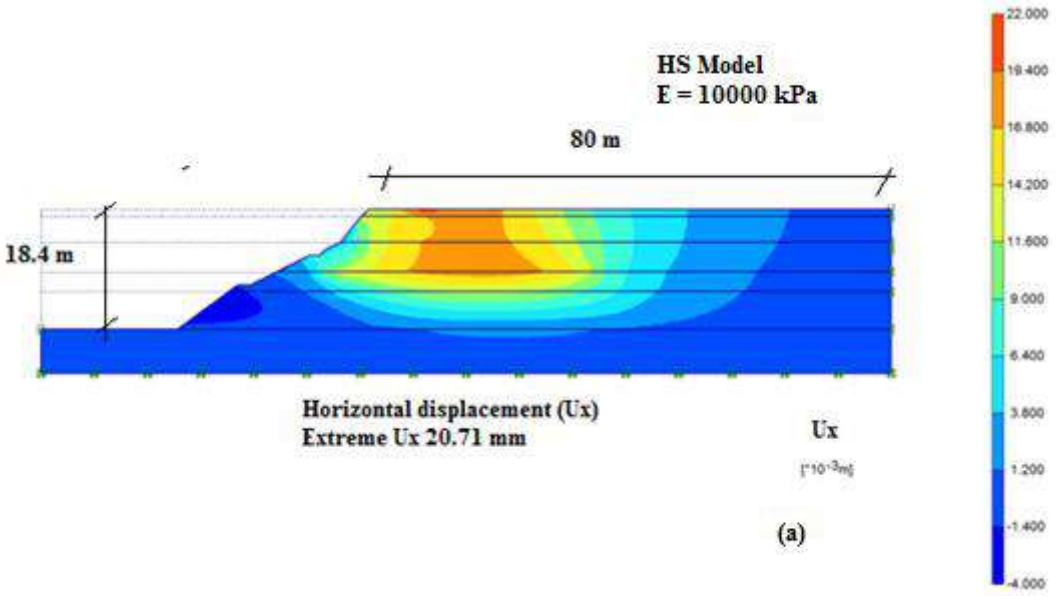
HS Model
E = 10000 kPa
80 m
18.4 m
Horizontal displacement (Ux)
Extreme Ux 20.71 mm
Ux
[*10^-3m]
22.000
19.400
16.800
14.200
11.600
9.000
6.400
3.800
1.200
-1.400
-4.000

(a)

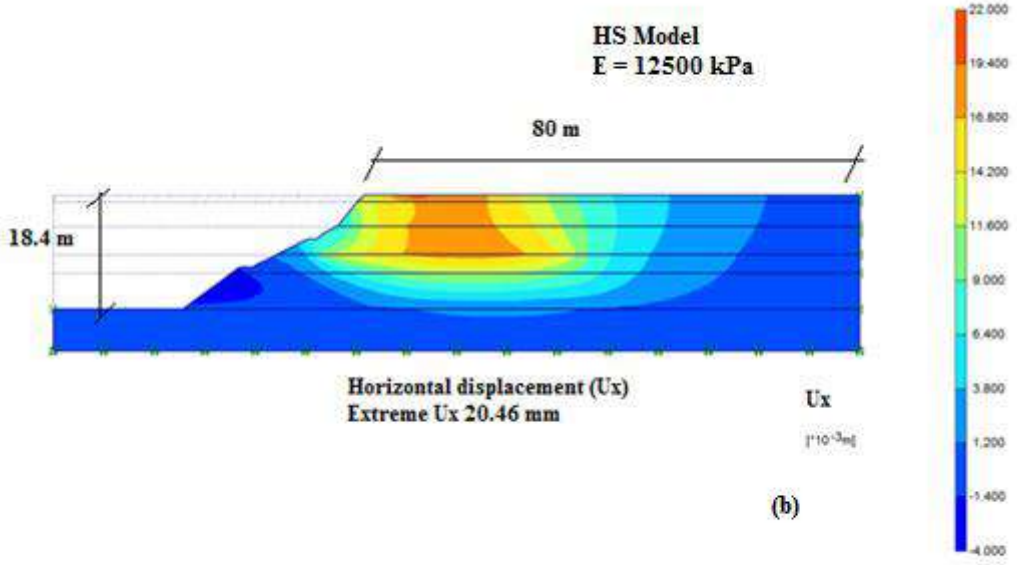
HS Model
E = 12500 kPa
80 m
18.4 m
Horizontal displacement (Ux)
Extreme Ux 20.46 mm
Ux
[*10^-3m]
22.000
19.400
16.800
14.200
11.600
9.000
6.400
3.800
1.200
-1.400
-4.000

(b)

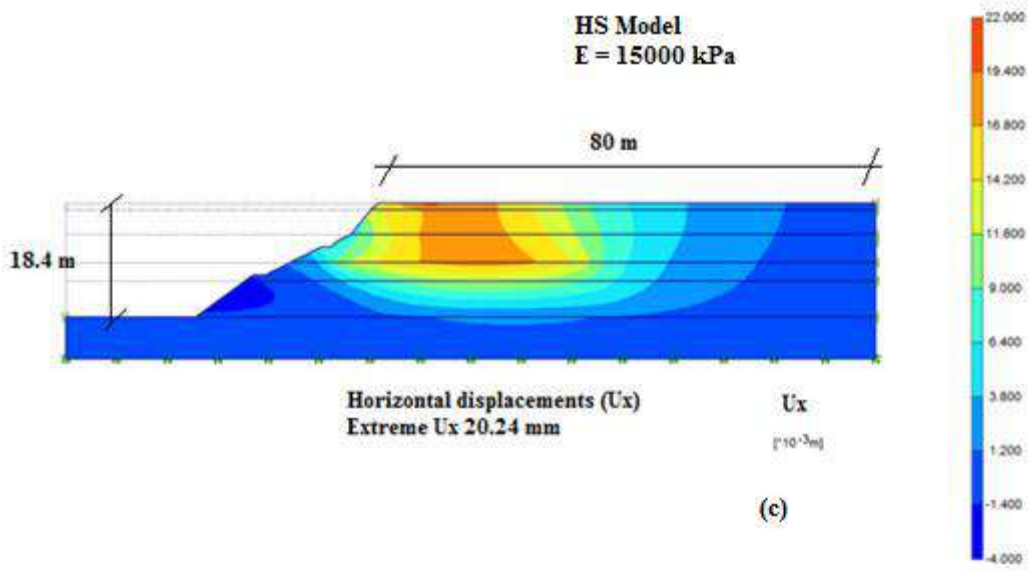

Fig 5.15 Horizontal displacement contour for HS model with E_{50}^{ref} (a) 10000 kPa (b) 12500 kPa (c) 15000 kPa

The settlement profiles obtained from the numerical analysis for various E_{50}^{ref} values using HS model are presented in Fig 5. 16 (a-c). As this figure shows the maximum displacement, the values are less than those indicated in Fig 5.14 which is obtained at a distance of 1.0 m away from the excavation.

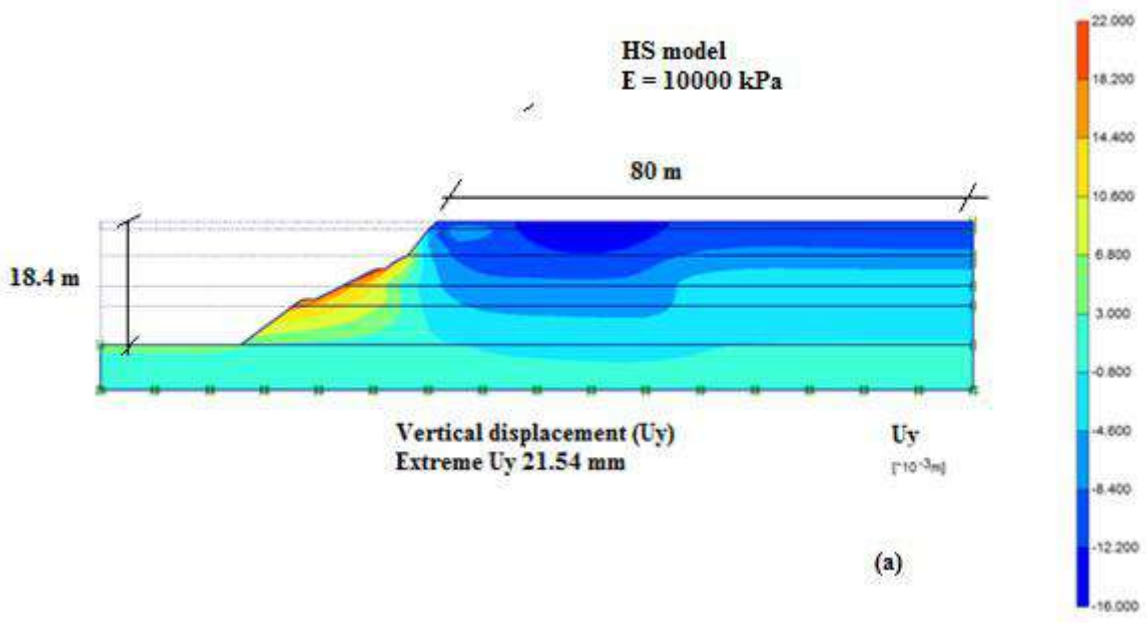

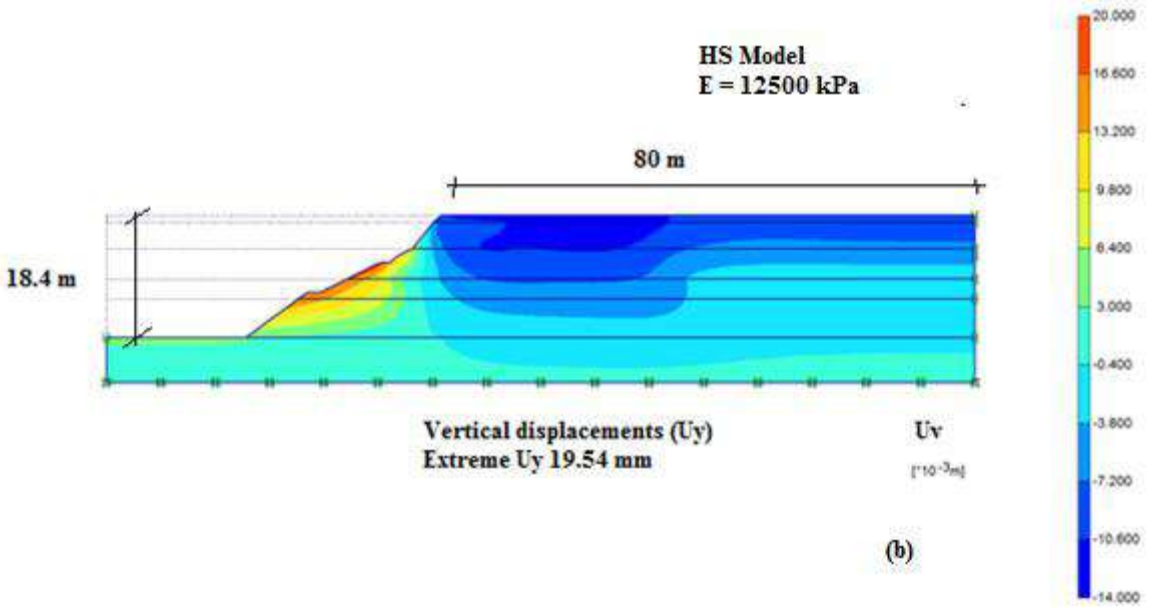

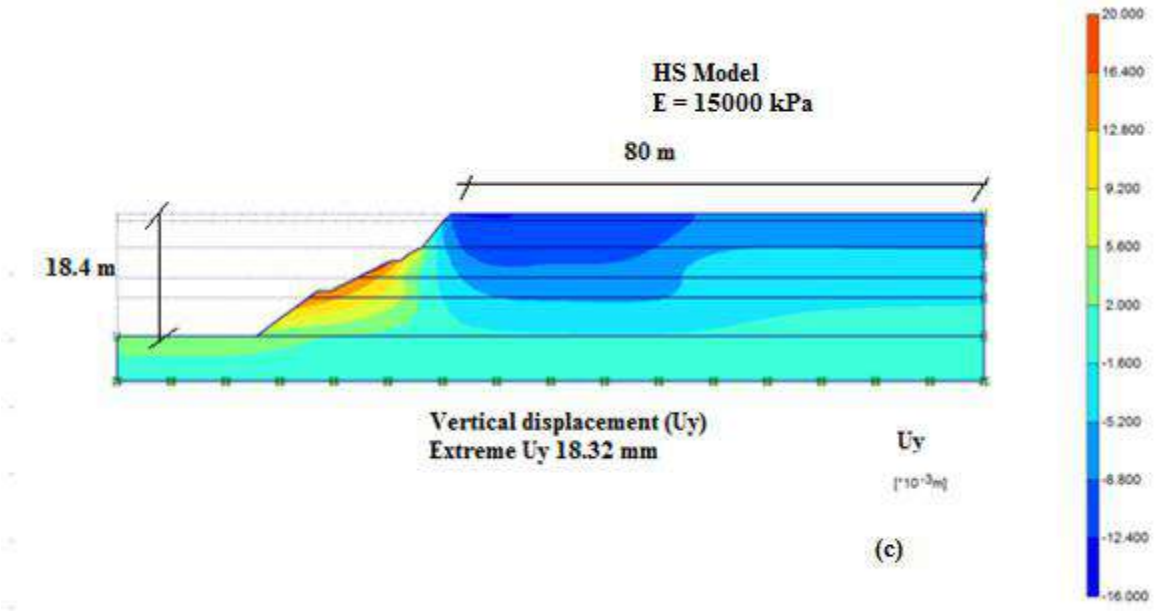

Fig 5.16: Settlement profile for HS model with E_{50}^{ref} (a) 10000 kPa (b) 12500 kPa (c) 15000 kPa

5.6 Summary

In this chapter, the behaviour of a deep excavation in terms of surface settlements and lateral deformation was studied for back filled soil. Values of soil parameters obtained from conventional field investigations were used as model inputs and a numerical analysis was carried out using basic MC Model in two dimensional FE model to predict the excavation behaviour. However, for the last phase of excavation, the displacement profile computed using soil stiffness obtained from conventional field investigations did not match with that of field monitored instrumentation data. Even though the horizontal displacements are within the order of 2 to 3 mm, the vertical displacement obtained from MC model is 41.58 mm which is higher than 24.58 mm that obtained from HS model. More over the horizontal displacement profile of MS model was not matching with that of field instrumentation records and HS model predicted the displacement profile close to field observed displacement values. This difference in numerical value and profile highlighted the requirement of higher order constitutive models and accurate stiffness parameters for predicting the behaviour of excavation in backfilled soil.

Employing higher order models in numerical analysis coupled with usage of field monitored displacement data for validating the model computed displacements can provide a frame work for accurate prediction of soil behaviour. This analysis can also be effectively used to evaluate the actual insitu stiffness of backfilled soil by conducting a series of back calculations in FE software matching the model based and observed displacements. The present study shows that the stiffness of backfilled soil obtained from conventional pressuremeter is conservative and the full scale plate load test overestimates the stiffness. The actual insitu stiffness of backfilled soil is almost 50% higher than that estimated from conventional pressuremeter test.

Usage of conservative stiffness parameters in excavation design would lead to lower slopes necessitating larger area and more excavation while over estimated stiffness properties in design can lead to excessive displacements and settlements that can lead to failure of adjacent structures within the zone of influence of excavation. Both are not desirable; the former from the economy of the infrastructure development and the later from safety consideration. Implementation of field instrumentation for monitoring excavation and comparing the field monitored data with numerical analysis prediction provides a better insight in to excavation behaviour which can be used for safe and economical design of excavation systems. This will also aid in accurate estimation of stiffness properties of backfilled soil that can be used in design of excavation systems in similar sites.

Chapter 6

Prediction of behaviour of retaining wall during future excavation

The current practice of deep excavation followed in the Indian nuclear industry is to design retaining walls during the planning stage and to construct them along with the main plant in constrained areas. Later, controlled backfilling is carried out around the retaining wall. During the expansion of the facility, excavation will be taken up with the help of this existing retaining wall. Even though these retaining walls are conventionally designed for strength and stability, the performance of retaining system and engineering backfilling during future excavation needs to be studied to evaluate the settlement of adjacent soil mass. Such studies will help in identifying critical areas of settlement and precautions to be taken up in order to limit the settlements within the permissible limit of 25 mm for isolated and strip footings of service supporting structures. Presently, empirical methods proposed by Clough & O'Rourke (1990), Goldberg et al., (1976), Ou et al., (1993) , Ou (2005),Peck (1969) are commonly used to predict the ground surface settlement and displacement of the retaining structures as described in Chapter 1. Even though these empirical methods are useful for a preliminary analysis and design of a deep excavation, a site-specific analysis accounting for the stiffness properties of the soil, retaining system and dewatering effect is warranted to identify the area of maximum settlement of soil mass to ensure the safety of the adjacent structures, which are to be supported on this soil mass. This outcome can be achieved by a numerical analysis of the deep excavation using site-specific strength and stiffness properties after accounting for the retaining system and continuous dewatering. In this chapter, an already constructed retaining wall which is to be used for assisting a future expansion excavation is analysed using the PLAXIS 2D finite element software, and the settlements of backfilled soil mass behind the excavation is computed using various soil constitutive laws. The displacement of wall also is computed.

6.1 Definition of the problem

While open excavation can be adopted at a virgin site where space is not a constraint, for sites adjacent to existing facilities, a supported excavation system must be adopted. Braced walls, sheet pile walls, contiguous and secant piles, diaphragm walls or slurry trenches, reinforced concrete retaining walls, etc. are commonly used in supported excavation systems. The choice of the type of support depends on various factors, such as soil strata, space availability, and cost. In the present case, a 185 m length counterfort retaining wall is conventionally designed for retaining earth for a depth of 23.7 m and constructed along with the main nuclear establishment to facilitate excavation during future expansion. The schematic details of the counterfort retaining wall section and its location with reference to the present and future excavation are indicated in Fig 6.1. After the construction of the retaining wall, uniform layer backfilling was carried out on both sides A and B of the retaining wall with the material obtained from the same site during excavation achieving 95 % of modified proctor compaction thus meeting compaction requirements. A future excavation is planned on the side opposite to the counterfort, which is indicated as A in Fig 6.1. During future construction for expanding the facility, excavation must be carried out in the backfill soil to the desired depth with the assistance of already constructed retaining wall. However, the effect of this deep excavation on the adjacent engineered backfilled soil mass in the zone B is to be assessed to evaluate the efficacy of engineered backfilling in limiting the settlement and to identify any additional precautions required as some of the services and lightly loaded structures will be supported on this backfilled soil.

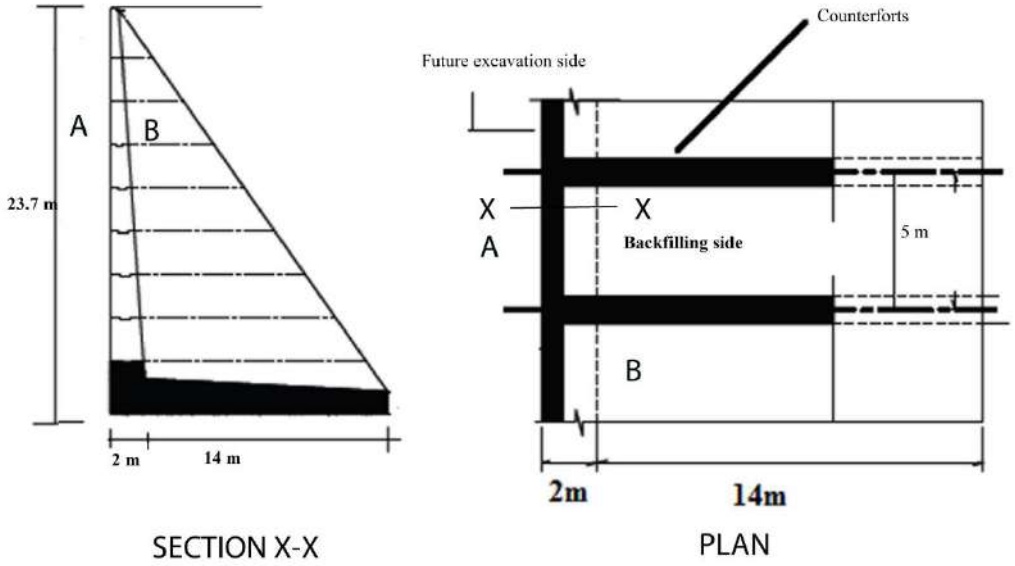

Fig 6.1 – Schematic diagram of retaining wall for future excavation

6.2 Numerical analysis of the problem

As the length of the retaining wall considered is 185 m, the problem defined in the section 6.1 was modelled in the PLAXIS 2D and analyzed as a plane strain case to study the behaviour of the retaining wall system during a future sequential excavation. The engineered backfilled soil is modelled as 15 noded triangular elements, and the retaining wall is modelled as five noded plate elements. The numerical model is shown in Fig 6.2. The extent of boundaries was considered as more than 4 times the depth of excavation to obtain ground settlement according to Ou (2014). The total depth of model is assumed as 40 m to capture the behaviour of retaining system. The equivalent stiffness of the counterfort was estimated per metre length of the retaining wall and was provided as an input to analysis (Table 6.1).

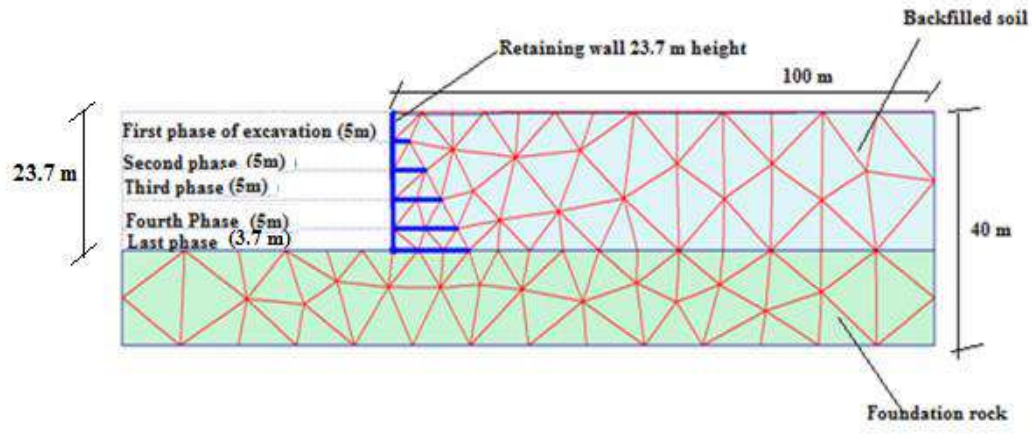

Fig 6.2 – Numerical model of the problem indicating various phases of excavation

Table 6.1: Parameters of backfilled soil and weathered rock

Parameter	***Engineering Back fill***	***Weathered rock***
Dry unit weight (γ_{dry}) kN/m^3	18	20
Saturated unit weight (γ_{sat}) kN/m^3	20	22
Secant stiffness (E_{50}^{ref}) MPa	8	5000
Cohesion (c) kN/m^2	5	100
Angle of internal friction (Φ) in Degree	30	35

Since the retaining system was constructed during the previous excavations and backfilling was carried out uniformly on both sides of the retaining wall, the process of construction of retaining wall was not modelled in this study as this study is aimed at understanding the behaviour of already constructed conventional retaining wall during deep excavation. Also, effect of interaction between soil and structure is to be studied. Standard fixities were adopted for the model boundary, where the vertical geometry line in the model is assumed to have a horizontal fixity, and the horizontal geometry line is assumed to have a total fixity. Finite element analysis was carried out using 12 Point Gauss Integration method.

The stress–strain relation of the backfilled soil is defined using Mohr-Coulomb (MC) model and the HS Model.

Table 6.2: Parameters for counter fort retaining wall

No.	***Identification***	***EA [kN/m]***	***EI [kNm²/m]***
1	Stem Portion 1	1.77E7	6.248E5
2	Stem Portion 2	2.59E7	1.95E6
3	Stem Portion 3	3.41E7	4.4E6
4	Stem Portion 4	4.3E7	8.8E6
5	Stem Portion 5	5.12E7	1.5E7
6	Base slab	3.6E7	5.6E6
7	Counterfort	3.6E7	8.5E7

The counter fort retaining wall is modelled by the Elasto Plastic constitutive law. The stiffness parameters for the HS Models were obtained from formulation described in chapter 4. The normal stiffness (*EA*) and bending stiffness (*EI*) of the plate element are calculated segment-wise for the stem. The stem is divided into 5 portions, and the stiffness is calculated for each portion. The spacing of the counter fort is 5.0 m, and the equivalent stiffness of the counterfort per metre length is estimated. The basic parameters required to define the MC and HS model is given in Table 6.2. The density of the concrete is 25 kN/m^3.

A drained analysis was carried out to predict the behaviour of the excavation assuming continuous dewatering at the time of excavation. The initial stresses were generated using the K_0 procedure. The initial water table is considered 2.0 m depth from the ground level. Each stage of the excavation is defined, and a sequential analysis is carried out. In each stage, a 5.0 m excavation is considered. After reaching 20 m, i.e., four stages, the last phase

of the excavation is 3.7 m. Thus, a total of five stages of excavation are analysed. The water table was lowered by 5m before each stage, i.e, to 7 m, 12 m, 17 m, 22 m and 27 m Through continous multi stage dewatering for the entire excavation zone. Stiffness of soil considered for this study corresponds to the field calibrated stiffness from the previous chapter which is 15000 kPa.

6.3 Results of the analysis

The numerical analyses were carried out using MC model and HS model with field-calibrated stiffness and other soil properties defined in the previous section. The results are discussed in the following sections.

6.3.1 Settlement and displacement from MC Model

The numerical analysis showed surface heaves in front of retaining walls and settlements behind the retaining wall. The horizontal displacements at a distance of 1.0 m behind the retaining wall and vertical settlement profiles in various stages of excavation are shown in Fig 6.3 and Fig 6.4 respectively. Maximum settlement behind retaining walls during the initial stages of excavation is 13 mm at a distance of 9.15 m behind the retaining wall. As the depth of excavation increases, during second stage, the settlement behind the retaining wall increases to 34 mm at a distance of 28.17 m behind the retaining wall which further increases to 59 mm during third stage. However, the location of maximum displacement shifts towards retaining wall and occurs at a distance of 16.5 m behind the retaining wall (Fig 6.3 a).

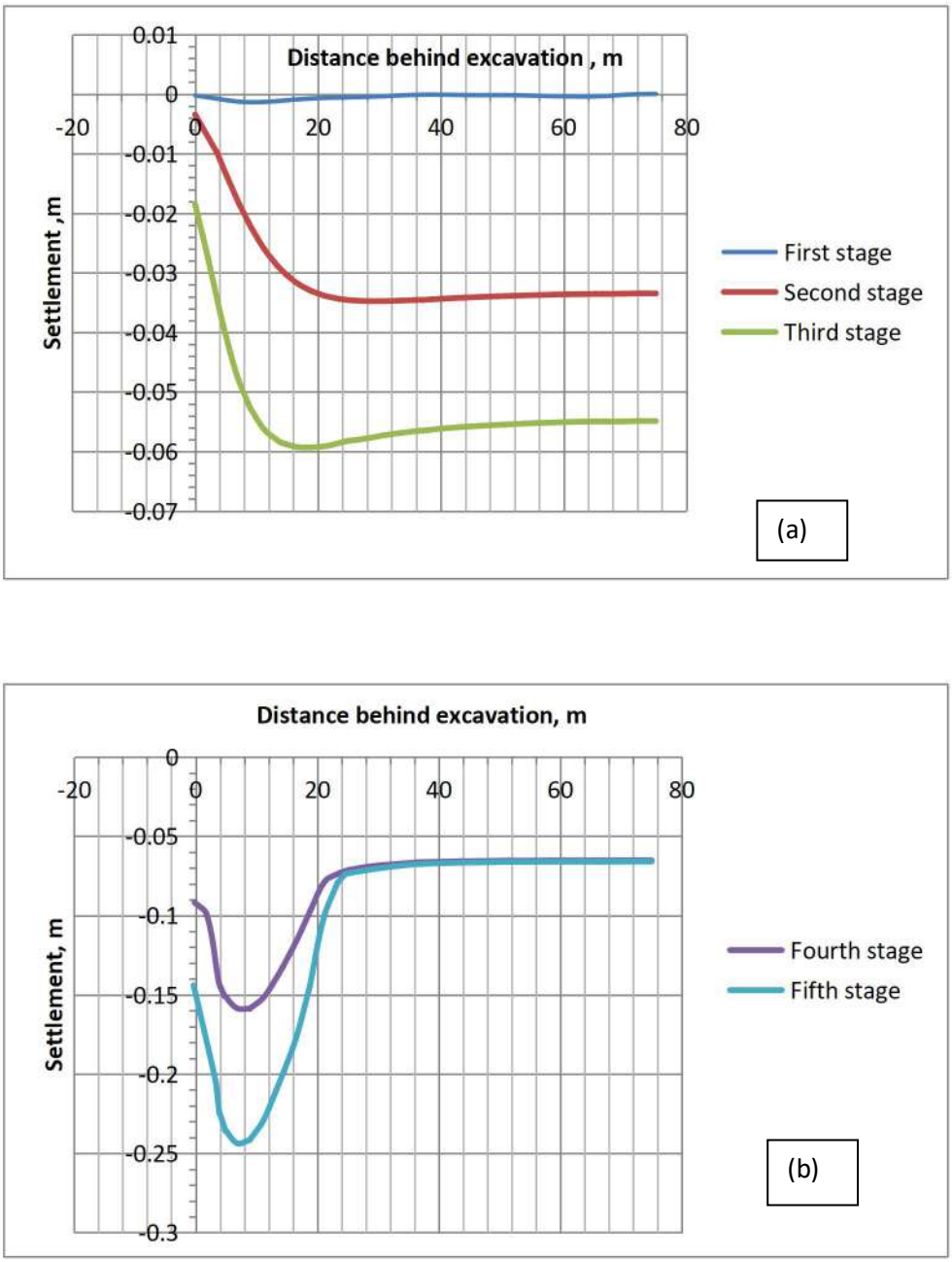

Fig 6.3 – Vertical settlement behind retaining wall for MC Model (a) first three stages and (b) fourth and fifth stages of excavation

The maximum settlement behind retaining wall at the end of fourth stage of excavation is 158 mm at a distance of 8.9 m behind the retaining wall. The settlement increases to 243.7 mm and occurs at a distance of 6.8 m behind the retaining wall as indicated in Fig 6.3 (b). The settlement does not go back to zero at any distance behind the wall which is attributable to the continuous multi stage dewatering carried out.

During the first stage of excavation, the displacement is away from the excavation and the maximum displacement is 3 mm at a depth of 5 m below the ground level. This is due to the passive earth pressure which is higher than active pressure. As the depth of excavation increases to 10 m, at the end of 2nd stage, the maximum displacement occurs towards retaining wall which is 15 mm at a depth of 15 m below ground level. At the end of third stage, the maximum displacement is 64.5 mm at a depth of 10 m below ground level (Fig 6.4 a). This shows that the location of maximum displacement shift towards ground level as the depth of excavation increases as shown in Fig 6.4 a. At the end of 4th stage of excavation, maximum displacement is 198 mm at a depth of 5.0 m below ground level, which increases to 348 mm and occurs at the surface at the end of excavation as shown in Fig 6.4 b

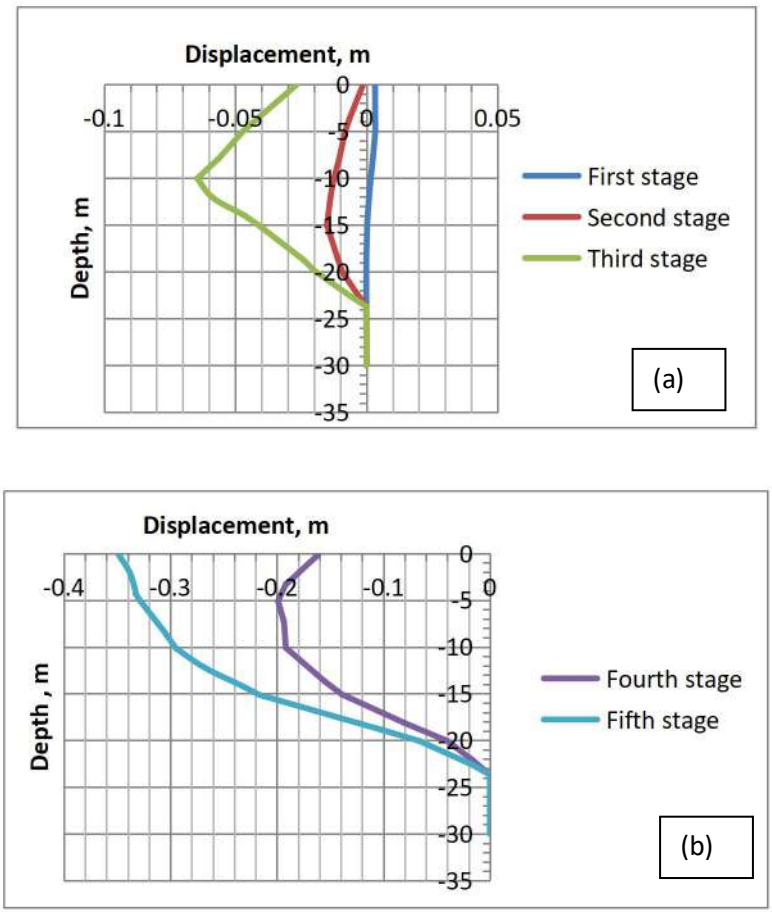

Fig 6.4 – Displacement profile behind retaining wall with MC Model (a) for the first three stage of excavation (b) fourth and fifth stages of excavation

The horizontal displacement and vertical settlement contours obtained from MC model for different phases are shown in Fig 6.5 and 6.6 respectively. The results show that the horizontal displacement at the beginning of the excavation is away from the excavation and the maximum horizontal displacement is 21.92 mm. As the depth of excavation increases the horizontal displacement is towards excavation and increases from -15.82 mm to -358.98 mm. As the depth of excavation increases, the height of earth which is to be retained increases and active pressure increases, which causes the location of maximum displacement to shift towards the surface. Surface heaves were computed for the first three phase of excavation which increases from 101.33 mm to 116.61 mm and then reduces to 110.76 mm. The settlement behind the excavation increases to -244.38 mm at the end of last phase of excavation.

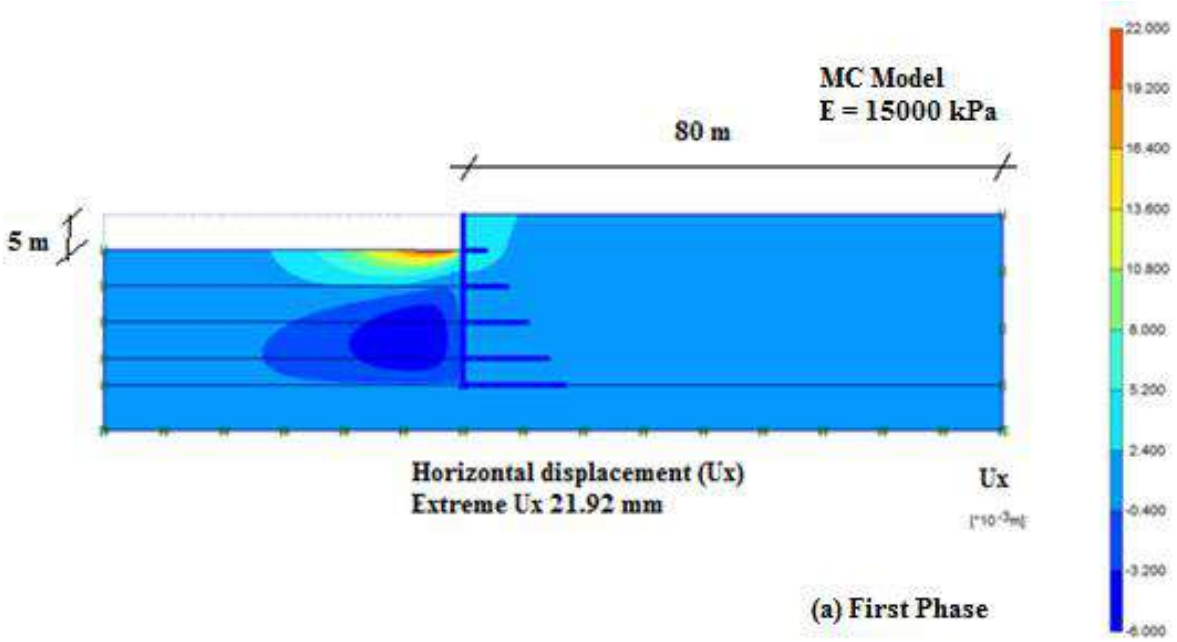

(a) First Phase

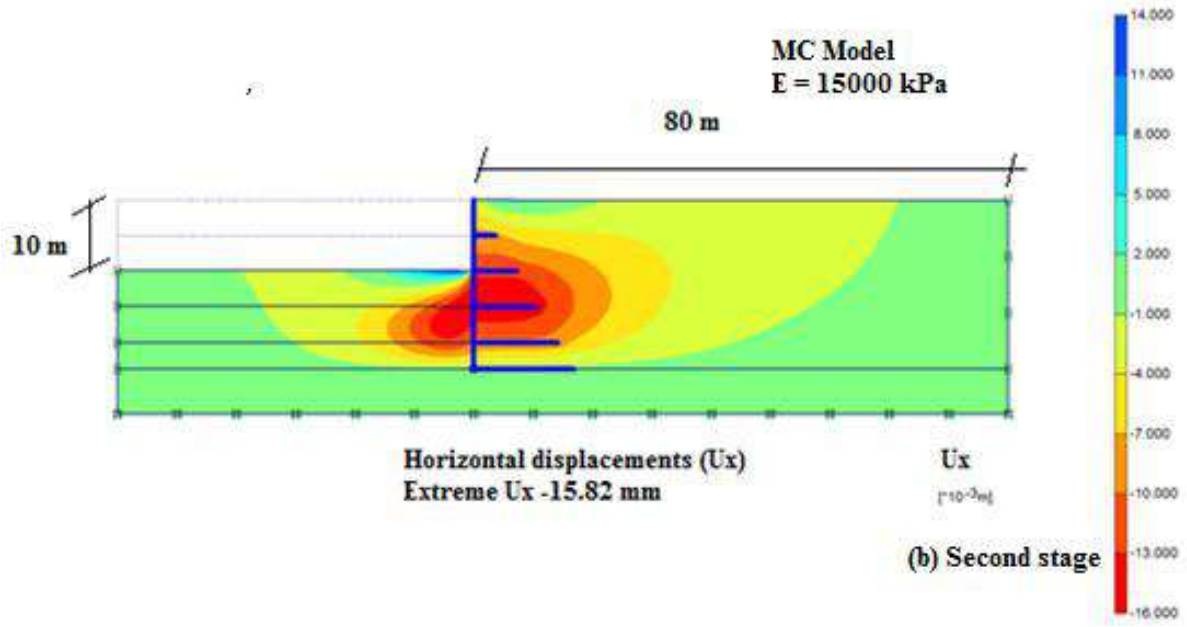

(b) Second stage

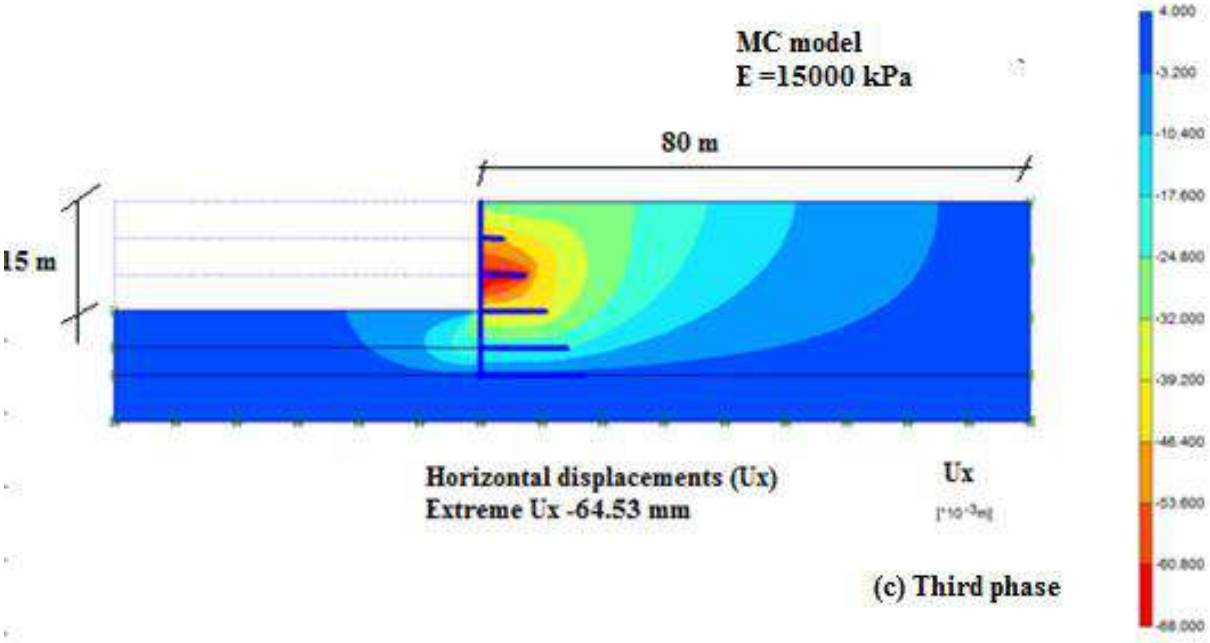

(c) Third phase

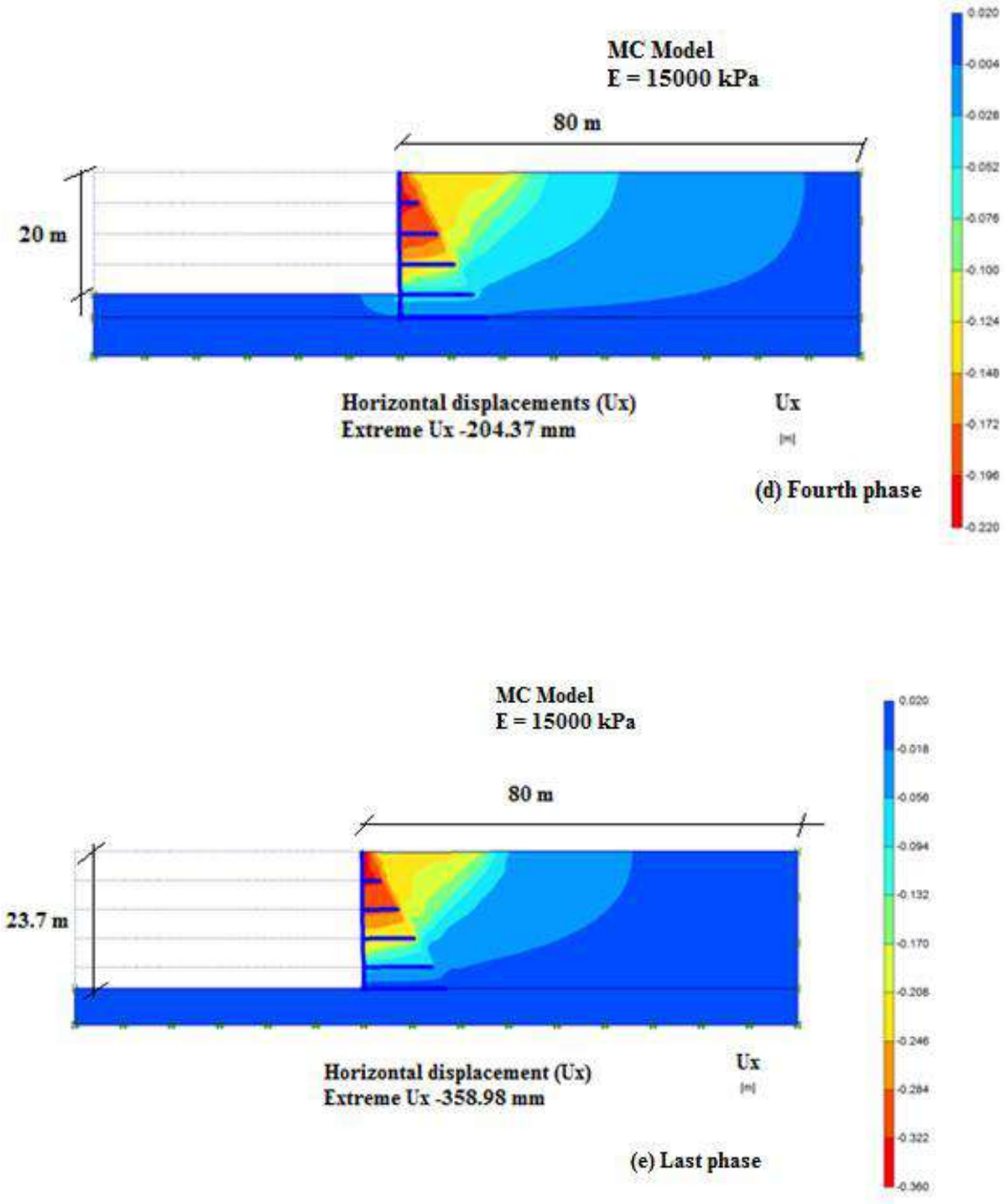

Fig 6.5: Progressive changes in horizontal displacement contours from MC Model (E =15000 kPa) at the end of different stages of excavation (a) 1st (b) 2nd (c) 3rd (d) 4th and (e) 5th

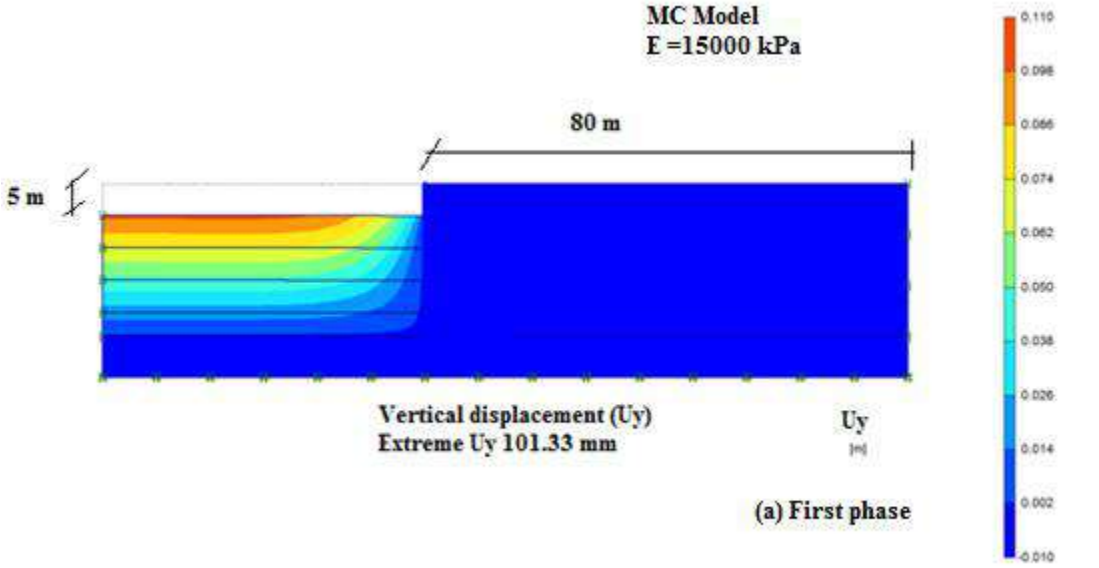

(a) First phase

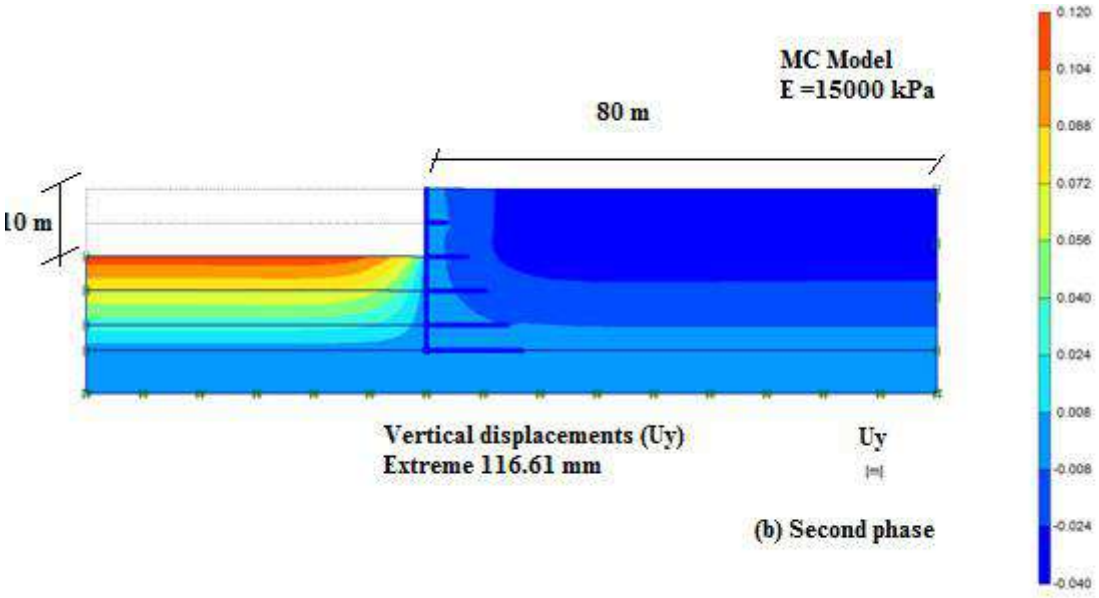

(b) Second phase

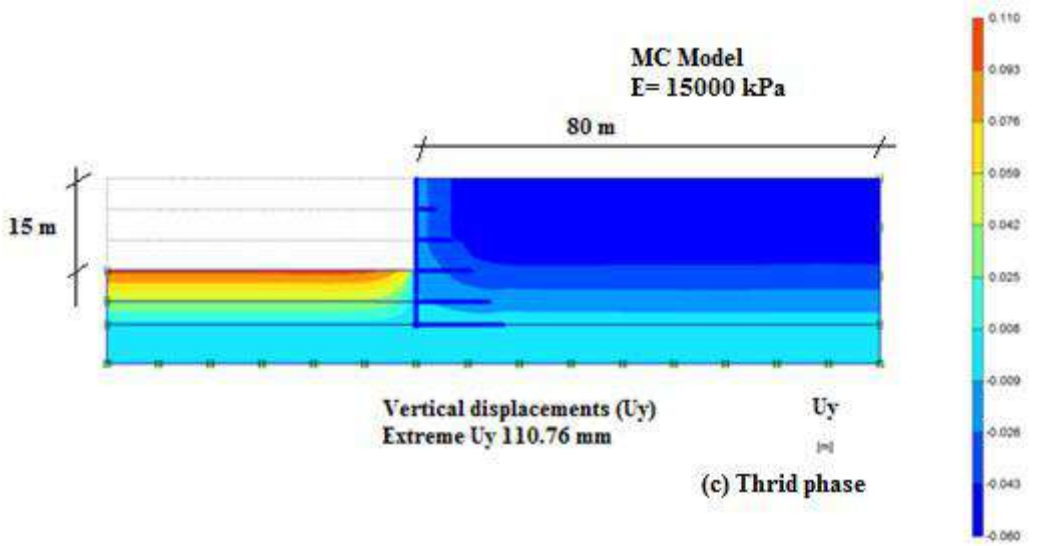

(c) Thrid phase

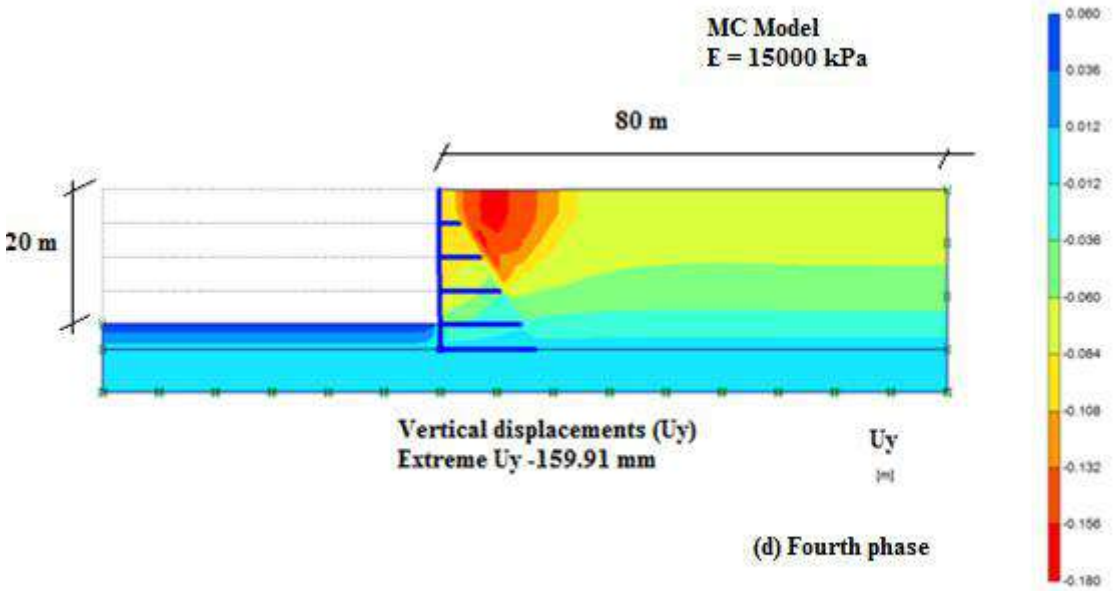

(d) Fourth phase

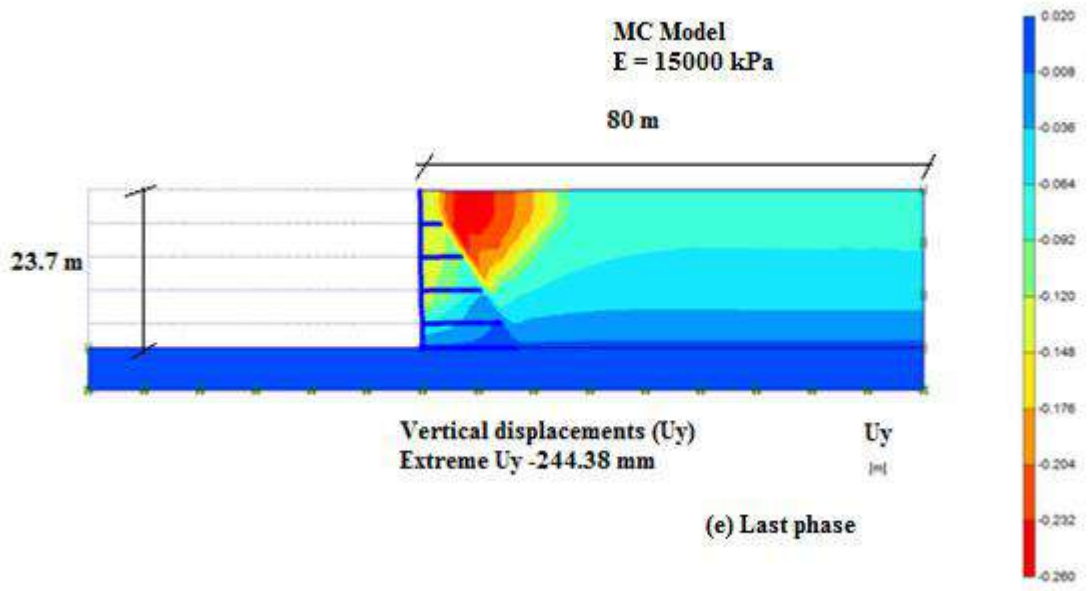

Fig 6.6: Progressive change in vertical settlement contour from MC Model (E =15000 kPa) at the end of different stages of excavation (a) 1st (b) 2nd (c) 3rd (d) 4th and (e) 5th

6.3.2 Settlements and displacements from HS Model

The vertical settlement profiles at surface in various stages of excavation are shown in Fig 6.7. At the end of first phase of excavation, the vertical settlement is 34 mm at a distance of 21.0 m behind the retaining wall, which increases as the depth of excavation increases. The settlement at the end of second phase is 69.7 mm at a distance of 15.0 m behind the excavation. As the depth of excavation further increases, the location of maximum settlement shifts towards retaining wall and at the end of third stage, the maximum settlement is 178 mm at a distance of 9.0 m behind the retaining wall. At the end of fourth and fifth stages of excavation, the maximum settlement is 320 mm and 397 mm respectively, which occurs at a distance of 8.9 m and 8.8 m from the retaining wall. This indicates that in HS model, the location of maximum settlement is almost occurs at a distance of 9.0 m behind retaining wall as shown in Fig 6.7. As the depth of excavation is less during the first stage, and passive earth pressure is higher than the active pressure developed, the soil behind the retaining wall heaves during the first stage of excavation. The settlement behind the excavation does not go

back to zero due to the continuous dewatering modelled for the entire zone of excavation. The entire excavation zone is assumed to be dewatered with continuous multi stage well point system.

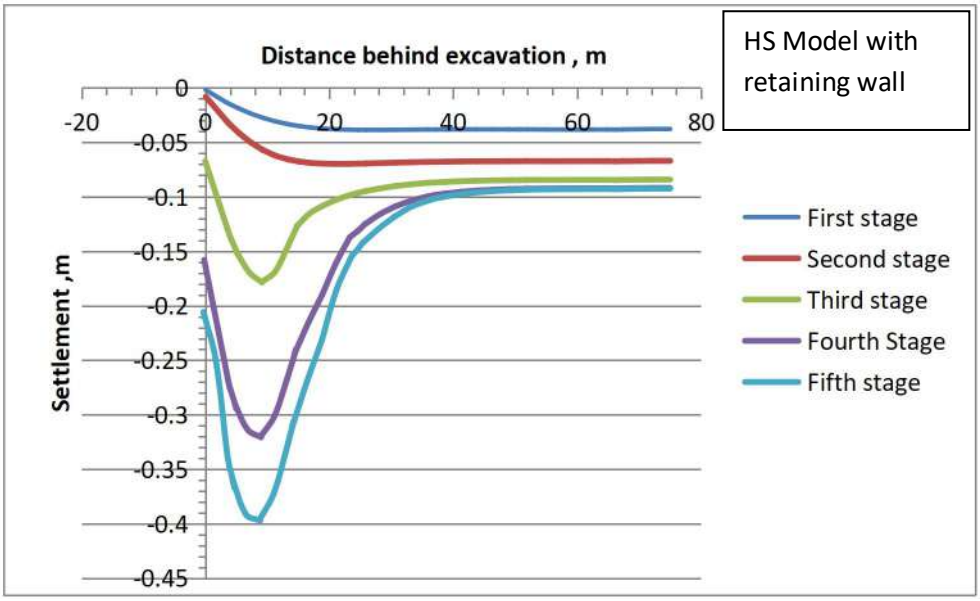

Fig 6.7: Vertical settlement profile behind retaining wall from HS model

The horizontal displacement profile behind excavation at a distance of 1.0 m is plotted in Fig 6.8. The maximum horizontal displacements at the end of first and second stages are 19 mm and 30 mm and occur at surface towards the excavation. As the depth of excavation increases, the displacement is away from the excavation. The location of maximum displacement shifts below ground level. The maximum displacements at the end of 3rd and 4th stages are 150 and 323 mm which occur at a depth of 10.0 m below ground level. At the end of excavation, the maximum displacement is 419 mm at a depth of 10.0 m as shown in Fig 6.8.

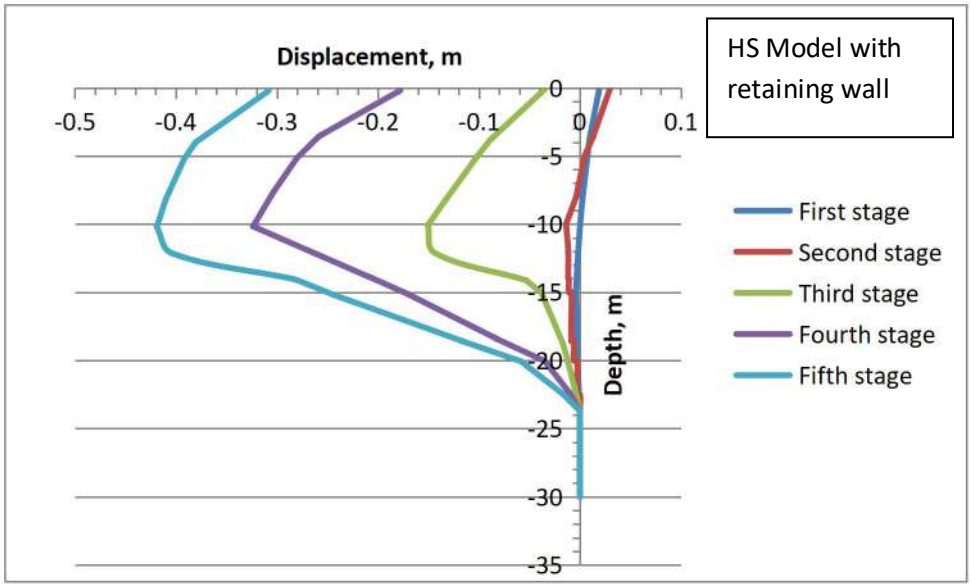

Fig 6.8 : Horizontal displacement behind retaining wall from HS model

The contours of vertical settlement and horizontal displacement are shown in Fig 6.9 (a-e) and 6.10 (a-e) respectively. The contour plot indicates that the horizontal displacement at the first phase of excavation is 19.41 mm towards the earth side and increases to 29.27 mm at the second phase of excavation. Further, the displacement is towards the excavation side and the displacement increases from -156.45 mm to -418.39 mm from third stage of excavation to last phase of excavation. No surface heaves were observed as noted in MC model and the settlement continuously increases from -38.61 mm (First Phase of excavation) to -399.69 mm (Last phase of excavation).

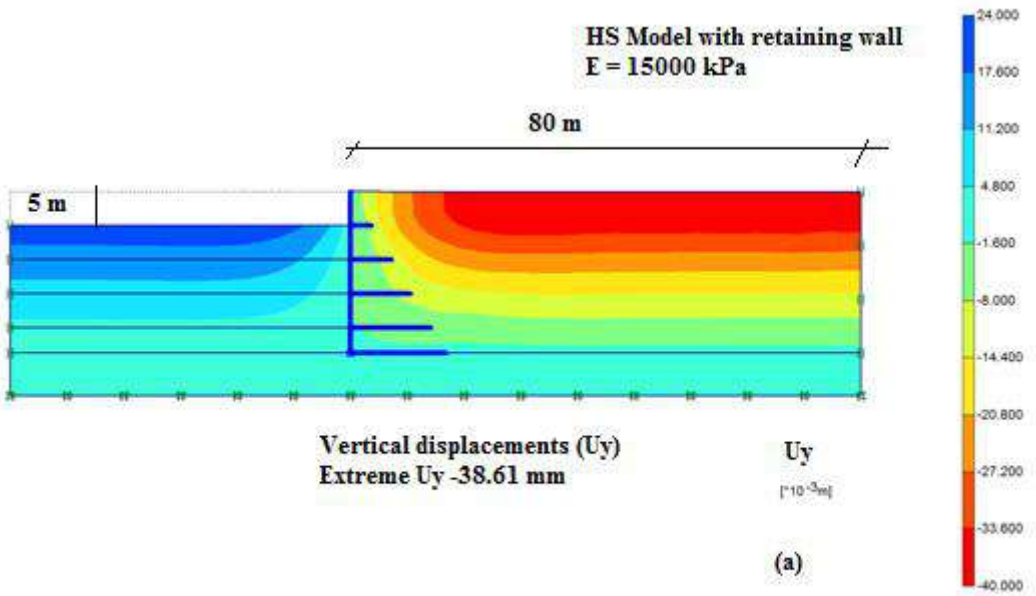
HS Model with retaining wall
E = 15000 kPa
80 m
5 m
Vertical displacements (Uy)
Extreme Uy -38.61 mm
Uy
[*10^-3 m]
24.000
17.600
11.200
4.800
-1.600
-8.000
-14.400
-20.800
-27.200
-33.600
-40.000

(a)

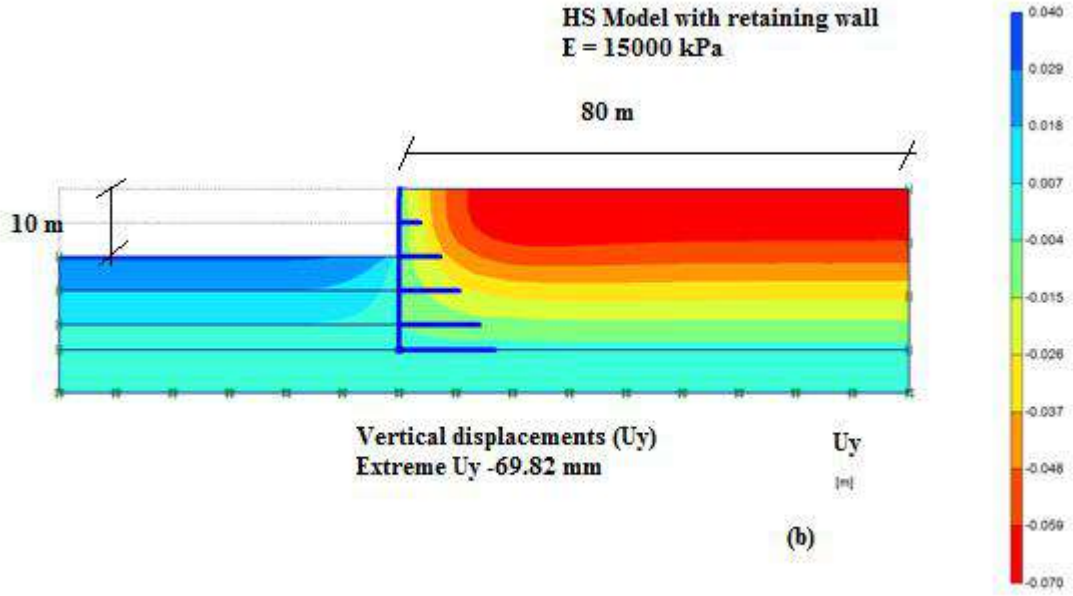
HS Model with retaining wall
E = 15000 kPa
80 m
10 m
Vertical displacements (Uy)
Extreme Uy -69.82 mm
Uy
[m]
0.040
0.029
0.018
0.007
-0.004
-0.015
-0.026
-0.037
-0.048
-0.059
-0.070

(b)

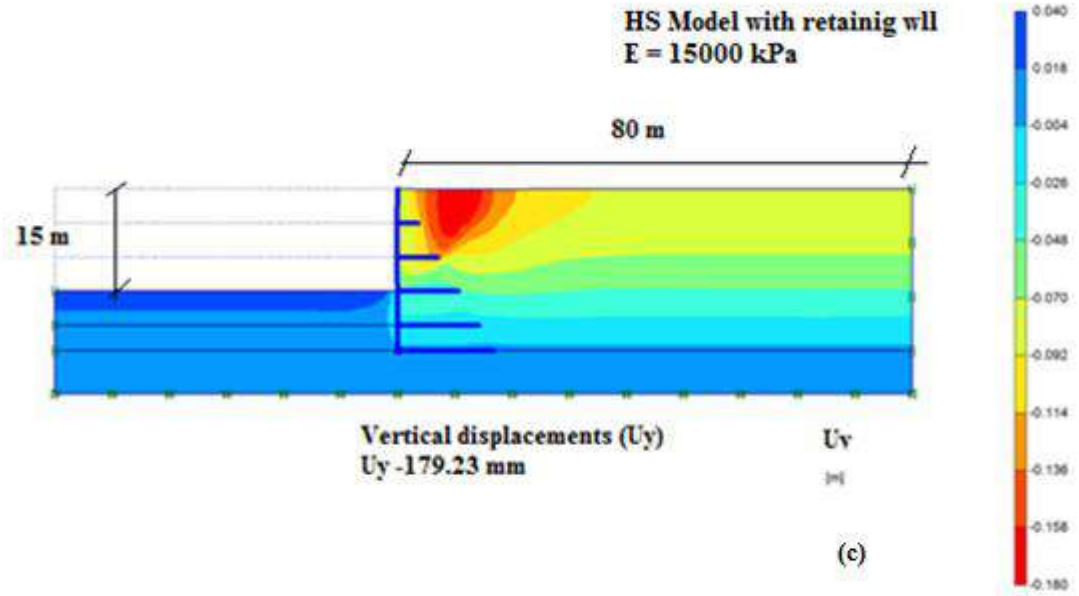
HS Model with retainig wll
E = 15000 kPa
80 m
15 m
Vertical displacements (Uy)
Uy -179.23 mm
Uv
[m]
0.040
0.018
-0.004
-0.026
-0.048
-0.070
-0.092
-0.114
-0.136
-0.158
-0.180

(c)

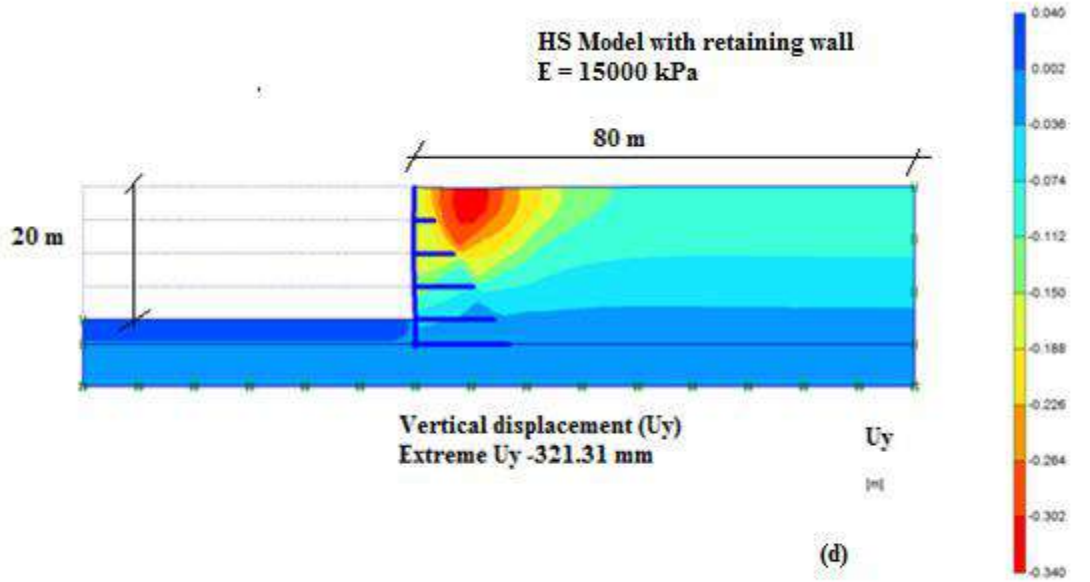
HS Model with retaining wall
E = 15000 kPa
80 m
20 m
Vertical displacement (Uy)
Extreme Uy -321.31 mm
Uy
[m]
0.040
0.002
-0.036
-0.074
-0.112
-0.150
-0.188
-0.226
-0.264
-0.302
-0.340

(d)

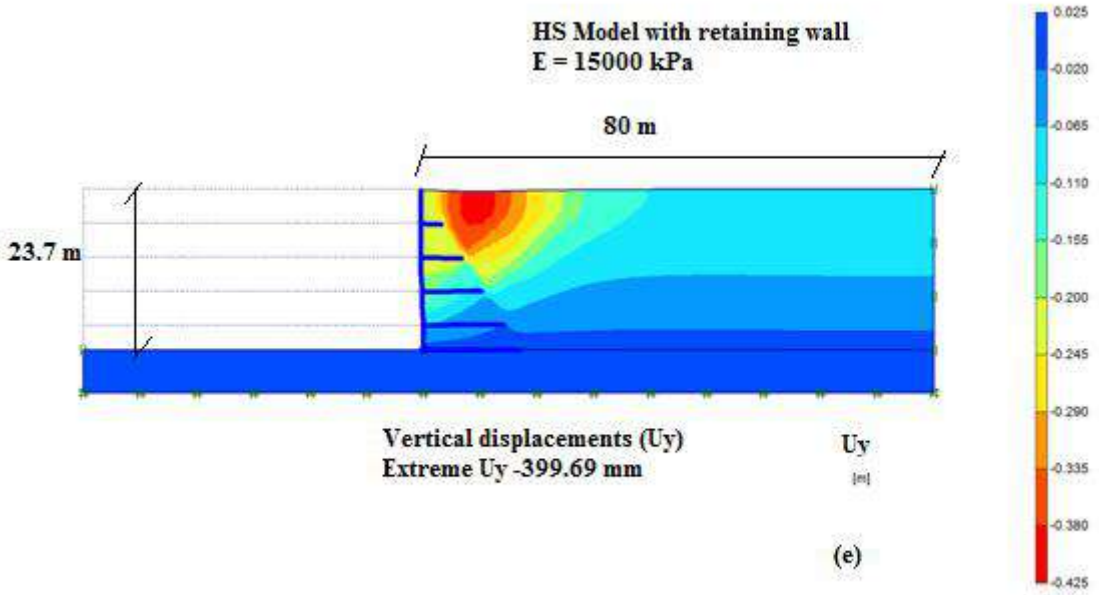

Fig 6.9: Vertical displacement contour from HS Model (E = 15000 kPa) at different stages of excavation (a) 1st (b) 2nd (c) 3rd (d) 4th and (e) 5th

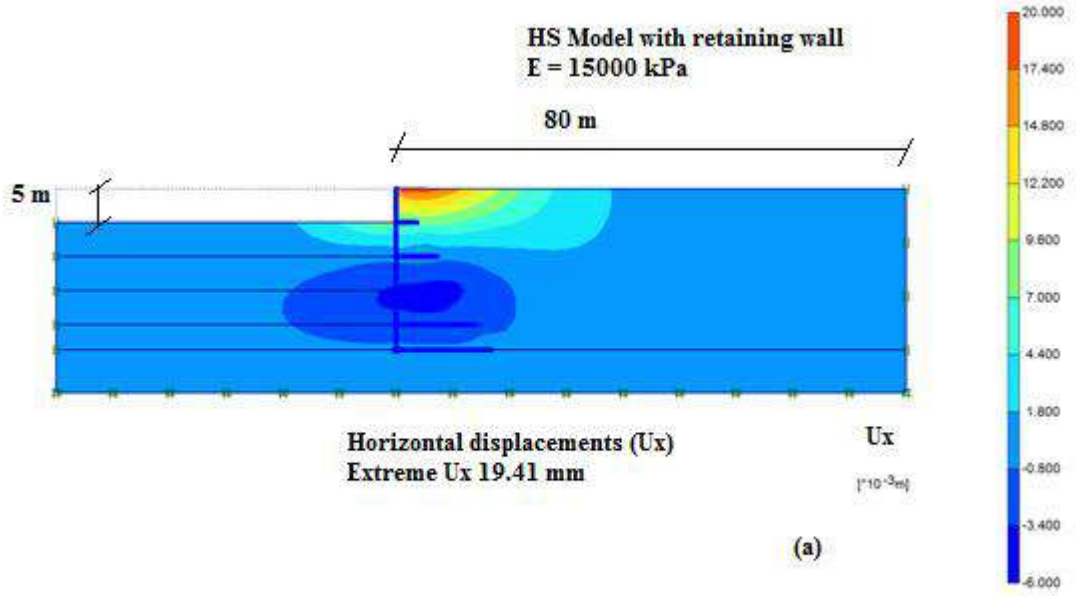

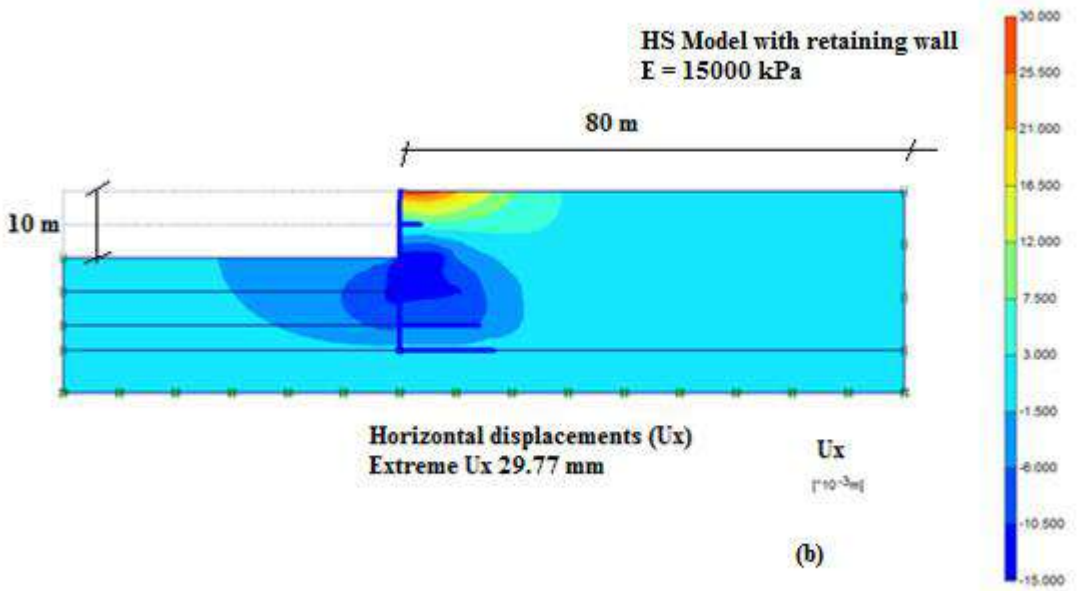
HS Model with retaining wall
E = 15000 kPa
80 m
10 m
Horizontal displacements (Ux)
Extreme Ux 29.77 mm
Ux
30.000
25.500
21.000
16.500
12.000
7.500
3.000
-1.500
-6.000
-10.500
-15.000

(b)

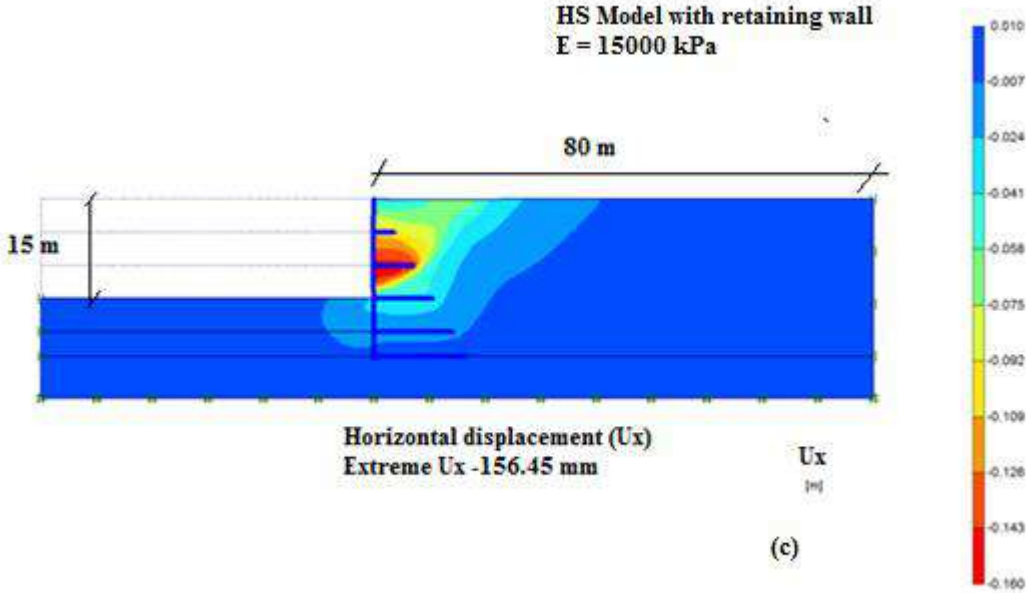
HS Model with retaining wall
E = 15000 kPa
80 m
15 m
Horizontal displacement (Ux)
Extreme Ux -156.45 mm
Ux
0.010
-0.007
-0.024
-0.041
-0.058
-0.075
-0.092
-0.109
-0.126
-0.143
-0.160

(c)

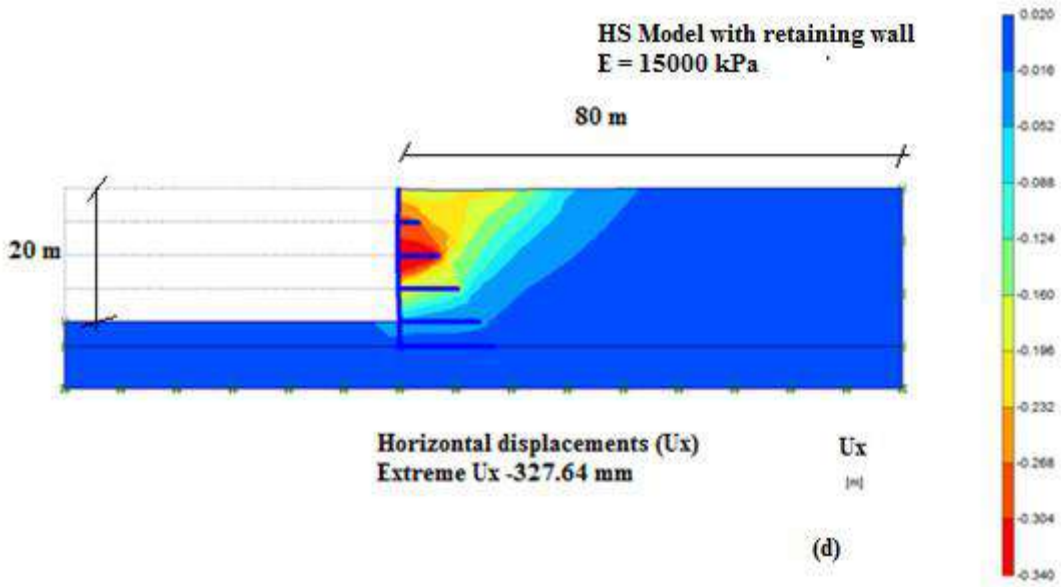

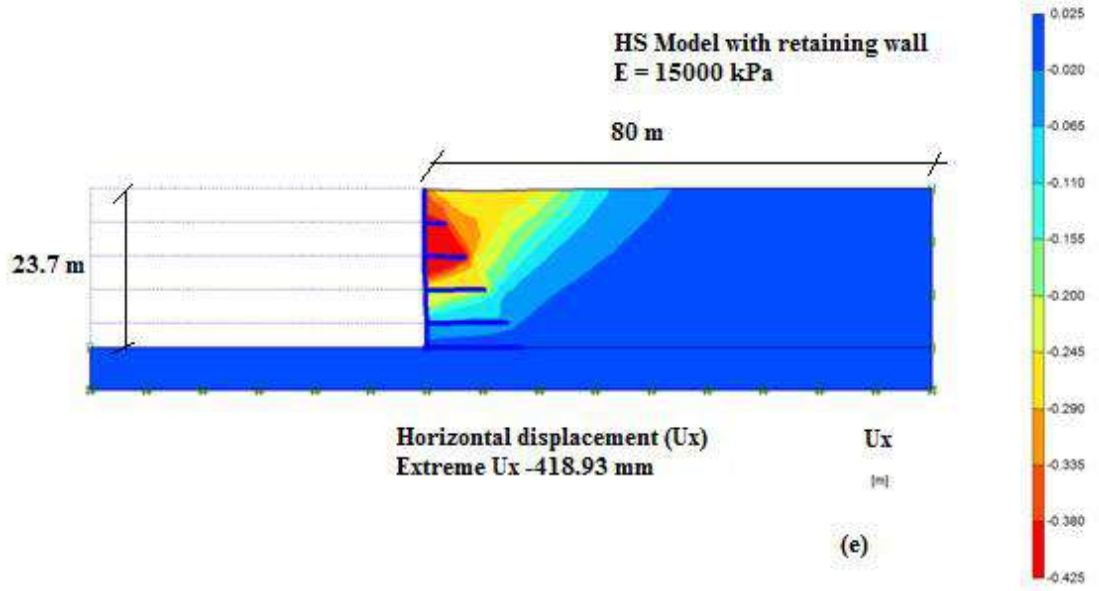

Fig 6.10: Horizontal displacement contour from HS Model (E =15000 kPa) at different stages of excavation (a) 1st (b) 2nd (c) 3rd (d) 4th (e) 5th

6.3.3 Comparison of results from various models

The horizontal displacement profiles obtained at a distance of 1.0 m behind retaining wall for various stages of excavation using different soil model are compared and shown in Fig 6.11 (a-e)

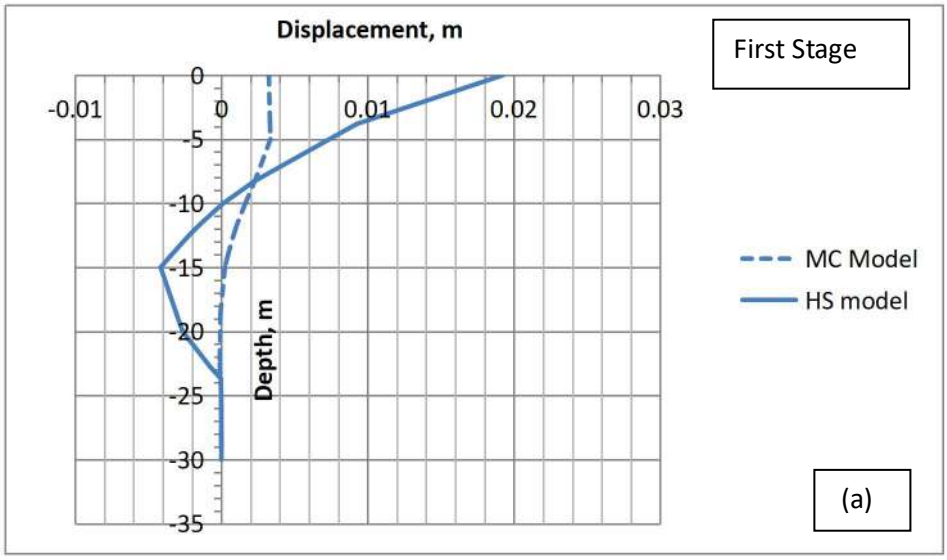

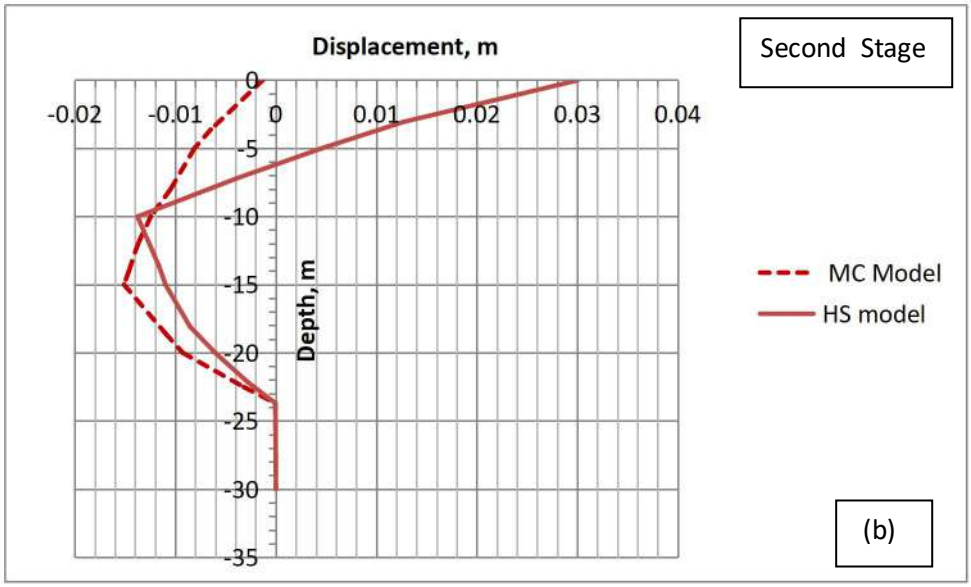

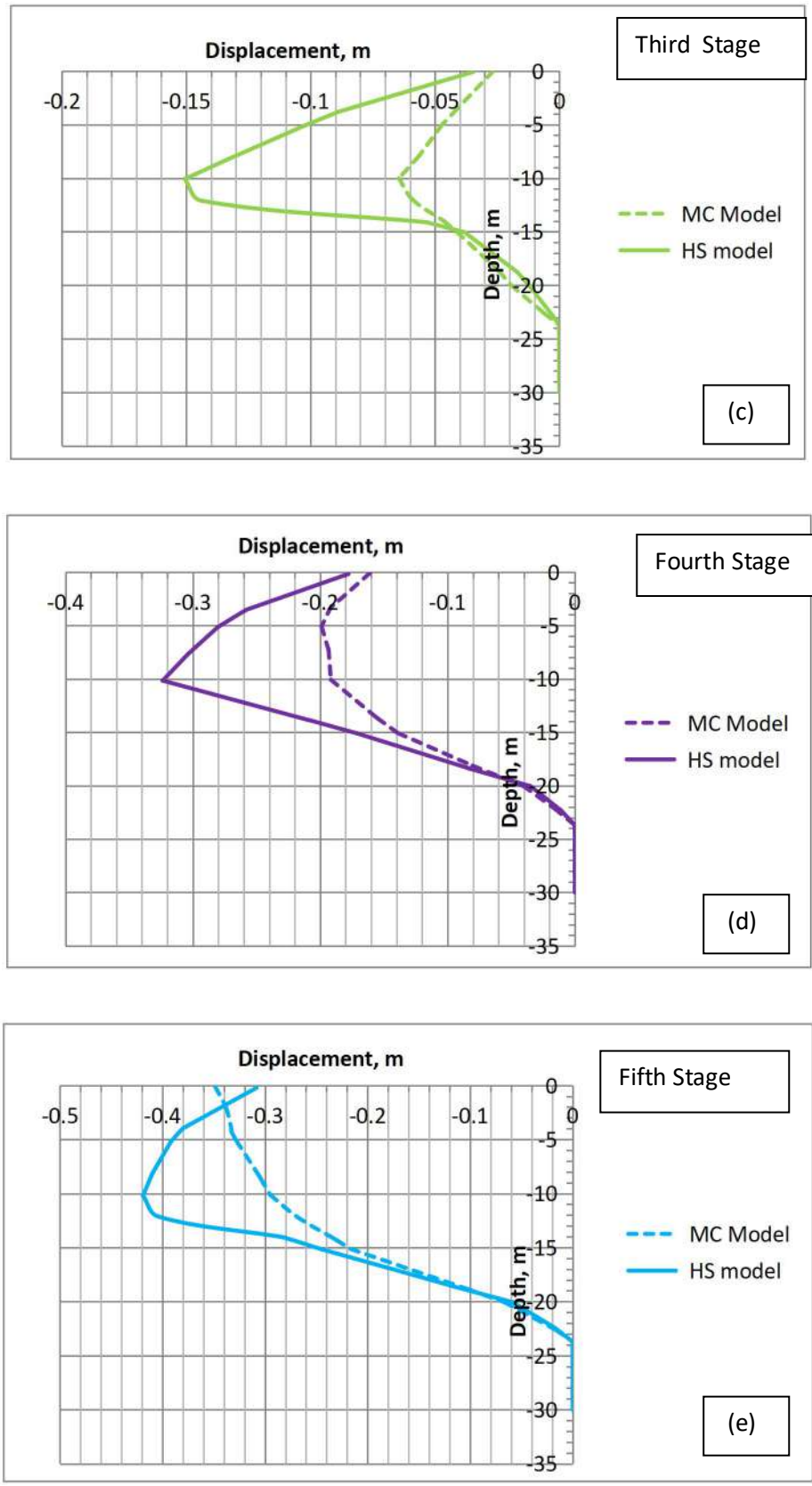

Fig 6.11: Comparison of displacement from different soil models at the end of various stages (a) 1st (b) 2nd (c) 3rd (d) 4th (e) 5th

The comparison shows that, the maximum displacement of soil is away from the excavation during first stage of excavation fig 6.11 (a) which is 3.3 mm at a depth of 3.6 m below ground level for MC model and is 19 mm at surface from HS Model. In the second stage, from MC model it is 15 mm towards excavation at a depth of 15 m below ground level while from HS Model it is 30 mm at surface. As the depth of excavation increases, the displacement increases. . The maximum displacements at the end of 3rd, 4th and 5th stages from MC model are 58.9 mm, 198 mm and 348 mm respectively. Interestingly, it was observed that the location of maximum displacement shifts towards surface from −12 m to during 3^{rd}, 4^{th} and 5^{th} stage of excavation. However, the displacement profiles obtained from HS model are different from that obtained from MC model and it was observed that displacement computed by HS model is higher than that obtained from MC model. The maximum displacements at the end of 3^{rd}, 4^{th} and 5^{th} stage are 150 mm, 323 mm and 418 mm which occurs at depths of about 10 m below ground level.

The settlement behind retaining wall for various stages of excavation obtained from both the models is shown in Fig 6.12 (a-e). The maximum Settlement at the end of first stage computed from MC model is 1.3 mm at a distance of 9.15 m behind retaining wall while that from HS model is 38 mm at a distance of 28 m behind retaining wall. The settlement profiles obtained from the models also vary widely.

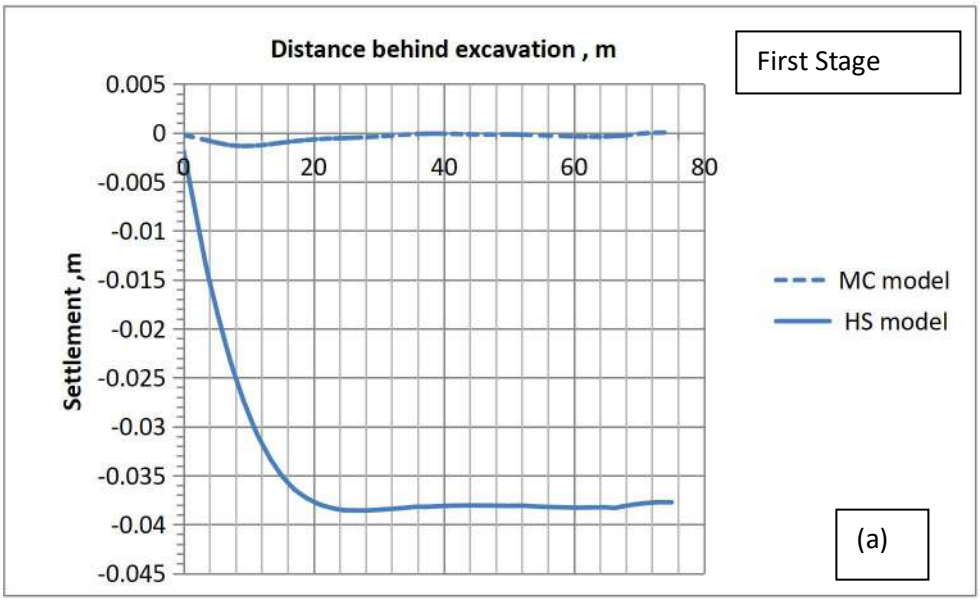
Distance behind excavation , m
First Stage
Settlement ,m
0.005
0
-0.005
-0.01
-0.015
-0.02
-0.025
-0.03
-0.035
-0.04
-0.045
0
20
40
60
80
MC model
HS model
(a)

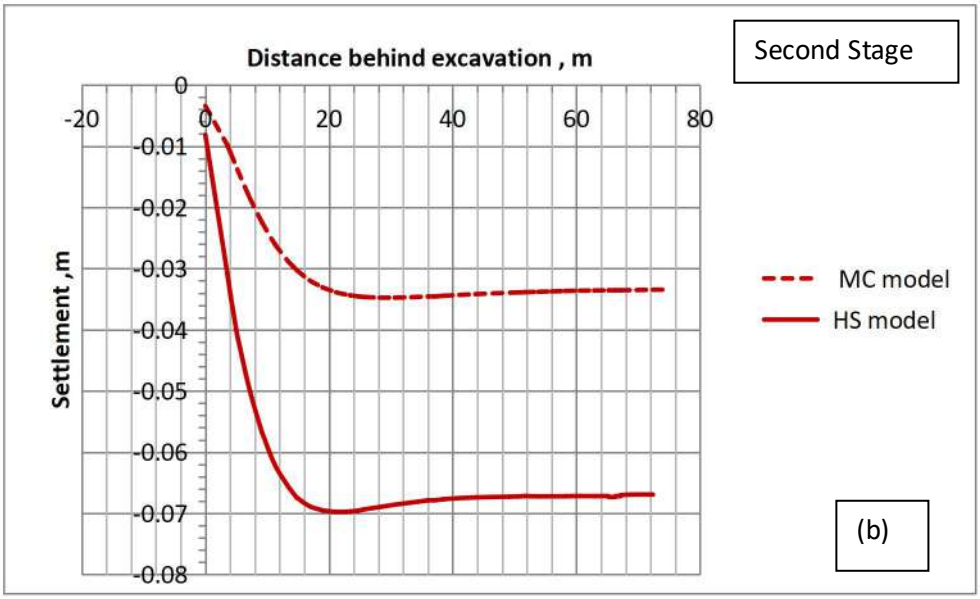
Distance behind excavation , m
Second Stage
Settlement ,m
0
-0.01
-0.02
-0.03
-0.04
-0.05
-0.06
-0.07
-0.08
-20
0
20
40
60
80
MC model
HS model
(b)

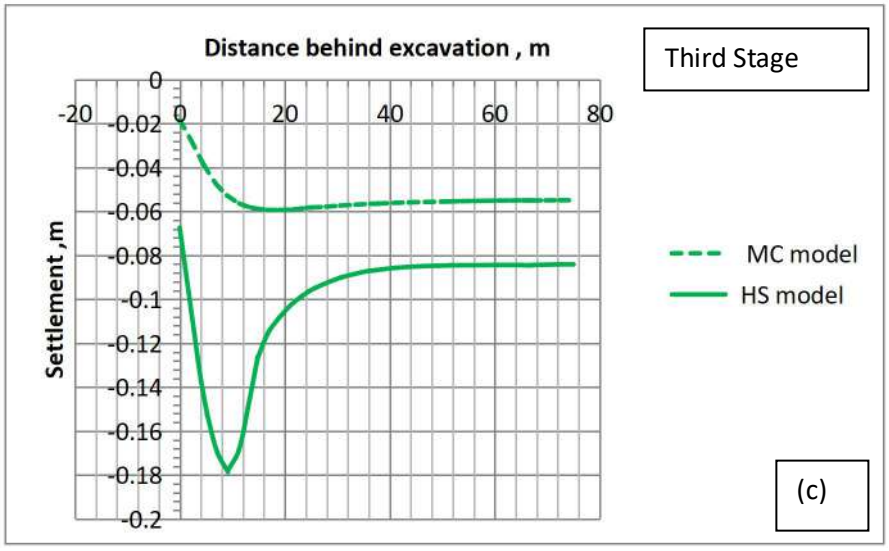
Distance behind excavation , m
Third Stage
Settlement ,m
0
-0.02
-0.04
-0.06
-0.08
-0.1
-0.12
-0.14
-0.16
-0.18
-0.2
-20
0
20
40
60
80
MC model
HS model
(c)

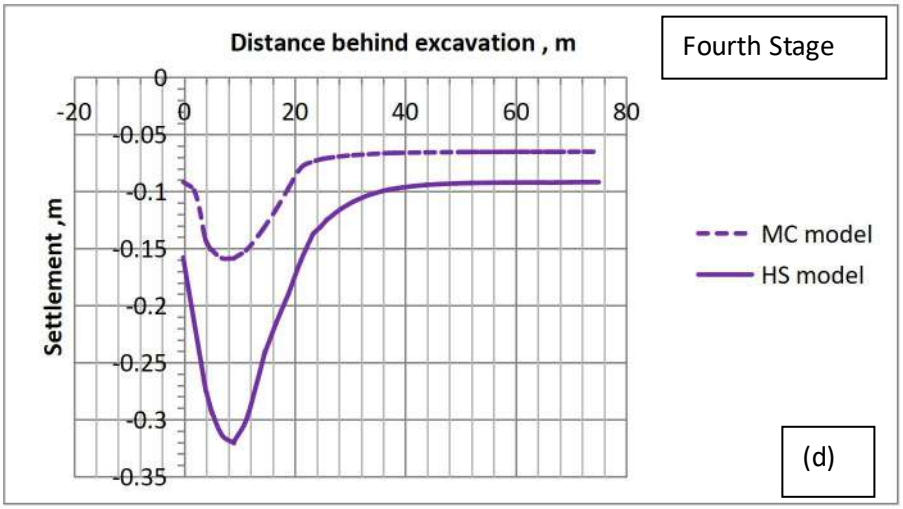

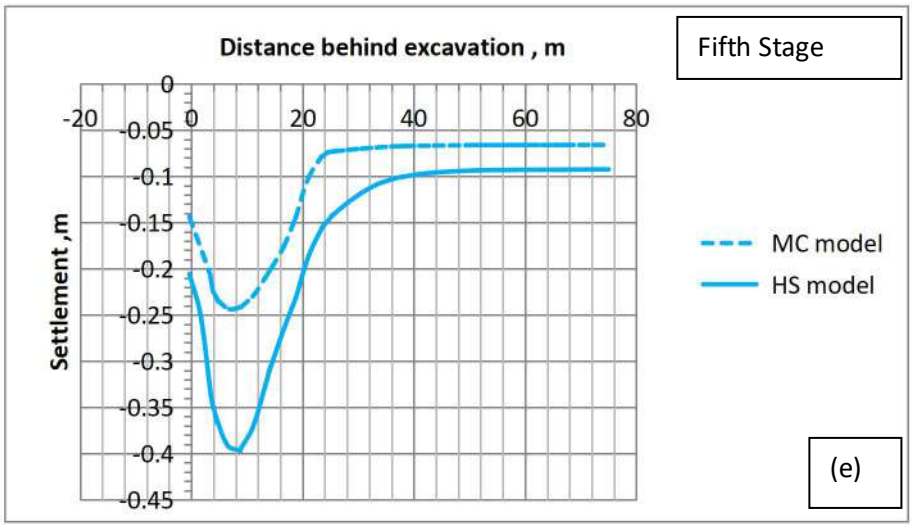

Fig 6.12: Comparison of vertical settlements behind retaining wall obtained from MC and HS models after different stages (a) 1st (b) 2nd (c) 3rd (d) 4th and (e) 5th

Settlement increases as the depth of excavation increases. At the end of second stage, after reaching 10 m depth, the maximum settlement from MC model is 34.75 mm at a distance of 28.1 m behind retaining wall, and that from HS model is 69.76 mm at a distance of 21 m behind retaining wall as shown in Fig 6.12 (b). After third stage, the values are 59.3 mm at a distance of 20 m from MC model and 178 mm at a distance of 9.1 m behind the retaining wall from HS model (Fig 6.12-c).

After the fourth stage, the maximum settlement from MC model is 158 mm at a distance of 6.7 m away from the retaining wall and from HS model; it is 320 mm at a distance of 9.0 m from retaining wall.

The maximum settlement at the end i.e, after reaching 23.7 m of excavation, obtained from both the MC and HS Model for the field calibrated E value of 15000 kPa shows a settlement of 243 mm and 397 mm behind excavation respectively at a distance of 6.85 m and 8.8 m behind retaining wall. The settlement profile is shown in Fig 6.12(e).

6.3.4 Comparison of settlement profile with empirical relations

The settlement induced by the excavation is of concave type and the primary influence zone of the excavation extends up to 25-30 m from both the models; approximately 1.05 to 1.25 times the depth of excavation. The location of maximum settlement is 8.8 m from both the models that is less than the 11.85 m computed by Ou et al., (1993) and Nicholson DP (1987). This analysis indicated the necessity of a site-specific numerical analysis in prediction of deep excavation behaviour and also the requirement for higher order soil models namely HS model in predicting the settlement induced by deep excavations. The settlement obtained from numerical analysis employing the HS model and the MC model were compared with those from the empirical methods proposed by Clough and O'Rourke (1990) and Ou et al., (1993) in Fig. 6.13.

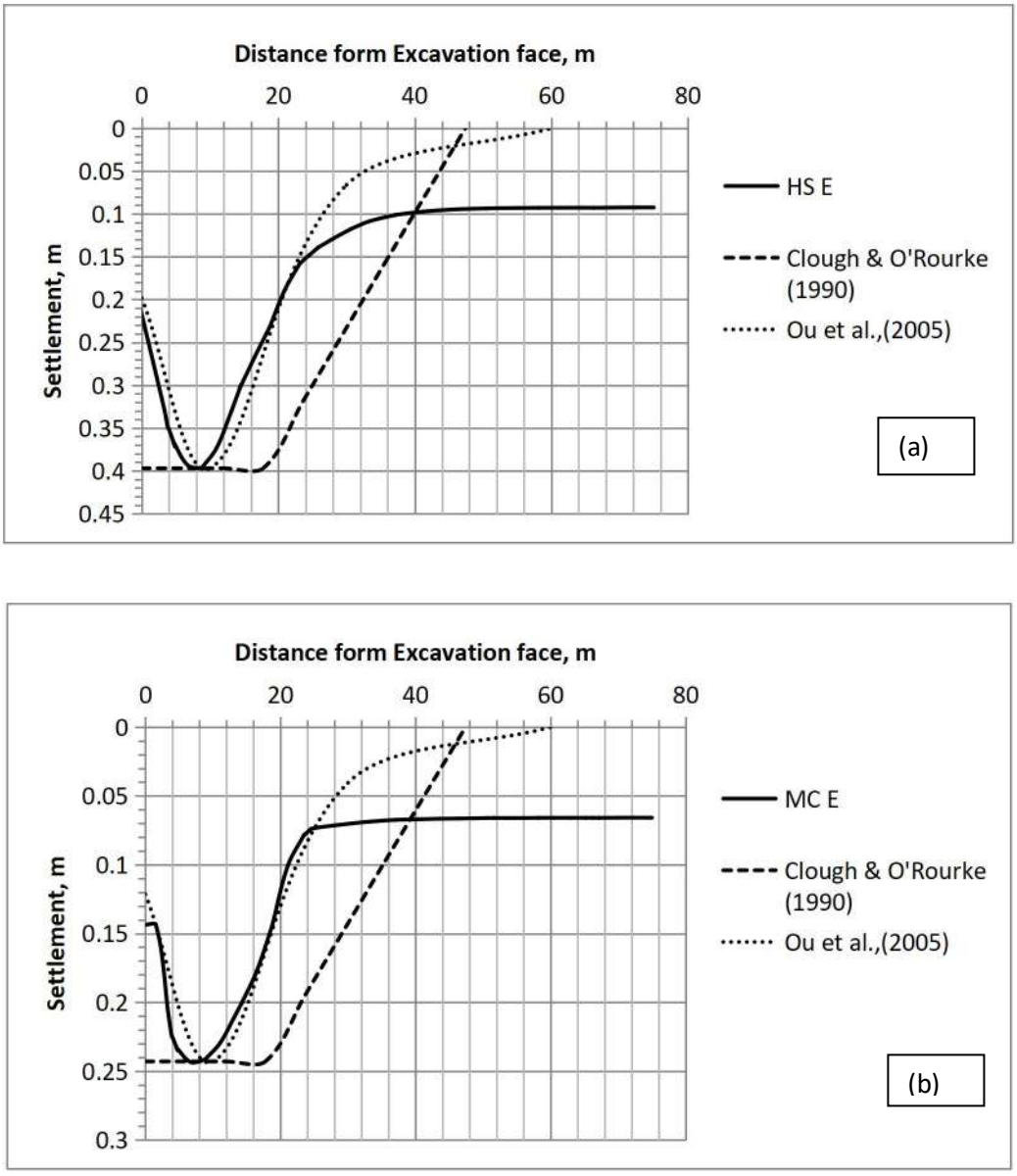

Fig 6.13- Comparison of computed settlement by (a) HS and (b) MC Mdoels with those from empirical methods

The analysis also indicates that the numerically computed results match well with the empirical charts provided by Ou et al., (2005) in the primary zone of influence, i.e. up to 20-25 m of distance. However, the settlement in the secondary zone of the influence zone (>25 m) does not match the empirical charts. This can be attributed to the effects of continuous dewatering adopted in the secondary zone of the excavation in the present study.

The settlement profile computed by Clough & O'Rourke (1990) envelopes the numerical values using both MC and HS model and the settlement computed from the charts Ou et al., (2005) for the primary settlement zone. However, the numerical model employing site-specific analysis indicates a higher value of settlement in the secondary settlement zone beyond 40 m, which is mainly attributable to the continuous dewatering, accounted in the numerical analysis. This shows that the empirical methods underestimate the settlements in secondary settlement zone. The settlement computed from the numerical analysis for the different soil models shows a wide variation of 243 mm to 397 mm and is not within the permissible limits of 25 to 40 mm generally adopted for the design of foundations. This order of settlement will affect the foundations of lightly loaded structures to be located near the influence zone. Thus, even though the retaining wall that is already designed for strength and stability will assist the future excavation, the adjacent structures will have settlements beyond the permissible limits of 25 mm to 40 mm, which needs to be addressed. Also, the study highlighted the possible effect of dewatering in settlement of secondary zone and inadequacy of stiffness of backfilled soil to control the settlements within the permissible limit.

6.4 Behaviour of excavation with strut load

As seen in the previous section, while carrying out future excavation using conventional retaining wall, settlement of already placed backfill with stiffness of 15000 kPa is beyond the permissible limit. Since these settlements can cause structural damages, remedial measures need to be implemented while carrying out future excavation to limit the settlement of adjacent soil mass within the permissible range of 25 to 45 mm. Commonly adopted methods to minimize the settlement are anchoring, strut loads and ground improvement to increase the effective stiffness properties of soil. In the present study, two analyses were carried out; the first one considers only strut load and the second one a

combination of strut and improvement of stiffness properties of already placed backfill soil. In this section, a strut load was applied to the model shown in the previous section after each stage of excavation.. The apparent earth pressure was estimated following (Peck, 1969) and the strut load of 500 kN/m was applied at a depth of 2.5 m from top of the excavation (1st strut load) and subsequently at every 5 m depth from the first strut (2nd to 4th strut load) . The 5th strut load of 450 kN/m is applied at a depth of 21.85 m below ground level. The struts need to be constructed after each phase of excavation before continuing excavation. The problem was analysed in PLAXIS and the settlements and displacement computed at each stage is shown in Fig 6.14 (a-f) and 6.15 (a-f). The analysis indicates that, the horizontal displacement of soil behind the retaining wall increases, progressively with increase of depth of excavation. However, the strut load application reduces the displacement comparing to the model without strut load. The maximum displacement at the end of excavation is 122.99 mm. The maximum settlement is 67.4 mm.

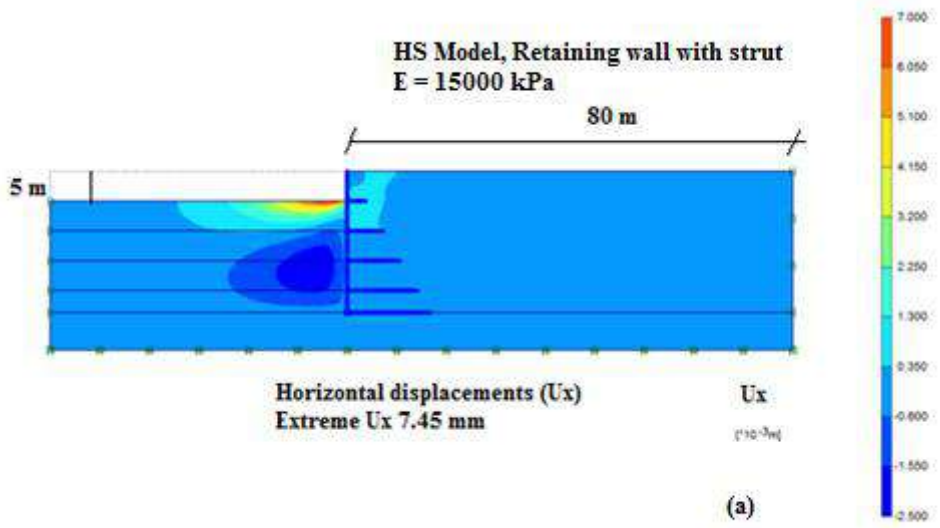

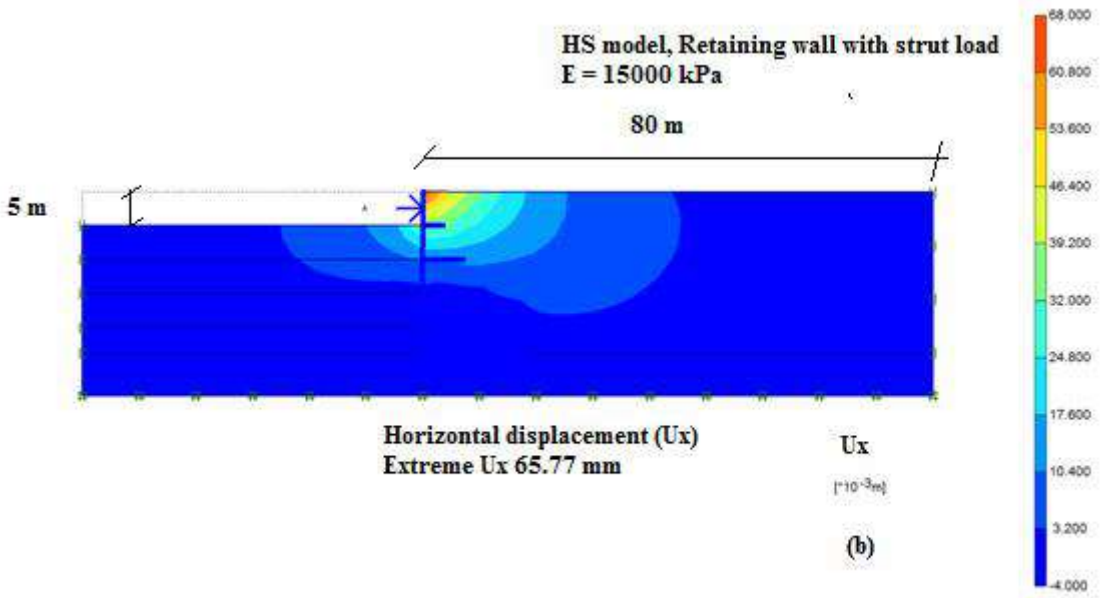
HS model, Retaining wall with strut load
E = 15000 kPa
80 m
5 m
Horizontal displacement (Ux)
Extreme Ux 65.77 mm
Ux
(b)
68.000
60.800
53.600
46.400
39.200
32.000
24.800
17.600
10.400
3.200
-4.000

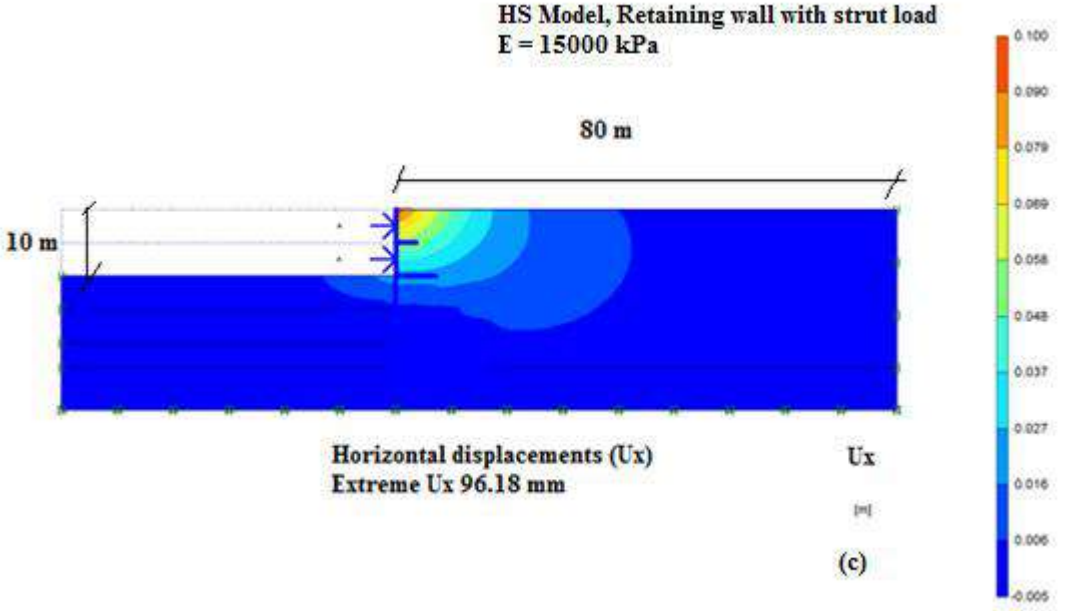
HS Model, Retaining wall with strut load
E = 15000 kPa
80 m
10 m
Horizontal displacements (Ux)
Extreme Ux 96.18 mm
Ux
(c)
0.100
0.090
0.079
0.069
0.058
0.048
0.037
0.027
0.016
0.006
-0.005

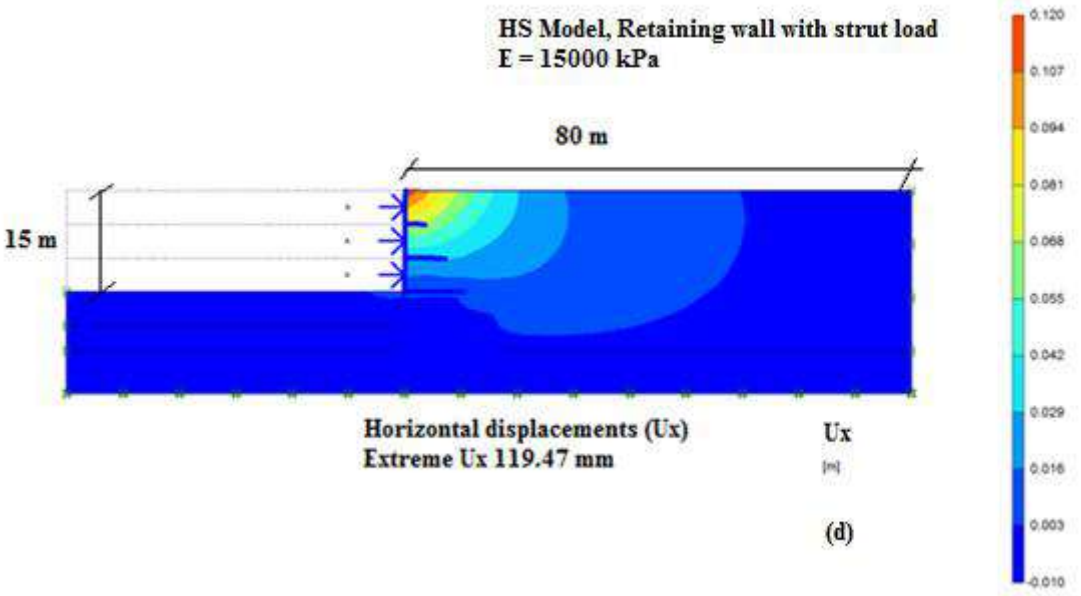
HS Model, Retaining wall with strut load
E = 15000 kPa
80 m
15 m
Horizontal displacements (Ux)
Extreme Ux 119.47 mm
Ux
[m]
0.120
0.107
0.094
0.081
0.068
0.055
0.042
0.029
0.016
0.003
-0.010

(d)

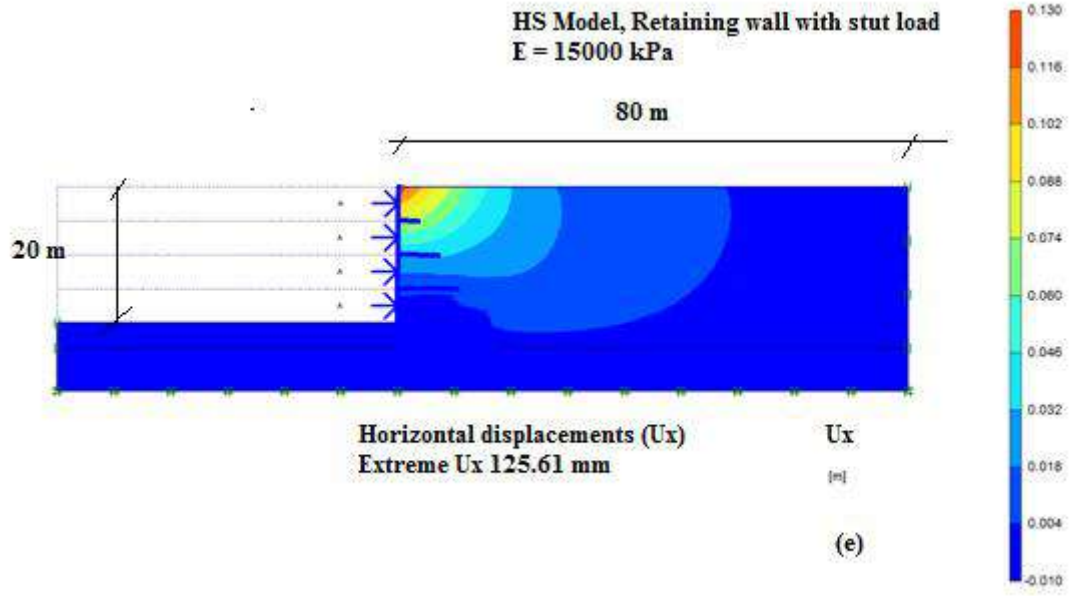
HS Model, Retaining wall with stut load
E = 15000 kPa
80 m
20 m
Horizontal displacements (Ux)
Extreme Ux 125.61 mm
Ux
[m]
0.130
0.116
0.102
0.088
0.074
0.060
0.046
0.032
0.018
0.004
-0.010

(e)

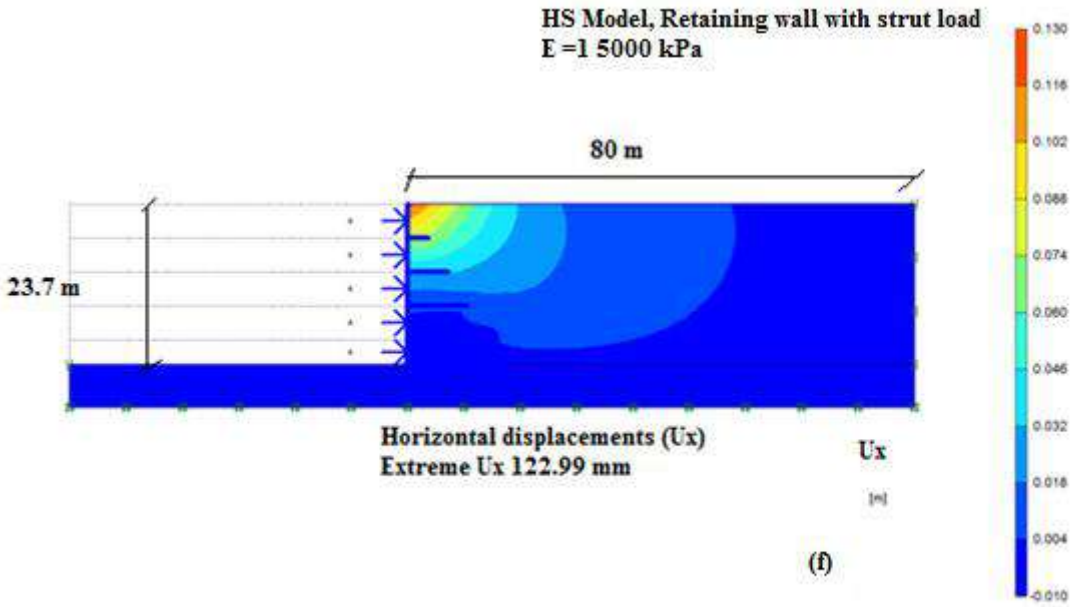

Fig 6.14 – Horizontal displacement profiles from HS model with strut load from different stages of excavation (a) Before sturt load (b) 1st level strut (c) 2nd level strut (d) 3rd level strut (e) 4th level strut (f) 5th level strut

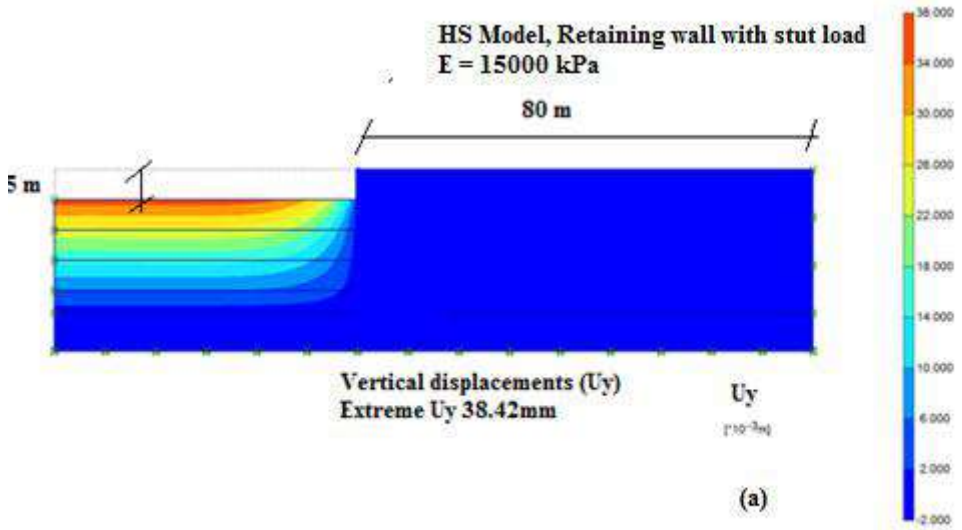

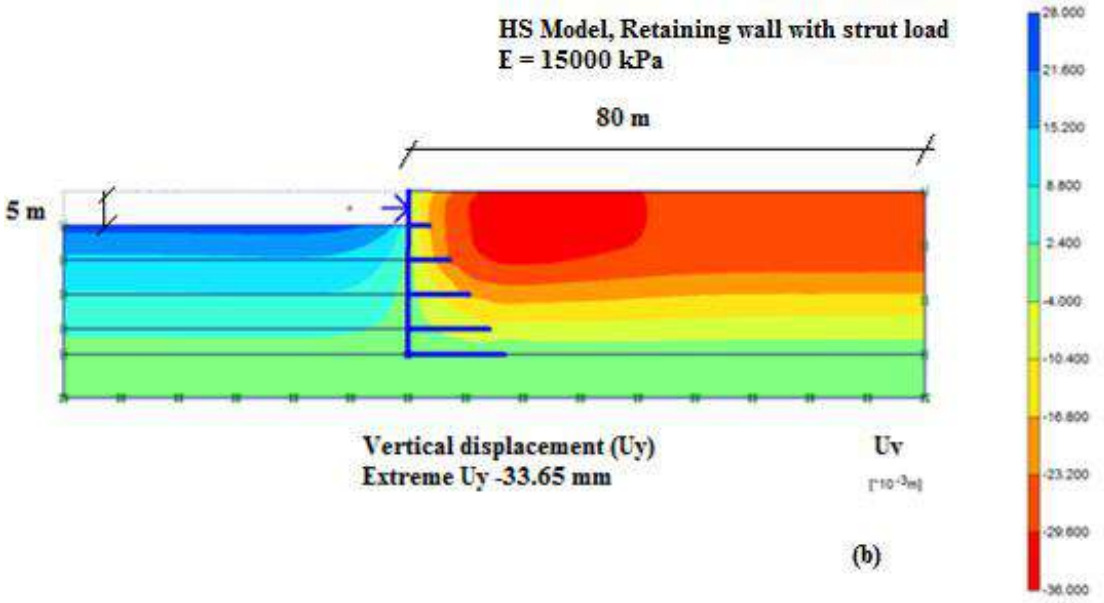
HS Model, Retaining wall with strut load
E = 15000 kPa
80 m
5 m
Vertical displacement (Uy)
Extreme Uy -33.65 mm
Uy
[*10^-3m]
28.000
21.600
15.200
8.800
2.400
-4.000
-10.400
-16.800
-23.200
-29.600
-36.000

(b)

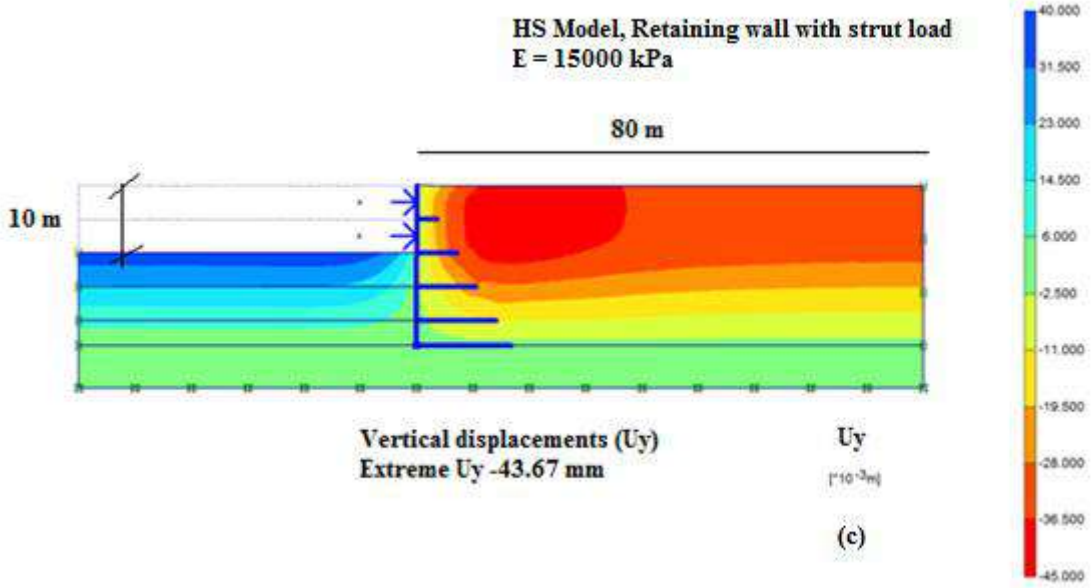
HS Model, Retaining wall with strut load
E = 15000 kPa
80 m
10 m
Vertical displacements (Uy)
Extreme Uy -43.67 mm
Uy
[*10^-3m]
40.000
31.500
23.000
14.500
6.000
-2.500
-11.000
-19.500
-28.000
-36.500
-45.000

(c)

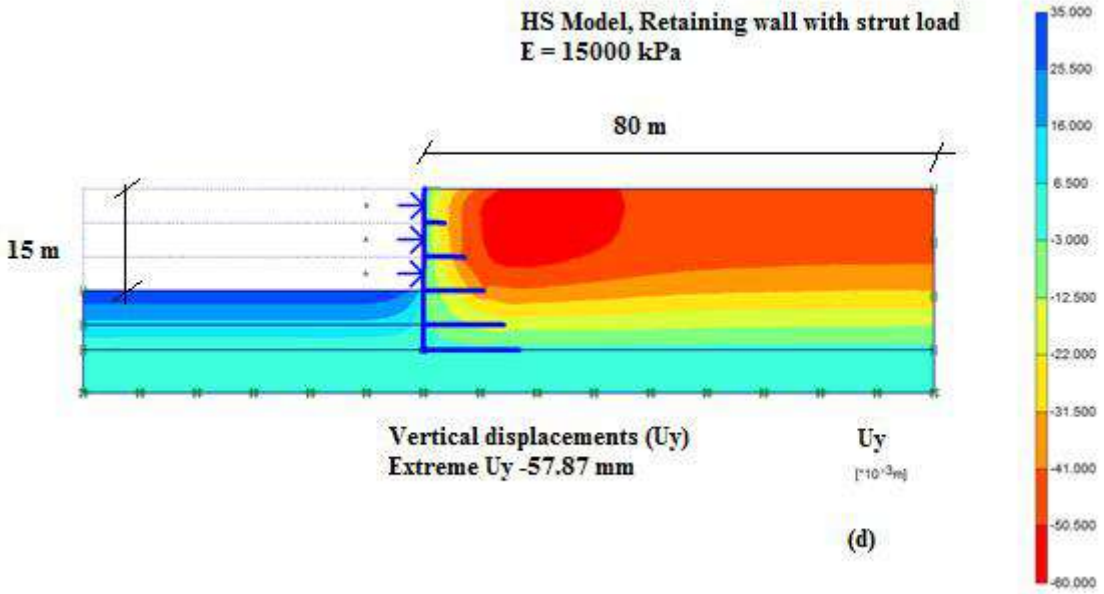
HS Model, Retaining wall with strut load
E = 15000 kPa
80 m
15 m
Vertical displacements (Uy)
Extreme Uy -57.87 mm
Uy
[*10^-3m]
35.000
25.500
16.000
6.500
-3.000
-12.500
-22.000
-31.500
-41.000
-50.500
-60.000

(d)

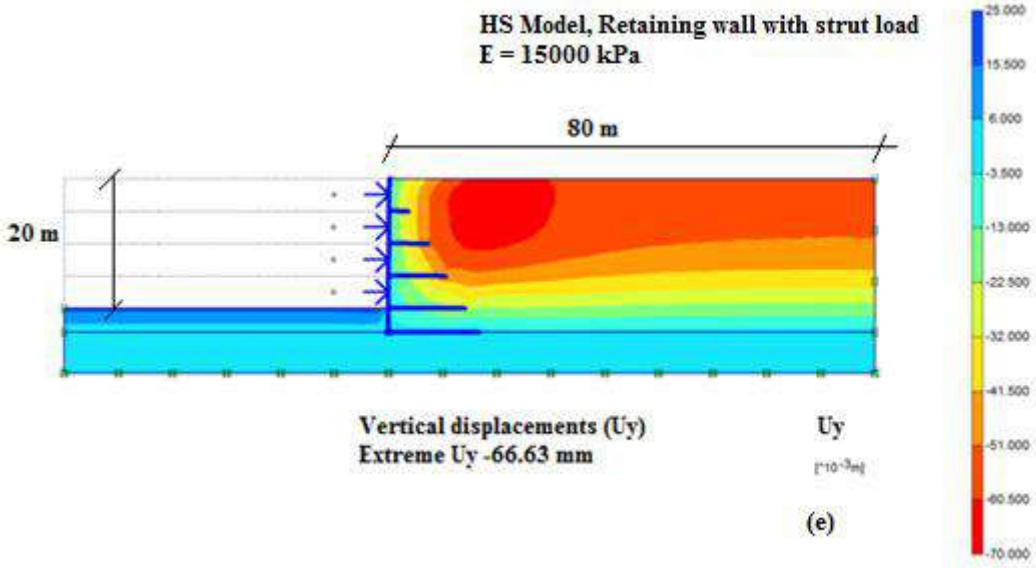
HS Model, Retaining wall with strut load
E = 15000 kPa
80 m
20 m
Vertical displacements (Uy)
Extreme Uy -66.63 mm
Uy
[*10^-3m]
25.000
15.500
6.000
-3.500
-13.000
-22.500
-32.000
-41.500
-51.000
-60.500
-70.000

(e)

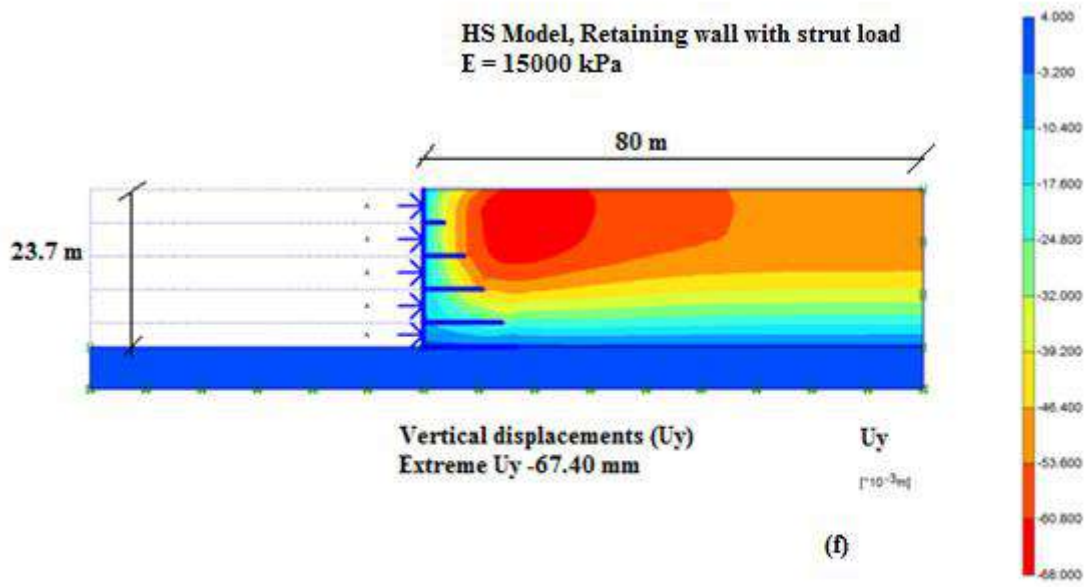

Fig 6.15 – Vertical displacement profiles from HS model (E = 15000 kPa) with strut load from different stages of excavation (a) Before strut load (b) 1st level strut (c) 2nd level strut (d) 3rd level strut (e) 4th level strut (f) 5th level strut

The settlement profiles of adjacent soil mass evaluated from the model for each stage of excavation shows that (Fig 6.16) the settlement can be minimized with the application of strut load. However, the maximum settlement is still higher than the permissible limit of 25 to 40 mm at the last phase of excavation, which is 67.4 mm at a distance of 13.4 m behind the excavation. Without strut load the maximum settlement at the last stage of excavation is 397 mm at a distance of 8.8 m. Comparison of the results indicates that in addition to reducing the settlement, the location of the maximum settlement is shifted away from the retaining wall after the application of strut load. Application of higher strut load can be used to reduce the settlement further to limit it within permissible limits.

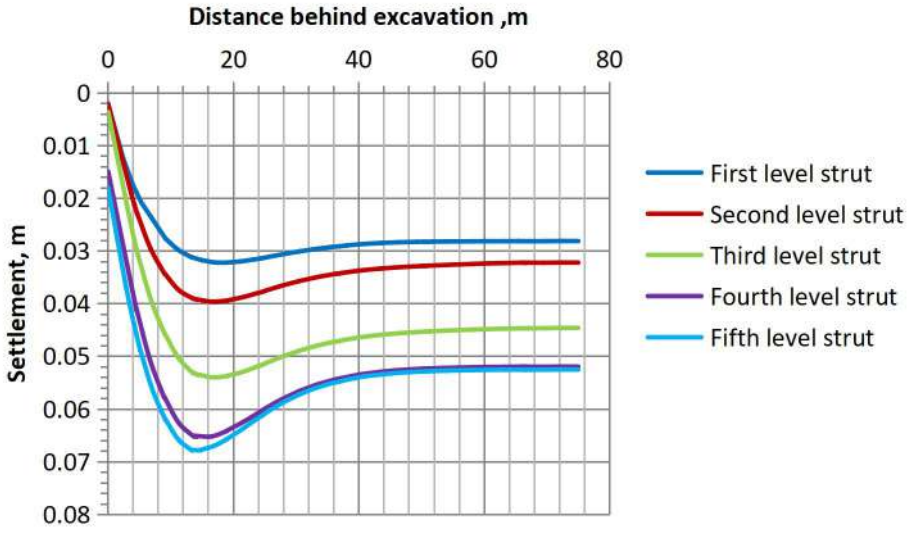

Fig 6.16: Vertical settlement behind excavation after installation of each stage struts

The displacement of soil behind excavation at a distance of 1.0 m is plotted against depth and shown in Fig 6.17.

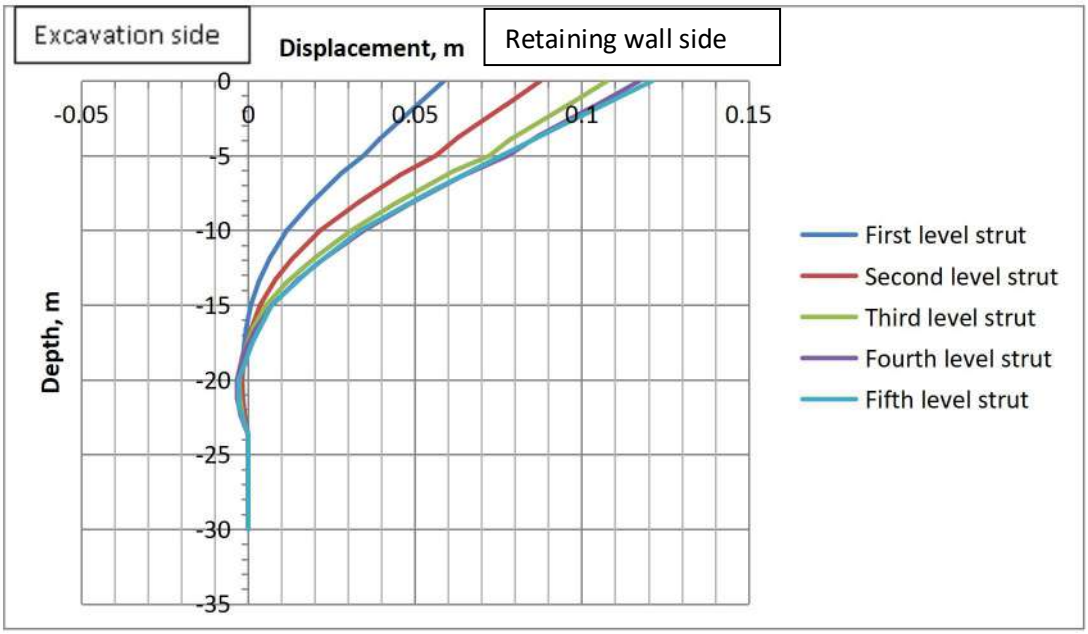

Fig 6.17 – Horizontal displacement behind the retaining wall after installation of each level strut

The horizontal displacement is away from the retaining wall after application of strut load and the displacement increases as the depth of excavation increases. The negative values indicate the movement of the retaining wall is towards excavation and positive values

indicates movement opposite to the excavation. The maximum displacement occurs at surface and is 121 mm at the end of excavation.

6.5 Behaviour of excavation with improved stiffness of soil

The results of analysis presented in the previous section indicates that even with installation of strut load, the settlement behind the retaining wall is beyond the permissible limit. Hence, additional measures are required to restrict the settlements within the permissible limits. Towards this, ground improvements are to be taken up to increase the stiffness of backfill soil along with the application of strut loading. A parametric study was carried out by increasing the insitu stiffness of backfilled soil to a value of 20000 and 25000 kPa and settlement of adjacent soil mass was estimated. In order to increase the stiffness of soil, appropriate methods like cement stabilization, lime stabilization and incorporation of geo grids need to be selected. Field trial needs to be conducted to select the appropriate ground improvement method and these aspects were presently not studied. The behaviour of adjacent soil mass is computed using HS model for stiffness value of 20000 kPa in addition to the already applied strut load and the settlement profile and displacement at a distance of 1.0 m behind the retailing wall at various stages of excavation is shown in Fig 6.18 (a-f) and Fig 6.19 (a-f). As the stiffness increases, the displacement and settlement reduces as indicated in these figure. The maximum displacement and settlement at the end of excavation is 91.91 mm and 50.77 mm for a stiffness of 20000 kPa and the maximum displacement and settlement reduces to 73.75 mm and 40. 7 mm for a stiffness of 25000 kPa.

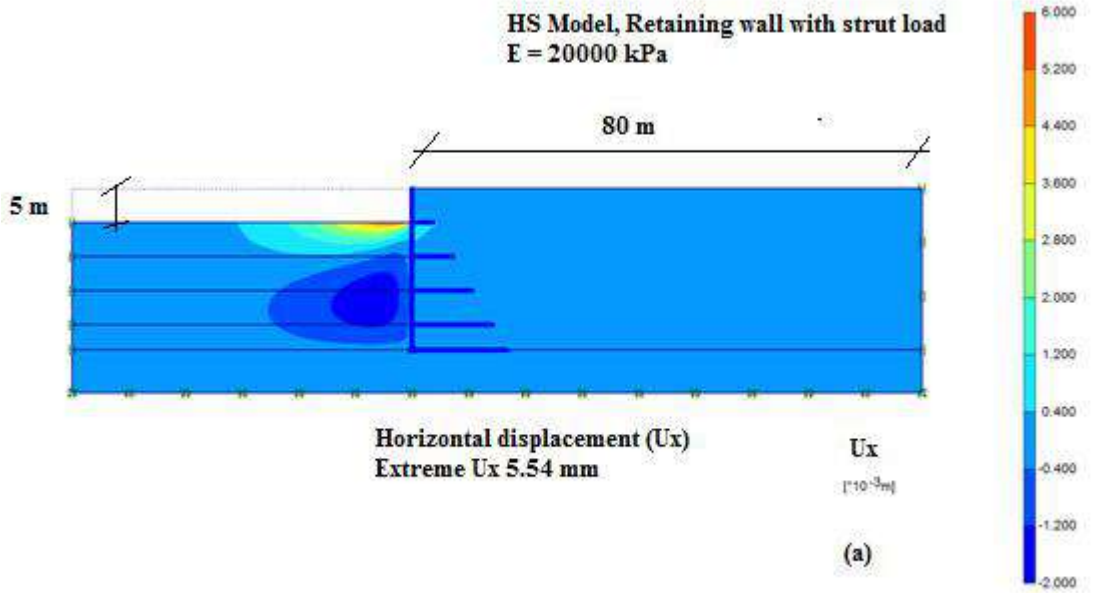
HS Model, Retaining wall with strut load
E = 20000 kPa
80 m
5 m
Horizontal displacement (Ux)
Extreme Ux 5.54 mm
Ux
[*10^-3m]
6.000
5.200
4.400
3.600
2.800
2.000
1.200
0.400
-0.400
-1.200
-2.000

(a)

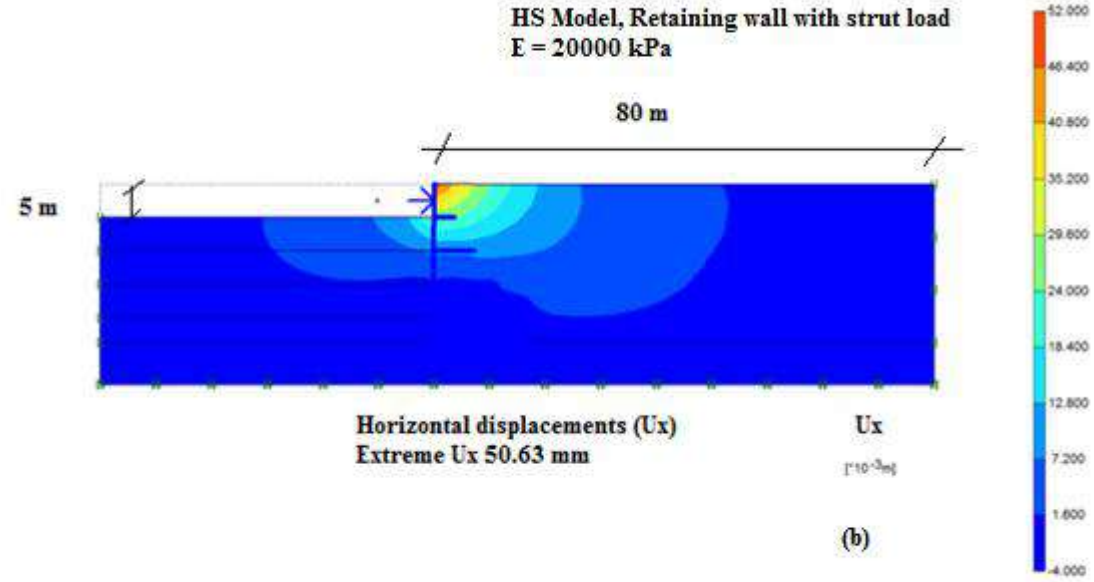
HS Model, Retaining wall with strut load
E = 20000 kPa
80 m
5 m
Horizontal displacements (Ux)
Extreme Ux 50.63 mm
Ux
[*10^-3m]
52.000
46.400
40.800
35.200
29.600
24.000
18.400
12.800
7.200
1.600
-4.000

(b)

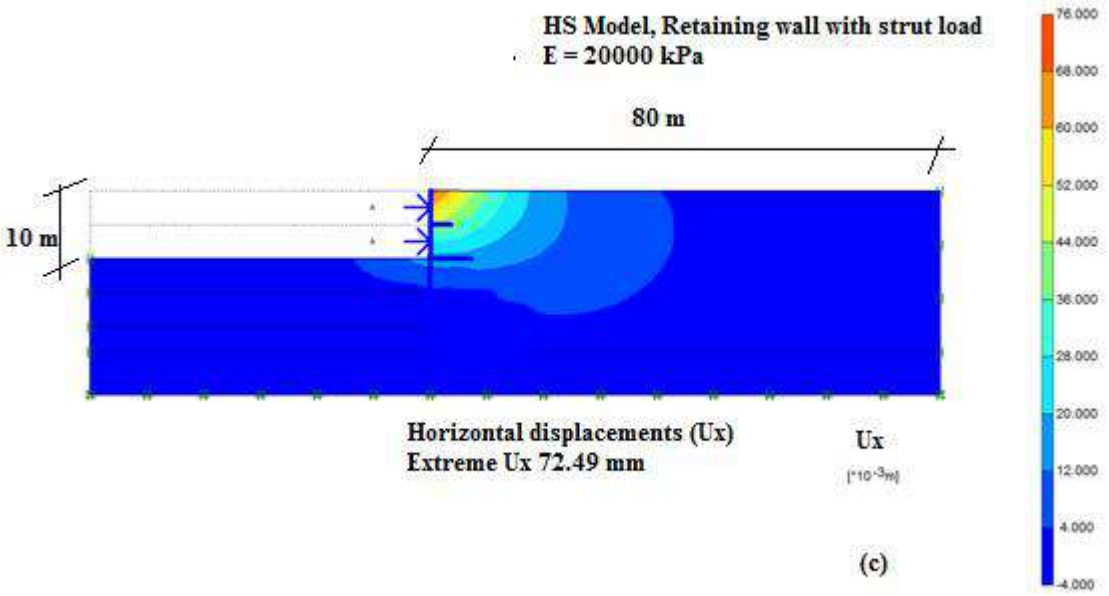
HS Model, Retaining wall with strut load
E = 20000 kPa
80 m
10 m
Horizontal displacements (Ux)
Extreme Ux 72.49 mm
Ux
[*10^-3m]
76.000
68.000
60.000
52.000
44.000
36.000
28.000
20.000
12.000
4.000
-4.000

(c)

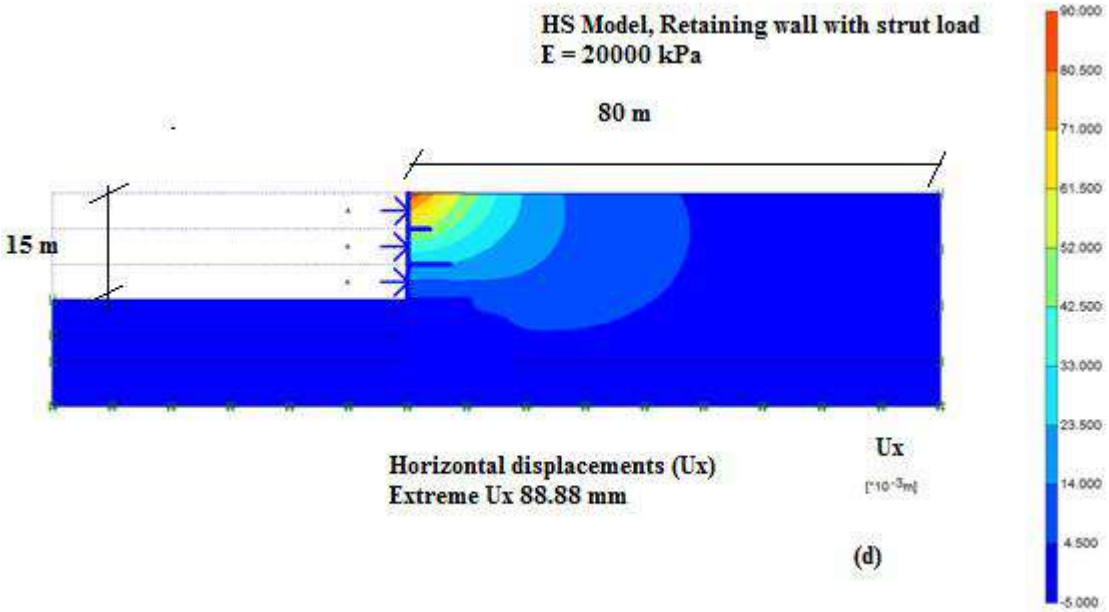
HS Model, Retaining wall with strut load
E = 20000 kPa
80 m
15 m
Horizontal displacements (Ux)
Extreme Ux 88.88 mm
Ux
[*10^-3m]
90.000
80.500
71.000
61.500
52.000
42.500
33.000
23.500
14.000
4.500
-5.000

(d)

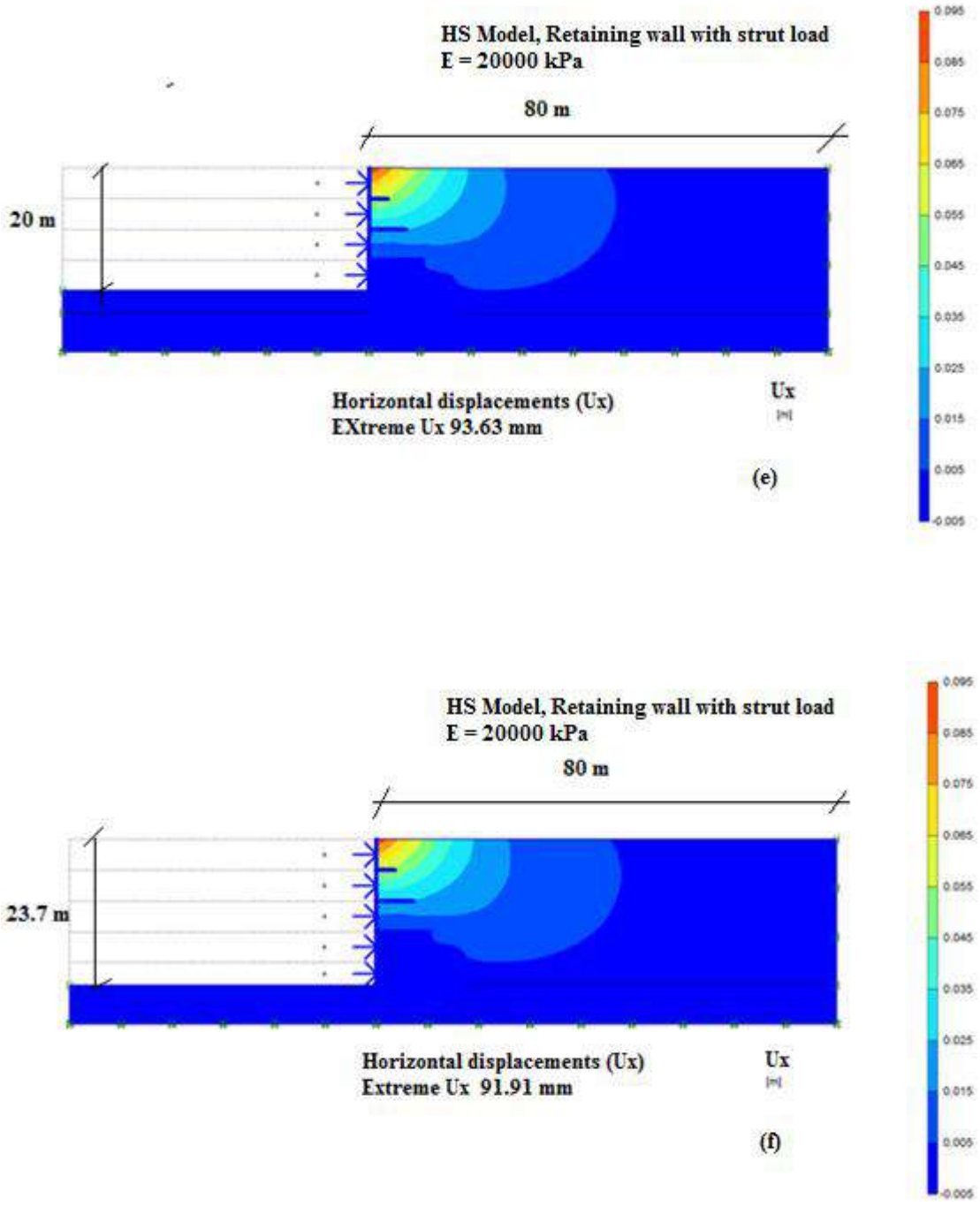

Fig 6.18: Horizontal displacement profiles from HS model (E = 20000 kPa) with strut load from different stages of excavation (a) Before strut load (b) 1st level strut (c) 2nd level strut (d) 3rd level strut (e) 4th level strut (f) 5th level strut

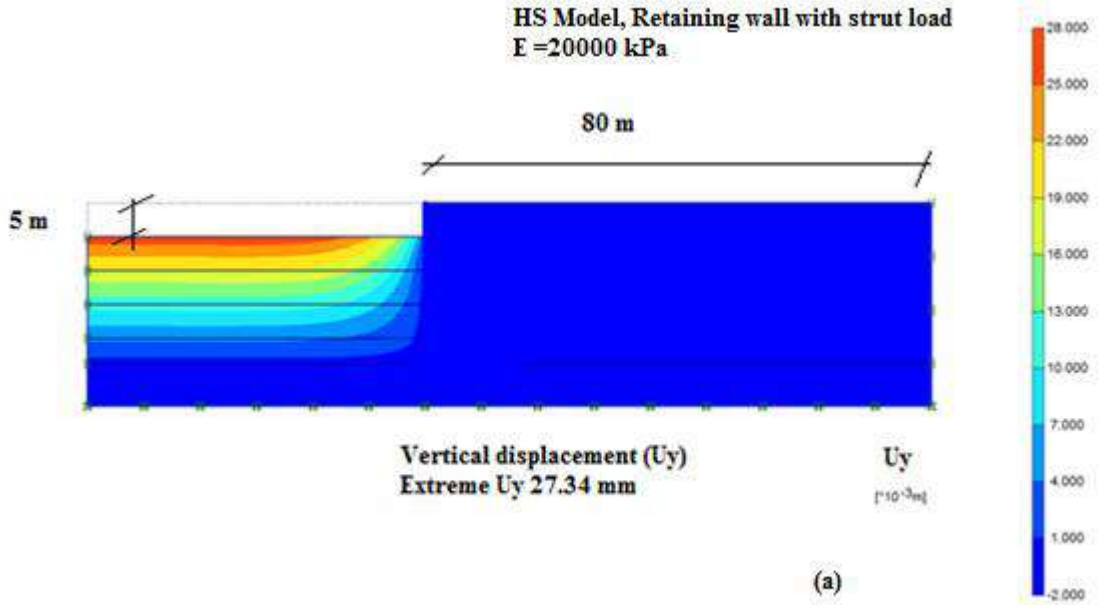
HS Model, Retaining wall with strut load
E =20000 kPa
80 m
5 m
Vertical displacement (Uy)
Extreme Uy 27.34 mm
Uy
28.000
25.000
22.000
19.000
16.000
13.000
10.000
7.000
4.000
1.000
-2.000

(a)

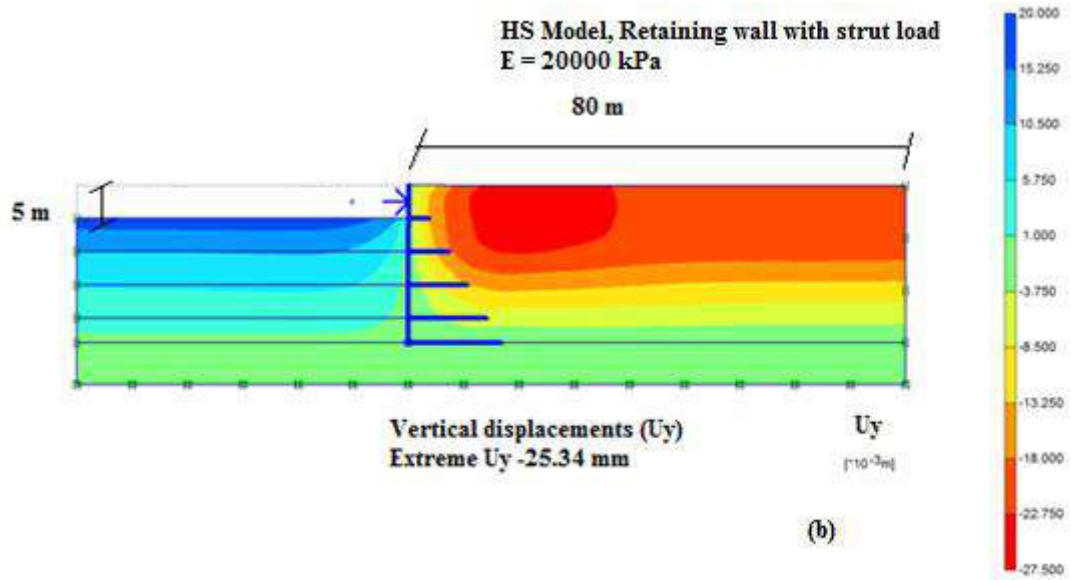
HS Model, Retaining wall with strut load
E = 20000 kPa
80 m
5 m
Vertical displacements (Uy)
Extreme Uy -25.34 mm
Uy
20.000
15.250
10.500
5.750
1.000
-3.750
-8.500
-13.250
-18.000
-22.750
-27.500

(b)

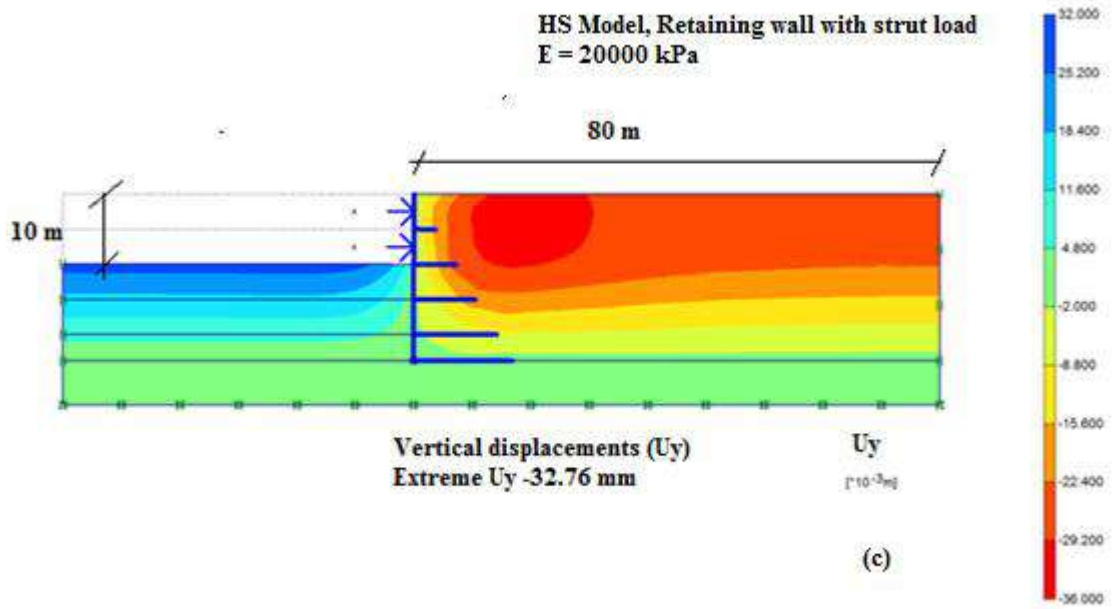
HS Model, Retaining wall with strut load
E = 20000 kPa
80 m
10 m
Vertical displacements (Uy)
Extreme Uy -32.76 mm
Uy
[*10^-3m]
32.000
25.200
18.400
11.600
4.800
-2.000
-8.800
-15.600
-22.400
-29.200
-36.000

(c)

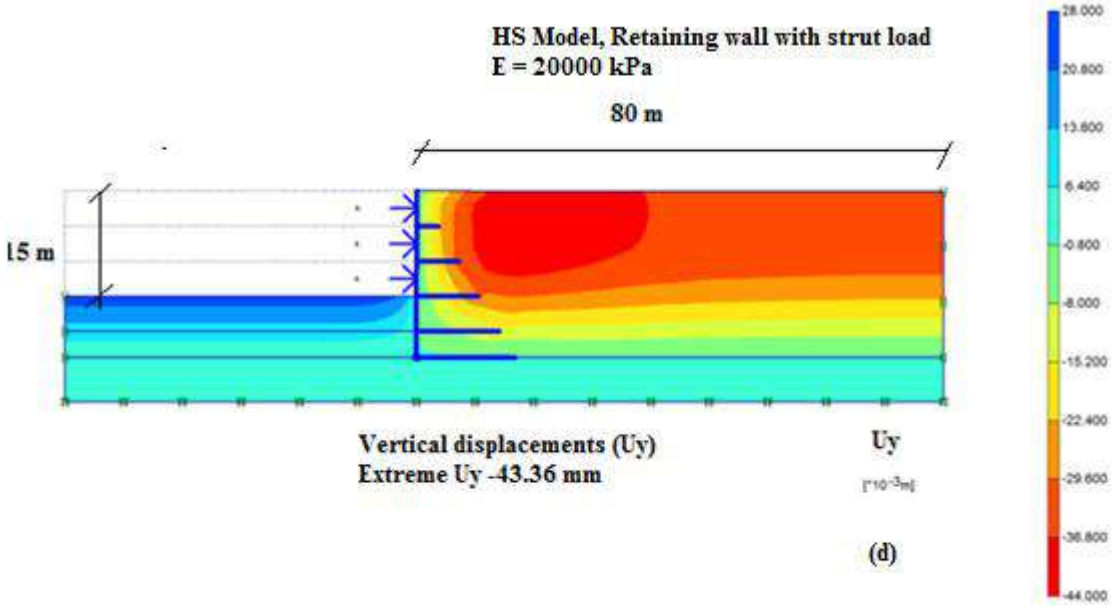
HS Model, Retaining wall with strut load
E = 20000 kPa
80 m
15 m
Vertical displacements (Uy)
Extreme Uy -43.36 mm
Uy
[*10^-3m]
28.000
20.800
13.600
6.400
-0.800
-8.000
-15.200
-22.400
-29.600
-36.800
-44.000

(d)

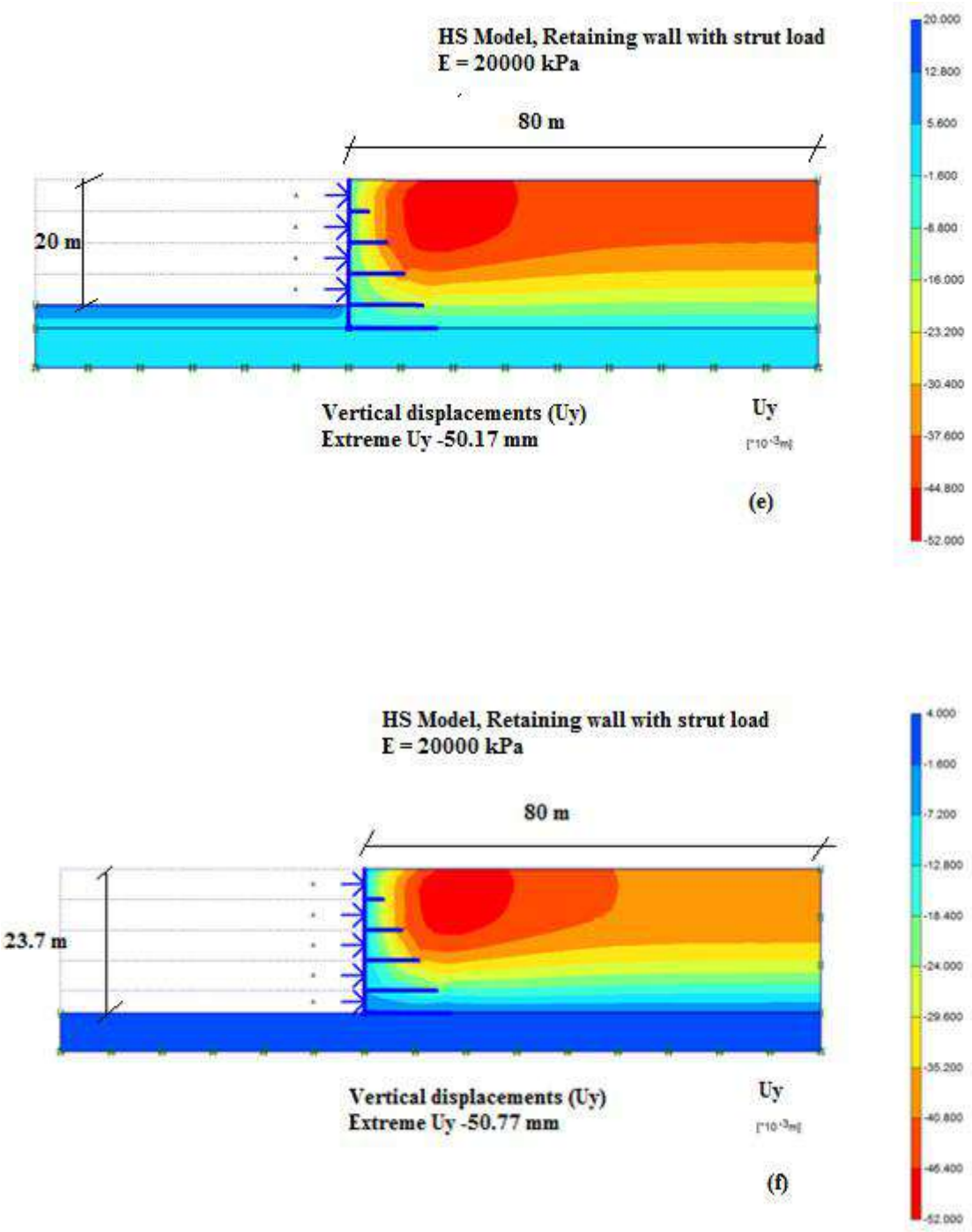

Fig 6.19: Vertical displacement profiles from HS model (E = 20000 kPa) with strut load from different stages of excavation (a) Before strut load (b) 1st level strut (c) 2nd level strut (d) 3rd level strut (e) 4th level strut (f) 5th level strut

The horizontal and vertical displacement contours computed using HS model for a soil stiffness of 25000 kPa is shown in Fig 6.20 (a-f) and 6.21 (a-f). The increase of stiffness of value decreases the horizontal displacement and settlement.

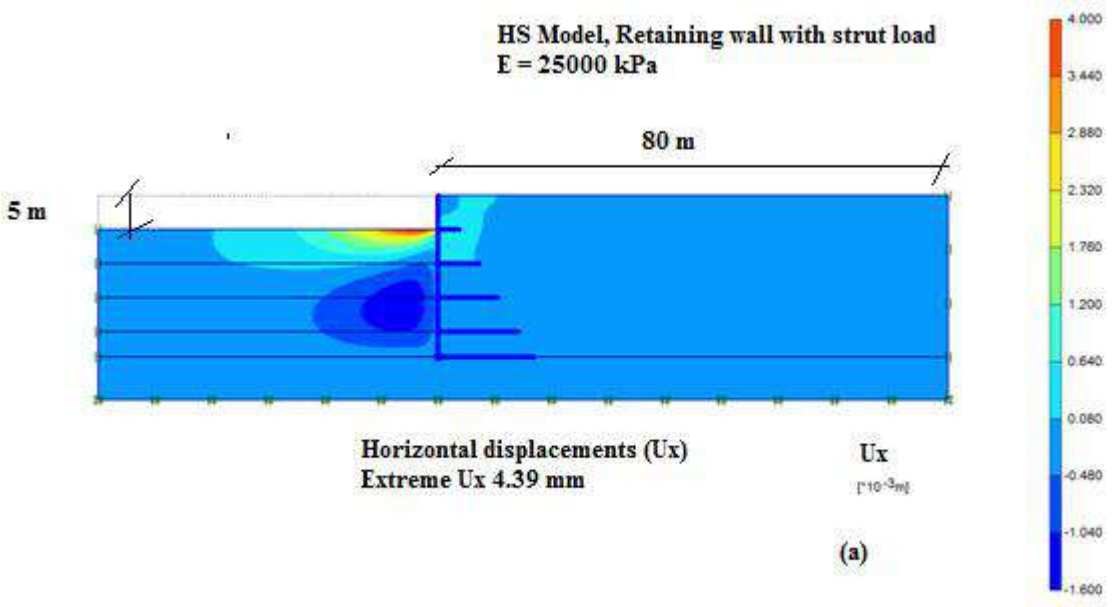

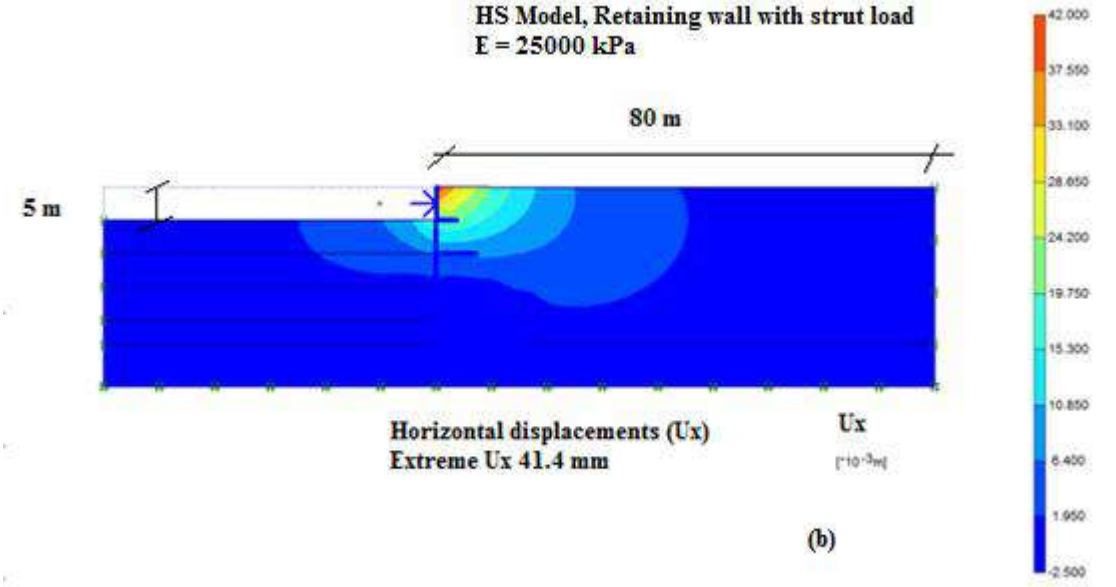

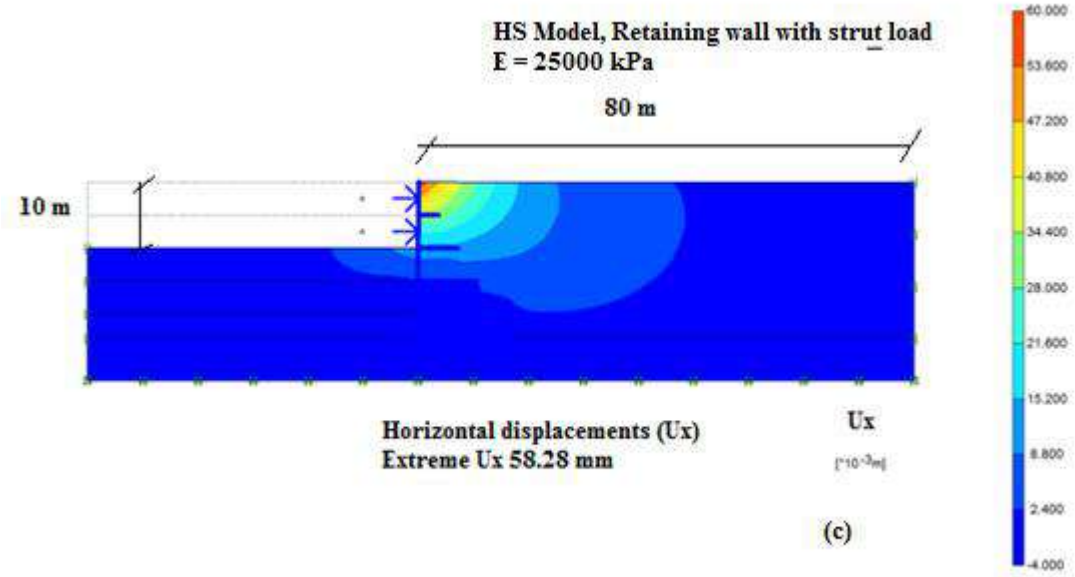
HS Model, Retaining wall with strut load
E = 25000 kPa
80 m
10 m
Horizontal displacements (Ux)
Extreme Ux 58.28 mm
Ux
[*10^-3m]
60.000
53.600
47.200
40.800
34.400
28.000
21.600
15.200
8.800
2.400
-4.000

(c)

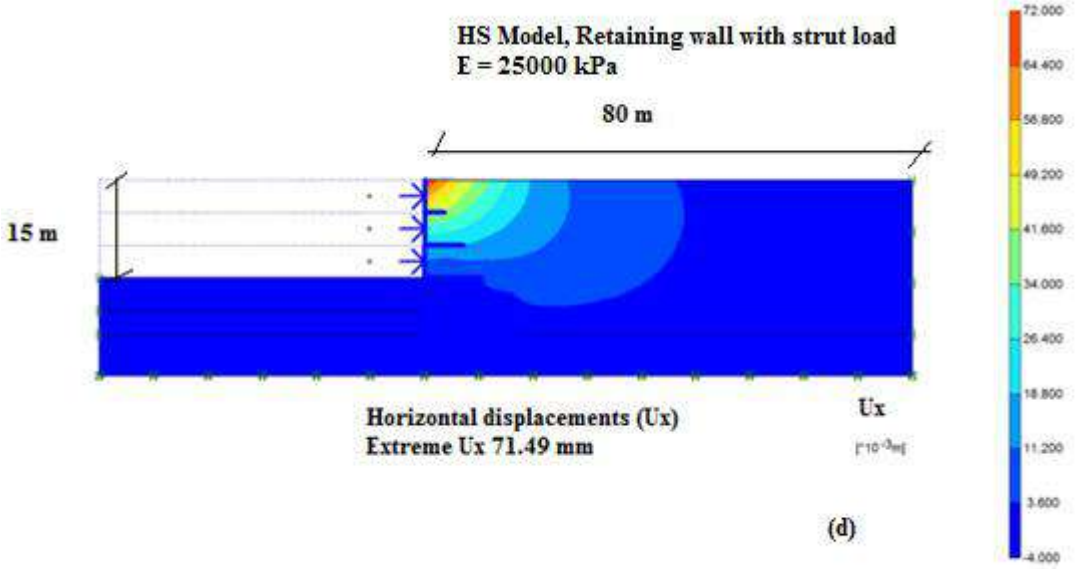
HS Model, Retaining wall with strut load
E = 25000 kPa
80 m
15 m
Horizontal displacements (Ux)
Extreme Ux 71.49 mm
Ux
[*10^-3m]
72.000
64.400
56.800
49.200
41.600
34.000
26.400
18.800
11.200
3.600
-4.000

(d)

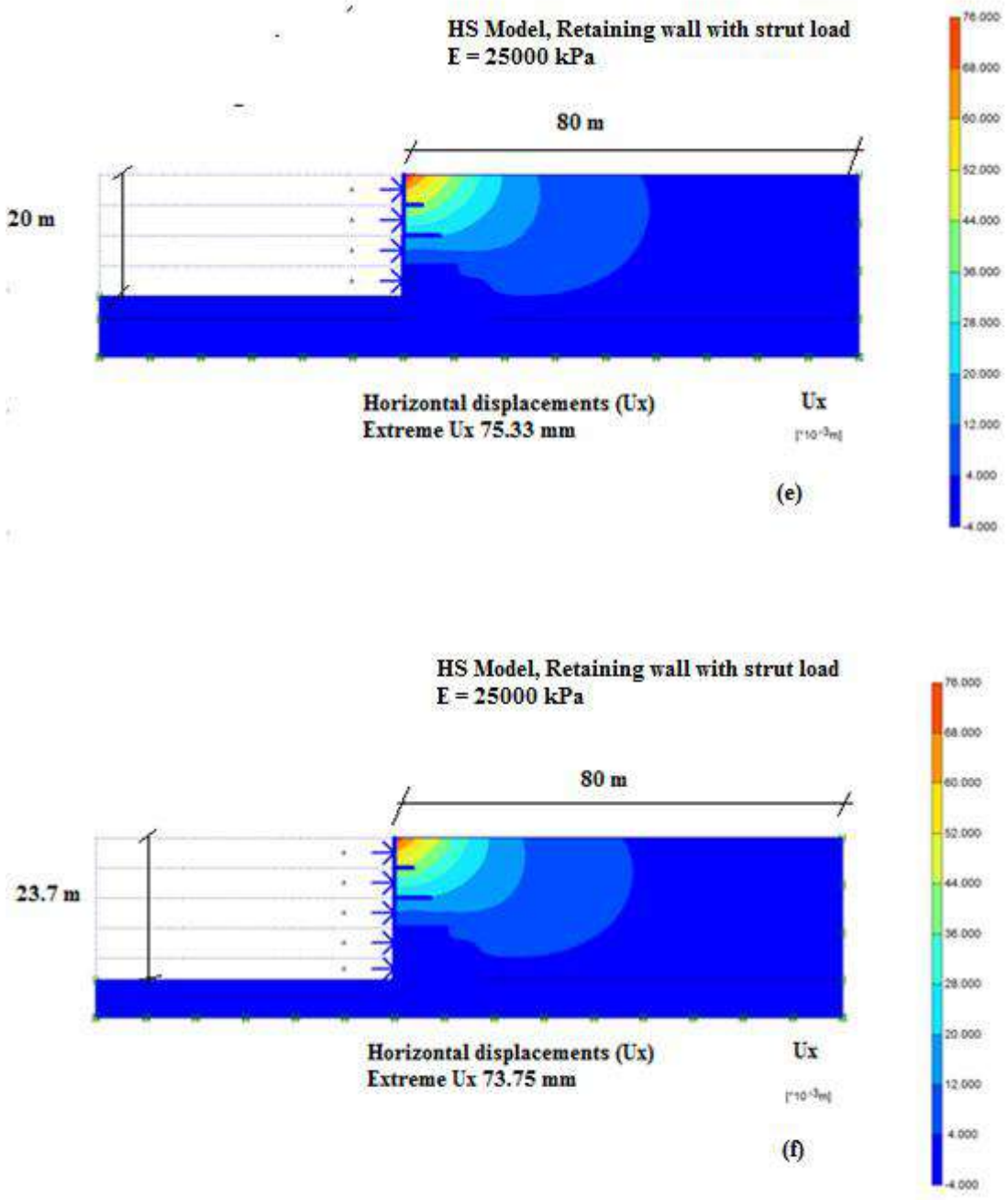

Fig 6.20– Horizontal displacement profiles from HS model (E = 25000 kPa) with strut load from different stages of excavation (a) Before strut load (b) 1st level strut (c) 2nd level strut (d) 3rd level strut (e) 4th level strut (f) 5th level strut

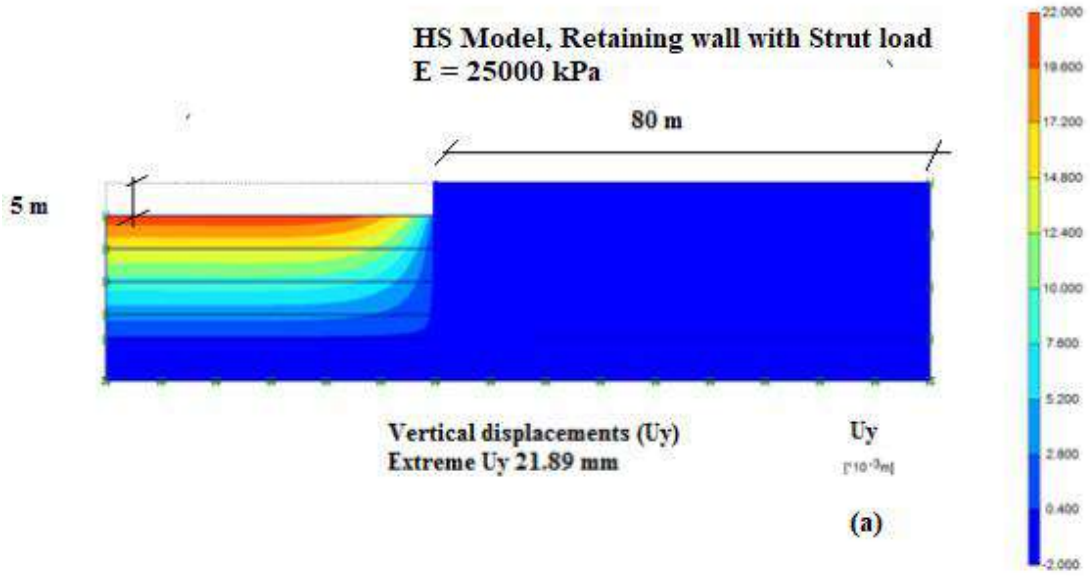
HS Model, Retaining wall with Strut load
E = 25000 kPa
80 m
5 m
Vertical displacements (Uy)
Extreme Uy 21.89 mm
Uy
[*10^-3m]
22.000
19.600
17.200
14.800
12.400
10.000
7.600
5.200
2.800
0.400
-2.000

(a)

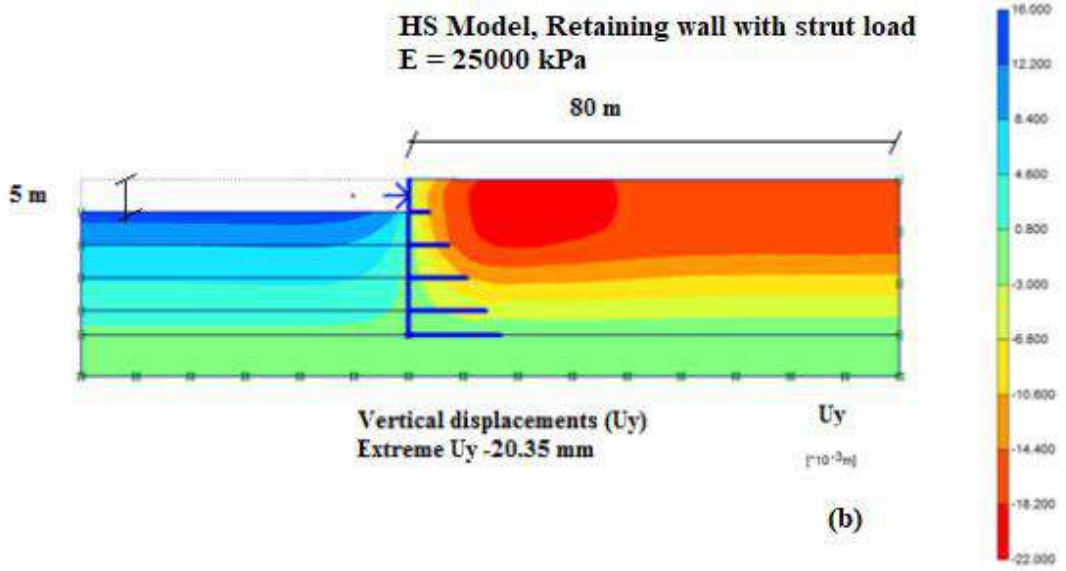
HS Model, Retaining wall with strut load
E = 25000 kPa
80 m
5 m
Vertical displacements (Uy)
Extreme Uy -20.35 mm
Uy
[*10^-3m]
16.000
12.200
8.400
4.600
0.800
-3.000
-6.800
-10.600
-14.400
-18.200
-22.000

(b)

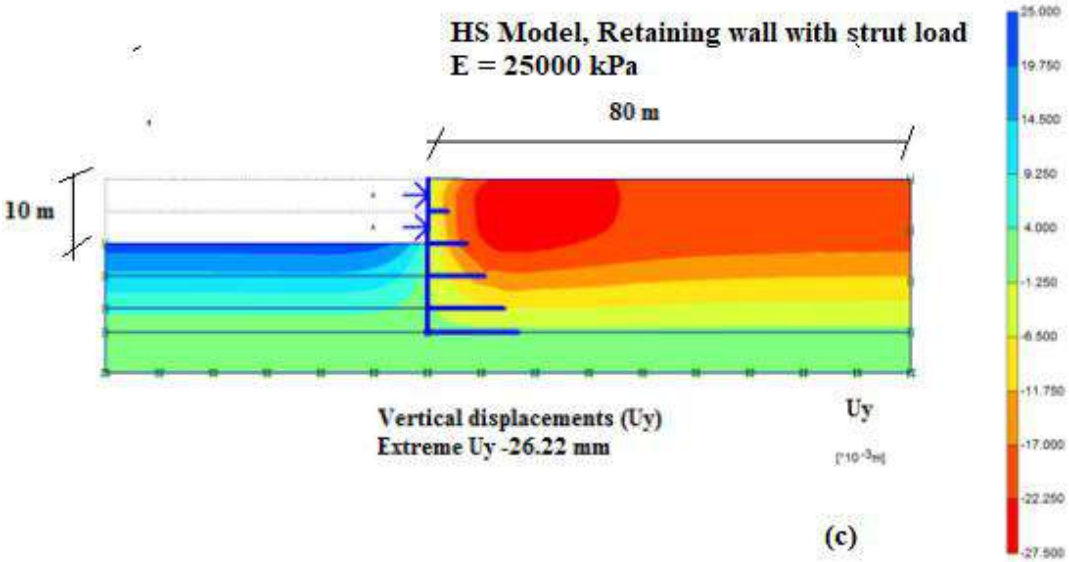
HS Model, Retaining wall with strut load
E = 25000 kPa
80 m
10 m
Vertical displacements (Uy)
Extreme Uy -26.22 mm
Uy
[*10^-3 m]
25.000
19.750
14.500
9.250
4.000
-1.250
-6.500
-11.750
-17.000
-22.250
-27.500

(c)

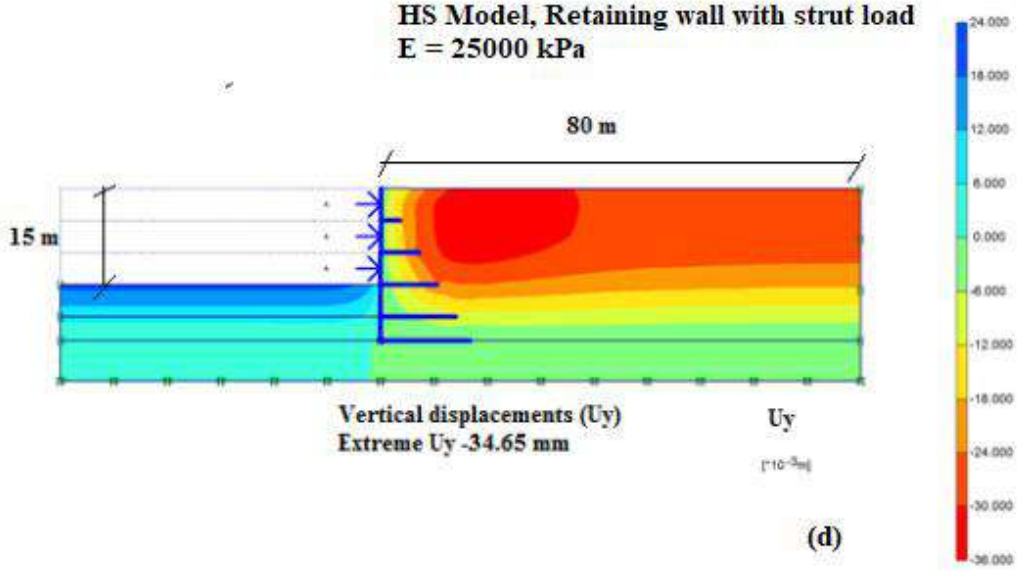
HS Model, Retaining wall with strut load
E = 25000 kPa
80 m
15 m
Vertical displacements (Uy)
Extreme Uy -34.65 mm
Uy
[*10^-3 m]
24.000
18.000
12.000
6.000
0.000
-6.000
-12.000
-18.000
-24.000
-30.000
-36.000

(d)

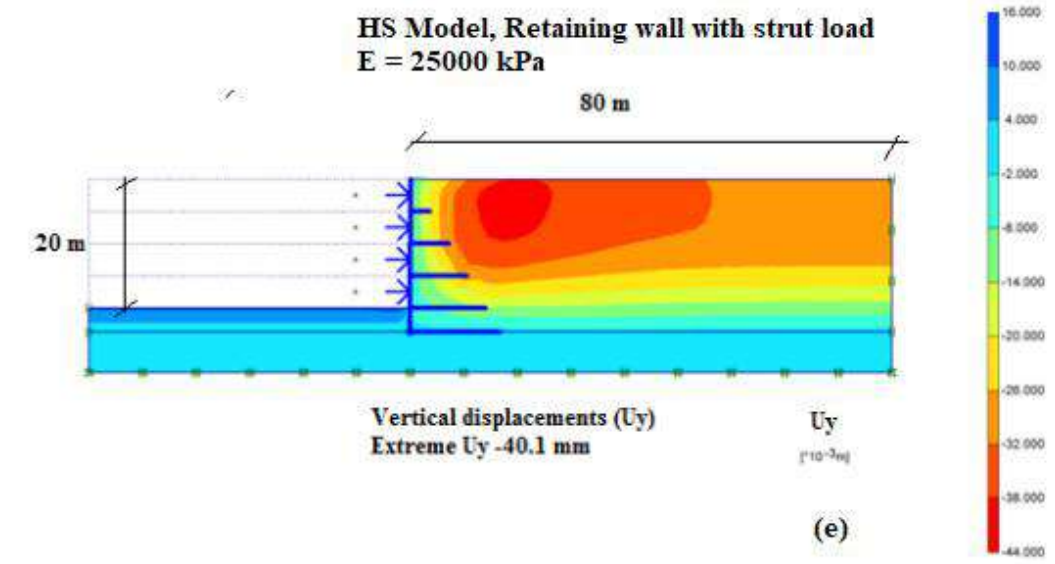

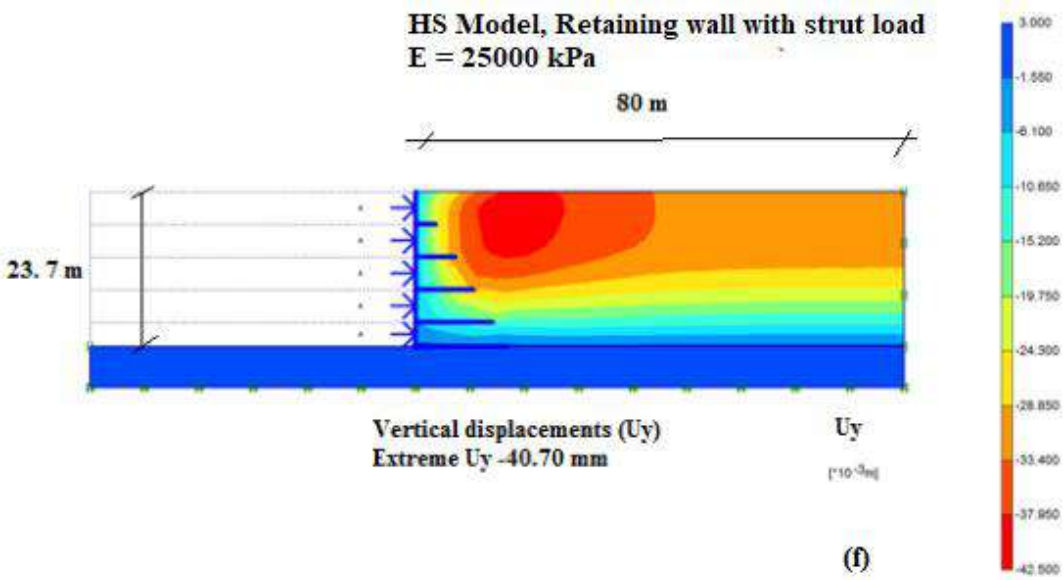

Fig 6.21– Vertical displacement profiles from HS model (E = 25000 kPa) with strut load from different stages of excavation (a) Before strut load (b) 1st level strut (c) 2nd level strut (d) 3rd level strut (e) 4th level strut (f) 5th level strut

The settlement at the final stage of excavation was found to be 48 mm and 39 mm respectively for stiffness values of 20000 kPa and 25000 kPa, which is compared with that obtained from application of strut load for stiffness value of 15000 kPa (Fig 6.22).

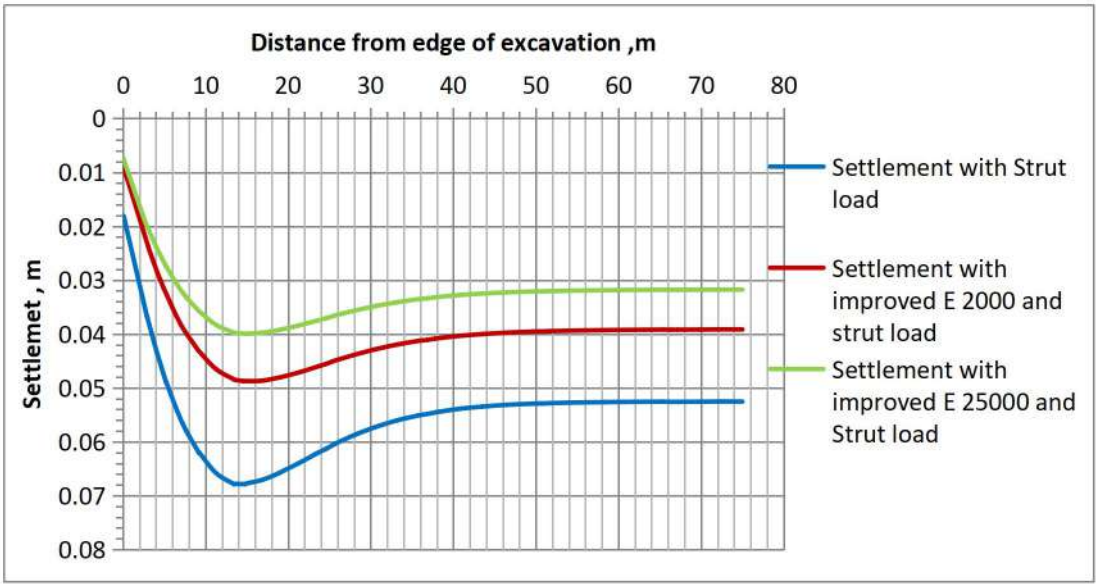

Fig 6.22 : Settlement profiles at the end of excavation for various cases.

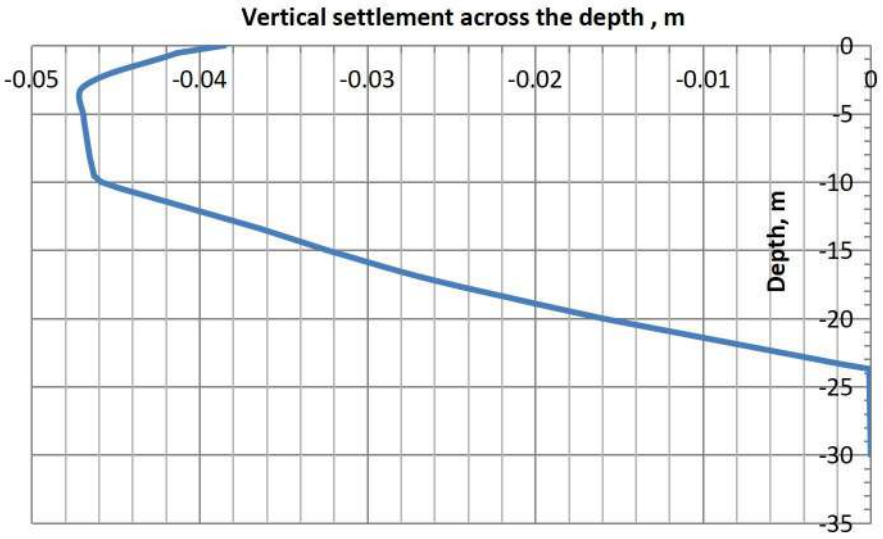

Fig 6.23 : Zone of vertical settlement at the end of excavation with strut load for E = 15000 kPa

The Figure 6.23 indicates that the maximum settlement zone extends from 3 m to 10 m and in this zone, stiffness improvement need to be carried out. This zone also extends upto

20 m behind the edge of retaining wall as shown in Fig 6.22. The analysis of results given in the previous sections and the discussions on remedial measures show that the settlement of adjacent soil mass during future excavation with the help of conventional retaining wall will be beyond permissible limit, and additional measures like strutting and ground improvement to increase the stiffness of the already placed backfilled soil is essential for limiting the settlements during excavation for adjacent structures.

The displacement profiles across the depth for various cases, i.e, strut load without soil improvement and strut load with improved stiffness of 20000 kPa and 25000 kPa shown in Fig 6.24 indicate that, the displacement reduces as the soil stiffness increases, and the maximum displacement is 70 mm at a distance of 1.0 m behind the retaining wall for the improved stiffness of 25000 kPa.

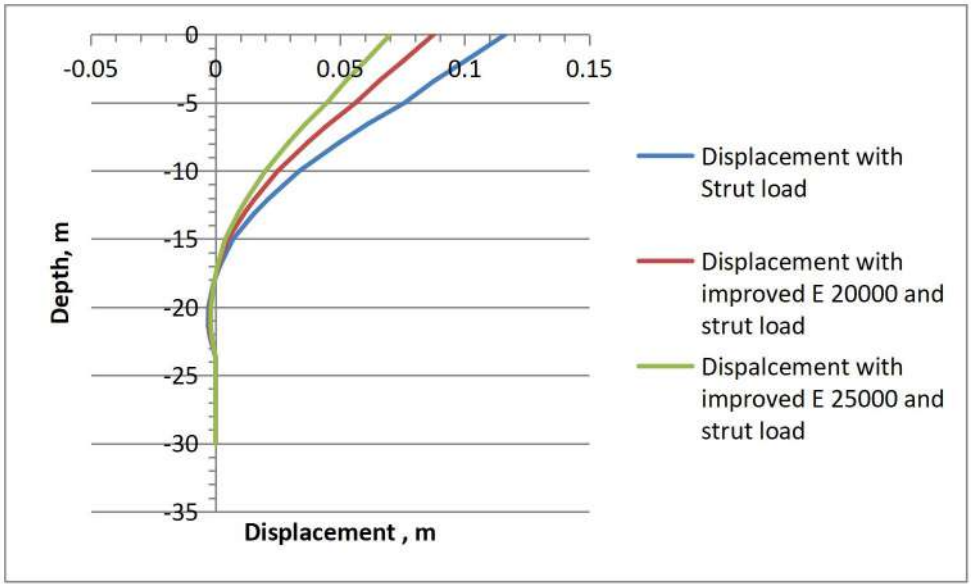

Fig 6.24 : Displacement profiles at 1 m behind the retaining wall at the end of excavation with improved soil stiffness

7.0 Summary

The current practice of deep excavation with the assistance of retaining wall, which is being followed in Indian nuclear industry, does not address the issue of settlement and displacement of adjacent engineered backfilled soil mass. The present study on the efficacy of engineered backfilling in limiting the settlements during future excavation highlighted the following:

- The empirical formulations predict the settlements accurately in primary settlement zones. However, the settlement computed using empirical formulations are lower than those computed using numerical models in the secondary settlement zone.
- The empirical relations established are from the observational case histories of diaphragm wall with limited dewatering. Hence the settlement due to continuous dewatering is not addressed in these formulations. For excavation assisted with counter fort retaining wall and multi stage well point system, these empirical formulations may not be adequate.
- The zone of dewatering is assumed conservatively up to the excavation boundary. However, the calculations using Terzaghi's one dimensional consolidation theory indicates a settlement of 60 mm in the secondary zone due to dewatering which is matching with that predicted from numerical model.
- As the settlement computed using conventional MC model is smaller than that obtained from HS model, the study also indicated the requirement of advanced models accounting non-linear behaviour of soil and non-conservatism involved in using conventional MC model.
- As the settlements computed in both the primary and secondary zones of settlement are higher than the permissible values, additional measures need to be adopted to limit

the settlements in order to ensure the stability of structures supported on this backfilled soil.

- Additional improvement methods like placement of strut load of 450 kN/m at each stage of excavation and improving the stiffness of soil to 25000 kPa for a depth of 15 m and distance of 20 m is essential to limit the settlements to within the permissible limit of 40 mm.

Chapter 7

Summary

Nuclear facilities are being constructed with provisions for future expansion, that will require excavation near existing operating facilities. Open excavations and supported excavation are the basic two type of excavations adopted. In the present study, current practice of deep excavation adopted in Indian Nuclear industry was critically reviewed and impact of these excavation induced ground deformations in close proximity, was numerically studied and calibrated with field monitored displacements and settlements.

The major works carried out during the study are mainly divided into three parts namely (a) Characterization of site for deep excavation problems, validation of results using field instrumentation and identifying appropriate soil constitutive models for analyzing deep excavation in multilayered soil sites (b) evaluation of stiffness properties of engineered backfill soil from numerical analysis and (c) numerical analysis of supported deep excavation in engineered backfill soil and study on efficacy of engineered backfill soil in limiting the settlements and displacements during deep excavation.

Towards this, site characterization was carried out using various methods and parameters required for soil constitutive models were arrived at. An open deep excavation carried out in a multi layered soil site as the part of locating a nuclear facility was analyzed and a suitable soil constitutive model was selected after comparison and validation of results with field data. This study was extended to evaluate the stiffness properties of engineered backfill soil after analyzing a deep excavation carried out in engineered back filled soil. Further, the behaviour of supported excavation in engineered backfilling was studied and the results indicated the inadequacy of the existing engineered backfilling in limiting the settlements and displacements.

7.1 Conclusion

The major conclusions from the study are as follows.

a) The analysis of open excavation indicated that, a single conventional constitutive model is not adequate to decipher the behaviour of deep excavation in a multi layered soil site. A combination of constitutive models namely MC model accounting for the dilatency and incremental increase in stiffness of the soil layer and HS model for silty/clayey sand layer is required to predict excavation behavior.

b) Conventional MC model is not always conservative in predicting the settlements and higher order models are essential.

c) The study indicated that the influence of open deep excavation is felt upto a distance of 20 m which is 1.08 times the depth of excavation.

d) Comparison of instrumentation data with numerical analysis results indicated the corner effects of deep excavation and indicated the necessity of three-dimensional analysis for excavation of such magnitude.

e) The settlement observed by field monitors in the primary settlement zone of the open excavation is less than the value computed by the models. However, the settlement beyond 10 m distance, the model computed values and field observed values are almost matching and the maximum settlement observed from the field is 42 mm at a distance of 20 m behind the excavation edge while the maximum computed settlement is 38.24 mm at a distance of 17.5 m behind the excavation.

f) The parametric study carried out for the variability of soil thickness indicated that the idealized soil profile predicts higher surface settlement and displacement than from the analysis accounting for the soil thickness variation.

g) The back calculation of displacement of open excavation indicated that available conventional correlations overestimates the stiffness of loose and medium sandy soil but underestimate that of the dense sand layer . Site-specific empirical relations were proposed which can be used for sites of similar geology and characteristics.

h) The stiffness properties of back filled soil evaluated from various field investigation methods vary widely and the present study shows that the stiffness parameter of backfilled soil obtained from conventional pressuremeter is conservative; the actual insitu stiffness of backfilled soil is 50% higher than that estimated from conventional pressuremeter test. The stiffness obtained from full-scale plate load tests overestimates the actual stiffness by 100%.

i) The empirical formulations for predicting the settlements of supported excavations predict the settlements accurately in primary settlement zones, while under predicting those in the secondary settlement zone due to site specific dewatering, which is not taken into account in the current empirical formulations.

j) The higher settlements in the entire secondary settlement zone is due to the assumption of continuous dewatering upto the excavation boundary.

k) As the settlement computed using conventional MC model is smaller than that obtained from HS model, the study also indicated the requirement for advanced models that account for the non-linear behaviour of soil. In addition, comparison of the data brought out the non-conservatism involved in using conventional MC model in predicting settlements.

l) The settlements computed in both the primary and secondary zones of settlements in the engineered backfilled soil are higher than the permissible values of 40 mm. These values

need to be limited to ensure the stability of structures supported on this backfilled soil. Additional measures like placement of struts and improving the stiffness of soil to an extent of 25000 kPa for a depth of 15 m and an extent of 20 m is essential to limit the settlements within the permissible limit of 40 mm.

7.2 Scope of Future work

The results obtained from the studies carried out as part of the thesis clearly establish the inadequacy of the present system of retaining wall assisted deep excavation in engineered backfilling to limit the settlements during future excavation. The conclusions drawn from the study are valuable inputs for the design of future excavation systems in engineered backfill soil. Further research needs to be taken up to identify the methods for improving the stiffness of engineered backfilling in the primary settlement zones. Cement stabilization, lime stabilization and the effect of geo grids in improving the stiffness properties need to be studied. Various laboratory and field investigations need to be carried out to evaluate the parameters of stabilized soil including pore pressure monitoring required for numerical analysis. Comprehensive study on instrumentation data from future excavations needs to be studied to identify the appropriate soil models and calibration of soil models used in analysis. Also, three dimensional analysis needs to be carried out by employing further advanced models like Hardening Small Strain (HSS) modelto evaluate the corner effects in massive excavations.

REFERENCES

1. ASTM, D. (2000). 4719 Standard test method for prebored pressuremeter testing in soils. *American Society for Testing & Materials Standard*.
2. Baguelin, F., Jézéquel, J. F., & Shields, D. H. (1978). *The pressuremeter and foundation engineering* (Vol. 2). Clausthal, Germany: Trans Tech Publications.
3. Banerjee, S., & Gupta, H. P. (2017). The evolution of the Indian nuclear power programme. *Progress in Nuclear Energy*, *101*, 4-18.
4. Becker, P. (2013). Importance of Observational Method in View of Numerical Analyses for Retaining Structures in Soft Soils. In the Proceedings of the Seventh International conference on case histories in geotechnical engineering, 28.http://scholarsmine.mst.edu/icchge/7icchge/session01/28
5. Bhatkar, T., Barman, D., Mandal, A., & Usmani, A. (2017). Prediction of behaviour of a deep excavation in soft soil: a case study. *International Journal of Geotechnical Engineering*, *11*(1), 10-19.
6. Boominathan, A. (2004). Seismic site characterization for nuclear structures and power plants. *Current Science*, 1388-1397.
7. Bowles, J.E., (1998). Foundation analysis and design. 4th Edition, McGraw-Hill Book Company, New York, USA.
8. Brinkgreve, R. B. J. (2004). Time-dependent behaviour of soft soils during embankment construction–a numerical study. *Proc. NUMOG IX*, 631-637.
9. Brinkgreve, R. B. J., & Vermeer, A. (1992). On the use of Cam-Clay models. In *Symposium on Numerical Models in Geomechanics, Balkema, Rotterdam, Netherlands*.
10. Brinkgreve, R. B. J., Swolfs, W. M., Engin, E., Waterman, D., Chesaru, A., Bonnier, P. G., & Galavi, V. (2010). PLAXIS 2D 2010. *User manual, Plaxis bv*.
11. Clough, G. W. (1990). Construction induced movements of in situ walls. *Design and performance of earth retaining structures*, 439-470. Geotech. Spec.Publ. No.25, ASCE, NY, 439-470
12. Clough, G. W., Smith, E. M., & Sweeney, B. P. (1989). Movement control of excavation support systems by iterative design. In *Foundation engineering: current principles and practices* (pp. 869-884). ASCE.
13. Code, I. S. IS 1888–1982. *Method of load test on soils (second revision)*.
14. Code, I. S. IS 2720 (Part 13)–1986. *Direct shear test (second revision)*.

15. Code, I. S. IS 2720 (Part 15)–1986. *Determination of consolidation properties (first revision)*.
16. Code, I. S. IS 2720 (Part 5)–1985. *Determination of liquid and plastic limit (second revision)*.
17. Cornforth, D. (2005). *Landslides in practice: investigation, analysis, and remedial/preventative options in soils*. Wiley.
18. Duncan, J. M., & Chang, C. Y. (1970). Nonlinear analysis of stress and strain in soils. *Journal of Soil Mechanics & Foundations Div*.
19. Dunnicliff, J. (1993). Geotechnical Instrumentation for Monitoring Field Performance, John Wiley, New York, 1993, pp. 250–268.
20. Erikson, C. M., Kraemer, S. R., & Jonnson, E. G. (1992). Geotechnical instrumentation for deep excavations in Boston. *Civil Engineering Practice*, *7*(1), 47-66.
21. Gambin, M. P., & Rousseau, J. (1988). The Menard pressuremeter: interpretation and application of pressuremeter test results to foundation design. *ISSMFE Technical Committee on Pressuremeter and Dilatometer Testing, General Memorandum, Sols Soils*, (26), 50.
22. Goh, A. T. C., Zhang, F., Zhang, W., Zhang, Y., & Liu, H. (2017). A simple estimation model for 3D braced excavation wall deflection. *Computers and Geotechnics*, *83*, 106-113.
23. Goldberg, D. T., Jaworski, W. E., & Gordon, M. D. (1976). Lateral Support Systems and Underpinning. Volume I: Design And Construction.
24. Gorska, K., & Wyjadłowski, M. (2012). Analysis of displacement of excavation based on inclinometer measurements. *Studia Geotechnica et Mechanica*, *34*(4), 3-16.
25. Guide, A. S. (2008). Geotechnical aspects and Safety of foundation for buildings and structures important to safety of nuclear power plants.
26. Hatanaka, M., & Uchida, A. (1996). Empirical correlation between penetration resistance and internal friction angle of sandy soils. *Soils and foundations*, *36*(4), 1-9.
27. Hsieh, P. G. (1999). *Prediction of ground movements caused by deep excavation in clay* (Doctoral dissertation, Ph. D. dissertation, Department of Construction Engineering, National Taiwan University of Science and Technology, Taipei, Taiwan.[In Chinese.]).
28. Hsieh, P. G., & Ou, C. Y. (1998). Shape of ground surface settlement profiles caused by excavation. *Canadian geotechnical journal*, *35*(6), 1004-1017.

29. Hsiung, B. C. B. (2009). A case study on the behaviour of a deep excavation in sand. *Computers and Geotechnics*, *36*(4), 665-675.
30. Hsiung, B. C. B., & Dao, S. D. (2016). Impacts from three-dimensional effect on the wall deflection induced by a deep excavation in Kaohsiung, Taiwan. *Japanese Geotechnical Society Special Publication*, *2*(45), 1602-1607.
31. Hsiung, B. C. B., Yang, K. H., Aila, W., & Hung, C. (2016). Three-dimensional effects of a deep excavation on wall deflections in loose to medium dense sands. *Computers and Geotechnics*, *80*, 138-151.
32. Hsiung, B. C., & Dao, S. D. (2014). Evaluation of constitutive soil models for predicting movements caused by a deep excavation in sands. *Electronic Journal of Geotechnical Engineering*, *19*, 17325-17344.
33. Janbu, N. (1963). Soil compressibility as determined by odometer and triaxial tests. In *Proc. Europ. Conf. SMFE* ,Vol. 1, 19-25.
34. Khoiri, M., & Ou, C. Y. (2013). Evaluation of deformation parameter for deep excavation in sand through case histories. *Computers and Geotechnics*, *47*, 57-67.
35. Kulhawy, F. H., & Mayne, P. W. (1990). *Manual on estimating soil properties for foundation design* (No. EPRI-EL-6800). Electric Power Research Inst., Palo Alto, CA (USA); Cornell Univ., Ithaca, NY (USA). Geotechnical Engineering Group.
36. Lambe, T. W., & Whitman, R. V. (1969). Soil mechanics. John Willey & Sons. *Inc., New York*, *553*.
37. Laplante, J. P. (1998). *Instrumentation to monitor building damage from excavation induced ground movement* (Doctoral dissertation, Massachusetts Institute of Technology).
38. Law, K. H., Othman, S. Z., Hashim, R., & Ismail, Z. (2014). Determination of soil stiffness parameters at a deep excavation construction site in Kenny Hill Formation. *Measurement*, *47*, 645-650.
39. Likitlersuang, S., Surarak, C., Wanatowski, D., Oh, E., & Balasubramaniam, A. (2013). Finite element analysis of a deep excavation: A case study from the Bangkok MRT. *Soils and foundations*, *53*(5), 756-773.
40. Lin, D. G., & Woo, S. M. (2007). Three dimensional analyses of deep excavation in Taipei 101 construction project. *Journal of GeoEngineering*, *2*(1), 29-42.
41. Menard, L., & Broise, Y. (1976). Theoretical and practical aspects of dynamic consolidation. In *Ground treatment by deep compaction* (pp. 3-18). Thomas Telford Publishing.

42. Mikkelsen, P. E. (2003). Advances in inclinometer data analysis. In *Symposium on field Measurements in Geomechanics, FMGM*.
43. Mikkelsen, P.E, (1996). Chapter 11—Field Instrumentation. In TRB Special Report 247: Landslides: Investigation and Mitigation (A. K. Turner and R. L. Schuster, eds.), TRB, National Research Council, Washington, D.C., 1996, pp. 278–316.
44. Nicholson, D. P. (1987, April). The design and performance of the retaining walls at Newton Station. In *Proceedings of the Singapore Mass Rapid Transit Conference, Singapore* (pp. 6-9).
45. Nikolinakou, M. A., Whittle, A. J., Savidis, S., & Schran, U. (2011). Prediction and interpretation of the performance of a deep excavation in Berlin sand. *Journal of Geotechnical and Geoenvironmental Engineering*, *137*(11), 1047-1061.
46. Obrzud, R. (2010). *The hardening soil model: A practical guidebook*. Zace Services.
47. O'Rourke, T. D. (1981). Ground movements caused by braced excavations. *Journal of Geotechnical and Geoenvironmental Engineering*, *107*(ASCE 16511).
48. Ou, C. Y. (2014). *Deep excavation: Theory and practice*. Crc Press.
49. Ou, C. Y., & Lai, C. H. (1994). Finite-element analysis of deep excavation in layered sandy and clayey soil deposits. *Canadian geotechnical journal*, *31*(2), 204-214.
50. Ou, C. Y., Hsieh, P. G., & Chiou, D. C. (1993). Characteristics of ground surface settlement during excavation. *Canadian geotechnical journal*, *30*(5), 758-767.
51. Ou, C. Y., Hsieh, P. G., & Duan, S. M. (2005). *A simplified method to estimate the ground surface settlement induced by deep excavation*. Geotechnical Research Report.
52. Ou, C. Y., Liao, J. T., & Cheng, W. L. (2000). Building response and ground movements induced by a deep excavation. *Geotechnique*, *50*(3), 209-220.
53. Ou, C. Y., Liao, J. T., & Lin, H. D. (1998). Performance of diaphragm wall constructed using top-down method. *Journal of geotechnical and geoenvironmental engineering*, *124*(9), 798-808.
54. Ou, C.Y, Hsiesh, P.G., (2000) Prediction of Ground Surface Settlement induced by Deep excavation, Geotechnical Research Report No GT200008, Department of Construction Engineering, National Taiwan University of Science and Technology.
55. Ou,C.Y and Yang,L.L. (2000). Ground movement induced by the construction of diaphragm wall, Geotechical Research Report No GT200005, Department of Construction Engineering, National Taiwan University of Science and Technology.

56. Pakbaz, M. S., Imanzadeh, S., & Bagherinia, K. H. (2013). Characteristics of diaphragm wall lateral deformations and ground surface settlements: Case study in Iran-Ahwaz metro. *Tunnelling and Underground Space Technology*, *35*, 109-121.
57. Pan, X. Y., & Fu, H. Y. (2012). Numerical prediction of settlement adjacent to deep excavation of metro station in Ju-Zi-Zhou island, Changsha. In *Applied mechanics and materials* (Vol. 204, pp. 1484-1487). Trans Tech Publications.
58. Peck, R. B. (1969). Deep excavations and tunneling in soft ground. *Proc. 7th ICSMFE, 1969*, 225-290.
59. Peck, R.B., Hanson, W.E., and Thoruburn, T.H., (1977).Foundation engineering, John Wiley and Sons, New York.
60. Pender, M. J., Wesley, L. D., Duske, G. C., Pranjoto, S., & Twose, G. (2000, November 19). Compressibility Of Auckland Residual Soil. International Society for Rock Mechanics and Rock Engineering.
61. Poh,T.Y and Wong, I.H (1998). Effects of construction of diaphragm wall panels on adjacent ground: field trial, Journal of Geotechnical and Environmental Engineering, ASCE, Vol. 124, No.8, pp.745-756.
62. Safety Guides, N. S. G. (2004). 3.6/International Atomic Energy Agency, Geotechnical Aspects of Site Evaluation and Foundations for Nuclear Power Plants.
63. Schanz, T. (1998). A constitutive model for hard soils T. Schanz. *The Geotechnics of Hard Soils-Soft Rocks*, *2*, 861.
64. Schanz, T., & Vermeer, P. A. (1998). On the stiffness of sands. In *Pre-failure deformation behaviour of geomaterials* (pp. 383-387). Thomas Telford Publishing.
65. Sivakumar, C., & Elango, L. (2008). Assessment of water quality in Kalpakkam Region, Tamil. *Nat Environ Pollut Technol*, *7*(4), 687-691.
66. Smith,I.M., Grifith,D.V. (1982). Programming the finite element method.John Wiley & Sons, Chisester, U.K, Second edition.
67. Terzaghi, K. (1943). Theoretical Soil Mechanics. JohnWiley & Sons. *New York*, 11-15.
68. Timoshenko, S., Goodier, J.N. (1951). Theory of Elasticity, McGraw-Hill Publications, New York.
69. Usmani, A., Ramana, G. V., & Sharma, K. G. (2010, December). Analysis of braced excavation using hardening soil model. In *Indian geotechnical conference*.
70. Wesley, L., & Pender, M. Soil stiffness measured in oedometer tests. *Soil-Structure Interaction*, 57.

71. Whittle, A. J., Corral, G., Jen, L. C., & Rawnsley, R. P. (2014). Prediction and performance of deep excavations for courthouse station, Boston. *Journal of Geotechnical and Geoenvironmental Engineering*, *141*(4), 04014123.
72. Wilson, S. D., & Mikkelsen, P. E. (1977). *FOUNDATION INSTRUMENTATION/INCLINOMETER* (No. FHWA-TS-77-291 Final Rpt.).
73. Xanthakos, P. P. (1994). *Slurry walls as structural systems*, 2nd Edition, McGraw-Hill, New York
74. Yoo, C., & Lee, D. (2008). Deep excavation-induced ground surface movement characteristics–A numerical investigation. *Computers and Geotechnics*, *35*(2), 231-252.
75. Zheng, G., Zeng, C. F., Diao, Y., & Xue, X. L. (2014). Test and numerical research on wall deflections induced by pre-excavation dewatering. *Computers and Geotechnics*, *62*, 244-256.

NOMENCLATURE

γ_w	Unit weight of water
γ_{dry}	Dry unit weight of soil
γ_{sat}	Saturated unit weight of soil
δ_v	Maximum vertical settlement
$\delta_{H\,max}$	Maximum lateral deflection of wall
δ_{hm}	Horizontal displacement
ε	Total strain
$\varepsilon_{x,y,z}$	Principle strain in three direction
ε^e	Reversible elastic strain
ε^p	Irreversible plastic stain
θ	Angle between vertical and casing alignment
σ	Stress
σ^{ref}	Reference stress
$\sigma_{x,y,z}$	Principle stress
υ	Poissons ratio
υ_{ur}	Unloading Poisson's ratio
ϕ	Angle of internal friction
ϕ'	Drained angle of internal friction

NOMENCLATURE

Ψ	Angle of dilatency
BH	Boreholes
C	Cohesion
C'	Drained cohesion
CD	Consolidated drained
C_d	Correction factor for plate size
d	Distance behind excavation
E	Stiffness of soil
E_{50}	Secant stiffness at reference stress
EA	Normal stiffness of retaining system
EI	Stiffness of retaining system
E_{inc}	Increase in stiffness
E_{oed}	Stiffness from oedometer
E_p	Pressuremeter modulus
E_{ur}	Unloading-reloading stiffness
E_{oed}^{ref}	Tangent stiffness
f	Yield function
F_b	Factor of safety against basal heave
g	Plastic potential function
h	Distance between struts

NOMENCLATURE

h_{avg}	Average distance between struts
Hc	Depth of excavation
HS	Hardening soil model
H_t	Depth of trench
L	Reading interval
m	Power for stress level dependency
MC	Mohr Coulomb model
N_{60}	Corrected SPT N values for 60% hammer efficiency
P_a	Atmospheric pressure
PI	Plasticity index
PIZ	Primary influence zone
P_L	Limit Pressure
q	Load intensity
SIZ	Secondary influence zone
SPT	Standard Penetration Test
UU	Unconsolidated Undrained
Ux	Horizontal displacement
U_y	Vertical displacement